Universidad de Concepción
Dirección de Postgrado
Facultad de Ciencias Físicas y Matemáticas
Programa de Doctorado en Ciencias Aplicadas
con Mención en Ingeniería Matemática

Métodos de elementos virtuales para problemas en mecánica de sólidos

Virtual element methods for problems in solid mechanics

Tesis para optar al grado de
Doctor en Ciencias Aplicadas con mención en Ingeniería Matemática

Iván Darío Velásquez Ramos

Concepción–Chile, 15 de Noviembre de 2019

Virtual element methods for problems in solid mechanics

Iván Darío Velásquez Ramos

Directores de Tesis: David Mora, Universidad del Bío-Bío, Chile.
Rodolfo Rodríguez, Universidad del Concepción, Chile.
Carlo Lovadina, Università degli Studi di Milano, Italia.

Director de Programa: Rodolfo Rodríguez, Universidad de Concepción, Chile.

Comisión evaluadora

Prof. Andrea Cangiani, University of Nottingham, UK.

Prof. Ricardo Duran, Universidad de Buenos Aires, Argentina.

Prof. Paola Pietra, Institute for Applied Mathematics and Information Technologies IMATI, Italy.

Comisión examinadora

Firma: _____
Prof. David Mora, Universidad del Bío-Bío, Chile.

Firma: _____
Prof. Thomas Führer, Pontificia Universidad Católica de Chile, Chile.

Firma: _____
Prof. Rodolfo Rodríguez, Universidad de Concepción, Chile.

Firma: _____
Prof. Pablo Venegas, Universidad del Bío-Bío, Chile.

Concepción, 15 de noviembre de 2019

Abstract

The main goal of this doctoral thesis is to develop, analyze, implement and apply several virtual element methods (VEM) conforming in H^2 on general polygonal meshes for solving diverse fourth order problems that arise in solid mechanics, with the purpose of establishing an original contribution in the virtual element theory.

We firstly present two linear eigenvalue problems for thin plates, namely vibration and buckling problems of Kirchhoff plates. In relation to the vibration problem of Kirchhoff plates, the study is focused on developing a C^1-virtual element method for the analysis of the numerical approximation of the vibration frequencies and vibration modes of thin plates. A variational formulation based only on the transverse displacement of the plate is proposed. A conforming discretization of H^2 by means of VEM which is simple in terms of degrees of freedom and coding aspects is introduced. Under standard assumptions on the computational domain, it is established that the resulting scheme provides a correct approximation of the spectrum. In addition, optimal order error estimates for the eigenfunctions and a double order for the eigenvalues are proved.

On the other hand, a virtual element method of high order on polygonal meshes for solving the buckling problem governed by Kirchhoff equations is developed as second work of this thesis. Then, a C^1 conforming virtual element discretization of arbitrary order ≥ 2 is introduced. In addition, the standard spectral theory for compact operators is applied to prove that the resulting scheme provides a correct approximation of the spectrum. Moreover, optimal order error estimates for the buckling modes and a double order for the buckling coefficients are proved.

Subsequently, we introduce and analyze a C^1-virtual element method for solving a nonlinear problem of plates modelled by von Kármán equations. A variational formulation based on C^1-conforming discretization by means of VEM is proposed. The method has the advantages of supporting general polygonal meshes and is simple in terms of coding aspects. We prove that the discrete problem is well posed for h (letter usually chosen to denote the discretization parameter) small enough. Moreover, optimal error estimates are derived.

We finally propose and analyze a virtual element method for numerically solving a non-linear non-self-adjoint eigenvalue problem called the transmission eigenvalue problem. By introducing a new unknown (which belongs to H_0^1) in the system of equations the eigenvalue problem is linearized. Next, a variational formulation on $H_0^2 \times H_0^1$ is defined. Then, by defining a solution operator, which result to be non-self-adjoint with respect to usual seminorm of $H_0^2 \times H_0^1$ and compact, the spectrum of the variational formulation is characterized (which is the spectrum of the transmission eigenvalue problem). A $C^1 \times C^0$ -conforming discretization by means of the VEM is proposed. The classical

spectral theory for non-sel-fadjoint compact operators is employed in order to analyze the correct spectral approximation. The optimal order of convergence for the eigenvalues and the eigenfunctions is derived.

For all the situations described above, several numerical experiments illustrating good performance of the proposed methods, and confirming the theoretical analysis, are presented.

Resumen

El objetivo principal de esta tesis doctoral es proponer, analizar, desarrollar, implementar y aplicar varios métodos de elementos virtuales (VEM) conformes en H^2 sobre mallas poligonales generales, para resolver diversos problemas de cuarto orden que surgen en mecánica de sólidos, con el propósito de establecer una contribución original en la teoría de los elementos virtuales.

En primer lugar, presentamos dos problemas de autovalores para estructuras delgadas, a saber, el problema de vibración y el problema de pandeo de placas modeladas por las ecuaciones de Kirchhoff. En relación con el problema de vibración de placas delgadas, el estudio se centra en desarrollar un método de elementos virtuales C^1 para la aproximación numérica de las frecuencias de vibración y los modos de vibración de las placas de Kirchhoff. Se propone una formulación variacional basada únicamente en el desplazamiento transversal de la placa. Se introduce una discretización conforme de H^2 por medio del VEM, el cual es simple en términos de grados de libertad e implementación computacional. Bajo supuestos estándar en el dominio computacional, se establece que el esquema resultante proporciona una aproximación correcta del espectro. Además, se obtienen óptimas estimaciones del error para las funciones propias y un orden doble para los valores propios.

Por otro lado, como segundo trabajo de esta tesis, se desarrolla un método de elemento virtual de alto orden en mallas poligonales, para resolver el problema de pandeo de placas gobernado por las ecuaciones de Kirchhoff. Se introduce una discretización de elemento virtual conforme C^1 de orden arbitraria ≥ 2. Además, se aplica la teoría espectral estándar de operadores compactos para demostrar que el esquema resultante proporciona una aproximación correcta del espectro. Se derivan estimaciones del error de orden óptimas para los modos de pandeo y un orden doble para los coeficientes de pandeo.

Posteriormente, introducimos y analizamos un método de elementos virtuales C^1 para resolver un problema no lineal de placas modeladas por las ecuaciones de von Kármán. Se propone una formulación variacional continua en H^2 asociada a este problema. Luego, se introduce una discretización conforme por medio de elementos virtuales. El método tiene las ventajas de considerar mallas poligonales generales y es simple en términos de implementación computacional. Probamos que el problema discreto está bien planteado para h (letra generalmente elegida para denotar el parámetro de discretización) lo suficientemente pequeño. Además, se obtienen estimaciones de error óptimas.

Finalmente, proponemos y analizamos un método de elementos virtuales, para resolver numéricamente un problema de valores propios no lineal y no autoadjunto, conocido como el problema de valores propios de transmisión. El problema se linealiza al introducir una nueva incógnita (que pertenece a H_0^1) en el sistema de ecuaciones. Luego, se define una formulación variacional en $H_0^2 \times H_0^1$ y se caracteriza el espectro del problema a través de la definición de un operador solución, el cual resulta ser no au-

toadjunto y compacto, con respecto a la seminorma usual de $H_0^2 \times H_0^1$. Se propone una discretización conforme de $C^1 \times C^0$ por medio del VEM. Se emplea la teoría espectral clásica para operadores compactos no autoadjuntos con el objetivo de analizar la aproximación espectral. Se deriva el orden óptimo de convergencia para los valores propios y las funciones propias.

Para todos los problemas descritos anteriormente, se presentan varios experimentos numéricos que ilustran el buen desempeño de los métodos propuestos y que confirman el análisis teórico.

Agradecimientos

En primer lugar, doy gracias a Dios por permitirme finalizar con éxito mis estudios de doctorado. En segunda instancia, agradezco infinitamente a Astrid Sarmiento (novia-polola-prometida-pareja-...-señoya) a quien le debo gran parte de este nuevo logro en mi vida. Por su apoyo incondicional, tiempo, dedicación y sus excelentes consejos pedagógicos.

A mi familia, a mi madre Ana y a mi padre Ulises, que siempre han estado en contacto conmigo sin importar que tan lejos esté de casa. A mis hermanos, Luz Daris, Jorge, Mario, Miguel y Edwin. A mis prim@s, sobrin@s, tí@s, amig@s que me ayudaron a comprar un pasaje de avión para venir a Chile y estudiar un postgrado.

Agradezco a David Mora, quien además de ser un excelente profesor y director de tesis, ha sido un gran amigo (más bien como un hermano mayor) desde que llegué a Chile a realizar mis estudios de maestría y posteriormente, mis estudios de doctorado. Gran parte de mi formación académica en las matemáticas aplicadas es gracias a él. Le agradezco su paciencia, dedicación y disposición para trabajar conmigo. Por sus enseñanzas, consejos académicos y no-académicos.

A Rodolfo Rodríguez, por tener siempre espacio libre en su agenda para ayudarme a resolver las dudas y también por compartir sus conocimientos analíticos y computacionales conmigo. También le agradezco su excelente gestión como director del programa y solicitar financiamiento con el objetivo de terminar mis estudios de doctorado.

A Carlo Lovadina por compartir sus conocimientos del VEM, durante las 2 estadías que realicé en la Università degli Studi di Milano. Por su gestión para solicitar un espacio en las salas de estudios de la UNIMI y poder desarrollar parte de mi tesis.

A Gabriel Gatica, por su excelente gestión como director del CI^{2}MA, lo cual se refleja en muy buenas comodidades de trabajo (oficinas adecuadas, financiamientos para asistir a congresos, fotocopiadora, impresora,..., y café). También, por la formación profesional que logré a través de los 3 cursos a los cuales asistí.

A Raimund Bürguer, por su excelente gestión cuando fue director del programa de doctorado, lo cual se vio reflejado en los apoyos de financiamiento que gestionó para poder asistir a distintos congresos en Chile y también a la escuela de verano sobre método de elementos virtuales realizada en la ciudad de Dobbiaco.

Agradezco a los profesores que me hicieron clases en el doctorado: Gabriel Gatica, Raimund Bürguer, Romel Bustinza, Leonardo Figueroa, Dhanya Rajendran y Manuel Solano.

A todos los profesores que tuve en pregrado, en particular a Carlos Reales “el comandante”, por

sugerirme venir a Chile y porque fue la primera persona a quien le escuché hablar sobre los métodos de elementos finitos. Por sugerirme entrar al programa de doctorado. También a Abraham Arenas por motivarme a estudiar un postgrado fuera de mi país, sobre todo con su frase motivadora "aja ¿y no quieres ser doctor?".

A todos los amigos colombianos con los cuales he compartido buenos momentos, parecidos a los que se viven en mi tierra. En particular a: Saúl, Liliana, Luis Vigolla, Mauricio, Rafael, Andrés Jaramillo, Hernán, Myleidi, Yadiris, Pedro, Diana, Adriana, Alberth, Rubén, Juan, Wilber, Harold y Andy.

Agradezco a los amigos chilenos con los que he compartido durante toda esta etapa y también a los amigos de otras nacionalidades que han pertenecido (o están) en el CI^{2}MA. En particular, al "compa" Paulo, Eduardo, Sergio, Gonzalo (por sus importantes comentarios sobre el VEM), Felipe Lepe, Lorena, Bryan, Paul, Víctor, Rodrigo, Cristian, Yolanda, Yissedt y Néstor.

A Verónica, Fernando y Nitesh por sus comentarios y sugerencias para la redacción en inglés de algunos párrafos en la introducción de esta tesis.

Agradezco a CONICYT PFCHA/DOCTORADO NACIONAL/2015-21151152 por financiar parcialmente mis estudios de doctorado. Al programa de financiamiento BASAL para apoyo a centros científicos y tecnológicos de excelencia a través del PROYECTO BASAL AFB 170001. Al Departamento de Ingeniería Matemática DIM y por último y no por ello menos importante, a la secretaria del programa de doctorado, Cecilia Leiva, por su excelente y gentil disposición para realizar distintos tramites referentes al programa.

Iván Darío Velásquez Ramos

Contents

List of Tables

List of Figures

Introduction

Motivation

Several interesting physical phenomena with engineering applications can be classified and described according to its medium. In particular those that arise in "Solid Mechanics" and are modelled by linear and nonlinear partial differential equations. Many models are governed by higher order partial differential equations, for instance, problems related to deformations, failures and tensions of some materials or solid structures. These types of problems are very important in: Physics, Geology, Seismology, Civil Engineering, Aerospace Engineering, Aeronautical Engineering, among others. For instance, fourth order problems appear in the study of the vibration and buckling problems of Kirchhoff plates. In particular, the lowest vibration frequencies of the structures is extremely important in aspects as safety, mechanical resistance and cost for designing aircraft, cars, boats, bridges, etc. This is one of the reasons for which it is very important to study eigenvalue problems from both the mathematical and the numerical point of view.

It is well known that the equations that model these problems are difficult to solve analytically; thus, developing numerical methods that approach solutions computationally are indispensable. On the other hand, one of the most known numerical method to approximate these solutions is the finite element method (FEM). In particular, there are several conforming finite elements methods that approximate the solution of fourth order problems governed by partial differential equations. For instance, the conforming methods most commonly used are: the Argyris finite elements (which needs 21 degrees of freedom by triangle), the Bell finite elements (this needs 18 degrees of freedom by triangle), the Bogner-Fox-Schmit finite elements (which needs 16 degrees of freedom by rectangle), and the Hsieh-Clough-Tocher finite elements (which needs 12 degrees of freedom by triangle). These methods allow to define elements of class C^1 (in triangular or quadrilateral meshes), which are naturally required to approximate solutions of fourth order partial differential equations in two dimensions. To construct the C^1 elements the continuity of the first order partial derivative across adjacent finite elements are required. However, to relax this continuity requirement and in order to solve the fourth order problems some methods has been introduced in the literature. The Morley finite elements and mixed methods like the Ciarlet-Raviart method are well-known among them.

In this doctoral thesis, we are interested in analyzing, applying, and implementing C^1 virtual element methods on general polygonal meshes (including triangular meshes) for solving diverse fourth order problems (modelled by partial differential equations) that arise in solid mechanics.

Virtual element method

The *Virtual Element Method* (VEM) was introduced in [12] as a generalization of finite element methods, with the capability to deal with general polygonal/polyhedral meshes, including "hanging vertexes" and non-convex shapes. The VEM has been developed in many aspects and successfully applied to a wide range of problems. In fact, since the birth of the VEM in 2012 an evident growth of the scientific interest for Virtual Element Methods can be appreciated. For instance, making a simple search in an online bibliographic database (for example Mathscinet) related to VEM papers, we found: 4 papers in 2013, 7 articles in 2014, 7 articles in 2015, 16 works published in 2016, 30 papers in 2017, 41 articles in 2018 and 31 during 2019. We mention some of them, in linear elasticity problems we find [15, 77, 8, 9, 44], Virtual element methods applied to Stokes problem in [42, 61, 94, 23, 54, 6], and for Navier-Stokes equations [24, 80, 93]. Virtual element methods applied to plate problems can be found in [27, 41, 64, 128, 63, 127], in particular those applied to spectral problems in [28, 79, 122, 28, 103]. A posteriori error analysis has been developed in [62, 53, 104, 31, 26], etc.

According to [2, 12] the main idea of VEM can be summarized as follows:

- The discrete local spaces are constructed so that the trial and test functions contain the set of polynomials of degree $\leq k$ (whose degree determines the method accuracy), and other functions, which are not polynomials and whose exact values in the interior of the polygon/polyhedral are not known (hence, it is termed "virtual").
- The degrees of freedom must be chosen carefully so that the discrete forms (linear, bilinear and trilinear, etc), can be computed exactly, whenever we take a polynomial of degree $\leq k$ as trial entry, and using only the degrees of freedom of the test entry.

Since the computed solutions are represented by the degrees of freedom, the properties above imply that the solution is not known explicitly as a virtual function, unless one of the two entries is a global polynomial of degree $\leq k$. In other words, these properties ensure the **patch test** used by engineers, i.e., on any patch of elements: if the true solution is a global polynomial of degree $\leq k$, then the discrete and exact solution will coincide [41].

An important and very used result of VEM was established in [2]. The authors show a variant of the virtual element method presented in [12] to compute (directly from the degrees of freedom) the L^2 projections on all polynomials of degree $\leq k$. The motivation for this result is due to the fact that in many applications it is convenient to know explicitly the local projector Π_K^∇ and the local L^2 -orthogonal projector Π_k^0 on the polynomials of degree $\leq k$. It is known from [12] that the projector Π_k^0 is available only on polynomials of degree $\leq k-2$ (directly from the degrees of freedom). The authors in [2] proved that in a certain number of cases, just by changing slightly the definition of the non-polynomial local functions (which, in any case, are never computed!), it is possible to obtain a local space in which the operator Π_k^0 can be easily computed using Π_k^∇ and the local degrees of freedom. This result has been also used for C^1-VEM, we can mention the works [7, 64, 27].

On the other hand, there are some articles related to the implementation of Virtual Element Method, for instance [16, 18, 117]. We can say that [16] is the first article of implementation for VEM, which details meticulously how to compute the discrete linear and bilinear forms used to approximate the

solutions of the Poisson problem in two and three dimensions, the authors first present the steps to follow for computing (only using the degrees of freedom) the local matrices obtained from the linear and bilinear forms that discretize the Poisson problem in 2D. In addition, the implementation of the stabilizing terms of the methods are also reported. Subsequently, they extend the implementation steps for the Poisson problem in 3D. Moreover, an implementation guide of VEM for two-dimensional elliptic equations in primal and mixed form with variable coefficients is introduced in [18], the authors show an alternative to the one presented in [16] for implementing the discrete bilinear forms which approximate the inner product in H^1. In addition, the implementation details for the discrete forms defined in the conforming virtual space of $H(div)$ (introduced in [17]) are also presented. A 50-line MATLAB implementation of the lowest order virtual element method for the two-dimensional Poisson problem is analyzed and showed in [117]. The author approximates the solution using the virtual discretization presented in [12] and includes the lines of the code in his article.

Until now the VEM has been extended successfully to different applied problems that arise in fluid and solid mechanics including those that require continuity of the higher order derivatives. In particular, to solve fourth order problems using conforming methods of H^2.

Therefore, according with the main goal of this doctoral thesis, we will describe briefly some contributions that have been introduced to VEM literature for solving fourth order problems (for instance [41, 64, 7]) by means of C^1-VEM.

C^1-Virtual element method

The first C^1-VEM (in two dimensions) was introduced in [41] to solve the linear bending plate problem described with Kirchhoff-Love equations, i.e.

$$D\Delta^2 u = f \quad \text{in } \Omega,$$

where Ω is a convex and bounded polygonal domain, $D = \frac{Et^3}{12(1-\nu^2)}$ is the bending rigidity, t the thickness, E the Young modulus, and ν the Poisson ratio. The weak formulation of the problem above is given by: given $f \in L^2(\Omega)$, find $u \in H_0^2(\Omega)$ such that

$$a(u,v) := D\Big((1-\nu)\int_\Omega D^2u : D^2v + \nu\int_\Omega \Delta u \Delta v\Big) = \int_\Omega fv \quad \forall v \in H_0^2(\Omega).$$

The basic idea considered by the authors can be summarized as follows: First, to propose some degrees of freedom at the interelement boundaries in order to identify in a unique way the traces of globally C^1 functions whose restriction on each side e of a polygon K is a polynomial of degree $\leq r$, and with normal derivative of degree $\leq s$ on each edge e of the polygon. Subsequently, a suitable quantity of the internal degrees of freedom must be added. In addition, for each polygon K the discrete subspace on K is defined by means of a local plate bending problem.

Therefore, if the discrete subspace is constructed with the previous steps then, the following properties hold:

- On each polygon K, the local spaces are designed to contain polynomials of degree$\leq k$, where k depends on r and s.

- On each polygon K the bilinear form $a(\cdot,\cdot)$ can be computed exactly whenever we take a polynomial of degree $\leq k$ as trial entry, and using only the degrees of freedom of the test entry (and not the fact that the test function solves a local plate problem).
- In order to obtain stability, the bilinear form $a(\cdot,\cdot)$ can be computed exactly even when both entries are not necessary polynomials.

As a consequence of the above properties the **patch test** is guaranteed. Moreover, by considering additional assumptions on the mesh, on the discrete space and on the bilinear form $a(\cdot,\cdot)$ (stability and consistency properties), the authors of [41] construct a family of C^1 elements which depend on three integer indices (r,s,m), related to the degree of accuracy $k \geq 2$ by:

$$r = \max\{k,3\}, \quad s = k-1 \quad \text{and} \quad m = k-4.$$

More precisely, the virtual local space V_h^K and degrees of freedom introduced in [41] are given by:

(i) The evaluation of the virtual functions on each vertex of the polygon;

(ii) The evaluation of the partial derivatives of the virtual functions on each vertex of the polygon;

(iii) For $r > 3$ the moments $\displaystyle\int_e qv$, for all q polynomial defined on e and of degree $\leq r-4$;

(iv) For $s > 1$, the moments $\displaystyle\int_e q\partial_n v$, for all q polynomial defined on e and of degree $\leq s-2$;

(v) For $m \geq 0$, the moments $\displaystyle\int_K qv$, for all q polynomial defined on K and of degree $\leq m$;

and

$$V_h^K := \{v \in H^2(K) : \Delta^2 v \in \mathbb{P}_m(K), \quad v|_e \in \mathbb{P}_r(e), \quad \partial_n v|_e \in \mathbb{P}_s(e) \quad \forall e \in \partial K\},$$

where, $\mathbb{P}_m(K), \mathbb{P}_r(e)$ and $\mathbb{P}_s(e)$ denote the set of polynomial of degree less than m, r and s, respectively, and $\partial_n v|_e$ denotes the normal derivative of v on e. An important fact, is that (v) allows to compute exactly the standard L^2-projector onto the set of polynomials of degree $\leq k-4$.

Additionally, the authors of [41] proved some particular examples of this family of virtual elements, optimal convergence and error estimates in the energy H^2 seminorm, we refer to [41] for further details.

Later, convergence and optimal error estimates in L^2 and in H^1 via classical duality arguments are introduced in [64]. Based on the arguments presented in [2], the authors modify the discrete subspaces defined in [41]. As a consequence, this modification allows to compute exactly the L^2-orthogonal projector onto the set of polynomials of degree $\leq k-2$. The model problem considered in [64] is the same which is considered in [41].

Another important contribution related to C^1-VEM is the lowest order ($k = 2$) virtual elements developed in [7] for the approximation of the Cahn-Hilliard equation. Based on the arguments presented in [2], the authors obtain a particular space of the family C^1-VEM established in [41]. The difference between the elements obtained in [7] and the ones obtained in [41, 64] is that the L^2-orthogonal

projection on polynomials of degree $k = 2$ can be exactly computed directly from the degrees of freedom.

Moreover, it is important to mention that C^1 virtual element methods for three dimensional fourth order problems have been recently developed in [19].

According to the above description, the main objective of this doctoral thesis is to analyze, apply and implement several C^1 virtual element methods (in two dimensions) on general polygonal meshes to solve fourth order problems that arise in solid mechanics. More precisely, we are interested in solving the vibration and buckling problems of Kirchhoff plates, von Kármán plates and a transmission eigenvalue problem.

Now, we will summarize the content of our study.

Vibration problem of Kirchhoff plates

The vibration problem of Kirchhoff plates is a fourth order partial differential equation modelling the transverse displacement of the mean surface of a thin plate, and a parameter that represent the vibration frequencies of the system (plate). The main characteristic of this model, is that the displacements of the mid-surface are vertical and straight with respect to deformed mid-surface even after the deformation. The study of the vibration problem of Kirchhoff plates appears in interesting applications of aerospace, marine and structural engineering, since it is important for the design of different solid structures.

In order to approximate the vibration frequencies and vibration modes (also called eigenfunctions), C^1-elements are required. However, to relax such continuity, several methods based on hybrid, non-conforming, and mixed finite elements have been developed in the last decades. For instance, in [57] a hybrid finite element method was introduced to approximate the vibration frequencies of a clamped plate. In [90] a semi-discrete and the fully discrete Morley finite element methods were analyzed to solve the vibration Kirchhoff problem. A C^0-IPG method is analyzed in [36] to solve the biharmonic eigenvalue problem with three types of boundary conditions. Next, the authors of [106] proposed and analyzed a piecewise linear finite element method to approximate the eigenvalues and eigenfunctions of the vibration and buckling problem of a thin plate modelled with Kirchhoff-Love equations. On the other hand, the most-well known mixed method (called Ciarlet-Raviart' method) to solve the biharmonic problem is introduced by Ciarlet and Raviart in [69]. In particular, this method has been studied to solve the vibration Kirchhoff problem (see [56, 99]). Regarding to C^1-elements, it is well known that the standard finite elements employed to solve the model problem of this chapter are Argyris and Bell finite elements. However, these elements need a lot of degrees of freedom (for instance, Argyris and Bell triangle need 21 and 18 degrees of freedom in a triangle), since otherwise they are difficult to implement (for instance Hsieh-Clough-Tocher element), we refer to [67, Chapter 6] for further details.

Typically, triangular or quadrilateral meshes are used to define finite element methods. However, in complex simulations can be more convenient to employ polygonal meshes. We are interested in studying, developing and implementing a C^1-virtual element method applied to general polygonal meshes (including non-convex elements and hanging nodes) to approximate the spectrum of the vibration

problem of Kirchhoff plates.

More precisely, **Chapter 1** of the thesis introduces the mathematical and numerical analysis of the vibration problem of a thin plate. First, we introduce a variational formulation where the unknown is the transverse displacement of the plate which belongs to H_0^2. Next, in order to characterize the spectrum of the problem we define a solution operator which is compact. Then, a C^1-virtual element discretization based on the elements introduced in [7] is written. Next, since the standard theory of abstract spectral approximation (see [11]) cannot be applied to analyze this problem, the theory presented in [73, 74] is adapted in this chapter to obtain convergence and error estimates of our method. Finally, a set of numerical examples which verify the performance of the method are tested.

The contents of this chapter gave rise to the following article:

- D. Mora, G. Rivera and I. Velásquez: *A virtual element method for the vibration problem of Kirchhoff plates*, ESAIM Math. Model. Numer. Anal., **52**, (2018), pp. 1437–1456.

Buckling problem of Kirchhoff plates

The buckling problem of Kirchhoff plates is an eigenvalue problem modelled by a fourth order partial differential equation. The main unknown of this model is the transverse displacement of the mean surface of the plate when it is subjected to horizontal forces through a plane stress tensor field. In this problem, the smallest eigenvalue corresponds to the critical load when the buckling occurs. One difficulty of this model is to approximate the buckling coefficients (eigenvalues) and buckling modes (eigenfunctions) when it is assumed that the stress tensor field is not necessary positive definite. Moreover, since the buckling problem is governed by a fourth order partial differential equation, it is well known that conforming methods require straight finite elements of class C^1 [67, Chapter 6].

This problem has attracted great interest to scientists and engineers for a long time [69, 91, 106, 36], due to their wide use in engineering applications, such as bridge, ship, cars and aircraft design.

There are numerous publications in the engineering literature about the various finite element that can be applied for solving the buckling problem of Kirchhoff plates. Since the conforming finite element methods of H^2 need many degrees of freedom or they do not have an easy implementation (see [67, Chapter 6]), several alternatives such as C^0, nonconforming, mixed and hybrid finite element methods have been studied to approximate the eigenvalues and vibration modes of the buckling problem. For instance, in [106] it was analyzed a mixed formulation to approximate the spectrum of the buckling problem. The authors employed the C^0-finite element method introduced in [3] for solving the bending moments of Kirchhoff-Love plates. In [100] was proposed and analyzed a mixed formulation based on the idea introduced by Ciarlet and Raviart [69]. The authors approximated the lowest buckling coefficients of a simply supported plate modelled with the Kirchhoff equations, and they derived optimal order error estimates for the eigenfunctions and a double order for the eigenvalues. Later, a C^0-IPG method, which consider three types of boundary conditions, namely, clamped plate, simply supported plate and the Cahn-Hilliard type has been introduced in [36]. In particular, the authors proved convergence and optimal error estimates results associated to the approximated eigenvalues and eigenfunctions.

In this part of the thesis, we are interested in proposing and analyzing a C^1 virtual element method to approximate the eigenvalues and eigenfunctions of the buckling problem of Kirchhoff plates.

Chapter 2 of the thesis proposes and analyzes a C^1- virtual element discretization to solve the buckling problem of Kirchhoff plates. First, assuming that the stress tensor field is symmetric and is divergence free, we arrive to a spectral characterization of the model problem. This is made introducing a solution operator (which results to be compact) defined from the associated source problem (biharmonic equation). Next, a discrete scheme based on the C^1-virtual elements introduced in [64] is proposed. Subsequently, in order to obtain convergence and optimal error estimates, the well known spectral theory for compact operators [11] is applied. Several numerical tests with different kind of boundary conditions are reported at the end of the chapter, which confirm that the experimental convergence rates agree with the theoretical analysis developed.

The results contained in this chapter are in the following pre-print:

- D. Mora and I. Velásquez: *Virtual element for the buckling problem of Kirchhoff-Love plates.* Preprint 2019-16, Centro de Investigación en Ingeniería Matemática (CI^{2}MA), Universidad de Concepción Chile, (2019).

The von Kármán equations

The first two chapters of this thesis deal with vibration and buckling problems of a thin plate. These problems are governed by a linear fourth order partial differential equation. In both cases the unknown is the transverse displacement of the mean surface of the plate. Now, in this chapter we will study a nonlinear system of partial differential equations modelling a very thin plate by using the von Kármán equations [65]. This model is a nonlinear system of fourth order differential equations, which describe two unknowns, namely, the displacement of the mean surface of the plate and the boundary stresses of the plate. The main difference between von Kármán and Kirchhoff models is the linearization of the strain tensor, which in fact, leads to the non-linearity in von Kármán model [68, Chapter 1].

This model was introduced in 1910 by von Kármán [123] to describe the large deflections of very thin elastic plates. Due to its applications in engineering design, this problem has been studied in a great number of papers in this area [92, 101, 40, 95, 96, 37, 59]. The von Kármán equations also has been analyzed to be applied in biology [109].

The von Kármán equations do not have a unique solution. However, sufficient conditions to approximate the isolated solutions of this problem has been established in [40]. The purpose of this part of the thesis is to propose and analyze a virtual element method to approximate the isolated solutions of von Kármán plates.

In **Chapter 3**, we describe the canonical von Kármán equations. Next, by introducing a new parameter that depends on the lateral forces on the plate and which allows to relate the von Kármán model with the buckling problem of Kirchhoff plate, we arrive to an equivalent system of equations. Using the existence result of the isolated solutions presented in [65] and assuming the sufficient conditions result (to approximate the isolated solutions) established in [40], a well-posed continuous variational formulation is written. Then, in order to discretize the variational formulation, we use the C^1 virtual

elements proposed in [7]. In particular, we introduce a discrete trilinear form defined with C^1 virtual elements. Next, to guarantee that the discrete problem is well posed, we use the general theory established in [40], which allows to approximate the isolated solutions of von Kármán plate by using fixed point arguments. As consequence, we obtain convergence and optimal error estimates results for the isolated solutions. Finally, several numerical tests that confirm the theoretical analysis developed are reported at the end of this chapter.

The results contained in this chapter are in the following pre-print:

- C. Lovadina D. Mora and I. Velásquez: *A virtual element method for the von Kármán equations.* Preprint 2019-36, Centro de Investigación en Ingeniería Matemática (CI^{2}MA), Universidad de Concepción Chile, (2019).

Transmission eigenvalues problem

The transmission eigenvalue model is non-self-adjoint and a non-elliptic problem arising from the study of the inverse scattering problem of inhomogeneous media which is governed by a second order system of partial differential equations [71]. However, it can be rewritten as a system of fourth order partial differential equations [46, 49]. This alternative gives a non-linear (because it is written as a quadratic eigenvalue problem) and non-self-adjoint eigenvalue problem [49, 60]. This problem plays an important role in the uniqueness and reconstruction in inverse scattering theory [47, 71]. Since it is highly non-trivial to develop effective numerical methods for approximating the eigenvalues and eigenfunctions of this kind non-self-adjoint problems, this mathematical model results to be a challenging spectral problem.

The transmission eigenvalue problem has been abundantly studied in the last years from the mathematical and numerical standpoint. For instance, the authors of [72] analyzed and proposed the first numerical treatment of the transmission eigenvalue problem. They introduced three finite element methods to approximate the eigenvalues of this problem. Later, using Argyris finite element methods convergence and optimal error estimates results are presented in [49] to eigenvalue transmission. In addition, a C^0 finite element method is studied in [60] to approximate the transmission eigenvalues using a gradient recovery operator.

Since the transmission eigenvalue problem is written by a quadratic fourth order eigenvalue system, in this part of the thesis, we linearize the problem by introducing a new unknown (see for instance [49, 50, 115]) in H_0^1 as the unique solution of the Laplace problem with homogeneous Dirichlet boundary conditions. According to the above and in order to exploit the capability of the virtual element method to construct discrete spaces with high regularity, in **Chapter 4** we propose, analyze and apply a $(C^1 \times C^0)$-VEM to solve the transmission eigenvalue problem.

More precisely, in this chapter, we focus on analyzing, a $(C^1 \times C^0)$-VEM for solving a non-self-adjoint spectral problem derived from the fourth order transmission eigenvalue problem. With this aim, first, a solution operator (which results to be compact) is defined, which characterizes the spectrum of the linearized eigenvalue problem. Next, a conforming virtual element discretization of $H_0^2 \times H_0^1$ based on the virtual elements is introduced and analyzed. Using the approximation theory for compact

non-self-adjoint operators [11], optimal order error estimates are derived. In addition, since the model problem is non-self-adjoint, the adjoint problems of the continuous and discrete eigenvalue problems are considered. The optimal order of convergence for the eigenvalues and the eigenfunctions of the adjoint problems are also reported. Numerical tests that confirm the theoretical results are presented at the end of the chapter.

The results contained in this chapter are in the following article:

- D. Mora and I. Velásquez: *A virtual element method for the transmission eigenvalue problem*, Math. Models Methods Appl. Sci., **28**, (2018), pp. 2803–2831.

Introducción

Motivación

Varios fenómenos físicos interesantes con aplicaciones de ingeniería pueden ser clasificados y descritos según su medio. En particular, aquellos que surgen en " Mecánica de sólidos " y se modelan mediante ecuaciones diferenciales parciales lineales y no lineales. Muchos modelos se rigen por ecuaciones diferenciales parciales de orden superior, por ejemplo, problemas relacionados con deformaciones, fallas y tensiones de algunos materiales o estructuras sólidas. Estos tipos de problemas son muy importantes en: Física, Geología, Sismología, Ingeniería Civil, Ingeniería Aeroespacial, Ingeniería Aeronáutica, entre otros. Por ejemplo, los problemas de valores aparecen en el estudio de los problemas de vibración y de pandeo de las placas Kirchhoff. En particular, las frecuencias de vibración más bajas de las estructuras es extremadamente importante en aspectos como seguridad, resistencia mecánica y el costo para diseñar aeronaves, automóviles, barcos, puentes, etc. Esta es una de las razones por las cuales es muy importante estudiar este tipo de problemas tanto desde el punto de vista matemático como numérico.

Es bien sabido que las ecuaciones que modelan estos problemas son difíciles de resolver analíticamente; por lo tanto, el desarrollo de métodos numéricos que aproximen computacionalmente las soluciones, son indispensables. Por otro lado, uno de los métodos numéricos más conocidos para aproximar estas soluciones es el método de elementos finitos (FEM). En particular, existen varios métodos de elementos finitos conformes que aproximan la solución de problemas de cuarto orden, gobernados por ecuaciones diferenciales parciales. Por ejemplo, los métodos conformes más comúnmente utilizados son: los elementos finitos de Argyris (los cuales necesitan 21 grados de libertad por triángulo), los elementos finitos de Bell (estos necesitan 18 grados de libertad por triángulo), los elementos finitos de Bogner-Fox-Schmit (que necesitan 16 grados de libertad por rectángulo), y los elementos finitos Hsieh-Clough-Tocher (los cuales no son fáciles de implementar). Estos métodos permiten definir elementos de clase C^1 (en mallas de triángulos y rectángulos), que naturalmente se requieren para aproximar las soluciones de ecuaciones diferenciales parciales de cuarto orden en dos dimensiones. Para construir los elementos de clase C^1, se requiere la continuidad de la derivada parcial de primer orden a través de elementos finitos adyacentes. Sin embargo, para relajar este requisito de continuidad y para resolver los problemas de cuarto orden, se han introducido algunos métodos en la literatura. Los elementos finitos de Morley y los métodos mixtos como el método Ciarlet-Raviart son bien conocidos entre ellos.

En esta tesis doctoral, estamos interesados en analizar, aplicar e implementar métodos de elementos virtuales C^1 en mallas poligonales generales para resolver diversos problemas de cuarto orden

(modelados por ecuaciones diferenciales parciales) que surgen en la mecánica de sólidos.

Método de elementos virtuales

El *Métodos de Elementos Virtuales* (VEM) se introdujo en [12] como una generalización del método de elementos finitos, con la capacidad de usar mallas poligonales/polihédricas generales, incluyendo "nodos colgantes" y elementos no convexos. El VEM se ha desarrollado en muchos aspectos y se ha aplicado con éxito a una amplia gama de problemas. De hecho, desde el nacimiento del VEM en 2012 se puede apreciar un crecimiento evidente del interés científico por los Métodos de los Elementos Virtuales. Por ejemplo, al realizar una búsqueda simple en una base de datos bibliográfica en línea (por ejemplo, Mathscinet) relacionada con papers acerca del VEM, encontramos: 4 artículos en 2013, 7 artículos en 2014, 7 artículos en 2015, 16 trabajos publicados en 2016, 30 artículos en 2017, 41 artículos en 2018 y 31 durante 2019. Mencionamos algunos de ellos: en problemas de elasticidad lineal encontramos [8, 9, 15, 44, 77], métodos de elementos virtuales aplicados a el problema de Stokes en [6, 23, 42, 54, 61, 94], y para las ecuaciones de Navier-Stokes [24, 80, 93]. Los métodos de elementos virtuales aplicados a los problemas de placas se pueden encontrar en [27, 41, 63, 64, 127, 128], en particular los aplicados a problemas de valores propios en [28, 79, 103, 122]. Análisis de error a posteriori se han desarrollado en [26, 31, 53, 62, 104], etc.

Según [2, 12] la idea principal de VEM se puede resumir de la siguiente manera:

- Los espacios locales discretos se construyen de modo que las funciones "test" y "trial" contengan el conjunto de polinomios de grado $\leq k$ (cuyo grado determina la precisión del método), y otras funciones, que no son polinomios y cuyos valores exactos en el interior del polígono/poliedro no se conoce (de ahí, se denomina "virtual").

- Los grados de libertad deben elegirse cuidadosamente para que las formas discretas (lineales, bilineales, trilineales, etc.) puedan calcularse exactamente, siempre que tomemos a un polinomio de grado $\leq k$ como una función "trial", y usando sólo los grados de libertad de la función "test".

Dado que las soluciones calculadas están representadas por los grados de libertad, las propiedades descritas en los dos items anteriores, implican que la solución no se conoce explícitamente como una función virtual, a menos que una de las dos entradas sea un polinomio global de grado $\leq k$. En otras palabras, estas propiedades aseguran el **patch test** utilizada por los ingenieros, es decir, si la solución verdadera es un polinomio global de grado $\leq k$, entonces la solución discreta y exacta coincidirán [41].

Un resultado importante y muy usado del VEM se estableció en [2]. Los autores muestran una variante del método del elemento virtual presentado en [12] para calcular, directamente desde los grados de libertad, las proyecciones L^2 sobre todos los polinomios de grado $\leq k$. La razón de este resultado se debe al hecho de que en muchas aplicaciones es conveniente conocer explícitamente el proyector local Π_K^∇ y el proyector L^2 ortogonal local Π_k^0 sobre los polinomios de grado $\leq k$. De [12] se sabe que el proyector Π_k^0 está disponible solo en polinomios de grado $\leq k-2$ (directamente de los grados de libertad). Los autores en [2] demostraron que en un cierto número de casos, simplemente cambiando ligeramente la definición de las funciones locales no polinomiales (que, en cualquier caso, nunca se calculan), es posible obtener un espacio en el que el operador Π_k^0 se puede calcular fácilmente

utilizando Π_k^{∇} y los grados de libertad locales. Este resultado también se ha utilizado para elementos virtuales de clase C^1, podemos mencionar los trabajos [7, 27, 64].

Por otro lado, existen algunos artículos relacionados con la implementación del método de elementos virtuales, por ejemplo, [16, 18, 117]. Podemos decir que [16] es el primer artículo de implementación para VEM, que detalla meticulosamente cómo calcular las formas lineales y bilineales discretas utilizadas para aproximar las soluciones del problema de Poisson en dos y tres dimensiones. Los autores primero presentan los pasos a seguir para calcular (solo utilizando los grados de libertad) las matrices locales obtenidas de las formas lineales y bilineales que discretizan el problema de Poisson en 2D. Además, también se presentan la implementación de los términos de estabilización de los métodos. Posteriormente, extienden los pasos de implementación para el problema de Poisson en 3D. Por otra parte, en [18] se presenta una guía de implementación del VEM para ecuaciones elípticas bidimensionales, en forma primal y mixta con coeficientes variables. Los autores muestran una alternativa a la presentada en [16] para implementar las formas bilineales discretas que aproximan el producto interno en H^1. Además, también se presentan los detalles de implementación para las formas discretas definidas en el espacio virtual conforme de $H(div)$ (introducido en [17]). Una implementación en MATLAB de 50 líneas del método de elemento virtual de orden más bajo para el problema de Poisson bidimensional se analiza y se presenta en [117]. El autor aproxima la solución utilizando la discretización virtual presentada en [12] e incluye las líneas del código en su artículo.

Hasta ahora, el VEM se ha extendido con éxito a diferentes problemas aplicados que surgen en la mecánica de fluidos y sólidos, incluidos aquellos que requieren continuidad de las derivadas de orden superior. En particular, para resolver problemas de cuarto orden, utilizando métodos conformes de H^2.

Por lo tanto, de acuerdo con el objetivo principal de esta tesis doctoral, a continuación describiremos brevemente algunas contribuciones que se han introducido en la literatura VEM para resolver problemas de cuarto orden (por ejemplo, [7, 41, 64]) por medio de C^1-VEM.

C^1-Virtual element method

El primer C^1-VEM (en dos dimensiones) se introdujo en [41] para resolver el problema de flexión de una placa descrito con las ecuaciones de Kirchhoff-Love, es decir,

$$D\Delta^2 u = f \quad \text{in } \Omega,$$

donde Ω es un dominio poligonal convexo y acotado, $D = \frac{Et^3}{12(1-\nu^2)}$ es la rigidez a la flexión, t el grosor, E el módulo de Young, y ν el radio de Poisson. La formulación débil del problema anterior está dada por: dado $f \in L^2(\Omega)$, hallar $u \in H_0^2(\Omega)$ such that

$$a(u,v) := D\Big((1-\nu)\int_\Omega D^2u : D^2v + \nu\int_\Omega \Delta u \Delta v\Big) = \int_\Omega fv \quad \forall v \in H_0^2(\Omega).$$

La idea básica considerada por los autores se puede resumir de la siguiente manera: primero, proponer algunos grados de libertad en la frontera entre los elementos para identificar de manera única las trazas de funciones globalmente C^1, cuya restricción en cada lado e de un polígono K es un polinomio de grado $\leq r$, y con derivada normal de grado $\leq s$ en cada lado e del polígono.

Posteriormente, se debe agregar una cantidad adecuada de los grados de libertad internos. Además, para cada polígono K, el subespacio discreto en K se define por medio de un problema local de flexión de placas.

Por lo tanto, si el subespacio discreto se construye con los pasos anteriores, las siguientes propiedades se mantienen:

- En cada polígono K, los espacios locales están diseñados para contener polinomios de grado $\leq k$, donde k depende de r y s.
- En cada polígono K, la forma bilineal $a(\cdot,\cdot)$ se puede calcular exactamente cada vez que tomamos como función " trial " de entrada a un polinomio de grado $\leq k$, y usando solo los grados de libertad de la función test (y no el hecho de que la función " trial " resuelva un problema de placa local).
- Para obtener estabilidad, la forma bilineal $a(\cdot,\cdot)$ se puede calcular exactamente, incluso cuando ambas entradas no son necesariamente polinomios.

Como consecuencia de las propiedades anteriores, se garantiza el **patch test**. Además, al considerar supuestos adicionales en la malla, en el espacio discreto y en la forma bilineal $a(\cdot,\cdot)$ (propiedades de estabilidad y consistencia), los autores construyen una familia de elementos de C^1 en [41], que depende de tres índices enteros (r,s,m), relacionados con el grado de precisión $k \geq 2$ por:

$$r = \max\{k,3\}, \quad s = k-1 \quad \text{and} \quad m = k-4.$$

Más precisamente, el espacio local virtual V_h^K y los grados de libertad introducidos en [41] vienen dados por:

(i) La evaluación de las funciones virtuales en cada vértice del polígono;

(ii) La evaluación de las derivadas parciales de las funciones virtuales en cada vértice del polígono;

(iii) Para $r > 3$ los momentos $\displaystyle\int_e qv$, para todos los polinomios de q definidos en e y de grado $\leq r-4$;

(iv) Para $s > 1$, los momentos $\displaystyle\int_e q\partial_n v$, para todos los polinomios de q definidos en e y de grado $\leq s-2$;

(v) Para $m \geq 0$, los momentos $\displaystyle\int_K qv$, para todos los polinomios de q definidos en K y de grado $\leq m$;

y

$$V_h^K := \{v \in H^2(K) : \Delta^2 v \in \mathbb{P}_m(K), \quad v|_e \in \mathbb{P}_r(e), \quad \partial_n v|_e \in \mathbb{P}_s(e) \quad \forall e \in \partial K\},$$

donde, $\mathbb{P}_m(K), \mathbb{P}_r(e)$ y $\mathbb{P}_s(e)$ denota el conjunto de polinomios de grado menor que m, r y s, respectivamente, y $\partial_n v|_e$ denota la derivada normal de v sobre e. Un hecho importante es que (v) permite calcular exactamente el proyector estándar L^2 en el conjunto de polinomios de grado $\leq k-4$.

Además, los autores de [41] prueban algunos ejemplos particulares de esta familia de elementos virtuales, convergencia óptima y estimaciones de error en la seminorma de energía de H^2.

Más adelante, en [64] se introducen las estimaciones de convergencia y error óptimo en L^2 y en H^1, a través de los argumentos de dualidad clásica. Basados en los argumentos presentados en [2], los autores de [64] modifican los subespacios discretos definidos en [41]. Como consecuencia, esta modificación permite calcular exactamente el proyector ortogonal L^2 en el conjunto de polinomios de grado $\leq k-2$. El problema modelo considerado en [64] es el mismo que se considera en [41].

Otra contribución importante relacionada con C^1-VEM son los elementos virtuales de orden más bajo ($k=2$) desarrollados en [7] para la aproximación de la ecuación de Cahn-Hilliard. Basados en los argumentos presentados en [2], los autores obtienen un espacio particular de la familia C^1-VEM establecido en [41]. La diferencia entre los elementos obtenidos en [7] y los obtenidos en [41, 64], es que la proyección ortogonal L^2 sobre los polinomios de grado $k=2$ se puede calcular exactamente, a partir de los grados de libertad.

Además, es importante mencionar que, recientemente en [19] se desarrollan métodos de elementos virtuales C^1 para problemas tridimensionales de cuarto orden.

De acuerdo con la descripción anterior, el objetivo principal de esta tesis doctoral es, analizar, aplicar e implementar varios métodos de elementos virtuales C^1 (en dos dimensiones) sobre mallas poligonales generales, para resolver problemas de cuarto orden (modelados por ecuaciones diferenciales parciales) que surgen en la mecánica de sólidos. Más precisamente, estamos interesados en resolver los problemas de vibración y pandeo de las placas Kirchhoff, el problema de flexión de placas von Kármán y el problema de valores propios de transmisión.

Ahora, resumiremos el contenido de nuestro estudio.

Problema de vibración de las placas Kirchhoff

El problema de vibración de las placas Kirchhoff, es un problema de ecuaciones diferenciales parciales de cuarto orden que modela el desplazamiento transversal de la superficie media de una placa delgada, y un parámetro que representa las frecuencias de vibración de la placa. La principal característica de este modelo, es que los desplazamientos de la superficie media son verticales y rectos con respecto a la superficie media deformada incluso después de la deformación. El estudio del problema de vibración de placas Kirchhoff aparece en interesantes aplicaciones de ingeniería aeroespacial, marina y estructural, ya que es importante para el diseño de diferentes estructuras sólidas.

Con el fin de aproximar los valores propios y los modos de vibración (también llamados funciones propias), se requieren C^1-elementos. Sin embargo, para relajar dicha continuidad, varios métodos de elementos finitos como híbridos, no conformes y mixtos, se han desarrollado en las últimas décadas. Por ejemplo, en [57] se introdujo un método híbrido de elementos finitos para aproximar las frecuencias de vibración de una placa empotrada. En [90], se analizaron métodos de elementos finitos de Morley semi-discretos y totalmente discretos, para resolver el problema de la vibración de Kirchhoff. En [36] se analizó un método C^0-IPG para resolver el problema de valores propios biharmónico con tres tipos de condiciones de contorno. Luego, los autores de [106] propusieron y analizaron un método de elementos

finitos lineales a trozos, para aproximar los valores propios y las funciones propias de los problemas de vibración y pandeo de una placa delgada modelada con las ecuaciones de Kirchhoff-Love. Por otro lado, el método mixto más conocido (llamado método Ciarlet-Raviart) para resolver el problema biharmónico, fue introducido por Ciarlet y Raviart en [69]. En particular, este método se ha estudiado para resolver el problema de la vibración de Kirchhoff (ver [56, 99]). Con respecto a los elementos C^1, es bien sabido que los elementos finitos estándar empleados para resolver el problema del modelo de este capítulo, son los elementos finitos de Argyris y Bell. Sin embargo, estos elementos necesitan muchos grados de libertad (por ejemplo, los elementos finitos de Argyris y los de Bell necesitan 21 y 18 grados de libertad en un triángulo), ya que de lo contrario son difíciles de implementar (por ejemplo, Hsieh-Clough, para ver más detalles refiérase a [67, Capítulo 6].

Es bien conocido que los métodos de elementos finitos en dos dimensiones se definen sobre mallas triangulares o de cuadriláteros. Sin embargo, en simulaciones complejas puede ser conveniente emplear mallas poligonales. Estamos interesados en estudiar, desarrollar e implementar un método de elementos virtuales C^1 aplicado a mallas poligonales generales (que incluyan elementos no convexos y nodos colgantes) para aproximar el espectro del problema de vibración de las placas Kirchhoff.

Más precisamente, el **Capítulo 1** de la tesis introduce el análisis matemático y numérico del problema de vibración de una placa delgada modelada con las ecuaciones de Kirchhoff. Primero, introducimos una formulación variacional para caracterizar el espectro del problema modelo. A continuación, definimos un operador solución, el cual es compacto, cuyo espectro está relacionado con el de la formulación variacional. Luego, se introduce una discretización de elementos virtuales C^1 basada en los elementos establecidos en [7]. Posteriormente, la teoría presentada en [73, 74] se analiza en este capítulo para obtener estimaciones de convergencia y error de nuestro método, dado que la teoría estándar de aproximación espectral abstracta (ver [11]) no se puede aplicar para analizar este problema. Finalmente, se prueba un conjunto de ejemplos numéricos que verifican el desempeño del método.

El contenido de este capítulo dio origen al siguiente artículo:

- D. Mora, G. Rivera and I. Velásquez: *A virtual element method for the vibration problem of Kirchhoff plates*, ESAIM Math. Model. Numer. Anal., **52**, (2018), pp. 1437–1456.

Problema de pandeo de las placas de Kirchhoff

El problema de pandeo de las placas Kirchhoff, es un problema de autovalores modelado por una ecuación diferencial parcial de cuarto orden, la cual describe el desplazamiento transversal de la superficie media de la placa cuando se somete a fuerzas horizontales a través de un campo tensorial de esfuerzo plano. En este problema, el valor propio más pequeño corresponde a la carga crítica cuando se produce el pandeo. Una de las dificultades de este modelo, es aproximar los valores propios y los modos de pandeo cuando se supone que el campo tensorial de esfuerzo no es necesariamente definido positivo. Además, como el problema de pandeo se rige por ecuaciones diferenciales parciales de cuarto orden, los métodos conformes requieren directamente elementos finitos de clase C^1 [67, Chapter 6].

Este problema ha atraído un gran interés por parte de los científicos e ingenieros durante mucho

tiempo, debido a su amplio uso en aplicaciones de ingeniería, tales como el diseño de puentes, barcos, automóviles y aeronaves.

Existen numerosas publicaciones en la literatura de ingeniería, sobre los diversos elementos finitos que se pueden aplicar para resolver el problema de pandeo de las placas de Kirchhoff. Dado que los métodos de elementos finitos conformes de H^2 necesitan muchos grados de libertad, ó no tienen una implementación fácil (ver [67, Capítulo 6]), varias alternativas, como métodos de elementos finitos, C^0, mixtos e híbridos se han estudiado para aproximar los valores propios y las autofunciones del problema de pandeo. Por ejemplo, en [106] se analizó una formulación mixta para aproximar el espectro del problema de pandeo. Los autores emplearon el método de elementos finitos C^0 introducido en [3] para resolver los momentos de flexión de las planchas de Kirchhoff-Love. En [100] se propuso y se analizó una formulación mixta, la cual se basó en la idea presentada por Ciarlet y Raviart [69]. Los autores de [100] aproximaron los valores propios más bajos de una placa simplemente apoyada y modelada con las ecuaciones de Kirchhoff, además, derivaron estimaciones del error con un orden óptimo para las autofunciones, y un orden doble para los valores propios. Recientemente, un método de C^0-IPG, que considera tres tipos de condiciones de contorno, a saber, placa empotrada, placa simplemente soportada y condiciones de tipo Cahn-Hilliard se ha introducido en [36]. En particular, los autores demostraron resultados de convergencia y estimaciones de error óptimas asociadas a los valores propios y funciones propias aproximadas.

En esta parte de la tesis, estamos interesados en proponer y analizar un método de elementos virtuales C^1 para aproximar los valores propios y autofunciones del problema de pandeo de las placas de Kirchhoff.

El **Capítulo 2** de la tesis propone y analiza una discretización de elementos virtuales C^1, para resolver el problema de pandeo de las placas Kirchhoff. Primero, asumiendo que el campo tensorial de esfuerzo es simétrico y de divergencia libre, llegamos a una caracterización espectral del problema del modelo. Esto se hace introduciendo un operador solución (que resulta ser compacto), definido a partir del problema fuente asociado (ecuación biharmónica). A continuación, se propone un esquema discreto basado en los elementos virtuales C^1 introducidos en [64]. Posteriormente, para obtener convergencia y estimaciones de error óptimas, y se aplica la conocida teoría espectral para operadores compactos [11]. Al final del capítulo se reportan varias pruebas numéricas con diferentes tipos de condiciones de contorno, las cuales confirman que las tasas de convergencia experimental coinciden con el análisis teórico desarrollado.

Los resultados contenidos en este capítulo se encuentran en la siguiente pre-publicación:

- D. Mora and I. Velásquez: *Virtual element for the buckling problem of Kirchhoff-Love plates.* Preprint 2019-16, Centro de Investigación en Ingeniería Matemática (CI^{2}MA), Universidad de Concepción Chile, (2019).

Las ecuaciones de von Kármán

Los primeros dos capítulos de esta tesis, tratan sobre los problemas de vibración y pandeo de una placa delgada modelada por las ecuaciones de Kirchhoff. En este capítulo estudiaremos un sistema

no lineal de ecuaciones diferenciales parciales que modelan una placa muy delgada, conocida como las ecuaciones de von Kármán [65]. Este modelo es un sistema no lineal de ecuaciones diferenciales de cuarto orden, que describe dos incógnitas, a saber, el desplazamiento de la superficie media de la placa y los esfuerzos de la frontera de la placa. La principal diferencia entre los modelos von Kármán y Kirchhoff es la linealización del tensor de esfuerzo, que de hecho, conduce a la no linealidad en el modelo de von Kármán [68, Capítulo 1].

Este modelo fue introducido en 1910 por von Kármán [123], para describir las grandes deformaciones de las placas elásticas muy delgadas. Debido a sus aplicaciones en el diseño de ingeniería, este problema se ha estudiado en una gran cantidad de artículos en esta área [37, 40, 59, 92, 95, 96, 101]. Las ecuaciones de von Kármán también se han analizado para ser aplicadas en biología [109]. Debido a la no linealidad y la incógnita adicional (los esfuerzos de frontera) de este modelo de placa, este problema resulta atractivo de resolver. Además, se necesitan elementos C^1 para obtener aproximaciones conformes de las soluciones.

Las ecuaciones de von Kármán no tienen una solución única. Sin embargo, en [40] se han dado las condiciones suficientes para aproximar las soluciones aisladas de este problema. Por lo tanto, el propósito de esta parte de la tesis, es proponer y analizar un método de elementos virtuales para aproximar las soluciones aisladas de las placas de von Kármán.

En el **Capítulo 3**, introducimos las ecuaciones canónicas de von Kármán. Luego, al introducir un nuevo parámetro que depende de las fuerzas laterales de la placa y que permite relacionar el modelo von Kármán con el problema de pandeo de la placa Kirchhoff, llegamos a un sistema de ecuaciones equivalente. Usando el resultado de existencia de las soluciones aisladas presentadas en [65] y asumiendo el resultado de condiciones suficientes (para aproximar las soluciones aisladas) establecido en [40], se introduce una formulación variacional continua bien planteada. Usamos los elementos virtuales C^1 propuestos en [7]. En particular, se define una forma trilinear discreta a partir de funciones virtuales de clase C^1. Luego, con el objetivo de garantizar el buen planteamiento del problema discreto, usamos la teoría general establecida en [40], la cual permite aproximar las soluciones aisladas de una placa modelada por las ecuaciones de von Kármán, usando argumentos de punto fijo. Como consecuencia, obtenemos resultados de convergencia y de estimaciones del error de orden óptimas para las soluciones aisladas. Al final de este capítulo se informan varias pruebas numéricas que confirman el análisis teórico desarrollado.

Los resultados contenidos en este capítulo se encuentran en la siguiente pre-publicación:

- C. Lovadina D. Mora and I. Velásquez: *A virtual element method for the von Kármán equations.* Preprint 2019-36, Centro de Investigación en Ingeniería Matemática (CI^{2}MA), Universidad de Concepción Chile, (2019).

Problema de valores propios de transmisión

El modelo de valores propios de transmisión, es un problema no autoadjunto y no elíptico, que surge del estudio del problema de dispersión inversa de medios no homogéneos, el cual se modela por un sistema de ecuaciones diferenciales parciales de segundo orden [71]. Sin embargo, se puede reescribir

como un sistema de ecuaciones diferenciales parciales de cuarto orden [46, 49]. Esta alternativa resulta en un problema de autovalores no lineal (ya que se reescribe como un problema de valores propios cuadrático) y no autoadjunto [49, 60]. Este problema juega un papel importante en la singularidad y reconstrucción en la teoría de dispersión inversa [47, 71]. Este modelo matemático resulta ser un problema espectral desafiante, puesto que, no es trivial desarrollar métodos numéricos efectivos para aproximar los valores propios y las funciones propias de este tipo de problemas no autoadjuntos.

El problema de valores propios de transmission ha sido estudiado en los últimos años, desde el punto de vista matemático y numérico. Por ejemplo, los autores de [72] analizaron y propusieron el primer tratamiento numérico del problema de valores propios de transmisión. Introdujeron tres métodos de elementos finitos para aproximar los valores propios de este problema. Más adelante, en [49] se usan los métodos de los elementos finitos de Argyris, para presentar resultados óptimos de convergencia y estimaciones de error de los valores propios de transmisión. Además, en [60] se estudia un método de elementos finitos C^0, para aproximar los valores propios de transmisión, usando un operador de recuperación de gradiente.

Dado que el problema de valores propios de transmisión está escrito por un sistema de valores propios cuadrático de cuarto orden, en esta parte de la tesis, linealizamos el problema introduciendo una nueva incógnita (ver por ejemplo [49, 50, 115]) en H_0^1 como la solución única del problema de Laplace con condiciones de contorno homogéneas de Dirichlet. De acuerdo con lo anterior y con el fin de explotar la capacidad de implementación fácil del método del elemento virtual para construir espacios discretos con alta regularidad, en el **Capítulo 4** proponemos, analizamos y aplicamos un $(C^1 \times C^0)$-VEM para resolver el problema del valores propios de transmisión.

Más precisamente, en este capítulo nos centramos en analizar un $(C^1 \times C^0)$-VEM para resolver un problema espectral no autoadjunto derivado del problema de autovalores de transmisión de cuarto orden. Con este objetivo, primero se define un operador solución (que resulta ser compacto), el cual caracteriza el espectro del problema. A continuación, se analiza una discretización de elemento virtual conforme de $H_0^2 \times H_0^1$ basada en los elementos virtuales introducidos en [7] y [2]. Usando la teoría de la aproximación para operadores compactos no autoadjuntos [11], se derivan las estimaciones del error y los órdenes óptimas de convergencia. Además, dado que el problema no es autoadjunto, se consideran los problemas adjuntos de los problemas de valores propios continuos y discretos. También se demuestra el orden óptimo de convergencia para los valores propios y las funciones propias de los problemas adjuntos. Al final del capítulo se presentan resultados numéricos, los cuales confirman los resultados teóricos.

Los resultados contenidos en este capítulo se encuentran en el siguiente artículo:

- D. Mora and I. Velásquez: *A virtual element method for the transmission eigenvalue problem*, Math. Models Methods Appl. Sci., **28**, (2018), pp. 2803–2831.

CHAPTER 1

A virtual element method for the vibration problem of Kirchhoff plates

1.1 Introduction

The *Virtual Element Method* (VEM), introduced in [12, 16], is a recent generalization of the Finite Element Method which is characterized by the capability of dealing with very general polygonal/polyhedral meshes. The interest in numerical methods that can make use of general polytopal meshes has recently undergone a significant growth in the mathematical and engineering literature; among the large number of papers on this subject, we cite as a minimal sample [12, 52, 75, 114, 118].

Indeed, polytopal meshes can be very useful for a wide range of reasons, including meshing of the domain (such as cracks) and data (such as inclusions) features, automatic use of hanging nodes, use of moving meshes, adaptivity. Moreover, the VEM presents the advantage to easily implement highly regular discrete spaces. Indeed, by avoiding the explicit construction of the local basis functions, the VEM can easily handle general polygons/polyhedrons without complex integrations on the element (see [16] for details on the coding aspects of the method). The VEM has recently been applied successfully to a wide range of problems, see for instance [2, 21, 25, 42, 55, 64, 77, 79, 103, 111, 125].

The numerical approximation of eigenvalue problems for partial differential equations encountered in engineering applications is the object of great interest, from both the practical and theoretical points of view. We refer to [33, 34] and the references therein for the state of the art in this subject area. In particular, this chapter focuses on the so called thin plate vibration problem, which involves the biharmonic operator. Among the existing techniques to solve this problem, various finite element methods have been introduced and analyzed. In particular, we mention nonconforming methods and different mixed formulations for the Kirchhoff model, see for instance [11, 56, 99, 106, 113]. More recently, in [36] a discontinuous Galerkin method has been proposed and analyzed for the vibration and buckling problems of thin plates. On the other hand, the construction of conforming finite elements for $H^2(\Omega)$ is difficult in general, since they usually involve a large number of degrees of freedom (see [67]).

Recently, thanks to the flexibility of VEM, it has been showed in [25, 41] that virtual elements can be used to build global discrete spaces of arbitrary regularity that are simple in terms of degrees

of freedom and coding aspects (see also [7, 27]). Thus, in the present contribution, we follow a similar approach in order to solve an eigenvalue problem modelling the two-dimensional plate vibration problem considering a conforming C^1 discrete formulation.

The aim of this paper is to introduce and analyze a C^1-VEM which applies to general polygonal meshes, made by possibly non-convex elements, for the two-dimensional plate vibration problem. We begin with a variational formulation of the spectral problem relying only on the transverse displacement of the plate. Then, we exploit the capability of VEM to build highly regular discrete spaces and propose a conforming $H^2(\Omega)$ discrete formulation. In particular, we consider the discrete virtual space introduced in [7] to solve the Cahn-Hilliard equation, which is a modification of the C^1 virtual elements in [25, 41]. More precisely, the functions of the discrete space will have continuous values and continuous gradients across edges. Therefore, it will be contained in $H^2(\Omega)$ and yields a conforming solution. The resulting discrete bilinear form is continuous and elliptic. This method makes use of a very simple set of degrees of freedom, namely 3 degrees of freedom per vertex of the mesh. By using the abstract spectral approximation theory (see [73, 74]), under rather mild assumptions on the polygonal meshes, we establish that the resulting scheme provides a correct approximation of the spectrum and prove optimal order error estimates for the eigenfunctions and a double order for the eigenvalues. We remark that the present method is new on triangular meshes for the discretization of fourth order eigenvalue problems and this case it employs $3N_v$ degrees of freedom, where N_v denotes the number of vertices, which represents a significant proxy for the computational cost, thus it provides a very competitive alternative in comparison to other classical techniques based on finite elements.

The outline of this article is as follows: In Section 1.2, we introduce the variational formulation of the vibration eigenvalue problem, define a solution operator and establish its spectral characterization. In Section 1.3, we introduce the virtual element discrete formulation, describe the spectrum of a discrete solution operator and prove some auxiliary results. In Section 1.4, we prove that the numerical scheme provides a correct spectral approximation and establish optimal order error estimates for the eigenvalues and eigenfunctions. Finally, several numerical tests that allow us to assess the convergence properties of the method, to confirm that it is not polluted with spurious modes and to check whether the experimental rates of convergence agree with the theoretical ones are reported in Section 1.5.

Throughout the article we will use standard notations for Sobolev spaces, norms and seminorms. Moreover, we will denote by C a generic constant independent of the mesh parameter h, which may take different values in different occurrences.

Finally, given a linear bounded operator $T : X \to X$, defined on a Hilbert space X, we denote its spectrum by $\mathrm{sp}(T) := \{z \in \mathbb{C} : (zI - T) \text{ is not invertible}\}$ and by $\rho(T) := \mathbb{C} \setminus \mathrm{sp}(T)$ the resolvent set of T. Moreover, for any $z \in \rho(T)$, $R_z(T) := (zI - T)^{-1} : X \to X$ denotes the resolvent operator of T corresponding to z.

1.2 The spectral problem

Let $\Omega \subset \mathbb{R}^2$ be a polygonal bounded domain corresponding to the mean surface of a plate in its reference configuration, clamped on its whole boundary Γ. The plate is assumed to be homogeneous, isotropic, linearly elastic, and sufficiently thin as to be modeled by Kirchhoff-Love equations. We

denote by w the transverse displacement of the mean surface of the plate.

The plate vibration problem reads as follows:

Find $(\lambda, w) \in \mathbb{R} \times H^2(\Omega)$, $w \neq 0$, such that

$$\begin{cases} \Delta^2 w = \lambda w & \text{in } \Omega, \\ w = \partial_n w = 0 & \text{on } \Gamma, \end{cases} \tag{1.2.1}$$

where $\lambda = \omega^2$, with $\omega > 0$ being the vibration frequency, and ∂_n denotes the normal derivative. To simplify the notation we have taken the Young modulus and the density of the plate, both equal to 1.

To obtain a weak formulation of the spectral problem (1.2.1), we multiply the corresponding equation by $v \in H_0^2(\Omega)$ and integrate twice by parts in Ω. Thus, we obtain:

Find $(\lambda, w) \in \mathbb{R} \times H_0^2(\Omega)$, $w \neq 0$, such that

$$a(w, v) = \lambda b(w, v) \qquad \forall v \in H_0^2(\Omega), \tag{1.2.2}$$

in (1.2.2) the bilinear forms are defined for any $w, v \in H_0^2(\Omega)$ by

$$a(w, v) := \int_\Omega D^2 w : D^2 v,$$
$$b(w, v) := \int_\Omega wv,$$

with " : " denotes the usual scalar product of 2×2-matrices, $D^2 v := (\partial_{ij} v)_{1 \leq i,j \leq 2}$ denotes the Hessian matrix of v. We note that those are bounded bilinear symmetric forms. Moreover, it is immediate to prove that the eigenvalues of the problem above are real and positive.

Next, we define the solution operator associated with the variational eigenvalue problem (1.2.2):

$$\begin{aligned} T : \ H_0^2(\Omega) &\longrightarrow H_0^2(\Omega), \\ f &\longmapsto Tf := u, \end{aligned}$$

where $u \in H_0^2(\Omega)$ is the solution of the corresponding source problem:

$$a(u, v) = b(f, v) \qquad \forall v \in H_0^2(\Omega). \tag{1.2.3}$$

The following lemma allows us to establish the well-posedness of this source problem.

Lemma 1.2.1. *There exists a constant $\alpha_0 > 0$, depending on Ω, such that*

$$a(v, v) \geq \alpha_0 \|v\|_{2,\Omega}^2 \qquad \forall v \in H_0^2(\Omega).$$

Proof. The result follows immediately from the fact that $\|D^2 v\|_{0,\Omega}$ is a norm on $H_0^2(\Omega)$, equivalent with the usual norm. □

We deduce from Lemma 1.2.1 that the linear operator T is well defined and bounded. Notice that $(\lambda, w) \in \mathbb{R} \times H_0^2(\Omega)$ solves problem (1.2.2) (and hence problem (1.2.1)) if and only if $Tw = \mu w$ with

$\mu \neq 0$ and $w \neq 0$, in which case $\mu := \frac{1}{\lambda}$. Moreover, it is easy to check that T is self-adjoint with respect to the $a(\cdot,\cdot)$ inner product. Indeed, given $f, g \in H_0^2(\Omega)$,

$$a(Tf, g) = b(f, g) = b(g, f) = a(Tg, f) = a(f, Tg).$$

The following is an additional regularity result for the solution of problem (1.2.3) and consequently, for the eigenfunctions of T.

Lemma 1.2.2. *There exist $s \in (\frac{1}{2}, 1]$ and $C > 0$ such that, for all $f \in L^2(\Omega)$, the solution u of problem (1.2.3) satisfies $u \in H^{2+s}(\Omega)$ and*

$$\|u\|_{2+s,\Omega} \leq C\|f\|_{0,\Omega}.$$

Proof. The proof follows from the classical regularity result for the biharmonic problem with its right-hand side in $L^2(\Omega)$ (cf. [85]). □

The constant s, in the lemma given above, is the Sobolev regularity for the biharmonic equation with homogeneous Dirichlet boundary conditions. This constant only depends on the domain Ω. If Ω is convex, then $s = 1$. Otherwise, the lemma holds for all $s < s_0$, where $s_0 \in (\frac{1}{2}, 1)$ depends on the largest reentrant angle of Ω (see [85] for the precise equation determining s_0). Hence, because of the compact inclusion $H^{2+s}(\Omega) \hookrightarrow H_0^2(\Omega)$, T is a compact operator. Therefore, we have the following spectral characterization result.

Lemma 1.2.3. *The spectrum of T satisfies $\mathrm{sp}(T) = \{0\} \cup \{\mu_k\}_{k\in\mathbb{N}}$, where $\{\mu_k\}_{k\in\mathbb{N}}$ is a sequence of real positive eigenvalues which converges to 0. The multiplicity of each eigenvalue is finite.*

1.3 Spectral approximation

In this section, first we recall the mesh construction and the assumptions considered to introduce the discrete virtual element spaces. Then, we will introduce a virtual element discretization of the eigenvalue problem (1.2.2) and provide a spectral characterization of the resulting discrete eigenvalue problem.

Let $\{\mathcal{T}_h\}_h$ be a sequence of decompositions of Ω into polygons K. Let h_K denote the diameter of the element K and h the maximum of the diameters of all the elements of the mesh, i.e., $h := \max_{K\in\mathcal{T}_h} h_K$. In what follows, we denote by N_K the number of vertices of K, by e a generic edge of $\mathcal{T}_h$ and for all $e \in \partial K$, we define a unit normal vector $\boldsymbol{n}_K^e$ that points outside of K.

For the analysis, we will make the following assumptions as in [12, 27]: there exists a positive real number $C_{\mathcal{T}}$ such that, for every h and every $K \in \mathcal{T}_h$,

A1: the ratio between the shortest edge and the diameter h_K of K is larger than $C_{\mathcal{T}}$;

A2: $K \in \mathcal{T}_h$ is star-shaped with respect to every point of a ball of radius $C_{\mathcal{T}} h_K$.

For any subset $S \subseteq \mathbb{R}^2$ and nonnegative integer k, we indicate by $\mathbb{P}_k(S)$ the space of polynomials of degree up to k defined on S.

Now, we consider a simple polygon K (meaning open simply connected set whose boundary is a non-intersecting line made of a finite number of straight line segments) and we define the following finite-dimensional space

$$V_h^K := \big\{ v_h \in H^2(K) : \Delta^2 v_h \in \mathbb{P}_2(K), v_h|_{\partial K} \in C^0(\partial K), v_h|_e \in \mathbb{P}_3(e) \ \forall e \in \partial K, \\ \nabla v_h|_{\partial K} \in C^0(\partial K)^2, \partial_n v_h|_e \in \mathbb{P}_1(e) \ \forall e \in \partial K \big\}.$$

We observe that any $v_h \in V_h^K$ satisfies the following conditions:

- the trace (and the trace of the gradient) on the boundary of K is continuous;
- $\mathbb{P}_2(K) \subseteq V_h^K$.

We now introduce two sets $\mathbf{D_1}$ and $\mathbf{D_2}$ of linear operators from V_h^K into $\mathbb{R}$. For all $v_h \in V_h^K$, they are defined as follows:

- $\mathbf{D_1}$ contains linear operators evaluating v_h at the N_K vertices of K;
- $\mathbf{D_2}$ contains linear operators evaluating ∇v_h at the N_K vertices of K.

Note that, as a consequence of definition of V_h^K, the output values of the two sets of operators $\mathbf{D_1}$ and $\mathbf{D_2}$ are sufficient to uniquely determine v_h and ∇v_h on the boundary of K.

In order to construct the discrete scheme, we need some preliminary definitions. First, we split the bilinear forms $a(\cdot,\cdot)$ and $b(\cdot,\cdot)$, introduced in the previous section, as follows:

$$a(u,v) = \sum_{K \in \mathcal{T}_h} a_K(u,v), \qquad u,v \in H_0^2(\Omega),$$

$$b(u,v) = \sum_{K \in \mathcal{T}_h} b_K(u,v), \qquad u,v \in H_0^2(\Omega),$$

with

$$a_K(u,v) := \int_K D^2 u : D^2 v, \qquad u,v \in H^2(K),$$

and

$$b_K(u,v) := \int_K uv, \qquad u,v \in H^2(K).$$

Now, we define the projector $\Pi_K^\Delta : V_h^K \longrightarrow \mathbb{P}_2(K) \subseteq V_h^K$ for each $v \in V_h^K$ as the solution of

$$a_K\big(\Pi_K^\Delta v, q\big) = a_K(v,q) \qquad \forall q \in \mathbb{P}_2(K), \tag{1.3.1a}$$

$$((\Pi_K^\Delta v, q))_K = ((v,q))_K \qquad \forall q \in \mathbb{P}_1(K), \tag{1.3.1b}$$

where $((\cdot,\cdot))_K$ is defined as follows:

$$((u,v))_K = \sum_{i=1}^{N_K} u(P_i) v(P_i) \qquad \forall u,v \in C^0(\partial K),$$

where $P_i, 1 \leq i \leq N_K$, are the vertices of K. We note that the bilinear form $a_K(\cdot,\cdot)$ has a non-trivial kernel, given by $\mathbb{P}_1(K)$. Hence, the role of condition (1.3.1b) is to select an element of the kernel of the operator. In order to show that the projector Π_K^Δ is computable, we integrate twice by parts on the right hand side of (1.3.1a) to obtain:

$$a_K\big(\Pi_K^\Delta v, q\big) = \int_{\partial K} (D^2 q \boldsymbol{n}_K^e) \cdot \nabla v_h \qquad \forall q \in \mathbb{P}_2(K). \tag{1.3.2}$$

Thus, from the definition of $((\cdot,\cdot))_K$, we observe that the right hand sides of (1.3.2) and (1.3.1b) are computable only on the basis of the output values of the operators in $\mathbf{D_2}$ and $\mathbf{D_1}$, respectively.

Now, we introduce our local virtual space:

$$W_h^K := \left\{ v_h \in V_h^K : \int_K (\Pi_K^\Delta v_h) q = \int_K v_h q \qquad \forall q \in \mathbb{P}_2(K) \right\}.$$

It is easy to check that $W_h^K \subseteq V_h^K$. Therefore, the operator Π_K^Δ is well defined on W_h^K and computable only on the basis of the output values of the operators in $\mathbf{D_1}$ and $\mathbf{D_2}$.

In [7, Lemma 2.1] has been established that the set of operators $\mathbf{D_1}$ and $\mathbf{D_2}$ constitutes a set of degrees of freedom for the space W_h^K. Moreover, it is easy to check that $\mathbb{P}_2 \subseteq W_h^K$. This will guarantee the good approximation properties for the space.

Additionaly, we have that the $L^2(\Omega)$ projection operator $\Pi_K^0 : W_h^K \to \mathbb{P}_2(K)$ is computable from the set of degrees freedom. In fact, for all $v_h \in W_h^K$, the function $\Pi_K^0 v_h \in \mathbb{P}_2(K)$ is defined by:

$$\int_K (\Pi_K^0 v_h) q = \int_K v_h q \qquad \forall q \in \mathbb{P}_2(K). \tag{1.3.3}$$

Now, due to the particular property appearing in definition of the space W_h^K, the right hand side in (1.3.3) is computable using $\Pi_K^\Delta v_h$, and thus $\Pi_K^0 v_h$ depends only on the values of the degrees of freedom for v_h and ∇v_h. Actually, it is easy to check that on the space W_h^K the projectors $\Pi_K^0 v_h$ and $\Pi_K^\Delta v_h$ are the same operator. In fact:

$$\int_K (\Pi_K^0 v_h) q = \int_K v_h q = \int_K (\Pi_K^\Delta v_h) q \qquad \forall q \in \mathbb{P}_2(K). \tag{1.3.4}$$

In what follows, we keep the notation Π_K^Δ for both operators.

We can now present the global virtual space: for every decomposition $\mathcal{T}_h$ of Ω into simple polygons K, we define

$$W_h := \left\{ v_h \in H_0^2(\Omega) : \ v_h|_K \in W_h^K \right\}.$$

A set of degrees of freedom for W_h is given by all pointwise values of v_h on all vertices of $\mathcal{T}_h$ together with all pointwise values of ∇v_h on all vertices of $\mathcal{T}_h$, excluding the vertices on Γ (where the values vanishes). Thus, the dimension of W_h is three times the number of interior vertices.

On the other hand, let $s_K(\cdot,\cdot)$ and $s_K^0(\cdot,\cdot)$ be any symmetric positive definite bilinear forms to be chosen as to satisfy:

$$c_0 a_K(v_h, v_h) \leq s_K(v_h, v_h) \leq c_1 a_K(v_h, v_h) \quad \forall v_h \in W_h^K \quad \text{with} \quad \Pi_K^\Delta v_h = 0, \tag{1.3.5}$$

$$c_2 b_K(v_h, v_h) \leq s_K^0(v_h, v_h) \leq c_3 b_K(v_h, v_h) \quad \forall v_h \in W_h^K. \tag{1.3.6}$$

We will introduce bilinear forms $s_K(\cdot,\cdot)$ and $s_K^0(\cdot,\cdot)$ satisfying (1.3.5)-(1.3.6) in Section 1.5.

Then, we set

$$a_h(u_h,v_h) := \sum_{K\in\mathcal{T}_h} a_{h,K}(u_h,v_h), \qquad u_h,v_h\in W_h,$$
$$b_h(u_h,v_h) := \sum_{K\in\mathcal{T}_h} b_{h,K}(u_h,v_h), \qquad u_h,v_h\in W_h,$$

where $a_{h,K}(\cdot,\cdot)$ and $b_{h,K}(\cdot,\cdot)$ are the local bilinear forms on $W_h^K\times W_h^K$ defined by

$$a_{h,K}(u_h,v_h) := a_K\big(\Pi_K^\Delta u_h,\Pi_K^\Delta v_h\big) + s_K\big(u_h-\Pi_K^\Delta u_h, v_h-\Pi_K^\Delta v_h\big), \qquad u_h,v_h\in W_h^K, \tag{1.3.7}$$
$$b_{h,K}(u_h,v_h) := b_K\big(\Pi_K^\Delta u_h,\Pi_K^\Delta v_h\big) + s_K^0\big(u_h-\Pi_K^\Delta u_h, v_h-\Pi_K^\Delta v_h\big), \qquad u_h,v_h\in W_h^K. \tag{1.3.8}$$

The construction of the bilinear forms $a_{h,K}(\cdot,\cdot)$ and $b_{h,K}(\cdot,\cdot)$ guarantees the usual consistency and stability properties of VEM, as noted in the proposition below. Since the proof follows standard arguments in the Virtual Element literature (see [7, 12, 22]), it is omitted.

Proposition 1.3.1. *The local bilinear forms $a_{h,K}(\cdot,\cdot)$ and $b_{h,K}(\cdot,\cdot)$ on each element K satisfy*

- *Consistency: for all $h>0$ and for all $K\in\mathcal{T}_h$, we have that*

$$a_{h,K}(p,v_h) = a_K(p,v_h) \qquad \forall p\in\mathbb{P}_2(K), \quad \forall v_h\in W_h^K, \tag{1.3.9}$$
$$b_{h,K}(p,v_h) = b_K(p,v_h) \qquad \forall p\in\mathbb{P}_2(K), \quad \forall v_h\in W_h^K. \tag{1.3.10}$$

- *Stability and boundedness: There exist positive constants $\alpha_i, i=1,2,3,4$, independent of K, such that:*

$$\alpha_1 a_K(v_h,v_h) \le a_{h,K}(v_h,v_h) \le \alpha_2 a_K(v_h,v_h) \qquad \forall v_h\in W_h^K, \tag{1.3.11}$$
$$\alpha_3 b_K(v_h,v_h) \le b_{h,K}(v_h,v_h) \le \alpha_4 b_K(v_h,v_h) \qquad \forall v_h\in W_h^K. \tag{1.3.12}$$

Now, we are in a position to write the virtual element discretization of problem (1.2.2).

Find $(\lambda_h,w_h)\in\mathbb{R}\times W_h$, $w_h\neq 0$, such that

$$a_h(w_h,v_h) = \lambda_h b_h(w_h,v_h) \qquad \forall v_h\in W_h. \tag{1.3.13}$$

We observe that by virtue of (1.3.11), the bilinear form $a_h(\cdot,\cdot)$ is bounded. Moreover, as shown in the following lemma, it is also uniformly elliptic.

Lemma 1.3.1. *There exists a constant $\beta>0$, independent of h, such that*

$$a_h(v_h,v_h) \ge \beta \|v_h\|_{2,\Omega}^2 \qquad \forall v_h\in W_h.$$

Proof. Thanks to (1.3.11) and Lemma 1.2.1, it is easy to check that the above inequality holds with $\beta := \alpha_0 \min\{\alpha_1,1\}$. □

The discrete version of the operator T is given by

$$\begin{aligned} T_h : \ W_h &\longrightarrow W_h, \\ f_h &\longmapsto T_h f_h := u_h, \end{aligned}$$

where $u_h \in W_h$ is the solution of the corresponding discrete source problem

$$a_h(u_h, v_h) = b_h(f_h, v_h) \qquad \forall v_h \in W_h.$$

Because of Lemma 1.3.1, the linear operator T_h is well defined and bounded uniformly with respect to h. Once more, as in the continuous case, $(\lambda_h, w_h) \in \mathbb{R} \times W_h$ solves problem (1.3.13) if and only if $T_h w_h = \mu_h w_h$ with $\mu_h \neq 0$ and $w_h \neq 0$, in which case $\mu_h := \frac{1}{\lambda_h}$. Moreover, T_h is self-adjoint with respect to $a_h(\cdot, \cdot)$. Because of this, it is easy to prove the following spectral characterization.

Theorem 1.3.1. *The spectrum of T_h consists of $M_h := \dim(W_h)$ eigenvalues, repeated according to their respective multiplicities. All of them are real and positive.*

In order to prove that the solutions of the discrete problem (1.3.13) converge to those of the continuous problem (1.2.2), the standard procedure would be to show that T_h converges in norm to T as h goes to zero. However, such a proof does not seem straightforward in our case. In fact, the operator T_h is not well defined for any $f \in H_0^2(\Omega)$, since the definition of bilinear form $b_{h,K}(\cdot, \cdot)$ in (1.3.8) needs the degrees of freedom and in particular the pointwise values of ∇f, but it is for any $f \in W_h$.

To circumvent this drawback, we will resort to the spectral theory from [73] and [74]. In spite of the fact that the main use of this theory is when T is a noncompact operator, it can also be applied to compact operators, and we will show that in our case it works.

With this aim, we first recall the following approximation result which is derived by interpolation between Sobolev spaces (see for instance [84, Theorem I.1.4]) from the analogous result for integer values of s. In its turn, the result for integer values is stated in [12, Proposition 4.2] and follows from the classical Scott-Dupont theory (see [38] and [7, Proposition 3.1]):

Proposition 1.3.2. *If the assumption* **A2** *is satisfied, then there exists a constant $C > 0$, such that for every $v \in H^{2+s}(K)$ with $s \in (1/2, 1]$, there exists $v_\pi \in \mathbb{P}_2(K)$ such that*

$$|v - v_\pi|_{\ell,K} \leq C h_K^{2+s-\ell} |v|_{2+s,K}, \quad \ell = 0, 1, 2.$$

For the analysis, we will introduce the broken H^2-seminorm:

$$|v|_{2,h}^2 := \sum_{K \in \mathcal{T}_h} |v|_{2,K}^2,$$

which is well defined for every $v \in L^2(\Omega)$ such that $v|_K \in H^2(K)$ for all polygon $K \in \mathcal{T}_h$.

Now, for $v \in W_h$, let Π_h be defined in $L^2(\Omega)$ by $(\Pi_h v)|_K := \Pi_K^\Delta v$ for all $K \in \mathcal{T}_h$, where Π_K^Δ has been defined in (1.3.1a)-(1.3.1b).

Lemma 1.3.2. *Let $v \in W_h$. Then, there exists $C > 0$ such that*

$$\|v - \Pi_h v\|_{0,\Omega} \leq C h^2 \|v\|_{2,\Omega}.$$

Proof. Let $v \in W_h$. Now, let $\Pi_K^\Delta v \in \mathbb{P}_2(K)$ as defined in (1.3.1a)-(1.3.1b). We have for all $r \in \mathbb{P}_2(K)$ that

$$\|v - \Pi_K^\Delta v\|_{0,K}^2 = \int_K (v - \Pi_K^\Delta v)(v - \Pi_K^\Delta v) = \int_K (v - \Pi_K^\Delta v)(v - r).$$

Thus,

$$\|v - \Pi_K^\Delta v\|_{0,K} \leq \inf_{r \in \mathbb{P}_2(K)} \|v - r\|_{0,K} \leq C h_K^2 \|v\|_{2,K},$$

where we have used (1.3.4) and [103, Proposition 4.1], and the result follows. □

Now, the remainder of this section is devoted to prove the following properties which will be used in the sequel:

Lemma 1.3.3. *There exists $C > 0$ such that, for all $f_h \in W_h$, if $u = Tf_h$ and $u_h = T_h f_h$, then*

$$\|(T - T_h) f_h\|_{2,\Omega} = \|u - u_h\|_{2,\Omega} \leq C \left(\|\Pi_h f_h - f_h\|_{0,\Omega} + \|u - u_I\|_{2,\Omega} + |u - u_\pi|_{2,h} \right),$$

for all $u_I \in W_h$ and for all $u_\pi \in L^2(\Omega)$ such that $u_\pi|_K \in \mathbb{P}_2(K) \quad \forall K \in \mathcal{T}_h$.

Proof. Let $f_h \in W_h$. For $u_I \in W_h$, we set $v_h := u_h - u_I$. Thus

$$||(T - T_h) f_h||_{2,\Omega} \leq ||u - u_I||_{2,\Omega} + ||v_h||_{2,\Omega}. \tag{1.3.14}$$

Now, thanks to Lemma 1.3.1, the definition of $a_{h,K}(\cdot,\cdot)$ and those of T and T_h, we have

$$\begin{aligned}
\beta ||v_h||_{2,\Omega}^2 \leq a_h(v_h, v_h) &= a_h(u_h, v_h) - a_h(u_I, v_h) = b_h(f_h, v_h) - \sum_{K \in \mathcal{T}_h} a_{h,K}(u_I, v_h) \\
&= b_h(f_h, v_h) - \sum_{K \in \mathcal{T}_h} \left\{ a_{h,K}(u_I - u_\pi, v_h) + a_{h,K}(u_\pi, v_h) \right\} \\
&= b_h(f_h, v_h) - \sum_{K \in \mathcal{T}_h} \left\{ a_{h,K}(u_I - u_\pi, v_h) + a_K(u_\pi - u, v_h) + a_K(u, v_h) \right\} \\
&= b_h(f_h, v_h) - b(f_h, v_h) - \sum_{K \in \mathcal{T}_h} \left\{ a_{h,K}(u_I - u_\pi, v_h) + a_K(u_\pi - u, v_h) \right\}.
\end{aligned} \tag{1.3.15}$$

Then, we bound the first term on the right hand side of the previous inequality as follows

$$\begin{aligned}
b_h(f_h, v_h) - b(f_h, v_h) &= \sum_{K \in \mathcal{T}_h} \left\{ b_{h,K}(f_h, v_h) - b_K(f_h, v_h) \right\} \\
&= \sum_{K \in \mathcal{T}_h} \left\{ b_{h,K}(f_h - \Pi_K^\Delta f_h, v_h) - b_K(f_h - \Pi_K^\Delta f_h, v_h) \right\} \\
&\leq \sum_{K \in \mathcal{T}_h} \left\{ b_{h,K}(f_h - \Pi_K^\Delta f_h, f_h - \Pi_K^\Delta f_h)^{1/2} b_{h,K}(v_h, v_h)^{1/2} + ||f_h - \Pi_K^\Delta f_h||_{0,K} ||v_h||_{0,K} \right\} \\
&\leq C \sum_{K \in \mathcal{T}_h} ||f_h - \Pi_K^\Delta f_h||_{0,K} ||v_h||_{0,K},
\end{aligned} \tag{1.3.16}$$

where we have used the consistency, Cauchy-Schwarz inequality and stability of $b_{h,K}(\cdot,\cdot)$.

Thus, from (1.3.15), using the above bound together with the Cauchy-Schwarz and triangular inequalities, we obtain

$$\begin{aligned}\beta \|v_h\|_{2,\Omega}^2 &\leq C \sum_{K\in\mathcal{T}_h} \left\|\Pi_K^{\Delta} f_h - f_h\right\|_{0,K} \|v_h\|_{0,K} + \sum_{K\in\mathcal{T}_h} \left(\alpha_2 |u_I - u_\pi|_{2,K} + |u_\pi - u|_{2,K}\right) |v_h|_{2,K} \\ &\leq C \left(\sum_{K\in\mathcal{T}_h} \left\|\Pi_K^{\Delta} f_h - f_h\right\|_{0,K}^2 + |u_I - u|_{2,K}^2 + |u_\pi - u|_{2,K}^2 \right)^{1/2} \|v_h\|_{2,\Omega} \\ &\leq C \left(\|\Pi_h f_h - f_h\|_{0,\Omega} + \|u_I - u\|_{2,\Omega} + |u_\pi - u|_{2,h} \right) \|v_h\|_{2,\Omega}.\end{aligned}$$

Therefore, the proof follows from (1.3.14) and the above inequality. □

The next step is to find an appropriate term u_I that can be used in the above lemma. Thus, we have the following result.

Proposition 1.3.3. *Assume **A1**–**A2** are satisfied, let $v \in H^{2+s}(\Omega)$ with $s \in (1/2, 1]$. Then, there exist $v_I \in W_h$ and $C > 0$ such that*

$$\|v - v_I\|_{2,\Omega} \leq C h^s |v|_{2+s,\Omega}.$$

Proof. The proof follows repeating the arguments from [27, Proposition 4.4] (see also [7, Proposition 3.1]). □

As we have mentioned before, to prove that T_h provides a correct spectral approximation of T, we will resort to the theory developed in [73] for noncompact operators. To this end, we first introduce some notations. For any linear operator $S : H_0^2(\Omega) \longrightarrow H_0^2(\Omega)$, we define the norm

$$\|S\|_h := \sup_{0\neq v_h\in W_h} \frac{\|S v_h\|_{2,\Omega}}{\|v_h\|_{2,\Omega}}.$$

Moreover, we recall the definition of the gap $\widehat{\delta}$ between two closed subspaces $\mathcal{X}$ and $\mathcal{Y}$ of $H_0^2(\Omega)$:

$$\widehat{\delta}(\mathcal{X}, \mathcal{Y}) := \max\{\delta(\mathcal{X}, \mathcal{Y}), \delta(\mathcal{Y}, \mathcal{X})\},$$

where

$$\delta(\mathcal{X}, \mathcal{Y}) := \sup_{x\in\mathcal{X}:\ \|x\|_{2,\Omega}=1} \delta(x, \mathcal{Y}) \quad \text{with} \quad \delta(x, \mathcal{Y}) := \inf_{y\in\mathcal{Y}} \|x - y\|_{2,\Omega}.$$

The theory from [73] guarantees approximation of the spectrum of T, provided the following two properties are satisfied:

- (P1): $\|T - T_h\|_h \to 0, \quad \text{as } h \to 0,$
- (P2): $\forall \phi \in H_0^2(\Omega), \quad \lim_{h\to 0} \delta(\phi, W_h) = 0.$

Property (P2) follows immediately from the approximation property of the virtual element space (see Proposition 1.3.3) and the density of smooth functions in $H_0^2(\Omega)$. Property (P1) is a consequence of the following lemma.

Lemma 1.3.4. *There exist $C > 0$ and $s \in (1/2, 1]$, independent of h, such that*

$$\|T - T_h\|_h \leq Ch^s.$$

Proof. Given $f_h \in W_h$, we have that (see Lemma 1.3.3)

$$\|(T - T_h)\, f_h\|_{2,\Omega} = \|u - u_h\|_{2,\Omega} \leq C \left(\|\Pi_h f_h - f_h\|_{0,\Omega} + \|u - u_I\|_{2,\Omega} + |u - u_\pi|_{2,h} \right),$$

now, using Lemma 1.3.2, Propositions 1.3.2 and 1.3.3, and Lemma 1.2.2, we have

$$\|(T - T_h)\, f_h\|_{2,\Omega} \leq C \left(h^2 \|f_h\|_{2,\Omega} + h^s \|f_h\|_{0,\Omega} \right) \leq Ch^s \|f_h\|_{2,\Omega}.$$

The proof is complete. □

1.4 Convergence and error estimates

In this section, we will adapt the arguments from [73, 74] to prove convergence of our spectral approximation as well as to obtain error estimates for the approximate eigenvalues and eigenfunctions.

The following results are consequence of property (P1) (see [73]):

Lemma 1.4.1. *Suppose that (P1) holds true and let $F \subset \rho(T)$ be closed. Then, there exist positive constants C and h_0 independent of h, such that for $h < h_0$*

$$\sup_{v_h \in W_h} ||R_z(T_h) v_h||_{2,\Omega} \leq C ||v_h||_{2,\Omega} \qquad \forall z \in F.$$

Theorem 1.4.1. *Let $U \subset \mathbb{C}$ be an open set containing $\mathrm{sp}(T)$. Then, there exists $h_0 > 0$ such that $\mathrm{sp}(T_h) \subset U$ for all $h < h_0$.*

An immediate consequence of this theorem is that the proposed virtual element method does not introduce spurious modes with eigenvalues interspersed among those with a physical meaning.

By applying the results from [73] to our problem, we conclude the spectral convergence of T_h to T as $h \to 0$. More precisely, let $\mu \neq 0$ be an isolated eigenvalue of T with multiplicity m and let $\mathcal{C}$ be an open circle in the complex plane centered at μ, such that μ is the only eigenvalue of T lying in $\mathcal{C}$ and $\partial\mathcal{C} \cap \mathrm{sp}(T) = \emptyset$. Then, according to Section 2 in [73] for h small enough there exist m eigenvalues $\mu_h^{(1)}, \ldots, \mu_h^{(m)}$ of T_h (repeated according to their respective multiplicities) which lie in $\mathcal{C}$. Therefore, these eigenvalues $\mu_h^{(1)}, \ldots, \mu_h^{(m)}$ converge to μ as h goes to zero.

The next step is to obtain error estimates for the spectral approximation. With this aim, we will use the theory from [74]. However, we cannot apply the results from this reference directly to our problem, because of the variational crimes in the bilinear forms used to define the operator T_h. Therefore, we need to extend the results from this reference to our case. With this purpose, we follow an approach recently presented in [28].

Consider the eigenspace $\mathcal{E}$ of T corresponding to μ and the T_h-invariant subspace $\mathcal{E}_h$ spanned by the eigenspaces of T_h corresponding to $\mu_h^{(1)}, \ldots, \mu_h^{(m)}$. As a consequence of Lemma 1.4.1, we have that

$$||(zI - T_h) v_h||_{2,\Omega} \geq C ||v_h||_{2,\Omega} \qquad \forall v_h \in W_h, \quad \forall z \in \partial\mathcal{C},$$

for h small enough.

Let $\mathcal{P}_h : H_0^2(\Omega) \to W_h \subseteq H_0^2(\Omega)$ be the projector with range W_h defined by the relation

$$a(\mathcal{P}_h u - u, v_h) = 0 \qquad \forall v_h \in W_h.$$

Notice that $\mathcal{P}_h$ is bounded uniformly on h (namely $||\mathcal{P}_h u||_{2,\Omega} \leq ||u||_{2,\Omega}$) and

$$|u - \mathcal{P}_h u|_{2,\Omega} = \inf_{v_h \in W_h} |u - v_h|_{2,\Omega}.$$

Let us define

$$\widehat{T}_h := T_h \mathcal{P}_h : H_0^2(\Omega) \to W_h.$$

Notice that $\mathrm{sp}(\widehat{T}_h) = \mathrm{sp}(T_h) \cup \{0\}$.

Next, we introduce the following spectral projectors (the second one, is well defined at least for h small enough):

- The spectral projector of T relative to μ: $F := \frac{1}{2\pi i} \int_{\partial \mathcal{C}} R_z(T) dz$;
- The spectral projector of $\widehat{T}_h$ relative to $\mu_h^{(1)}, \ldots, \mu_h^{(m)}$: $\widehat{F}_h := \frac{1}{2\pi i} \int_{\partial \mathcal{C}} R_z(\widehat{T}_h) dz$.

We have the following result (see Lemma 1 in [74]).

Lemma 1.4.2. *There exist $h_0 > 0$ and $C > 0$ such that*

$$||R_z(\widehat{T}_h)|| \leq C \qquad \forall z \in \partial \mathcal{C}, \quad \forall h \leq h_0.$$

Proof. It is identical to the proof of Lemma 11 in [28]. □

Consequently, for h small enough, the spectral projector $\widehat{F}_h$ is bounded uniformly in h.

Now, we define

$$\gamma_h := \delta(\mathcal{E}, W_h) \quad \text{and} \quad \eta_h := \sup_{w \in \mathcal{E}} \frac{||w - \Pi_h w||_{0,\Omega}}{||w||_{2,\Omega}}.$$

From Lemmas 1.2.2 and 1.3.2, we have that

$$\gamma_h \leq C h^{\tilde{s}} \qquad \text{and} \qquad \eta_h \leq C h^2, \tag{1.4.1}$$

where $\tilde{s} \in (1/2, 1]$ is such that $\mathcal{E} \subset H^{2+\tilde{s}}(\Omega)$.

The following result establishes an error estimate for the eigenfunctions.

Theorem 1.4.2. *If $\mathcal{E} \subset H^{2+\tilde{s}}(\Omega)$ with $\tilde{s} \in (1/2, 1]$, there exist positive constants h_0 and C such that, for all $h < h_0$,*

$$\widehat{\delta}(\mathcal{E}, \mathcal{E}_h) \leq C h^{\tilde{s}}.$$

Proof. It follows by arguing exactly as in the proof of Theorem 1 from [74] and using (1.4.1). □

Finally, we have the following result that provides an error estimate for the eigenvalues.

Theorem 1.4.3. *There exist positive constants C and h_0 independent of h, such that, for all $h < h_0$,*

$$\left|\lambda - \lambda_h^{(i)}\right| \leq Ch^{2\tilde{s}}, \qquad i = 1, \ldots, m,$$

where $\tilde{s} \in (1/2, 1]$ is such that $\mathcal{E} \subset H^{2+\tilde{s}}(\Omega)$.

Proof. Let w_h be such that $(\lambda_h^{(i)}, w_h)$ is a solution of (1.3.13) with $\|w_h\|_{2,\Omega} = 1$. According to Theorem 1.4.2, $\delta(w_h, \mathcal{E}) \leq Ch^{\tilde{s}}$. It follows that there exists (λ, w) eigenpair solution of (1.2.2) such that

$$\|w - w_h\|_{2,\Omega} \leq Ch^{\tilde{s}}. \tag{1.4.2}$$

From the symmetry of the bilinear forms and the facts that $a(w, v) = \lambda b(w, v)$ for all $v \in H_0^2(\Omega)$ (cf. (1.2.2)) and $a_h(w_h, v_h) = \lambda_h^{(i)} b_h(w_h, v_h)$ for all $v_h \in W_h$ (cf. (1.3.13)), we have

$$\begin{aligned} a(w - w_h, w - w_h) - \lambda b(w - w_h, w - w_h) &= a(w_h, w_h) - \lambda b(w_h, w_h) \\ &= a(w_h, w_h) - a_h(w_h, w_h) + \lambda_h^{(i)} b_h(w_h, w_h) - \lambda b(w_h, w_h) \\ &= a(w_h, w_h) - a_h(w_h, w_h) + \lambda_h^{(i)} \left[b_h(w_h, w_h) - b(w_h, w_h)\right] + (\lambda_h^{(i)} - \lambda) b(w_h, w_h), \end{aligned}$$

from which we obtain the following identity:

$$\begin{aligned} (\lambda_h^{(i)} - \lambda) b(w_h, w_h) = a(w - w_h, w - w_h) - \lambda b(w - w_h, w - w_h) \\ + \left(a_h(w_h, w_h) - a(w_h, w_h)\right) - \lambda_h^{(i)} \left[b_h(w_h, w_h) - b(w_h, w_h)\right]. \end{aligned} \tag{1.4.3}$$

The next step is to bound each term on the right hand side above. The first and the second ones are easily bounded using the Cauchy-Schwarz inequality and (1.4.2):

$$|a(w - w_h, w - w_h) - \lambda b(w - w_h, w - w_h)| \leq C\left(|w - w_h|_{2,\Omega}^2 + \|w - w_h\|_{0,\Omega}^2\right) \leq Ch^{2\tilde{s}}. \tag{1.4.4}$$

For the third term, for $w \in \mathcal{E}$, we consider $w_\pi \in L^2(\Omega)$ defined on each $K \in \mathcal{T}_h$ so that $w_\pi|_K \in \mathbb{P}_2(K)$ and the estimate of Proposition 1.3.2 holds true. Then, we use (1.3.9) and (1.3.11) to write

$$\begin{aligned} |a_h(w_h, w_h) - a(w_h, w_h)| &= \Big| \sum_{K \in \mathcal{T}_h} \Big\{ a_{h,K}(w_h - w_\pi, w_h) - a_K(w_h - w_\pi, w_h) \Big\} \Big| \\ &\leq \sum_{K \in \mathcal{T}_h} (1 + \alpha_2) a_K(w_h - w_\pi, w_h - w_\pi) \\ &\leq C \sum_{K \in \mathcal{T}_h} |w_h - w_\pi|_{2,K}^2. \end{aligned}$$

Then, adding and subtracting w, using triangular inequality, Proposition 1.3.2 and (1.4.2), we obtain

$$|a_h(w_h, w_h) - a(w_h, w_h)| \leq Ch^{2\tilde{s}}. \tag{1.4.5}$$

For the last term in (1.4.3), using that Π_K^Δ is also the L^2-projector (see (1.3.4)), we obtain

$$\begin{aligned} |b_h(w_h, w_h) - b(w_h, w_h)| &\leq C \sum_{K \in \mathcal{T}_h} \|w_h - \Pi_K^\Delta w_h\|_{0,K}^2 \\ &\leq C \sum_{K \in \mathcal{T}_h} \|w_h - w_\pi\|_{0,K}^2 \\ &\leq C \sum_{K \in \mathcal{T}_h} \left(\|w - w_\pi\|_{0,K}^2 + \|w - w_h\|_{0,K}^2\right) \leq Ch^{2\tilde{s}}, \end{aligned}$$

where we have used again Proposition 1.3.2 and (1.4.2).

On the other hand, using Lemma 1.3.1, we have

$$1 = \|w_h\|^2_{2,\Omega} \leq \frac{1}{\beta}\lambda_h^{(i)} b_h(w_h, w_h) \leq \lambda_h^{(i)} C \|w_h\|^2_{0,\Omega},$$

thus, the theorem follows from (1.4.3)–(1.4.5) and the inequalities above. □

1.5 Numerical results

We report in this section a couple of tests which have allowed us to assess the theoretical results proved above. With this aim, we have implemented in a MATLAB code the proposed VEM on arbitrary polygonal meshes, by following the ideas presented in [16].

Now, to complete the choice of the VEM, we had to fix the bilinear forms $s_K(\cdot,\cdot)$ and $s_K^0(\cdot,\cdot)$ satisfying (1.3.5) and (1.3.6), respectively. Proceeding as in [12], a natural choice for $s_K(\cdot,\cdot)$ is given by

$$s_K(u_h, v_h) := \sigma_K \sum_{i=1}^{N_K} [u_h(P_i)v_h(P_i) + h_{P_i}^2 \nabla u_h(P_i) \cdot \nabla v_h(P_i)] \quad \forall u_h, v_h \in W_h^K, \tag{1.5.1}$$

where $P_1, \ldots, P_{N_K}$ are the vertices of K, h_{P_i} corresponds to the maximum diameter of the elements with P_i as a vertex and $\sigma_K > 0$ is a multiplicative factor to take into account the magnitude of the material parameter and the h-scaling, for instance, in the numerical tests we have picked $\sigma_K > 0$ as the mean value of the eigenvalues of the local matrix $a_K\big(\Pi_K^\Delta u_h, \Pi_K^\Delta v_h\big)$. This ensures that the stabilizing term scales as $a_K(v_h, v_h)$. Now, a choice for $s_K^0(\cdot,\cdot)$ is given by

$$s_K^0(u_h, v_h) := \sigma_K^0 \sum_{i=1}^{N_K} [u_h(P_i)v_h(P_i) + h_{P_i}^2 \nabla u_h(P_i) \cdot \nabla v_h(P_i)] \quad \forall u_h, v_h \in W_h^K. \tag{1.5.2}$$

In this case, we have taken the parameter $\sigma_K^0 > 0$ as the mean value of the eigenvalues of the local matrix $b_K\big(\Pi_K^\Delta u_h, \Pi_K^\Delta v_h\big)$ to ensure (1.3.6). A proof of (1.3.5) and (1.3.6) for the above (standard) choices could be derived following the arguments in [22] (see also [7]). Finally, we mention that the above definitions of the bilinear forms $s_K(\cdot,\cdot)$ and $s_K^0(\cdot,\cdot)$ are according to the analysis presented in [103] in order to avoid spectral pollution.

We have tested the method by using different families of meshes (see Figure 1.1):

- $\mathcal{T}_h^1$: rectangular meshes;
- $\mathcal{T}_h^2$: hexagonal meshes;
- $\mathcal{T}_h^3$: non-structured hexagonal meshes made of convex hexagons;
- $\mathcal{T}_h^4$: trapezoidal meshes which consist of partitions of the domain into $N \times N$ congruent trapezoids, all similar to the trapezoid with vertices $(0,0)$, $(\frac{1}{2},0)$, $(\frac{1}{2},\frac{2}{3})$ and $(0,\frac{1}{3})$.

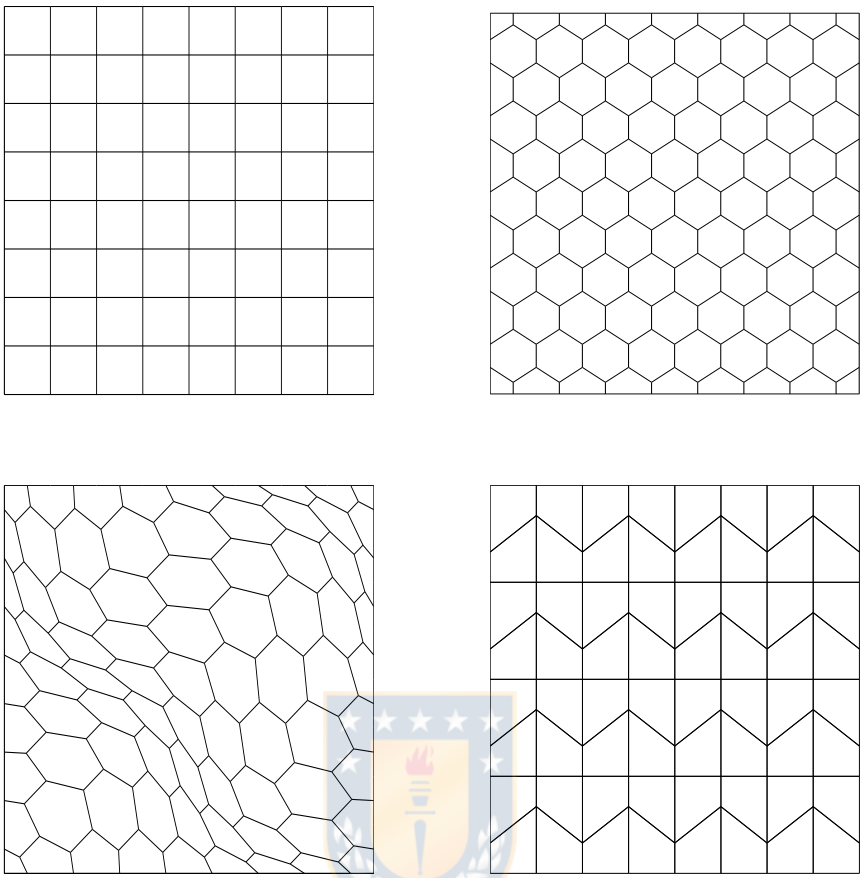

Figure 1.1: Sample meshes: $\mathcal{T}_h^1$ (top left), $\mathcal{T}_h^2$ (top right), $\mathcal{T}_h^3$ (bottom left) and $\mathcal{T}_h^4$ (bottom right), for $N = 8$ (figure produced by the author).

The refinement parameter N used to label each mesh is the number of elements on each edge of the plate.

1.5.1 Simply supported plate

First, we have considered a simply supported plate, because analytical solutions are available in this case (see [5, 11]). Even though our theoretical analysis has been developed only for clamped plates, we think that the results of the previous sections should hold true for more general boundary conditions as well. The results that follow give some numerical evidence of this. For the computations we took $\Omega := (0, 1)^2$.

In Table 1.1, we report the four lowest eigenvalues (λ_i, $i = 1, 2, 3, 4$) computed by our method with two different families of meshes and $N = 32, 64, 128$ for a simply supported plate. The table also includes the estimated orders of convergence, as well as more accurate values of the vibration

eigenvalues extrapolated from the computed ones by means of a least-squares fitting of the model

$$\lambda_i \approx \lambda_i + C_i h^{\alpha_i}.$$

This fitting has been done for each eigenvalue separately. The fitted parameters λ_i and α_i are the extrapolated vibration eigenvalue and the estimated order of convergence, respectively.

The last column shows the exact eigenvalues. It can be seen from Table 1.1 that the method converges to the exact values with an optimal quadratic order. Notice that, for the $\mathcal{T}_h^1$ meshes, the second computed eigenvalue is double, because the meshes preserve the symmetry of the domain leading to an eigenvalue of multiplicity 2 in the continuous problem.

Table 1.1: Lowest eigenvalues of a simply supported square plate computed on different meshes with the method analyzed in this chapter (table produced by the author).

	Mesh	$N = 32$	$N = 64$	$N = 128$	Order	Extrapolated	Exact
λ_1		390.0184	389.7307	389.6599	2.02	389.6366	389.6364
λ_2	$\mathcal{T}_h^1$	2430.2171	2433.9024	2434.8914	1.90	2435.2523	2435.2273
λ_3		2430.2171	2433.9024	2434.8914	1.90	2435.2523	2435.2273
λ_4		6259.8318	6240.2949	6235.6906	2.09	6234.2872	6234.1818
λ_1		389.0957	389.4908	389.5987	1.87	389.6395	389.63634
λ_2	$\mathcal{T}_h^2$	2412.1885	2429.0389	2433.6393	1.87	2435.3783	2435.2273
λ_3		2433.8095	2434.8277	2435.1197	1.80	2435.2376	2435.2273
λ_4		6199.2905	6224.8431	6231.7684	1.88	6234.3634	6234.1818

1.5.2 Clamped plate

In this numerical test, we took $\Omega := (0,1)^2$ and considered clamped boundary condition on the whole of $\partial\Omega$. We present numerical experiments which confirm the theoretical results proved above.

Table 1.2 shows the four lowest eigenvalues computed with successively refined meshes of each type for a clamped plate. The table includes orders of convergence, as well as accurate values extrapolated by means of a least-squares fitting. Moreover, we compare the performance of the proposed method with the one presented in [106] with a mixed formulation for solving the plate vibration problem and a Galerkin method based on piecewise linear and continuous finite elements. With this aim, we include in the last column of Table 1.2 the values obtained by extrapolating those computed with method in [106] on uniform triangular meshes as those shown in Figure 1.2, for the same problem.

It is clear that the eigenvalue approximation order of our method is quadratic and that the results obtained by the two methods agree perfectly well.

1.5.3 L-shaped plate

Now, we present two numerical experiments which confirm the theoretical results proved above. We have computed the eigenvalues of an L-shaped plate: $\Omega := (0,1) \times (0,1) \setminus [0.5,1) \times [0.5,1)$.

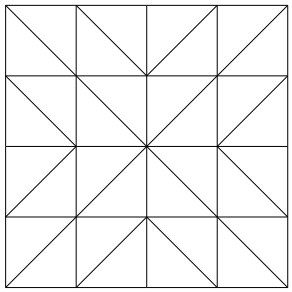

$N = 4$

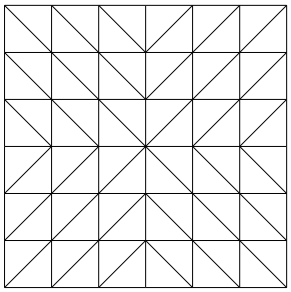

$N = 6$

Figure 1.2: Uniform meshes (figure produced by the author).

Table 1.2: Lowest eigenvalues of a clamped square plate computed on different meshes with the VEM method analyzed in this chapter and the one in [106] (table produced by the author).

	Mesh	$N = 32$	$N = 64$	$N = 128$	Order	Extrapolated	[106]
λ_1		1283.2286	1291.5607	1294.0225	1.76	1295.0526	1294.9369
λ_2	$\mathcal{T}_h^3$	5268.2854	5353.1383	5377.7322	1.79	5387.6973	5386.6675
λ_3		5326.6504	5368.5269	5381.6191	1.68	5387.5416	5386.6675
λ_4		11406.3068	11622.9583	11686.8981	1.76	11713.7035	11710.9076
λ_1		1289.7221	1293.6088	1294.6010	1.97	1294.9410	1294.9369
λ_2	$\mathcal{T}_h^4$	5318.4039	5368.9773	5382.1939	1.94	5386.8279	5386.6675
λ_3		5351.6510	5377.6743	5384.3950	1.95	5386.7517	5386.6675
λ_4		11664.9586	11698.2652	11707.5973	1.84	11711.1942	11710.9076

In the first test, we considered clamped boundary condition on the whole of $\partial\Omega$ and we have used uniform triangular meshes as those shown in Figure 1.3. Once again, we compare the performance of the proposed method with the one presented in [106].

We report in Table 1.3 the four lowest eigenvalues computed with the method analyzed in this chapter. The table includes orders of convergence, as well as accurate values extrapolated by means of a least-squares fitting. The last column shows the values obtained by extrapolating those computed with method in [106] on the same uniform triangular meshes.

In this case, for the first eigenvalue, the method converges with order close to 1.28, which is the expected one because of the singularity of the solution (see [85]). Instead, the method converges with larger orders for the second, third and fourth eigenvalues.

In this case, we mention the following advantages of the proposed VEM method: the computational cost of our method is smaller than the method studied in [106]. In fact, the number of unknowns for our VEM method is, $3N_v$, where N_v denotes the number of vertices, whereas in [106] is $4N_v$. Moreover, in this case, the eigenvalue problem to be solved is much simpler than the one arising from the formulation studied in [106]. In fact, the latter leads to a degenerate generalized matrix eigenvalue problem, which is shown to be well posed in [106, Appendix] but that cannot be solved with standard eigensolvers.

Table 1.3: Lowest eigenvalues of an L-shaped clamped plate computed on uniform triangular meshes with the VEM method analyzed in this chapter and the one in [106] (table produced by the author).

	$N = 32$	$N = 64$	$N = 128$	Order	Extrapolated	[106]
λ_1	6827.5421	6753.6207	6725.1315	1.28	6707.4264	6704.2982
λ_2	11128.5787	11073.4576	11059.3867	1.97	11054.5647	11055.5189
λ_3	14989.9367	14926.5156	14910.6489	2.00	14905.3676	14907.0816
λ_4	26325.7078	26195.9206	26163.4597	2.00	26152.6488	26157.9673

We show in Figure 1.3 the eigenfunctions corresponding to the four lowest eigenvalues for an L-shaped clamped plate.

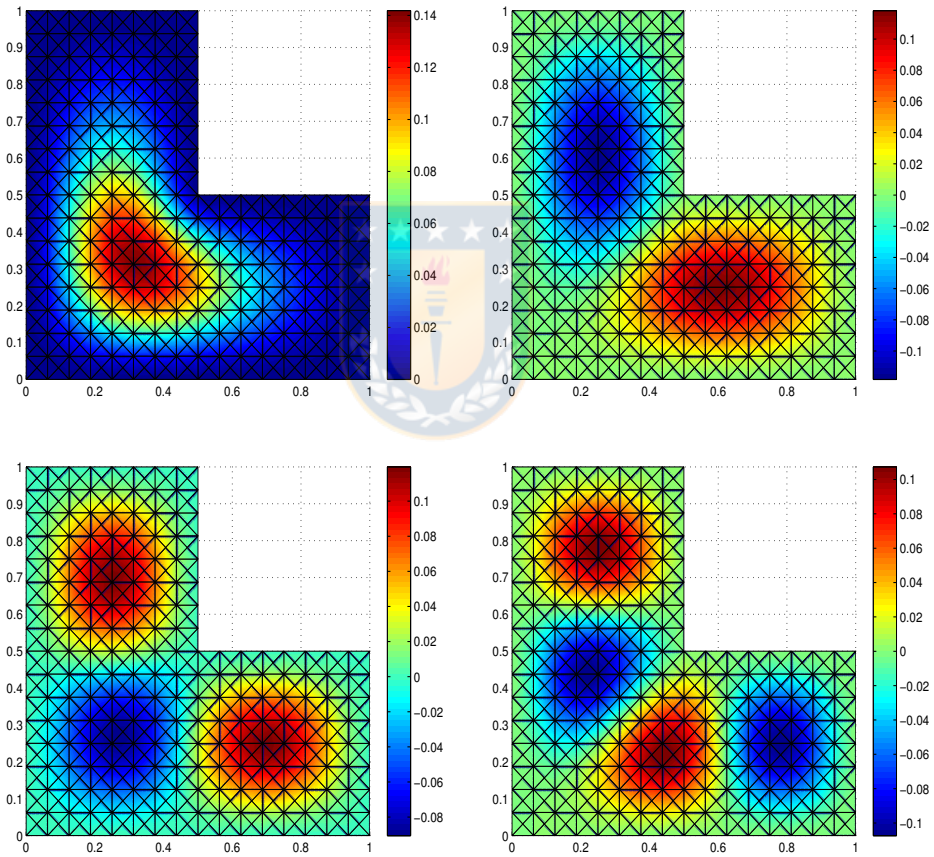

Figure 1.3: Eigenfunctions of the plate problem with clamped boundary condition associated with eigenvalues λ_1 (top left) λ_2 (top right), λ_3 (bottom left) and λ_4 (bottom right) (figure produced by the author).

Finally, Table 1.4 shows the four lowest eigenvalues computed with successively refined triangular meshes for an L-shaped clamped-free plate. The table includes orders of convergence, as well as accurate values extrapolated by means of a least-squares fitting. We observe from the results reported

in Table 1.4 that the order of convergence is again quadratic in this case.

Table 1.4: Lowest eigenvalues of an L-shaped clamped-free plate computed on triangular meshes with the VEM method analyzed in this chapter (table produced by the author).

	$N = 32$	$N = 64$	$N = 128$	Order	Extrapolated
λ_1	1198.2579	1195.3003	1194.4606	1.82	1194.1302
λ_2	4576.4950	4556.9217	4551.0233	1.73	4548.4764
λ_3	6807.0921	6785.8226	6780.4745	2.00	6778.6710
λ_4	15094.2896	15019.3352	14998.6457	1.86	14990.8077

We show in Figure 1.4 the eigenfunctions corresponding to the four lowest eigenvalues.

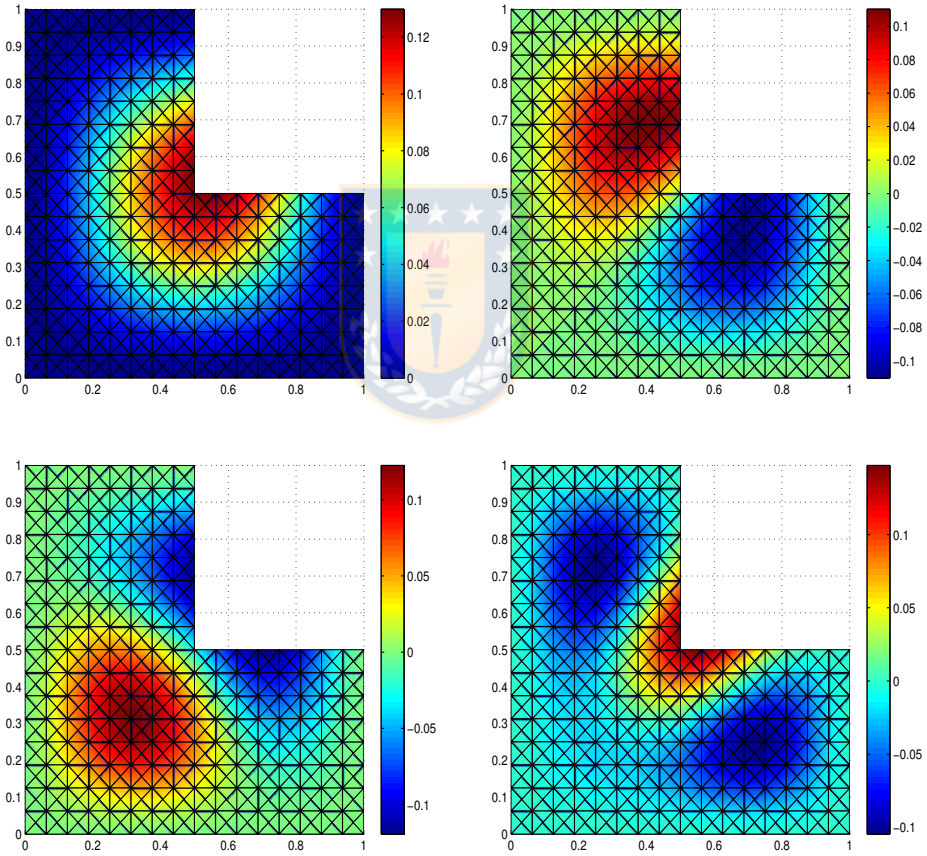

Figure 1.4: Eigenfunctions of the plate problem with mixed boundary condition associated with eigenvalues λ_1 (top left) λ_2 (top right), λ_3 (bottom left) and λ_4 (bottom right) (figure produced by the author).

1.5.4 Effect of the stability constants

The aim of this test is to analyze the influence of the stabilizing bilinear forms $s_K(\cdot,\cdot)$ and $s_K^0(\cdot,\cdot)$ introduced in (1.5.1) and (1.5.2), respectively, on the computed spectrum, to know whether the quality of the computations can be affected.

With this aim, for any $\alpha > 0$, we consider the following scaled stabilizing bilinear forms $\alpha s_K(\cdot,\cdot)$ and $\alpha s_K^0(\cdot,\cdot)$. In this test, we have taken the same configuration as in Section 1.5.2. Therefore, the results for $\alpha = 1$ on different meshes are reported in Table 1.2.

In Table 1.5, we report the lowest eigenvalues computed by the method with varying values of α on a fixed mesh $\mathcal{T}_h^4$ with refinement level $N = 16$ (see Figure 1.1). We have observed the eigenfunctions associated to each eigenvalue and no spurious eigenvalues were detected for any choice of the parameter α. Moreover, it can be seen in Table 1.5, that the computed spectrum is well approximated for a wide range of values of α. On the other hand, for small and large values of α, the computed eigenvalues are sensible to this parameter.

However, the eigenvalues for $\alpha \geq 1/4$ converge to the same values with an optimal quadratic order as the mesh is refined, this can be seen in Table 1.6, where we report the lowest eigenvalues computed with varying values of α on the family of meshes $\mathcal{T}_h^4$. The table also includes orders of convergence, as well as accurate values extrapolated by means of a least-squares fitting. The last column shows the values obtained by extrapolating those computed with the finite element method introduced in [106] on triangular meshes. On the other hand, from the same table, we see that for very small values of α the lowest eigenvalues converge to wrong results and finer meshes are needed for the computed eigenvalues to lie close to the reference value.

Table 1.5: Computed lowest eigenvalues for $\alpha = 4^k$ with $-3 \leq k \leq 3$ (table produced by the author).

	$\alpha = 1/64$	$\alpha = 1/16$	$\alpha = 1/4$	$\alpha = 1$	$\alpha = 4$	$\alpha = 16$	$\alpha = 64$
λ_1	678.2631	884.2427	1116.2400	1275.3202	1427.0062	1818.0463	3282.2829
λ_2	1573.9238	2458.2514	3892.7704	5146.3829	6083.8491	8275.8511	16596.5175
λ_3	2981.4564	3623.2656	4477.9219	5259.3630	6266.1534	8638.6246	17136.2878
λ_4	3159.0171	5555.2757	9188.7834	11581.8220	15108.1552	25967.6692	54081.8017

This analysis suggests, that the user of VEM for this kind of spectral problems, has to be aware of the risk of degeneration of the eigenvalues for certain values of the parameter α. The way of minimizing this risk in this case is to take values of $\alpha \in [1/4, 4]$, where the method is robust with respect to the parameter.

Table 1.6: Lowest eigenvalues for different values of α of a clamped square plate computed on the family of meshes $\mathcal{T}_h^4$ with the VEM method analyzed in this chapter and the one in [106] (table produced by the author).

	α	$N = 32$	$N = 64$	$N = 128$	Order	Extrapolated	[106]
λ_1		945.2274	1154.7930	1253.1204	1.09	1340.3447	1294.9369
λ_2	$\alpha = 1/64$	2528.0163	3884.5960	4867.1361	0.47	7412.8204	5386.6675
λ_3		4303.2208	4996.5611	5270.7107	1.34	5449.4967	5386.6675
λ_4		7700.0166	9702.2703	11006.5891	0.62	13433.8908	11710.9076
λ_1		1133.7070	1247.0043	1282.3102	1.68	1298.3651	1294.9369
λ_2	$\alpha = 1/16$	3851.0044	4852.8168	5238.5617	1.38	5478.5748	5386.6675
λ_3		4732.4857	5194.7780	5336.1008	1.71	5398.3001	5386.6675
λ_4		9357.1501	10894.0565	11482.6150	1.38	11851.4313	11710.9076
λ_1		1241.0596	1280.6680	1291.3094	1.90	1295.1848	1294.9369
λ_2	$\alpha = 1/4$	4858.3819	5238.8944	5348.5413	1.80	5392.4526	5386.6675
λ_3		5106.2979	5311.7571	5367.5790	1.88	5388.4009	5386.6675
λ_4		10796.1790	11450.7700	11643.3385	1.77	11722.7741	11710.9076
λ_1		1328.6944	1303.4367	1297.0628	1.99	1294.9288	1294.9369
λ_2	$\alpha = 4$	5565.8430	5431.8202	5397.9674	1.99	5386.6545	5386.6675
λ_3		5610.9332	5443.2945	5400.8574	1.98	5386.4086	5386.6675
λ_4		12601.1773	11936.9889	11767.6059	1.97	11709.4491	11710.9076
λ_1		1785.9613	1420.0748	1326.7370	1.97	1294.7091	1294.9369
λ_2	$\alpha = 64$	8146.0204	6081.0251	5561.9715	1.99	5386.8201	5386.6675
λ_3		8194.4611	6098.0923	5569.3074	1.99	5392.1072	5386.6675
λ_4		25490.6782	15186.1020	12597.4474	1.99	11722.9278	11710.9076

CHAPTER 2

Virtual element for the buckling problem of Kirchhoff plates

2.1 Introduction

In this chapter we analyze a conforming C^1 virtual element approximation of an eigenvalue problem arising in Structural Mechanics: the elastic stability of plates, in particular the so-called buckling problem. This problem has attracted much interest since it is frequently encountered in several engineering applications such as car or aircraft design. In particular, we will focus on thin plates which are modeled by the Kirchhoff–Love equations.

The buckling problem for plates can be formulated as a spectral problem of fourth order whose solution is related with the limit of elastic stability of the plate (i.e., eigenvalues-buckling coefficients and eigenfunctions-buckling modes). This problem has been studied with several finite element methods, for instance, conforming and non-conforming discretizations, mixed formulations. We cite as a minimal sample of them [36, 58, 70, 89, 91, 100, 106, 113].

The aim of the present chapter is to introduce and analyze a virtual element method (VEM) to solve the buckling problem. The VEM has been introduced in [12] and has been applied successfully in a large range of problems in fluid and solid mechanics; see for instance [6, 7, 9, 13, 14, 15, 21, 23, 30, 35, 42, 43, 55, 64, 98, 112, 121, 125]. Regarding VEM for spectral problems, we mention the following recent works [28, 78, 79, 102, 103, 105, 107].

One important advantage of VEM is the possibility of easily implement highly regular discrete spaces to solve fourth order partial differential equations [7, 41, 64]. It is very well known that the construction of conforming finite elements to H^2 is difficult in general, since they generally involve a large number of degrees of freedom (see [67]). Here, we follow the VEM approach presented in [41, 64] to build global discrete spaces of C^1 of arbitrary order that are simple in terms of degrees of freedom and coding aspects to solve an eigenvalue problem modelling the plate buckling problem.

More precisely, we will propose a C^1 Virtual Element Method of arbitrary order $k \geq 2$ to approximate the buckling coefficients and modes of the plate buckling problem on general polygonal meshes. Based on the transverse displacements of the midplane of a thin plate subjected to a symmetric stress tensor field, we propose and analyze a variational formulation in H^2. We characterize the continuous spectrum of the problem through a certain continuous, compact and self-adjoint operator. Then, we

exploit the ability of VEM in order to construct highly regular discrete spaces and propose a conforming discretization of the buckling eigenvalue problem in H^2 which is an extension of the discrete virtual space introduced in [7, 41]. We construct projection operators in order to write bilinear forms that are fully computable. In particular, to discretize the right hand side of the eigenvalue problem we propose a simple bilinear form which does not need any stabilization. This make possible to use directly the so-called Babuška–Osborn abstract spectral approximation theory (see [11]) to show that under standard shape regularity assumptions the resulting virtual element scheme provides a correct approximation of the spectrum and prove optimal order error estimates for the eigenfunctions and a double order for the eigenvalues. The proposed VEM method provides an attractive and competitive alternative to solve the fourth order plate buckling eigenvalue problem in term of its computational cost. For instance, in the lowest order configuration ($k = 2$), our method employs $3N_v$ of degrees of freedom, where N_v denotes the number of vertices in the polygonal mesh. For $k = 3$, the total of dofs is $3N_v + N_e$, where N_e denotes the number of edges in the polygonal mesh, which represents a significant proxy for the computational cost of the method.

This chapter is structured as follows: In Section 2.2, we present the variational formulation for the plate buckling eigenvalue problem. We define a solution operator whose spectrum allows us to characterize the spectrum of the buckling problem. In Section 2.3 we introduce the virtual element discretization of arbitrary degree $k \geq 2$, describe the spectrum of a discrete solution operator and prove some auxiliary results. In Section 2.4, we prove that the numerical scheme presented in this work provides a correct spectral approximation and establish optimal order error estimates for the eigenvalues and eigenfunctions. Finally, in Section 2.5 we report some numerical tests that confirm the theoretical analysis developed.

Throughout the article we will use standard notations for Sobolev spaces, norms and seminorms. Moreover, we will denote by C a generic constant independent of the mesh parameter h, which may take different values in different occurrences.

2.2 Presentation of the continuous spectral problem

Let $\Omega \subseteq \mathbb{R}^2$ be a polygonal bounded domain corresponding to the mean surface of a plate in its reference configuration. The plate is assumed to be homogeneous, isotropic, linearly elastic, and sufficiently thin as to be modeled by Kirchhoff-Love equations. The buckling eigenvalue problem of a clamped plate, which is subjected to a plane stress tensor field $\boldsymbol{\eta} : \Omega \to \mathbb{R}^{2\times 2}$ with $\boldsymbol{\eta} \neq 0$ reads as follows:

$$\begin{cases} \Delta^2 u = -\lambda \operatorname{div}(\boldsymbol{\eta}\nabla u) & \text{in } \Omega, \\ u = \partial_\nu u = 0 & \text{on } \Gamma. \end{cases} \tag{2.2.1}$$

The unknowns of this eigenvalue problem are the deflection of the plate u (buckling modes) and the eigenvalue λ (scaled buckling coefficients). We have denoted by ∂_ν the normal derivative. To simplify the notation we have taken the Young modulus and the density of the plate, both equal to 1. In addition, the stress tensor field is assumed to satisfy the following equilibrium equations:

$$\begin{aligned} \boldsymbol{\eta}^{\mathrm{t}} &= \boldsymbol{\eta} \quad \text{in } \Omega, \\ \mathbf{div}\, \boldsymbol{\eta} &= 0 \quad \text{in } \Omega. \end{aligned}$$

In the remain of this section and in Section 2.3, it is enough to consider $\boldsymbol{\eta} \in L^\infty(\Omega)^{2\times 2}$. However, we will assume some additional regularity which will be used in the proof of Theorem 2.4.4. In addition, we do not need to assume $\boldsymbol{\eta}$ to be positive definite. Let us remark that, in practice, $\boldsymbol{\eta}$ is the stress distribution on the plate subjected to in-plane loads, which does not need to be positive definite [120].

2.2.1 The continuous formulation

In this section we will present and analyze a variational formulation associated with the spectral problem. We will also introduce the so-called solution operator whose spectra will be related to the solutions of the continuous spectral problem (2.2.1).

In order to write the variational formulation of the spectral problem, we introduce the following symmetric bilinear forms in $H_0^2(\Omega)$:

$$a(u,v) := \int_\Omega D^2u : D^2v, \qquad b(u,v) := \int_\Omega (\boldsymbol{\eta}\nabla u)\cdot \nabla v,$$

where " : " denotes the usual scalar product of 2×2-matrices, $D^2v := (\partial_{ij}v)_{1\le i,j\le 2}$ denotes the Hessian matrix of v. It is easy to see that $a(\cdot,\cdot)$ is an inner-product in $H_0^2(\Omega)$.

The variational formulation of the eigenvalue problem (2.2.1) is given as follows:

Problem 1. *Find $(\lambda, u) \in \mathbb{R}\times H_0^2(\Omega)$, $u \neq 0$, such that*

$$a(u,v) = \lambda b(u,v) \qquad \forall v \in H_0^2(\Omega). \tag{2.2.2}$$

The following result establishes that the bilinear form $a(\cdot,\cdot)$ is elliptic in $H_0^2(\Omega)$.

Lemma 2.2.1. *There exists a constant $\alpha_0 > 0$, depending on Ω, such that*

$$a(v,v) \ge \alpha_0 \|v\|_{2,\Omega}^2 \qquad \forall v \in H_0^2(\Omega).$$

Proof. The result follows immediately from the fact that $\|D^2v\|_{0,\Omega}$ is a norm on $H_0^2(\Omega)$, equivalent with the usual norm. □

Remark 2.2.1. *We have that $\lambda \neq 0$ in problem (2.2.2). Moreover, it is easy to prove, using the symmetry of $\boldsymbol{\eta}$, that all the eigenvalues are real (not necessarily positive). We also have that $b(u,u) \neq 0$.*

Next, in order to analyze the variational eigenvalue problem (2.2.2), we introduce the following solution operator:

$$\begin{aligned} T : \ H_0^2(\Omega) &\longrightarrow H_0^2(\Omega), \\ f &\longmapsto Tf := w, \end{aligned}$$

where $w \in H_0^2(\Omega)$ is the unique solution (as a consequence of Lemma 2.2.1) of the following source problem:

$$a(w,v) = b(f,v) \qquad \forall v \in H_0^2(\Omega). \tag{2.2.3}$$

We have that the linear operator T is well defined and bounded. Notice that $(\lambda, u) \in \mathbb{R} \times H_0^2(\Omega)$ solves problem (2.2.2) if and only if $Tu = \mu u$ with $\mu \neq 0$ and $u \neq 0$, in which case $\mu := \frac{1}{\lambda}$. In addition, using the symmetry of $\boldsymbol{\eta}$, we can deduce that T is self-adjoint with respect to the inner product $a(\cdot, \cdot)$ in $H_0^2(\Omega)$. Indeed, given $f, g \in H_0^2(\Omega)$,

$$a(Tf, g) = b(f, g) = b(g, f) = a(Tg, f) = a(f, Tg).$$

On the other hand, the following is an additional regularity result for the solution of problem (2.2.3) and consequently, for the eigenfunctions of T.

Lemma 2.2.2. *There exists $s_\Omega > 1/2$ such that the following results hold:*

(i) For all $f \in H^1(\Omega)$, there exists a positive constant $C > 0$ such that any solution w of the source problem (2.2.3) satisfies $w \in H^{2+\tilde{s}}(\Omega)$ with $\tilde{s} := \min\{s_\Omega, 1\}$ and

$$\|w\|_{2+\tilde{s},\Omega} \leq C\|f\|_{1,\Omega}.$$

(ii) If (λ, u) is an eigenpair of the spectral problem (2.2.2), there exist $s > 1/2$ and a positive constant C depending only on Ω such that $u \in H^{2+s}(\Omega)$ and

$$\|u\|_{2+s,\Omega} \leq C\|u\|_{2,\Omega}.$$

Proof. The proof follows from the classical regularity result for the biharmonic problem with its right-hand side in $L^2(\Omega)$ (cf. [85]). □

Therefore, because of the compact inclusion $H^{2+s}(\Omega) \hookrightarrow H_0^2(\Omega)$, T is a compact operator. Thus, we finish this section with the following spectral characterization result.

Lemma 2.2.3. *The spectrum of T satisfies $\mathrm{sp}(T) = \{0\} \cup \{\mu_k\}_{k\in\mathbb{N}}$, where $\{\mu_k\}_{k\in\mathbb{N}}$ is a sequence of real eigenvalues which converges to 0. The multiplicity of each eigenvalue is finite.*

2.3 Spectral approximation.

In this section, we will write a VEM discretization of the spectral problem (2.2.2). With this aim, we start with the mesh construction and the assumptions considered to introduce the discrete virtual element spaces.

Let $\{\mathcal{T}_h\}_h$ be a sequence of decompositions of Ω into polygons K we will denote by h_K the diameter of the element K and h the maximum of the diameters of all the elements of the mesh, i.e., $h := \max_{K\in\mathcal{T}_h} h_K$. In what follows, we denote by N_K the number of vertices of K, by e a generic edge of $\{\mathcal{T}_h\}_h$ and for all $e \in \partial K$, we define a unit normal vector ν_K^e that points outside of K.

In addition, we will make the following assumptions as in [12, 28]: there exists a positive real number $C_\mathcal{T}$ such that, for every h and every $K \in \mathcal{T}_h$,

A1: $K \in \mathcal{T}_h$ is star-shaped with respect to every point of a ball of radius $C_\mathcal{T} h_K$;

A2: the ratio between the shortest edge and the diameter h_K of K is larger than $C_{\mathcal{T}}$.

In order to introduce the discretization, for every integer $k \geq 2$ and for every polygon K, we define the following finite dimensional space:

$$\widetilde{V}_h^K := \big\{ v_h \in H^2(K) : \Delta^2 v_h \in \mathbb{P}_{k-2}(K), v_h|_{\partial K} \in C^0(\partial K), v_h|_e \in \mathbb{P}_r(e) \ \forall e \in \partial K, \\ \nabla v_h|_{\partial K} \in C^0(\partial K)^2, \partial_{\nu_K^e} v_h|_e \in \mathbb{P}_s(e) \ \forall e \in \partial K \big\},$$

where $r := \max\{3, k\}$ and $s := k - 1$.

This space has been recently considered in [64] to obtain optimal error estimates for fourth order PDEs and it can be seen as an extension of the C^1 virtual space introduced in [41] to solve the bending problem of thin plates. Here, we will consider the same space together with an enhancement technique (cf. [2]) to build a computable right hand of the buckling eigenvalue problem.

It is easy to see that any $v_h \in \widetilde{V}_h^K$ satisfies the following conditions:

- the trace (and the trace of the gradient) on the boundary of K is continuous;
- $\mathbb{P}_k(K) \subseteq \widetilde{V}_h^K$.

In $\widetilde{V}_h^K$ we define the following five sets of linear operators. For all $v_h \in \widetilde{V}_h^K$:

D$_1$: evaluation of v_h at the N_K vertices of K;

D$_2$: evaluation of ∇v_h at the N_K vertices of K;

D$_3$: For $r > 3$, the moments $\int_e q(\xi) v_h(\xi) d\xi \qquad \forall q \in \mathbb{P}_{r-4}(e), \quad \forall$ edge e;

D$_4$: For $s > 1$, the moments $\int_e q(\xi) \partial_{\nu_K^e} v_h(\xi) d\xi \quad \forall q \in \mathbb{P}_{s-2}(e), \quad \forall$ edge e;

D$_5$: For $k \geq 4$, the moments $\int_K q(\boldsymbol{x}) v_h(\boldsymbol{x}) d\boldsymbol{x} \qquad \forall q \in \mathbb{P}_{k-4}(K), \quad \forall$ polygon K.

In order to construct the discrete scheme, we need some preliminary definitions. First, we note that bilinear form $a(\cdot,\cdot)$, introduced in the previous section, can be split as follows:

$$a(u,v) = \sum_{K \in \mathcal{T}_h} a_K(u,v), \qquad u, v \in H_0^2(\Omega),$$

with

$$a_K(u,v) := \int_K D^2 u : D^2 v, \qquad u, v \in H^2(K).$$

Now, we define the projector $\Pi_K^{k,D} : \widetilde{V}_h^K \to \mathbb{P}_k(K) \subseteq \widetilde{V}_h^K$ as the solution of the following local problems (in each element K):

$$a_K\big(\Pi_K^{k,D} v, q\big) = a_K(v,q) \qquad \forall q \in \mathbb{P}_k(K) \quad \forall v \in H^2(K), \tag{2.3.1a}$$

$$\widehat{\Pi_K^{k,D} v} = \widehat{v}, \quad \widehat{\nabla \Pi_K^{k,D} v} = \widehat{\nabla v}, \tag{2.3.1b}$$

where $\widehat{v}$ is defined as follows:

$$\widehat{v} := \frac{1}{N_K}\sum_{i=1}^{N_K} v(\mathrm{v}_i) \qquad \forall v \in C^0(\partial K)$$

and $\mathrm{v}_i, 1 \leq i \leq N_K$, are the vertices of K.

We observe that bilinear form $a_K(\cdot,\cdot)$ has a non-trivial kernel given by $\mathbb{P}_1(K)$. Hence, the role of condition (2.3.1b) is to select an element of the kernel of the operator.

It is easy to see that operator $\Pi_K^{k,D}$ is well defined on $\widetilde{V}_h^K$. Moreover, the following result states that for all $v \in \widetilde{V}_h^K$ the polynomial $\Pi_K^{k,D} v$ can be computed using the output values of the sets $\mathbf{D_1} - \mathbf{D_5}$.

Lemma 2.3.1. *The operator $\Pi_K^{k,D} : \widetilde{V}_h^K \to \mathbb{P}_k(K)$ is explicitly computable for every $v \in \widetilde{V}_h^K$, using only the information of the linear operators in $\mathbf{D_1} - \mathbf{D_5}$.*

Proof. For all $v_h \in \widetilde{V}_h^K$ we integrate twice by parts on the right-hand side of (2.3.1a). We obtain

$$\begin{aligned} a(v_h, q) &= \int_K D^2 v_h : D^2 q \\ &= \int_K \Delta^2 q v_h - \int_{\partial K} \mathbf{div}(D^2 q)\cdot \nu_K v_h + \int_{\partial K} D^2 q \nu_K \cdot \nabla v_h. \end{aligned} \tag{2.3.2}$$

It is easy to see that since $\Delta^2 q \in \mathbb{P}_{k-4}(K)$ hence the first integral in the right-hand side of (2.3.2) is computable using the output values of the set $\mathbf{D_5}$. We also note that the boundary integrals of (2.3.2) only depends on the boundary values of v_h and ∇v_h, so they are computable using the output values of the sets $\mathbf{D_1} - \mathbf{D_4}$. On the other hand, the kernel part of $\Pi_K^{k,D}$ (cf. (2.3.1b)) is computable using the output values of the sets $\mathbf{D_1} - \mathbf{D_2}$. □

We introduce our local virtual space:

$$V_h^K := \left\{ v_h \in \widetilde{V}_h^K : \int_K (\Pi_K^{k,D} v_h) q = \int_K v_h q \qquad \forall q \in \mathbb{P}^*_{k-3}(K) \cup \mathbb{P}^*_{k-2}(K) \right\}.$$

where $\mathbb{P}^*_\ell(K)$ denotes homogeneous polynomials of degree ℓ with the convention that $\mathbb{P}^*_{-1}(K) = \{0\}$.

Note that $V_h^K \subseteq \widetilde{V}_h^K$. Thus, the linear operator $\Pi_K^{k,D}$ is well defined on V_h^K and computable only using the output values of the sets $\mathbf{D_1} - \mathbf{D_5}$. We also have that $\mathbb{P}_k(K) \subseteq V_h^K$. This will guarantee the good approximation properties of the space.

Moreover, it has been established in [64] that the set of linear operators $\mathbf{D_1} - \mathbf{D_5}$ constitutes a set of degrees of freedom for V_h^K.

Now, we consider the $L^2(K)$ orthogonal projector onto $\mathbb{P}_{k-2}(K)$ as follows: we define $\Pi_K^{k-2} : L^2(K) \to \mathbb{P}_{k-2}(K)$ for each $v \in L^2(K)$ by

$$\int_K (\Pi_K^{k-2} v) q = \int_K v q \qquad \forall q \in \mathbb{P}_{k-2}(K). \tag{2.3.3}$$

Next, due to the particular property appearing in definition of the space V_h^K, it can be seen that the right hand side in (2.3.3) is computable using $\Pi_K^{k,D} v$, and the degrees of freedom given by $\mathbf{D_5}$ and thus $\Pi_K^{k-2} v$ depends only on the values of the degrees of freedom given by $\mathbf{D_1} - \mathbf{D_5}$ when $v \in V_h^K$.

In order to discretize the right hand side of the buckling eigenvalue problem, we will consider the following projector onto $\mathbb{P}_{k-1}(K)^2$: we define $\mathbf{\Pi}_K^{k-1} : H^1(K) \to \mathbb{P}_{k-1}(K)^2$ for each $v \in H^1(K)$ by

$$\int_K (\mathbf{\Pi}_K^{k-1}\nabla v)\cdot \mathbf{q} = \int_K \nabla v \cdot \mathbf{q} \quad \forall \mathbf{q} \in \mathbb{P}_{k-1}(K)^2.$$

In addition, we observe that the for any $v_h \in V_h^K$, the vector function $\mathbf{\Pi}_K^{k-1}\nabla v_h$ can be explicitly computed from the degrees of freedom $\mathbf{D_1} - \mathbf{D_5}$. In fact, in order to compute $\mathbf{\Pi}_K^{k-1}\nabla v_h$, for all $K \in \mathcal{T}_h$ we must be able to calculate the following:

$$\int_K \nabla v_h \cdot \mathbf{q} \qquad \forall \mathbf{q} \in \mathbb{P}_{k-1}(K)^2.$$

From an integration by parts, we have

$$\begin{aligned}\int_K \nabla v_h \cdot \mathbf{q} &= -\int_K v_h \ \mathrm{div}\, \mathbf{q} + \int_{\partial K} v_h(\mathbf{q}\cdot \nu_K) \qquad \forall \mathbf{q} \in \mathbb{P}_{k-1}(K)^2,\\ &= -\int_K \Pi_K^{k-2} v_h \ \mathrm{div}\, \mathbf{q} + \int_{\partial K} v_h(\mathbf{q}\cdot \nu_K) \qquad \forall \mathbf{q} \in \mathbb{P}_{k-1}(K)^2.\end{aligned}$$

The first term on the right-hand side above depends only on the $\Pi_K^{k-2}v_h$ and this depends on the values of the degrees of freedom $\mathbf{D_1} - \mathbf{D_5}$ (cf. (2.3.3)). The second term can also be computed since $\mathbf{q}$ is a polynomial of degree $k-1$ on each edge and therefore is uniquely determined by the values of $\mathbf{D_1} - \mathbf{D_5}$.

Now, we are ready to define our global virtual space to solve the plate buckling eigenvalue problem, this is defined as follows:

$$V_h := \Big\{ v_h \in H_0^2(\Omega) : v_h|_K \in V_h^K \Big\}. \tag{2.3.4}$$

In what follows, we discuss the construction of the discrete version of the local forms. With this aim, we consider $s_K^D(\cdot,\cdot)$ any symmetric positive definite and computable bilinear form to be chosen as to satisfy:

$$c_0 a_K(v_h, v_h) \le s_K^D(v_h, v_h) \le c_1 a_K(v_h, v_h) \quad \forall v_h \in V_h^K \quad \text{with} \quad \Pi_K^{k,D} v_h = 0. \tag{2.3.5}$$

Then, we set

$$\begin{aligned} a_h(u_h, v_h) &:= \sum_{K\in\mathcal{T}_h} a_{h,K}(u_h, v_h), \qquad u_h, v_h \in V_h,\\ b_h(u_h, v_h) &:= \sum_{K\in\mathcal{T}_h} b_{h,K}(u_h, v_h), \qquad u_h, v_h \in V_h,\end{aligned}$$

with $a_{h,K}(\cdot,\cdot)$ and $b_{h,K}(\cdot,\cdot)$ are the local bilinear forms on $V_h^K \times V_h^K$ defined by

$$\begin{aligned} a_{h,K}(u_h, v_h) &:= a_K\big(\Pi_K^{k,D}u_h, \Pi_K^{k,D}v_h\big) + s_K^D\big(u_h - \Pi_K^{k,D}u_h, v_h - \Pi_K^{k,D}v_h\big),\\ b_{h,K}(u_h, v_h) &:= \int_K \boldsymbol{\eta}\mathbf{\Pi}_K^{k-1}\nabla u_h \cdot \mathbf{\Pi}_K^{k-1}\nabla v_h. \end{aligned} \tag{2.3.6}$$

Notice that the bilinear form $s_K^D(\cdot,\cdot)$ has to be actually computable for $u_h, v_h \in V_h^K$.

Proposition 2.3.1. *The local bilinear form $a_{h,K}(\cdot,\cdot)$ on each element K satisfy*

- *Consistency: for all $h>0$ and for all $K\in\mathcal{T}_h$, we have that*

$$a_{h,K}(p,v_h)=a_K(p,v_h)\qquad\forall p\in\mathbb{P}_k(K),\quad\forall v_h\in V_h^K, \tag{2.3.7}$$

- *Stability and boundedness: There exist two positive constants α_1,α_2, independent of K, such that:*

$$\alpha_1 a_K(v_h,v_h)\leq a_{h,K}(v_h,v_h)\leq\alpha_2 a_K(v_h,v_h)\qquad\forall v_h\in V_h^K. \tag{2.3.8}$$

2.3.1 The discrete eigenvalue problem

Now, we are in a position to write the virtual element discretization of Problem 1 as follows.

Problem 2. *Find $(\lambda_h,u_h)\in\mathbb{R}\times V_h$, $u_h\neq 0$, such that*

$$a_h(u_h,v_h)=\lambda_h b_h(u_h,v_h)\qquad\forall v_h\in V_h. \tag{2.3.9}$$

We observe that by virtue of (2.3.8), the bilinear form $a_h(\cdot,\cdot)$ is bounded. Moreover, as shown in the following lemma, it is also uniformly elliptic.

Lemma 2.3.2. *There exists a constant $\alpha>0$, independent of h, such that*

$$a_h(v_h,v_h)\geq\alpha\,\|v_h\|_{2,\Omega}^2\qquad\forall v_h\in V_h.$$

Proof. Thanks to (2.3.8) and Lemma 2.2.1, it is easy to check that the above inequality holds with $\alpha:=\alpha_0\min\{\alpha_1,1\}$. □

In order to analyze the discrete problem, we introduce the solution operator associated to Problem 2 as follows:

$$\begin{aligned}T_h:H_0^2(\Omega)&\longrightarrow H_0^2(\Omega),\\ f&\longmapsto T_hf:=w_h,\end{aligned}$$

with w_h the unique solution of the following source problem

$$a_h(w_h,v_h)=b_h(f,v_h)\qquad\forall v_h\in V_h. \tag{2.3.10}$$

Note that the ellipticity of $a_h(\cdot,\cdot)$ established in Lemma 2.3.2, the boundedness of the right hand side (cf. (2.3.6)) and Lax-Milgram Lemma guarantee that T_h is well defined. Moreover, as in the continuous case, $(\lambda_h,u_h)\in\mathbb{R}\times V_h$ solves problem (2.3.9) if and only if $T_hu_h=\mu_hu_h$ with $\mu_h\neq 0$ and $u_h\neq 0$, in which case $\mu_h:=\frac{1}{\lambda_h}$.

Remark 2.3.1. *The same arguments leading to Remark 2.2.1 allow us to show that any solution of (2.3.9) satisfies $\lambda_h\neq 0$. Moreover, $b_h(u_h,u_h)\neq 0$ also holds true.*

Moreover from the definition of $a_h(\cdot,\cdot)$ and $b_h(\cdot,\cdot)$ we can check that T_h is self-adjoint with respect to inner product $a_h(\cdot,\cdot)$. Therefore, we can describe the spectrum of the solution operator T_h.

Now, we are in position to write the following characterization of the spectrum of the solution operator.

Theorem 2.3.1. *The spectrum of T_h consists of $M_h := \dim(V_h)$ eigenvalues, repeated according to their respective multiplicities. The spectrum decomposes as follows: $\mathrm{sp}(T_h) = \{0\} \cup \{\mu_h\}_{k=1}^{\kappa}$, where $\kappa = M_h - \dim Z_h$ with $Z_h := \{u_h \in V_h : b_h(u_h, v_h) = 0 \quad \forall v_h \in V_h\}$. The eigenvalues μ_h are all real and non-zero.*

2.4 Convergence and error estimates

In this section we will establish convergence and error estimates of the proposed VEM discretization. With this aim, we will prove that T_h provides a correct spectral approximation of T using the classical theory for compact operators (see [11]).

We start with the following approximation result, on star-shaped polygons, which is derived by interpolation between Sobolev spaces (see for instance [84, Theorem I.1.4] from the analogous result for integer values of s). We mention that this result has been stated in [12, Proposition 4.2] for integer values and follows from the classical Scott-Dupont theory (see [38] and [7, Proposition 3.1]):

Proposition 2.4.1. *There exists a constant $C > 0$, such that for every $v \in H^\delta(K)$ there exists $v_\pi \in \mathbb{P}_k(K)$, $k \geq 0$ such that*

$$|v - v_\pi|_{\ell,K} \leq C h_K^{\delta-\ell} |v|_{\delta,K} \quad 0 \leq \delta \leq k+1, \ell = 0, \ldots, [\delta],$$

with $[\delta]$ denoting largest integer equal or smaller than $\delta \in \mathbb{R}$.

In what follows, we write several auxiliary results which will be useful in the forthcoming analysis. First, we write standard error estimations for the projector $\mathbf{\Pi}_K^{k-1}$.

Lemma 2.4.1. *There exists $C > 0$ independent of h such that for all $\mathbf{v} \in H^\delta(K)^2$*

$$\|\mathbf{v} - \mathbf{\Pi}_K^{k-1}\mathbf{v}\|_{0,K} \leq C h_K^{\delta} |\mathbf{v}|_{\delta,K} \quad 0 \leq \delta \leq k+1.$$

Now, we present an interpolation result in the virtual space V_h (see [7, 27]).

Proposition 2.4.2. *Assume **A1**–**A2** are satisfied, then for all $v \in H^s(K)$ there exist $v_I \in V_h$ and $C > 0$ independent of h such that*

$$||v - v_I||_{l,K} \leq C h_K^{s-l} |v|_{s,K}, \quad l = 0, 1, 2, \quad 2 \leq s \leq k+1.$$

Now, in order to prove the convergence of our method, we introduce the following broken H^s-seminorm ($s = 1, 2$):

$$|v|_{s,h} := \Big(\sum_{K \in \mathcal{T}_h} |v|_{s,K}^2 \Big)^{1/2},$$

which is well defined for every $v \in L^2(\Omega)$ such that $v|_K \in H^s(K)$ for all polygon $K \in \mathcal{T}_h$.

Now, with these definitions we have the following results.

Lemma 2.4.2. *There exists $C>0$ such that, for all $f\in H_0^2(\Omega)$, if $w=Tf$ and $w_h=T_hf$, then*

$$\|(T-T_h)\,f\|_{2,\Omega}=\|w-w_h\|_{2,\Omega}\leq C\Big(h||f||_{2,\Omega}+\|w-w_I\|_{2,\Omega}+|w-w_\pi|_{2,h}\Big),$$

for all $w_I\in V_h$ and for all $w_\pi\in L^2(\Omega)$ such that $w_\pi|_K\in\mathbb{P}_k(K)\quad\forall K\in\mathcal{T}_h$.

Proof. Let $f\in H_0^2(\Omega)$, and $w=Tf$ and $w_h=T_hf$. For $w_I\in V_h$, we set $v_h:=w_h-w_I$. Thus

$$||(T-T_h)f||_{2,\Omega}\leq||w-w_I||_{2,\Omega}+||v_h||_{2,\Omega}. \tag{2.4.1}$$

Now, thanks to Lemma 2.3.2, the definition of $a_{h,K}(\cdot,\cdot)$ and those of T and T_h, we have

$$\begin{aligned}
\alpha||v_h||_{2,\Omega}^2\leq a_h(v_h,v_h)&=a_h(w_h,v_h)-a_h(w_I,v_h)=a_h(w_h,v_h)-\sum_{K\in\mathcal{T}_h}a_{h,K}(w_I,v_h)\\
&=a_h(w_h,v_h)-\sum_{K\in\mathcal{T}_h}\Big\{a_{h,K}(w_I-w_\pi,v_h)+a_{h,K}(w_\pi,v_h)\Big\}\\
&=a_h(w_h,v_h)-\sum_{K\in\mathcal{T}_h}\Big\{a_{h,K}(w_I-w_\pi,v_h)+a_K(w_\pi-w,v_h)+a_K(w,v_h)\Big\}\\
&=a_h(w_h,v_h)-a(w,v_h)-\sum_{K\in\mathcal{T}_h}\Big\{a_{h,K}(w_I-w_\pi,v_h)+a_K(w_\pi-w,v_h)\Big\}.
\end{aligned}\tag{2.4.2}$$

We bound each term on the right hand side of (2.4.2). The first term can be estimated as follows

$$\begin{aligned}
&a_h(w_h,v_h)-a(w,v_h)=b_h(f,v_h)-b(f,v_h)\\
&=\sum_{K\in\mathcal{T}_h}\left\{\int_K\{\boldsymbol{\eta}\boldsymbol{\Pi}_K^{k-1}\nabla f\cdot\boldsymbol{\Pi}_K^{k-1}\nabla v_h-\boldsymbol{\eta}\nabla f\cdot\nabla v_h\}\right\}\\
&=\sum_{K\in\mathcal{T}_h}\left\{\int_K\{\boldsymbol{\eta}\boldsymbol{\Pi}_K^{k-1}\nabla f\cdot\boldsymbol{\Pi}_K^{k-1}\nabla v_h-\boldsymbol{\eta}\nabla f\cdot\boldsymbol{\Pi}_K^{k-1}\nabla v_h+\boldsymbol{\eta}\nabla f\cdot\boldsymbol{\Pi}_K^{k-1}\nabla v_h-\boldsymbol{\eta}\nabla f\cdot\nabla v_h\}\right\}\\
&=\sum_{K\in\mathcal{T}_h}\left\{\int_K\{\boldsymbol{\eta}\left(\boldsymbol{\Pi}_K^{k-1}\nabla f-\nabla f\right)\cdot\boldsymbol{\Pi}_K^{k-1}\nabla v_h+\boldsymbol{\eta}\nabla f\cdot\left(\boldsymbol{\Pi}_K^{k-1}\nabla v_h-\nabla v_h\right)\}\right\}\\
&\leq\sum_{K\in\mathcal{T}_h}C\left\{\|\boldsymbol{\Pi}_K^{k-1}\nabla f-\nabla f\|_{0,K}\|\boldsymbol{\Pi}_K^{k-1}\nabla v_h\|_{0,K}+\|\nabla f\|_{0,K}\|\boldsymbol{\Pi}_K^{k-1}\nabla v_h-\nabla v_h\|_{0,K}\right\}\\
&\leq Ch\|f\|_{2,\Omega}\|v_h\|_{2,\Omega},
\end{aligned}$$

where we have used Lemma 2.4.1 in the last inequality. Notice taht the constant $C>0$ depends on $\|\boldsymbol{\eta}\|_\infty$.

Next, using the stability of $a_{h,K}(\cdot,\cdot)$, the Cauchy-Schwarz and triangular inequalities in the second term on the right hand side of (2.4.2), we have

$$\alpha\,\|v_h\|_{2,\Omega}^2\leq C\Big(h||f||_{2,\Omega}+\|w-w_I\|_{2,\Omega}+|w-w_\pi|_{2,h}\Big)\|v_h\|_{2,\Omega}.$$

Thus, the result follows from the previous bounds together with (2.4.2). □

Now we are in a position to prove that the operator T_h converges in norm to T.

Theorem 2.4.1. *For all $f \in H_0^2(\Omega)$, there exist $\tilde{s} \in (\frac{1}{2}, 1]$ and $C > 0$ independent of h such that*

$$||(T - T_h)f||_{2,\Omega} \leq Ch^{\tilde{s}}||f||_{2,\Omega}.$$

Proof. The proof is obtained from Lemma 2.4.2 and Propositions 2.4.1 and 2.4.2 and Lemma 2.2.2. □

Next, we will use the classical theory for compact operators (see [11] for instance) in order to prove convergence and error estimates for eigenfunctions and eigenvalues. Indeed, an immediate consequence of Theorem 2.4.1 is that isolated parts of $\mathrm{sp}(T)$ are approximated by isolated parts of $\mathrm{sp}(T_h)$. It means that if μ is a nonzero eigenvalue of T with algebraic multiplicity m, hence there exist m eigenvalues $\mu_h^{(1)}, \ldots, \mu_h^{(m)}$ of T_h (repeated according to their respective multiplicities) that will converge to μ as h goes to zero.

Now, let us denote by $\mathcal{E}$ and $\mathcal{E}_h$ the eigenspace associated to the eigenvalue μ and the spanned of the eigenspaces associated to $\mu_h^{(1)}, ..., \mu_h^{(m)}$, respectively.

We also recall the definition of the *gap* $\widehat{\delta}$ between two closed subspaces $\mathcal{X}$ and $\mathcal{Y}$ of a Hilbert space $\mathcal{V}$:

$$\widehat{\delta}(\mathcal{X}, \mathcal{Y}) := \max\left\{\delta(\mathcal{X}, \mathcal{Y}), \delta(\mathcal{Y}, \mathcal{X})\right\},$$

where

$$\delta(\mathcal{X}, \mathcal{Y}) := \sup_{\mathbf{x} \in \mathcal{X}:\ \|x\|_{\mathcal{V}}=1} \delta(x, \mathcal{Y}), \quad \text{with } \delta(x, \mathcal{Y}) := \inf_{y \in \mathcal{Y}} \|x - y\|_{\mathcal{V}}.$$

We also define

$$\gamma_h := \sup_{f \in \mathcal{E}: ||f||_{2,\Omega}=1} ||(T - T_h)f||_{2,\Omega}.$$

The following error estimates for the approximation of eigenvalues and eigenfunctions hold true which is obtained from Theorems 7.1 and 7.3 from [11].

Theorem 2.4.2. *There exists a strictly positive constant C such that*

$$\begin{aligned} \widehat{\delta}(\mathcal{E}, \mathcal{E}_h) &\leq C\gamma_h, \\ \left|\mu - \mu_h^{(j)}\right| &\leq C\gamma_h \qquad \forall j = 1, \ldots, m. \end{aligned}$$

Moreover, employing the additional regularity of the eigenfunctions, we immediately obtain the following bound.

Theorem 2.4.3. *There exist $s > 1/2$ and $C > 0$ independent of h such that*

$$||(T - T_h)f||_{2,\Omega} \leq Ch^{\min\{s,k-1\}}||f||_{2,\Omega} \qquad \forall f \in \mathcal{E}, \tag{2.4.3}$$

and as a consequence,

$$\gamma_h \leq Ch^{\min\{s,k-1\}}. \tag{2.4.4}$$

Proof. The inequality (2.4.3) can be obtained by repeating the same steps like in the proof of the Theorem 2.4.1 and Lemma 2.2.2. Estimate (2.4.4) follows from the definition of γ_h and (2.4.3). □

Remark 2.4.1. *The error estimate obtained for the eigenpair (μ, u) of T in Theorem 2.4.2 implies similar estimates for the eigenpair $(\lambda := 1/\mu, u)$ of Problem 1 by means of the discrete eigenvalues $\lambda_h^{(j)} = 1/\mu_h^{(j)}, 1 \leq j \leq m$.*

Now, in what follows we will prove a double order of convergence for the eigenvalue approximation. To prove this, we are going to assume that $\boldsymbol{\eta}$ is a smooth enough tensor.

Theorem 2.4.4. *There exists a positive constant independent of h such that*

$$|\lambda - \lambda_h^{(j)}| \leq Ch^{2\min\{s,k-1\}} \qquad \forall j = 1, \ldots, m.$$

Proof. Let $u_h \in \mathcal{E}_h$ be an eigenfunction corresponding to one of the eigenvalues $\lambda_h^{(j)}$, $j = 1, \ldots, m$, with $||u_h||_{2,\Omega} = 1$. From Theorem 2.4.2, we have that there exists $u \in \mathcal{E}$ satisfying

$$||u - u_h||_{2,\Omega} \leq C\gamma_h. \tag{2.4.5}$$

It is easy to see that from the symmetry of the bilinear forms in the continuous and discrete spectral problems (cf. Problem 1 and Problem 2), we have

$$\begin{aligned} a(u-u_h, u-u_h) - \lambda b(u-u_h, u-u_h) &= a(u_h, u_h) - \lambda b(u_h, u_h) \\ &= a(u_h, u_h) - a_h(u_h, u_h) + \lambda_h^{(j)} b_h(u_h, u_h) - \lambda b(u_h, u_h) \\ &= a(u_h, u_h) - a_h(u_h, u_h) + (\lambda_h^{(j)} - \lambda) b_h(u_h, u_h) + \lambda[b_h(u_h, u_h) - b(u_h, u_h)], \end{aligned}$$

and therefore we have the following identity

$$\begin{aligned} (\lambda_h^{(i)} - \lambda) b_h(u_h, u_h) = a(u-u_h, u-u_h) - \lambda b(u-u_h, u-u_h) \\ + (a_h(u_h, u_h) - a(u_h, u_h)) + \lambda \left[b(u_h, u_h) - b_h(u_h, u_h)\right]. \end{aligned} \tag{2.4.6}$$

Now, we will bound each term on the right hand side of (2.4.6). For the first and second term we deduce

$$a(u-u_h, u-u_h) = |u-u_h|_{2,\Omega}^2 \leq C\gamma_h^2,$$

and

$$b(u-u_h, u-u_h) = \int_\Omega \boldsymbol{\eta} \boldsymbol{\Pi}_K^{k-1} \nabla(u-u_h) \cdot \boldsymbol{\Pi}_K^{k-1} \nabla(u-u_h) \leq \|\boldsymbol{\eta}\|_\infty ||u-u_h||_{2,\Omega}^2 \leq C\gamma_h^2.$$

Thus, we obtain

$$|a(u-u_h, u-u_h) - \lambda b(u-u_h, u-u_h)| \leq C\gamma_h^2. \tag{2.4.7}$$

Next, to bound the third term, we consider $u_\pi \in L^2(\Omega)$ such that $u_\pi|_K \in \mathbb{P}_k(K)$ for all $K \in \mathcal{T}_h$ and the Proposition 2.4.1 holds true. Hence, using the properties (2.3.7) and (2.3.8) of $a_{h,K}(\cdot,\cdot)$, we have

$$\begin{aligned} |a_h(u_h, u_h) - a(u_h, u_h)| &= \Big| \sum_{K \in \mathcal{T}_h} \Big\{ a_{h,K}(u_h - u_\pi, u_h) - a_K(u_h - u_\pi, u_h) \Big\} \Big| \\ &\leq \sum_{K \in \mathcal{T}_h} (1 + \alpha_2) a_K(u_h - u_\pi, u_h - u_\pi) \\ &\leq C \sum_{K \in \mathcal{T}_h} |u_h - u_\pi|_{2,K}^2. \end{aligned}$$

Then, adding and subtracting u, using the triangular inequality, Proposition 2.4.1 and (2.4.5), we get

$$|a_h(w_h, w_h) - a(w_h, w_h)| \leq C\{\gamma_h^2 + h^{2\min\{s,k-1\}}\}. \tag{2.4.8}$$

On the other hand, the fourth term can be treated as follows:

$$\begin{aligned} b(u_h, u_h) - b_h(u_h, u_h) &= \sum_{K\in\mathcal{T}_h} \left\{ \int_K \boldsymbol{\eta}\nabla u_h \cdot \nabla u_h - \int_K \boldsymbol{\eta}\boldsymbol{\Pi}_K^{k-1}\nabla u_h \cdot \boldsymbol{\Pi}_K^{k-1}\nabla u_h \right\}. \\ &= \sum_{K\in\mathcal{T}_h} \left\{ \underbrace{\int_K \boldsymbol{\eta}\nabla u_h \cdot (\nabla u_h - \boldsymbol{\Pi}_K^{k-1}\nabla u_h)}_{E_1} + \underbrace{\int_K (\nabla u_h - \boldsymbol{\Pi}_K^{k-1}\nabla u_h) \cdot \boldsymbol{\eta}\boldsymbol{\Pi}_K^{k-1}\nabla u_h}_{E_2} \right\}. \end{aligned}$$

Now, we bound the terms E_1 and E_2. We start with E_1:

$$\begin{aligned} E_1 &= \int_K (\boldsymbol{\eta}\nabla u_h - \boldsymbol{\Pi}_K^{k-1}(\boldsymbol{\eta}\nabla u)) \cdot (\nabla u_h - \boldsymbol{\Pi}_K^{k-1}\nabla u_h) \\ &= \int_K \Big(\boldsymbol{\eta}\nabla u_h - \boldsymbol{\eta}\nabla u + \boldsymbol{\eta}\nabla u - \boldsymbol{\Pi}_K^{k-1}(\boldsymbol{\eta}\nabla u)\Big) \cdot \Big(\nabla u_h - \nabla u + \nabla u - \boldsymbol{\Pi}_K^{k-1}\nabla u + \boldsymbol{\Pi}_K^{k-1}(\nabla u - \nabla u_h)\Big) \\ &\leq Ch^{2\min\{s,k-1\}}, \end{aligned}$$

where in the last inequality we have used the triangular inequality, the approximation properties for $\boldsymbol{\Pi}_K^{k-1}$ (cf. Lemma 2.4.1), the additional regularity for the stress tensor $\boldsymbol{\eta}$ and the additional regularity for the eigenfunctions and finally (2.4.5) together with (2.4.4).

For the term E_2, we repeat the same arguments used to bound E_1, we obtain that

$$E_2 \leq Ch^{2\min\{s,k-1\}}. \tag{2.4.9}$$

On the other hand, from Problem 2, Lemma 2.3.2 and the fact $\lambda_h^{(j)} \to \lambda$ when $h \to 0$, we have

$$|b_h(u_h, u_h)| = |\frac{1}{\lambda_h^{(j)}} a_h(u_h, u_h)| \geq \frac{\alpha}{|\lambda_h^{(j)}|}||u_h||_{2,\Omega}^2 = \frac{\alpha}{|\lambda_h^{(j)}|} = C > 0$$

Thus, the proof follows from the above bound together with estimates (2.4.6)-(2.4.9). □

2.5 Numerical results

In this section, we report some numerical experiments to approximate the buckling coefficients considering different configurations of the problem, in order to confirm the theoretical results presented in this work for the cases $k = 2$ and $k = 3$. With this purpose, we have implemented in a MATLAB code the proposed discretization, following the arguments presented in [16].

To complete the construction of the discrete bilinear form, we have taken the symmetric form $s_K^D(\cdot,\cdot)$ as the euclidean scalar product associated to the degrees of freedom, properly scaled to satisfy (2.3.5) (see [7, 64, 105] for further details).

On the other hand, we have tested the method by using different families of meshes (see Figure 2.1):

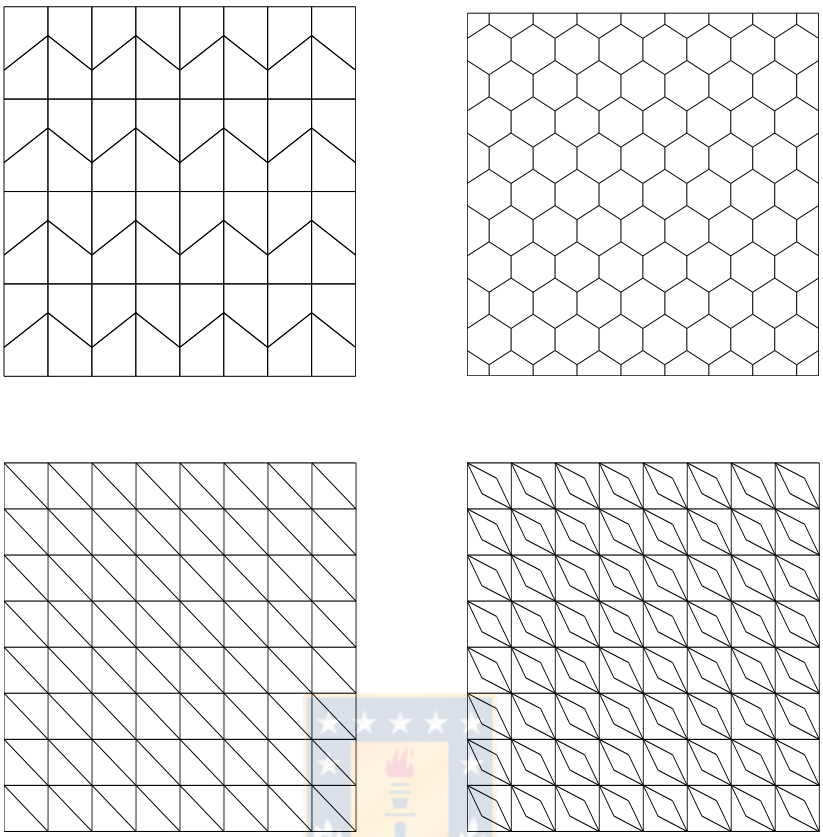

Figure 2.1: Sample meshes: $\mathcal{T}_h^1$ (top left), $\mathcal{T}_h^2$ (top right), $\mathcal{T}_h^3$ (bottom left) and $\mathcal{T}_h^4$ (bottom right), for $N = 8$ (figure produced by the author).

- $\mathcal{T}_h^1$: trapezoidal meshes which consist of partitions of the domain into $N \times N$ congruent trapezoids, all similar to the trapezoid with vertices $(0,0)$, $(1/2,0)$, $(1/2,2/3)$ and $(0,1/3)$;
- $\mathcal{T}_h^2$: hexagonal meshes;
- $\mathcal{T}_h^3$: triangular meshes;
- $\mathcal{T}_h^4$: distorted concave rhombic quadrilaterals.

We have used successive refinements of an initial mesh (see Figure 2.1). The refinement parameter N used to label each mesh is the number of elements on each edge of the plate.

We have chosen two configurations for the computational domain Ω: $\Omega_S := (0,1) \times (0,1)$ and $\Omega_L := (0,1) \times (0,1) \backslash [1/2,1) \times [1/2,1)$. Even though our theoretical analysis has been developed only for clamped plates, we will consider in Section 2.5.3 other boundary conditions.

In order to compare our results for the buckling problem, we introduce a non-dimensional buckling

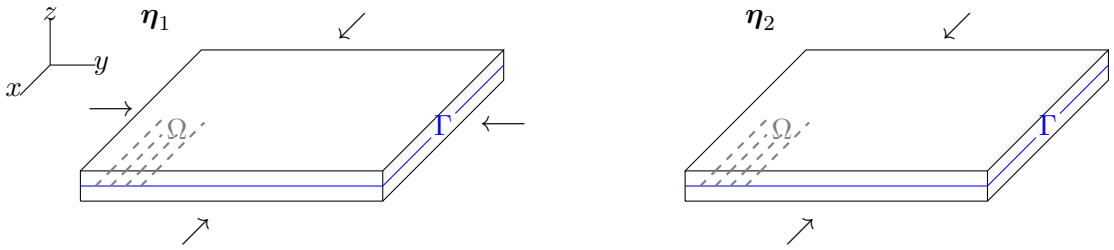

Figure 2.2: $\boldsymbol{\eta}_1$ (left) correspond to a uniformly compressed plate (in the x, y directions) and $\boldsymbol{\eta}_2$ (right) correspond to a plate subjected to uniaxial compression (in the x direction) (figure produced by the author).

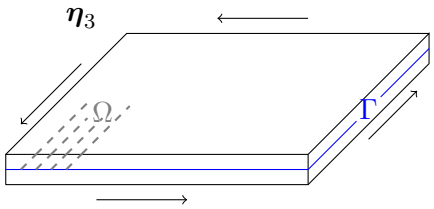

Figure 2.3: $\boldsymbol{\eta}_3$ correspond to a plate subjected to shear load (figure produced by the author).

coefficient, which is defined as:

$$\widehat{\lambda}_h^{(j)} := \frac{\lambda_h^{(j)} L}{\pi^2}, \tag{2.5.10}$$

where L is the plate side length.

Moreover, we will consider different in-plane compressive stress $\boldsymbol{\eta}$. More precisely, we will compute the non-dimensional buckling coefficients using the following $\boldsymbol{\eta}$:

$$\boldsymbol{\eta}_1 := \begin{pmatrix} 1 & 0 \\ 0 & 1 \end{pmatrix}, \qquad \boldsymbol{\eta}_2 := \begin{pmatrix} 1 & 0 \\ 0 & 0 \end{pmatrix}, \qquad \boldsymbol{\eta}_3 := \begin{pmatrix} 0 & 1 \\ 1 & 0 \end{pmatrix}.$$

The physical meaning of the tensors $\boldsymbol{\eta}_1, \boldsymbol{\eta}_2$ and $\boldsymbol{\eta}_3$ is illustrated in Figures 2.2 and 2.3, respectively.

2.5.1 Clamped square plate

In this numerical test we compute the non-dimensional buckling coefficients (cf. 2.5.10) for a uniformly compressed square plate Ω_S. This corresponds to the stress field $\boldsymbol{\eta}_1$

We report in Table 2.1 the four lowest non-dimensional buckling coefficients computed with the virtual element method analyzed in this chapter. The polynomial degrees are given by $k = 2, 3$ and with two different families of meshes and $N = 32, 64, 128$. The table includes orders of convergence as well as accurate values extrapolated by means of a least-squares fitting. In the last row of the table, we show the values obtained by extrapolating those computed with different method presented in [106].

Table 2.1: Lowest non-dimensional buckling coefficients $\widehat{\lambda}_h^i$, $i = 1, 2, 3, 4$ of a clamped square plate subjected to a plane stress field $\boldsymbol{\eta}_1$ (table produced by the author).

Mesh	k	N	$\widehat{\lambda}_h^1$	$\widehat{\lambda}_h^2$	$\widehat{\lambda}_h^3$	$\widehat{\lambda}_h^4$
		32	5.2724	9.1716	9.2744	12.8252
		64	5.2952	9.2906	9.3174	12.9461
$\mathcal{T}_h^2$	2	128	5.3014	9.3229	9.3297	12.9786
		Order	1.86	1.88	1.80	1.89
		Extrap.	5.3038	9.3350	9.3347	12.9907
		32	5.3037	9.3345	9.3347	12.9918
		64	5.3036	9.3342	9.3342	12.9904
$\mathcal{T}_h^2$	3	128	5.3036	9.3342	9.3342	12.9904
		Order	3.95	3.95	3.94	3.93
		Extrap.	5.3036	9.3342	9.3342	12.9903
		32	5.3192	9.3581	9.3968	13.0934
		64	5.3075	9.3401	9.3498	13.0162
$\mathcal{T}_h^4$	2	128	5.3046	9.3356	9.3381	12.9968
		Order	2.00	2.00	2.00	1.99
		Extrap.	5.3036	9.3342	9.3341	12.9903
		32	5.3039	9.3348	9.3353	12.9939
		64	5.3036	9.3342	9.3342	12.9906
$\mathcal{T}_h^4$	3	128	5.3036	9.3342	9.3342	12.9904
		Order	3.94	3.93	3.93	3.91
		Extrap.	5.3036	9.3342	9.3342	12.9903
[106]			5.3037	9.3337	9.3337	12.9909

In this case, since Ω_S is convex, the problem have smooth eigenfunctions, as a consequence, when using degree k, the order of convergence is $2(k-1)$ as the theory predicts (cf. Theorem 2.4.4). Moreover, the results obtained by the two methods agree perfectly well.

In the next test we compute once again the non-dimensional buckling coefficients (in absolute value) of the same plate as in the previous example, subjected to a uniform shear load. This corresponds to the stress field $\boldsymbol{\eta}_3$.

In Table 2.2 we report the four lowest non-dimensional buckling coefficients (in absolute value) considering the stress field $\boldsymbol{\eta}_3$. Once again, the polynomial degrees are given by $k = 2, 3$ and with two different families of meshes and $N = 32, 64, 128$. The table includes orders of convergence as well as accurate values extrapolated by means of a least-squares fitting. In the last row of the table, we show the values obtained by extrapolating those computed with different method presented in [106].

Once again, it can be clearly observed from Table 2.2 that our method computes the scaled buckling coefficients (cf.2.5.10) with an optimal order of convergence and that the agreement with the method from [106] is excellent.

We show in Figure 2.4 the buckling mode associated with the lowest scaled buckling coefficient.

Table 2.2: Lowest non-dimensional buckling coefficients (in absolute value) $\widehat{\lambda}_h^i$, $i = 1, 2, 3, 4$ of a clamped square plate subjected to a plane stress tensor field $\boldsymbol{\eta}_3$ (table produced by the author).

Mesh	k	N	$\widehat{\lambda}_h^1$	$\widehat{\lambda}_h^2$	$\widehat{\lambda}_h^3$	$\widehat{\lambda}_h^4$
		32	14.6083	16.8405	33.2148	35.2101
		64	14.6331	16.8983	33.3053	35.2700
$\mathcal{T}_h^1$	2	128	14.6397	16.9137	33.3319	35.2888
		Order	1.89	1.92	1.77	1.67
		Extrap.	14.6422	16.9191	33.3429	35.2974
		32	14.6470	16.9242	33.3795	35.3423
		64	14.6423	16.9192	33.3437	35.2986
$\mathcal{T}_h^1$	3	128	14.6420	16.9189	33.3413	35.2957
		Order	3.93	3.95	3.90	3.89
		Extrap.	14.6420	16.9188	33.3411	35.2954
		36	14.6330	16.9071	33.2479	35.1883
		64	14.6398	16.9159	33.3178	35.2685
$\mathcal{T}_h^3$	2	128	14.6415	16.9181	33.3353	35.2887
		Order	2.02	2.01	1.99	1.99
		Extrap.	14.6420	16.9188	33.3412	35.2955
		32	14.6455	16.9214	33.3536	35.3098
		64	14.6423	16.9190	33.3421	35.2966
$\mathcal{T}_h^3$	3	128	14.6420	16.9189	33.3412	35.2955
		Order	3.63	3.71	3.65	3.62
		Extrap.	14.6420	16.9188	33.3411	35.2954
[106]			14.6420	16.9195	33.3376	-

2.5.2 Clamped L-shaped plate

In this numerical test, we consider an L-shaped domain: Ω_L. We have used triangular and concave meshes as those shown in $\mathcal{T}_h^3$ and $\mathcal{T}_h^4$, respectively (see Figure 2.1). Once again, the refinement parameter N is the number of elements on each edge.

Table 2.3 reports the four lowest non-dimensional buckling coefficient computed with the method analyzed in this chapter with polynomial degree $k = 2$. We include in this table orders of convergence, as well as accurate values extrapolated by means of a least-squares fitting again. In the last row of the table, we show the values obtained by extrapolating those computed with different method presented in [106].

We observe that for the lowest non-dimensional buckling coefficient, the method converges with order close to 1.089, which is the expected one because of the singularity of the solution (see [85]). For the other non-dimensional buckling coefficients, the method converges with larger orders.

We show in Figure 2.5 the buckling mode associated with the lowest scaled buckling coefficient.

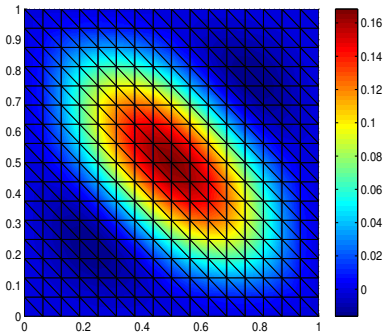

Figure 2.4: Test 1. Buckling mode associated to the first non-dimensional buckling coefficient of a square plate subjected to a plane stress tensor field $\boldsymbol{\eta}_3$ (figure produced by the author).

Table 2.3: Four lowest non-dimensional buckling coefficient of a clamped L-shaped plate and subjected to a plane stress tensor field $\boldsymbol{\eta}_1$ (table produced by the author).

Mesh	k	N	$\widehat{\lambda}_{1h}$	$\widehat{\lambda}_{2h}$	$\widehat{\lambda}_{3h}$	$\widehat{\lambda}_{4h}$
		32	13.1749	15.0809	17.0798	19.9445
		64	13.0847	15.0234	17.0203	19.8758
$\mathcal{T}_h^3$	2	128	13.0495	15.0083	17.0042	19.8582
		Order	1.36	1.93	1.89	1.97
		Extrap.	13.0271	15.0029	16.9983	19.8522
		32	13.1949	15.1399	17.1801	20.1590
		64	13.0903	15.0388	17.0453	19.9297
$\mathcal{T}_h^4$	2	128	13.0511	15.0124	17.0105	19.8717
		Order	1.41	1.94	1.95	1.98
		Extrap.	13.0274	15.0031	16.9983	19.8519
		[106]	13.0290	15.0036	16.9949	-

2.5.3 Simply supported-free square plate

In this final test, which is not covered by our theory since our theoretical results has been developed only for clamped plates, we have computed the non-dimensional buckling coefficient of a simply supported-free square plate, subjected to linearly varying in-plane load in one direction (x direction). This corresponds to a plane stress field given by

$$\widetilde{\boldsymbol{\eta}}_2 := \begin{pmatrix} 1-\alpha\frac{y}{L} & 0 \\ 0 & 0 \end{pmatrix}, \tag{2.5.11}$$

with values of α in $\{0, 2/3, 1, 4/3, 2\}$. We observe that for $\alpha = 0$, we obtain the plane stress tensor field $\boldsymbol{\eta}_2$.

We take an square plate Ω_S which has two simply supported edges and two free edges.

We report in Table 2.4 the non-dimensional buckling coefficient. The polynomial degrees are given

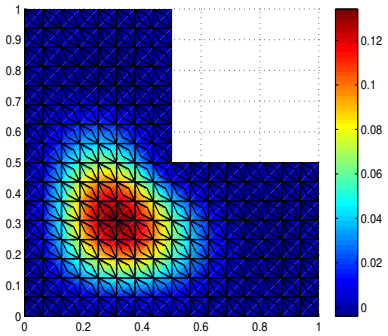

Figure 2.5: Test 2. Buckling mode associated to the first non-dimensional buckling coefficient of a clamped L-shaped plate subjected to a plane stress tensor field $\boldsymbol{\eta}_1$ (figure produced by the author).

by $k = 2, 3$ and the family of meshes $\mathcal{T}_h^2$ with $N = 32, 64, 128$. The table includes computed orders of convergence and extrapolated more accurate values of each eigenvalue obtained by means of a least-squares fitting.

Table 2.4: Non-dimensional buckling coefficient $\widehat{\lambda}_{1h}$ for different values of α of a square plate with mixed boundary conditions and subjected to linearly varying in-plane load in one direction $\widetilde{\boldsymbol{\eta}}_2$ (table produced by the author).

Mesh	k	N	$\alpha = 0$	$\alpha = 2/3$	$\alpha = 1$	$\alpha = 4/3$	$\alpha = 2$
		32	0.9984	1.4474	1.7763	2.1687	3.0676
		64	0.9996	1.4490	1.7782	2.1709	3.0702
$\mathcal{T}_h^2$	2	128	0.9999	1.4495	1.7787	2.1715	3.0710
		Order	1.91	1.90	1.90	1.88	1.85
		Extrap.	1.0000	1.4496	1.7789	2.1717	3.0713
		32	1.0000	1.4496	1.7789	2.1717	3.0712
		64	1.0000	1.4496	1.7789	2.1717	3.0712
$\mathcal{T}_h^2$	3	128	1.0000	1.4496	1.7789	2.1717	3.0712
		Order	4.00	4.00	4.00	4.00	4.00
		Extrap.	1.0000	1.4496	1.7789	2.1717	3.0712

It can be clearly observed from Table 2.4 that the proposed virtual scheme computes the scaled buckling coefficient (cf. 2.5.10) with an optimal order of convergence for all the values of α.

Finally, we show in Figure 2.6 the buckling mode associated with the lowest scaled buckling coefficient for different values of the parameter α.

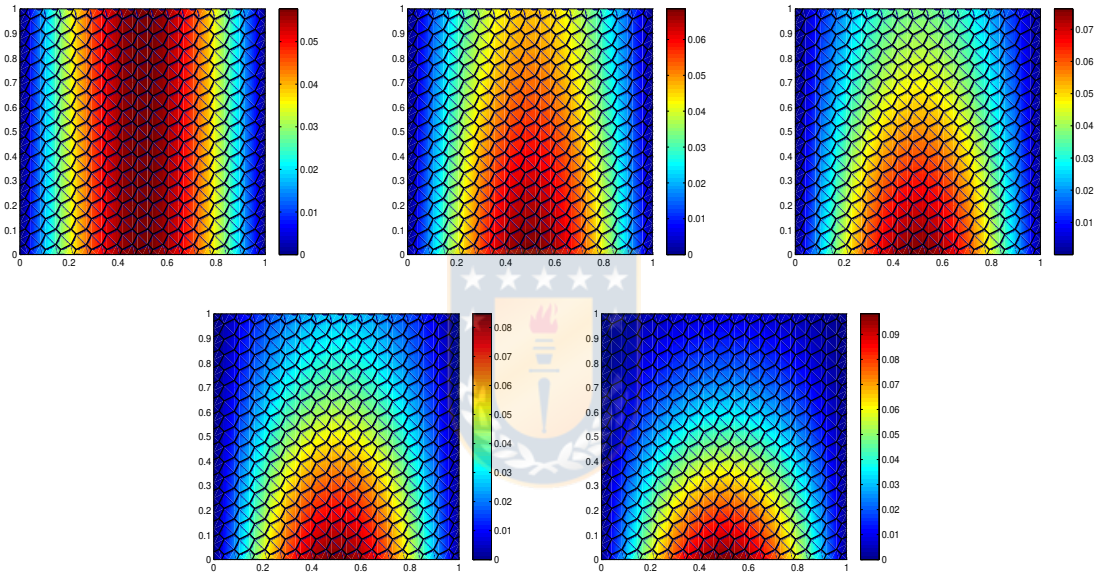

Figure 2.6: Test 3. Buckling modes associated to the first non-dimensional buckling coefficient $\widehat{\lambda}_{1h}$ of a square plate with mixed boundary conditions and subjected to linearly varying in-plane load in one direction $\widetilde{\boldsymbol{\eta}}_2$ (cf. (2.5.11)): $\alpha = 0$ (top left), $\alpha = 2/3$ (top middle), $\alpha = 1$ (top right), $\alpha = 4/3$ (bottom left), $\alpha = 2$ (bottom right) (figure produced by the author).

CHAPTER 3

A virtual element method for the von Kármán equations

3.1 Introduction

The von Kármán equations is a fourth order system of nonlinear partial differential equations that model the deformation of very thin plates. This system consists of two unknowns, which describe the transverse displacement and the boundary stresses of the plate, respectively [65]. This model has attracted great interest in the scientific community since it is frequently encountered in several engineering applications such as the design of cars and aircrafts (see [82, 124]).

Results on existence of solutions of the von Kármán system have been stated in [65, 68]. In general the problem has not a unique solution. However, sufficient conditions that guarantee uniqueness of isolated solutions are established in [40]. Due to the importance of this problem, several finite element methods have been developed to approximate the isolated solutions of a von Kármán plate. For instance, a general technique based on any conforming discretization was introduced in [40], convergence and optimal error bounds in the energy norm are presented considering the standard formulation in H^2. Then, in [96] a conforming finite element method was analyzed to approximate the isolated solutions of the von Kármán problem, using Bogner-Fox-Schmit elements, and they also obtained error estimates in H^1 and L^2 norms using a duality argument. On the other hand, to avoid C^1 finite elements, nonconforming discretizations based on Morley finite element methods were proposed in [95] and [97]. In these works, a priori error estimates for displacement and Airy stress functions have been established. Lately, a C^0 interior penalty method has been introduced in [37]. The method uses quadratic Lagrange elements to approximate both the transverse displacement and the Airy stress function. Optimal order error estimates are derived. More recently, a discontinuous Galerkin method has been developed in [59]. The authors prove a priori and a posteriori error estimates for the isolated solution of von Kármán equations.

It is well known that conforming finite element spaces of H^2 are of complex implementation and contain high order polynomials (see [67]), for instance, Argyris and Bell finite elements (21 and 18 degrees of freedom per triangle, respectively) or Bogner-Fox-Schmit finite elements (16 degrees of freedom in a rectangle), respectively. In this paper, we will propose a C^1 VEM to approximate the isolated solutions of the von Kármán problem which can be applied to general polygonal meshes (made by possibly non-convex elements). The method will make use of a very simple set of degrees

of freedom. For instance, the total of degrees of freedom of the proposed VEM method will be $6N_v$, where N_v denotes the number of internal vertices of the polygonal mesh to approximate both the transverse displacement and the Airy stress function.

The VEM was introduced for the first time in [12], as a generalization of the finite element methods by considering polygonal or polyhedral meshes. One of its main characteristics is the possibility to construct and implement in an easy way discrete subspaces of C^α, $\alpha \in \mathbb{N}$. In recent years, the Virtual Elements Method has been a focus of great interest in the scientific community. Several virtual element methods based on conforming and non-conforming schemes have been developed to solve a wide variety of problems in Solid and Fluid Mechanics, for example [6, 7, 9, 13, 14, 15, 21, 35, 42, 55, 64, 98, 112, 121]. Moreover, the VEM for thin structures has been developed in [27, 41, 63, 64, 105, 108], whereas VEM for nonlinear problems have been introduced in [4, 24, 51, 80, 81, 125]

In this paper, we analyze a conforming C^1 Virtual Element Method to approximate the isolated solutions of the von Kármán equations. We consider a variational formulation in terms of the transverse displacement and the Airy stress function, which contains bilinear and trilinear forms. After introducing the local and global virtual space ([7, 41, 64]), we write the discrete problem by constructing discrete version of the bilinear and trilinear forms considering different projectors (polynomial functions) which are computable using only the information of the degrees of freedom of the discrete virtual space. For the analysis, we will adapt some ideas presented in [40] to deal with the variational crimes in the forms and in the right hand side. More precisely, in order to prove that the discrete scheme is well posed, an operator T is defined. Next, it is established that each solution of the discrete problem is a fixed point of this operator (and reciprocally). To prove existence and uniqueness the classical Banach fixed point theorem is employed and some assumptions on the mesh are considered. In particular, for h small enough, we establish that the operator T has a unique fixed point in a proper set which is the unique solution of the discrete problem. Optimal order of convergence in H^2-norm is established in this work for both unknowns.

The outline of this work is organized as follows. In Section 3.2 the physical model problem is described. An auxiliary variable that depends of the horizontal load forces applied to the plate is introduced, which allows us to rewrite an equivalent nonlinear system of partial differential equations. Hence, a variational formulation is obtained from this system. In Section 3.3, we introduce a conforming virtual element discretization and some auxiliary local results are proved. Then, in Section 3.4, fixed-point arguments are employed to establish that our discrete scheme is well posed. In addition, optimal convergence rate is obtained in this section. Finally, in Section 3.5, we report some numerical tests that confirm the theoretical analysis developed.

In this article, we will employ standard notations for Sobolev spaces, norms and seminorms. In addition, we will denote by C a generic constant independent of the mesh parameter h, which may take different values in different occurrences. In addition, let X, Y be Hilbert spaces. If $\Pi : X \to Y$ is a linear and bounded operator, we will denote by $\mathbf{\Pi} : X \times X \to Y \times Y$ the operator defined by $\mathbf{\Pi}(x, \tilde{x}) := (\Pi x, \Pi \tilde{x}), \forall (x, \tilde{x}) \in X \times X$.

3.2 The continuous problem

Let $\Omega \subset \mathbb{R}^2$ be a polygonal bounded domain with boundary $\Gamma := \partial\Omega$. The von Kármán system can be reads as follows (see e.g [65, 68]): Given a load force $f \in L^2(\Omega)$ and lateral load forces $(\varphi_0, \varphi_1) \in H^{5/2}(\Gamma) \times H^{3/2}(\Gamma)$ (see Fig. 3.1), find u and ϕ such that

$$\begin{aligned} \Delta^2 u &= [\phi, u] + f && \text{in } \Omega, \\ \Delta^2 \phi &= -\frac{1}{2}[u, u] && \text{in } \Omega, \\ u &= \partial_\nu u = 0 && \text{on } \Gamma, \\ \phi &= \varphi_0 && \text{on } \Gamma, \\ \partial_\nu \phi &= \varphi_1 && \text{on } \Gamma, \end{aligned} \tag{3.2.1}$$

where $[\phi, u]$ is defined by

$$[\phi, u] := \partial_{11}\phi\partial_{22}u + \partial_{22}\phi\partial_{11}u - 2\partial_{12}\phi\partial_{12}u, \tag{3.2.2}$$

and $\nu := (\nu_1(x, y), \nu_2(x, y))$ denotes the outer unit normal vector to Γ, for all $(x, y) \in \Gamma$.

In the system (3.2.1), u and φ represent the transverse displacement and the boundary stresses of the plate, respectively. This model is also known as the canonical von Kármán equations. This is a non-linear system of fourth-order partial differential equations established by T. von Kármán in 1910 (see [123]). The existence of solutions of this problem has been proved in [65, 68]. Moreover, it can be seen in [68, Section 2.2] that introducing $\theta_0 \in H_0^2(\Omega)$ as the unique solution of the following problem: find $\theta_0 \in H_0^2(\Omega)$ such that

$$\Delta^2\theta_0 = 0 \text{ in } \Omega, \qquad \theta_0 = \varphi_0, \quad \partial_\nu\theta_0 = \varphi_1 \quad \text{on } \Gamma, \tag{3.2.3}$$

we have that the system (3.2.1) can be written equivalently as follows: find $(u, \psi) \in [H_0^2(\Omega)]^2$ such that

$$\begin{aligned} \Delta^2 u &= [\psi, u] + [\theta_0, u] + f && \text{in } \Omega, \\ \Delta^2 \psi &= -\frac{1}{2}[u, u] && \text{in } \Omega, \\ u &= \partial_\nu u = \psi = \partial_\nu \psi = 0 && \text{on } \Gamma, \end{aligned}$$

where $\psi = \phi - \theta_0$.

Moreover, if the lateral load forces on Γ are chosen in (3.2.3) such that

$$\varphi_0 := -\frac{\lambda}{2}(x^2 + y^2) \quad \text{on } \Gamma, \qquad \varphi_1 := -\frac{\lambda}{2}\partial_\nu(x^2 + y^2) \quad \text{on } \Gamma,$$

where λ is a real number called bifurcation parameter that measures the intensity of the horizontal forces (see [68, Section 2.3] or [65, Section 5.9] for further details), hence we obtain that $\theta_0(x, y) = -\frac{\lambda}{2}(x^2 + y^2)$ in Ω solves problem (3.2.3). In addition, from the definition of $[\cdot, \cdot]$, we obtain that

$$[\theta_0, u] = -\lambda\Delta u \qquad \text{in } \Omega.$$

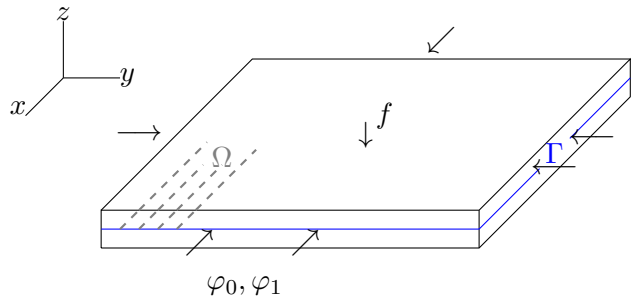

Figure 3.1: Plate subject to transversal and lateral forces $f \in L^2(\Omega)$ and $(\varphi_0, \varphi_1) \in H^{5/2}(\Gamma) \times H^{3/2}(\Gamma)$, respectively (figure produced by the author).

As a consequence of the previous definitions, from now on, our aim is to solve the following set of equations: given $(f, \lambda) \in L^2(\Omega) \times \mathbb{R}$, find $(u, \psi) \in [H_0^2(\Omega)]^2$ such that

$$\begin{aligned} \Delta^2 u &= [\psi, u] - \lambda \Delta u + f \qquad \text{in } \Omega, \\ \Delta^2 \psi &= -\frac{1}{2}[u, u] \qquad \text{in } \Omega, \\ u = \partial_\nu u &= \psi = \partial_\nu \psi = 0 \qquad \text{on } \Gamma. \end{aligned} \tag{3.2.4}$$

Remark 3.2.1. *The von Kármán model (3.2.4) does not have a unique solution: For instance, when $f = 0$ and $\lambda > \lambda^\star$, where $\lambda^\star$ is the lowest positive real number that satisfies*

$$\Delta^2 u = -\lambda \Delta u \quad \text{in } \Omega \qquad \text{and} \qquad u = \partial_\nu u = 0 \text{ on } \Gamma, \tag{3.2.5}$$

in this case, the problem (3.2.4) has at least three solutions: $u_0 = 0$, $u_1 \neq 0$, and $u_2 = -u_1$ (see [65, Theorem 5.9-2]). On the other hand, if f and λ are small enough then the system (3.2.4) has a unique solution.

Now, testing system (3.2.4) with functions in $H_0^2(\Omega)$, we arrive at the following weak formulation of the problem: given $(f, \lambda) \in L^2(\Omega) \times \mathbb{R}$, find $(u, \psi) \in [H_0^2(\Omega)]^2$ such that

$$a^\Delta(u, v) + \lambda a^\nabla(u, v) + b(u, \psi, v) + b(\psi, u, v) = F(v) \qquad \forall v \in H_0^2(\Omega), \tag{3.2.6}$$

$$a^\Delta(\psi, \varphi) - b(u; u, \varphi) = 0 \qquad \forall \varphi \in H_0^2(\Omega), \tag{3.2.7}$$

where $a^\Delta, a^\nabla : H_0^2(\Omega) \times H_0^2(\Omega) \to \mathbb{R}$ are bilinear forms, $b : H_0^2(\Omega) \times H_0^2(\Omega) \times H_0^2(\Omega) \to \mathbb{R}$ is a trilinear form and $F : H_0^2(\Omega) \to \mathbb{R}$ is a linear functional, all of them defined as follows:

$$a^\Delta(u, v) := \begin{cases} \int_\Omega \Delta u \Delta v \qquad \forall u, v \in H_0^2(\Omega) \\ \text{or} \\ \int_\Omega D^2 u : D^2 v \qquad \forall u, v \in H_0^2(\Omega), \end{cases} \tag{3.2.8}$$

$$a^\nabla(u, v) := -\int_\Omega \nabla u \cdot \nabla v \qquad \forall u, v \in H_0^2(\Omega), \tag{3.2.9}$$

$$b(w; u, v) := -\frac{1}{2} \int_\Omega [w, u] v \qquad \forall w, u, v \in H_0^2(\Omega), \tag{3.2.10}$$

$$F(v) := \int_\Omega fv \qquad \forall v \in H_0^2(\Omega). \tag{3.2.11}$$

Remark 3.2.2. *We have proposed two options to write the bilinear form associated to the bilaplacian operator. We will write the discrete method considering both options. In particular, we will employ the bilinear form* $a^\Delta(u,v) := \int_\Omega D^2u : D^2v$ *to construct the projector* $\Pi_K^{2,D}$ *(cf. (3.3.1a)-(3.3.1b)) which will be used to write the discrete schemes with the two options in (3.2.8).*

On the other hand, we endow the space $\mathbb{H} := [H_0^2(\Omega)]^2$ with the corresponding product norm, which we will simply denote by $||(\cdot,\cdot)||$.

We rewrite (3.2.6)-(3.2.7), in the following equivalent form: given $(f,\lambda) \in L^2(\Omega) \times \mathbb{R}$, find $\mathbf{u} := (u,\psi) \in \mathbb{H}$ such that

$$A^\Delta(\mathbf{u},\mathbf{v}) + \lambda A^\nabla(\mathbf{u},\mathbf{v}) + B(\mathbf{u};\mathbf{u},\mathbf{v}) = F(\mathbf{v}) \quad \forall\, \mathbf{v} := (v,\varphi) \in \mathbb{H}, \tag{3.2.12}$$

where, A^Δ, A^∇, B, F are defined as follows:

$$A^\Delta(\mathbf{u},\mathbf{v}) := a^\Delta(u,v) + a^\Delta(\psi,\varphi) \quad \forall\, \mathbf{u},\mathbf{v} \in \mathbb{H}, \tag{3.2.13}$$

$$A^\nabla(\mathbf{u},\mathbf{v}) := a^\nabla(u,v) \quad \forall\, \mathbf{u},\mathbf{v} \in \mathbb{H}, \tag{3.2.14}$$

$$B(\mathbf{w};\mathbf{u},\mathbf{v}) := b(w;\psi,v) + b(\xi;u,v) - b(w;u,\varphi) \quad \forall\, \mathbf{w} := (w,\xi), \mathbf{u},\mathbf{v} \in \mathbb{H}, \tag{3.2.15}$$

$$F(\mathbf{v}) := F(v) \quad \forall\, \mathbf{v} \in \mathbb{H}. \tag{3.2.16}$$

It is easy to see that the bilinear forms $a^\Delta(\cdot,\cdot)$ and $a^\nabla(\cdot,\cdot)$ are bounded and symmetric, the former is also positive definite on $H_0^2(\Omega) \times H_0^2(\Omega)$ and F is bounded. Moreover, from Lemma 2.2-2 in [68] we have that the trilinear form $b(\cdot;\cdot,\cdot)$ is bounded and symmetric independent of the arguments. Therefore, we have the following result.

Lemma 3.2.1. *The forms defined in (3.2.13)-(3.2.16) satisfy the following properties:*

$$|A^\Delta(\mathbf{u},\mathbf{v})| \le ||\,\mathbf{u}\,||\,||\,\mathbf{v}\,|| \quad \textit{and} \quad |A^\nabla(\mathbf{u},\mathbf{v})| \le |\lambda|\,||\,\mathbf{u}\,||\,||\,\mathbf{v}\,|| \qquad \forall\, \mathbf{u},\mathbf{v} \in \mathbb{H},$$

$$|F(\mathbf{v})| \le ||f||_{0,\Omega}||\,\mathbf{v}\,|| \qquad \forall\, \mathbf{u},\mathbf{v} \in \mathbb{H},$$

$$|B(\mathbf{w};\mathbf{u},\mathbf{v})| \le C||\,\mathbf{w}\,||\,||\,\mathbf{u}\,||\,||\,\mathbf{v}\,|| \qquad \forall\, \mathbf{w},\mathbf{u},\mathbf{v} \in \mathbb{H},$$

$$B(\mathbf{w};\mathbf{u},\mathbf{v}) = B(\mathbf{u};\mathbf{w},\mathbf{v}) \qquad \forall\, \mathbf{w},\mathbf{u},\mathbf{v} \in \mathbb{H}.$$

Now, from [65, Theorem 5.8-3(b)] (see also [92]) we have that the variational formulation (3.2.12) has at least one solution. Moreover, we present the following additional regularity result for the solution of the von Kármán problem (3.2.12), which has been proved in [37, Theorem 2.4].

Theorem 3.2.1. *Let* $\mathbf{u}$ *be a solution of von Kármán problem (3.2.12). Then, there exist* $s \in (1/2,1]$ *and* $C > 0$ *such that* $\mathbf{u} \in [H^{2+s}(\Omega)]^2$ *and*

$$||\,\mathbf{u}\,||_{2+s,\Omega} \le C||f||_{0,\Omega},$$

where, the constant $s \in (1/2,1]$ *is the Sobolev regularity for the biharmonic equation with the right-hand side in* $H^{-1}(\Omega)$ *and homogeneous Dirichlet boundary conditions (see e.g. [85]).*

Now, we will introduce some definitions that will be used to establish an existence result of the isolated solutions of the problem (3.2.12). Given $\mathbf{u} \in \mathbb{H}$ we introduce the following global form.

$$A_{\mathbf{u}}(\mathbf{w}, \mathbf{v}) := A^{\Delta}(\mathbf{w}, \mathbf{v}) + \lambda A^{\nabla}(\mathbf{w}, \mathbf{v}) + 2B(\mathbf{u}; \mathbf{w}, \mathbf{v}) \quad \forall \mathbf{w}, \mathbf{v} \in \mathbb{H}. \tag{3.2.17}$$

Definition 3.2.1. *(see [40]) A solution* $\mathbf{u}$ *of the system* (3.2.12) *is said to be isolated if and only if the linearized problem: given* $\mathbf{g} \in [L^2(\Omega)]^2$*, find* $\mathbf{w} \in \mathbb{H}$ *such that*

$$A_{\mathbf{u}}(\mathbf{w}, \mathbf{v}) = \int_{\Omega} \mathbf{g} \cdot \mathbf{v} \quad \forall \mathbf{v} \in \mathbb{H},$$

has a unique solution and satisfies the following a priori estimates

$$|| \mathbf{w} || \leq C || \mathbf{g} ||_{0,\Omega} \qquad \text{and} \qquad || \mathbf{w} ||_{2+s,\Omega} \leq C || \mathbf{g} ||_{0,\Omega},$$

where, the constant $s \in (1/2, 1]$ *is the Sobolev regularity for the biharmonic problem with the right-hand side in* $H^{-1}(\Omega)$ *and homogeneous Dirichlet boundary conditions (see e.g. [85]).*

Now, the following result gives a sufficient condition to obtain an isolated solution of the system (3.2.12) (see for instance [37, Remark 3.1], or [96, Remark 2.1]–[96, Theorem 2.3]).

Theorem 3.2.2. *If* $(f, \lambda) \in L^2(\Omega) \times \mathbb{R}$ *are small enough, then the von Kármán system* (3.2.12) *has a unique solution and it is isolated.*

We finish this section with the following result which will be used to approach the isolated solution of the von Kármán problem.

Theorem 3.2.3. *Assume that the bilinear form* $A_{\mathbf{u}}(\cdot, \cdot)$ *(cf.* (3.2.17)*) is non singular on* $\mathbb{H} \times \mathbb{H}$*, this means (see e.g [40, Lemma 1]) that there exist two positive constants* c_1 *and* c_2 *such that*

$$\sup_{\substack{\mathbf{v} \in \mathbb{H} \\ || \mathbf{v} || = 1}} A_{\mathbf{u}}(\mathbf{w}, \mathbf{v}) \geq c_1 || \mathbf{w} || \ \forall \mathbf{w} \in \mathbb{H}, \qquad \text{and} \qquad \sup_{\substack{\mathbf{w} \in \mathbb{H} \\ || \mathbf{w} || = 1}} A_{\mathbf{u}}(\mathbf{w}, \mathbf{v}) \geq c_2 || \mathbf{v} || \ \forall \mathbf{v} \in \mathbb{H}. \tag{3.2.18}$$

Then, there exists a positive constant δ *such that* $A_{\tilde{\mathbf{u}}}(\cdot, \cdot)$ *is non singular on* $\mathbb{H} \times \mathbb{H}$*, for all* $\tilde{\mathbf{u}}$ *that satisfies*

$$|| \mathbf{u} - \tilde{\mathbf{u}} || \leq \delta.$$

Proof. The proof can be obtained repeating the arguments in [40, Lemma 1]. □

3.3 Discrete problem

In this section, we will introduce a C^1-VEM discretization to approximate the isolated solutions of a von Kármán plate (cf. Theorem 3.2.2).

We begin with the mesh construction and the assumptions considered to introduce the discrete virtual element spaces (see e.g [2, 7, 12]). Let $\{\mathcal{T}_h\}_h$ be a sequence of decompositions of Ω into general polygonal elements K. We will denote by h_K the diameter of the element K and by h the maximum

of the diameters of all the elements of the mesh, i.e., $h := \max_{K\in\mathcal{T}_h} h_K$. In addition, we denote by N_K the number of vertices of K, by e a generic edge of $\{\mathcal{T}_h\}_h$ and for all $e \in \partial K$, we define a unit normal vector ν_K^e that points outside of K.

Moreover, we will make the following assumptions: there exists a positive real number $C_{\mathcal{T}}$ such that, for every h and every $K \in \mathcal{T}_h$:

A1: $K \in \mathcal{T}_h$ is star-shaped with respect to every point of a ball of radius $C_{\mathcal{T}} h_K$;

A2: the ratio between the shortest edge and the diameter h_K of K is larger than $C_{\mathcal{T}}$.

The hypotheses **A1** and **A2** though not too restrictive in several practical cases, can be further relaxed, as established in [22].

In order to write the method, we first define the following finite dimensional space (see [7]).

$$\widetilde{H}_h^K := \big\{ v_h \in H^2(K) : \Delta^2 v_h \in \mathbb{P}_2(K), v_h|_{\partial K} \in C^0(\partial K), v_h|_e \in \mathbb{P}_3(e)\ \forall e \in \partial K, \\ \nabla v_h|_{\partial K} \in C^0(\partial K)^2, \partial_{\nu_K^e} v_h|_e \in \mathbb{P}_1(e)\ \forall e \in \partial K \big\}.$$

It is easy to see that any $v_h \in \widetilde{H}_h^K$ satisfies the following conditions:

- the trace (and the trace of the gradient) on the boundary of K is continuous;
- $\mathbb{P}_2(K) \subseteq \widetilde{H}_h^K$.

On the other hand, we introduce two sets of linear operators from $\widetilde{H}_h^K$ into $\mathbb{R}$. For all $v_h \in \widetilde{H}_h^K$, they are defined as follows:

$\mathbf{D_1}$: evaluation of v_h at the N_K vertices of K;

$\mathbf{D_2}$: evaluation of ∇v_h at the N_K vertices of K.

Now, we will introduce some preliminary definitions in order to construct the discrete scheme. Let $a_K^D : H^2(K) \times H^2(K) \to \mathbb{R}$ be defined as follows:

$$a_K^D(u,v) := \int_K D^2 u : D^2 v, \qquad u, v \in H^2(K).$$

We build the projection operator $\Pi_K^{2,D} : \tilde{H}_h^K \to \mathbb{P}_2(K) \subseteq \tilde{H}_h^K$, defined by the unique solution of the following local problem:

$$a_K^D\big(\Pi_K^{2,D} v, q\big) = a_K^D(v,q) \qquad \forall q \in \mathbb{P}_2(K), \tag{3.3.1a}$$

$$\widehat{\Pi_K^{2,D} v} = \widehat{v}, \quad \widehat{\nabla \Pi_K^{2,D} v} = \widehat{\nabla v}, \tag{3.3.1b}$$

where $\widehat{v}$ is defined as follows:

$$\widehat{v} := \frac{1}{N_K} \sum_{i=1}^{N_K} v(\mathrm{v}_i) \qquad \forall v \in C^0(\partial K)$$

and $\mathrm{v}_i, 1 \leq i \leq N_K$, are the vertices of K.

We note that the bilinear form $a_K^D(\cdot,\cdot)$ has a non-trivial kernel, given by $\mathbb{P}_1(K)$. Thus, the role of condition (3.3.1b) is to choose an element of the kernel of the operator. Hence, we have that the operator $\Pi_K^{2,D}$ is well defined on $\widetilde{H}_h^K$ and is computable from the output values of the sets $\mathbf{D_1}$ and $\mathbf{D_2}$ (see [7, 41]).

Next, we introduce our local virtual space:

$$H_h^K := \left\{ v_h \in \widetilde{H}_h^K : \int_K (v_h - \Pi_K^{2,D} v_h) q = 0, \quad \forall q \in \mathbb{P}_2(K) \right\}.$$

Note that $H_h^K \subseteq \widetilde{H}_h^K$. This allows us to obtain the well definition of $\Pi_K^{2,D}$ on H_h^K, and therefore to prove that $\Pi_K^{2,D}$ is computable from the output values of operators $\mathbf{D_1}$ and $\mathbf{D_2}$. Moreover, it is easy to check that $\mathbb{P}_2(K) \subseteq H_h^K$. This will guarantee the good approximation properties for the virtual space.

On the other hand, the following result which has been proved in [7] guarantees that any function $v_h \in H_h^K$ is uniquely determined by the output values of the sets $\mathbf{D_1}$ and $\mathbf{D_2}$.

Lemma 3.3.1. *The set of operators* $\mathbf{D_1}$ *and* $\mathbf{D_2}$ *constitutes a set of degrees of freedom for the space* H_h^K.

Now, we are in a position to introduce our global virtual space for the transverse displacement and the Airy stress function:

$$H_h := \left\{ v_h \in H_0^2(\Omega) : v_h|_K \in H_h^K \right\}. \tag{3.3.2}$$

3.3.1 Construction of bilinear and trilinear forms and the loading term.

In this subsection we will propose discrete version of the local forms to construct the discrete virtual scheme.

We begin by introducing new projectors: For $\ell = 0, 1, 2$, we consider $\Pi_K^\ell : L^2(K) \to \mathbb{P}_\ell(K)$ the standard L^2-orthogonal projector defined as follows:

$$\int_K \Pi_K^\ell v q = \int_K v q \qquad \forall q \in \mathbb{P}_\ell(K) \quad \forall v \in L^2(K). \tag{3.3.3}$$

Now, due to the particular property appearing in definition of the space H_h^K, it can be seen that the right hand side in (3.3.3) is computable using $\Pi_K^{2,D} v$. Thus, $\Pi_K^\ell v, \ell = 0, 1, 2$ depends only on the values of the degrees of freedom given by the sets $\mathbf{D_1}$ and $\mathbf{D_2}$. Furthermore, it is easy to check that on the space H_h^K the projectors Π_K^2 and $\Pi_K^{2,D}$ are the same operator. In fact:

$$\int_K (\Pi_K^2 v_h) q = \int_K v_h q = \int_K (\Pi_K^{2,D} v_h) q \qquad \forall q \in \mathbb{P}_2(K), \quad \forall v_h \in H_h^K.$$

We introduce the projector $\Pi_K^{2,\nabla} : H^1(K) \longrightarrow \mathbb{P}_2(K)$, for each $v \in H^1(K)$ as the solution of

$$\begin{aligned} a_K^\nabla(\Pi_K^{2,\nabla} v, q) &= a_K^\nabla(v, q) \qquad \forall q \in \mathbb{P}_2(K), \\ \int_K \Pi_K^{2,\nabla} v &= \int_K v. \end{aligned}$$

The following lemma proved in [7] establishes that operator $\Pi_K^{2,\nabla}$ is fully computable on the local virtual space H_h^K.

Lemma 3.3.2. *The operator $\Pi_K^{2,\nabla} : H_h^K \to \mathbb{P}_2(K) \subseteq H_h^K$ is well defined and depends only on the values of the degrees of freedom given by the sets $\mathbf{D_1}$ and $\mathbf{D_2}$.*

Following the standard procedure in VEM literature (see for instance [2, 12, 41, 64]), we propose the following (computable) discrete local bilinear forms:

$$a_{h,K}^{\Delta} : H_h^K \times H_h^K \to \mathbb{R}; \quad \text{and} \quad a_{h,K}^{\nabla} : H_h^K \times H_h^K \to \mathbb{R}; \tag{3.3.5}$$

defined by

$$a_{h,K}^{\Delta}(u_h, v_h) := \begin{cases} \int_K \Delta\Pi_K^{2,D} u_h \Delta\Pi_K^{2,D} v_h + \overline{\alpha} s_K^D\big(u_h - \Pi_K^{2,D} u_h, v_h - \Pi_K^{2,D} v_h\big), \\ \text{or} \\ \int_K D^2\Pi_K^{2,D} u_h : D^2\Pi_K^{2,D} v_h + \overline{\alpha} s_K^D\big(u_h - \Pi_K^{2,D} u_h, v_h - \Pi_K^{2,D} v_h\big), \end{cases} \tag{3.3.6}$$

$$a_{h,K}^{\nabla}(u_h, v_h) := -\Big\{ \int_K \boldsymbol{\Pi}_K^1 \nabla u_h \cdot \boldsymbol{\Pi}_K^1 \nabla v_h + \widehat{\alpha} s_K^{\nabla}\big(u_h - \Pi_K^{2,\nabla} u_h, v_h - \Pi_K^{2,\nabla} v_h\big) \Big\}, \tag{3.3.7}$$

respectively, where $\boldsymbol{\Pi}_K^1 : L^2(K)^2 \to \mathbb{P}_1(K)^2$ is the standard L^2-orthogonal projector and $s_K^{\Delta}(\cdot,\cdot)$ and $s_K^{\nabla}(\cdot,\cdot)$ are two symmetric positive definite bilinear forms satisfying the following conditions:

$$c_0 a_K^D(v_h, v_h) \leq s_K^D(v_h, v_h) \leq c_1 a_K^D(v_h, v_h) \quad \forall v_h \in H_h^K \quad \text{with} \quad \Pi_K^{2,D} v_h = 0, \tag{3.3.8}$$

$$c_2 a_K^{\nabla}(v_h, v_h) \leq s_K^{\nabla}(v_h, v_h) \leq c_3 a_K^{\nabla}(v_h, v_h) \quad \forall v_h \in H_h^K \quad \text{with} \quad \Pi_K^{2,\nabla} v_h = 0, \tag{3.3.9}$$

respectively. In addition, in (3.3.6)-(3.3.7), $\overline{\alpha}$ and $\widehat{\alpha}$ are constants which depend on the physical parameters.

Remark 3.3.1. *In (3.3.7) the vector function $\boldsymbol{\Pi}_K^1 \nabla v_h$ is fully computable from the degrees of freedom given by the sets $\mathbf{D_1}$ and $\mathbf{D_2}$ (see for instance [108, Section 3] for further details).*

Now, we define the following global discrete bilinear forms on H_h.

$$a_h^{\Delta}(u_h, v_h) := \sum_{K \in \mathcal{T}_h} a_{h,K}^{\Delta}(u_h, v_h), \qquad u_h, v_h \in H_h,$$
$$a_h^{\nabla}(u_h, v_h) := \sum_{K \in \mathcal{T}_h} a_{h,K}^{\nabla}(u_h, v_h), \qquad u_h, v_h \in H_h.$$

The following result establishes the usual properties of consistency and stability for the local virtual forms.

Proposition 3.3.1. *The local bilinear forms $a_{h,K}^{\Delta}(\cdot,\cdot)$ and $a_{h,K}^{\nabla}(\cdot,\cdot)$ on each element K satisfy*

- *Consistency: for all $h > 0$ and for all $K \in \mathcal{T}_h$, we have that*

$$a_{h,K}^{\Delta}(q, v_h) = a_K^{\Delta}(q, v_h) \qquad \forall q \in \mathbb{P}_2(K), \quad \forall v_h \in H_h^K, \tag{3.3.10}$$
$$a_{h,K}^{\nabla}(q, v_h) = a_K^{\nabla}(q, v_h) \qquad \forall q \in \mathbb{P}_2(K), \quad \forall v_h \in H_h^K. \tag{3.3.11}$$

- *Stability and boundedness: There exist positive constants $\alpha_i, i = 1, \ldots, 4$ independent of K, such that:*

$$\alpha_1 a_K^D(v_h, v_h) \leq a_{h,K}^{\Delta}(v_h, v_h) \leq \alpha_2 a_K^D(v_h, v_h) \qquad \forall v_h \in H_h^K, \tag{3.3.12}$$

$$\alpha_3 a_K^{\nabla}(v_h, v_h) \leq a_{h,K}^{\nabla}(v_h, v_h) \leq \alpha_4 a_K^{\nabla}(v_h, v_h) \qquad \forall v_h \in H_h^K. \tag{3.3.13}$$

Proof. Since the proof can be followed from standard arguments in the Virtual Element literature (see [2, 35]), it is omitted. □

On the other hand, we will propose on each element K the following local (and computable) approximation for the trilinear form $b(\cdot;\cdot,\cdot)$ (cf. (3.2.10)):

$$b_{h,K}(w_h; u_h, v_h) := -\frac{1}{2}\int_K [\Pi_K^{2,D} w_h, \Pi_K^{2,D} u_h]\Pi_K^2 v_h. \tag{3.3.14}$$

Now, we are going to introduce the discrete version of (3.2.13)-(3.2.16). First, let us define $\mathbb{H}_h := H_h \times H_h$, $\mathbb{H}_h^K := H_h^K \times H_h^K$ and let $A_h^{\Delta}, A_h^{\nabla}, F_h, B_h$ be the discrete forms given by:

$$\begin{aligned}
&A_h^{\Delta} : \mathbb{H}_h \times \mathbb{H}_h \to \mathbb{R}; && A_h^{\Delta}(\mathbf{u}_h, \mathbf{v}_h) && := \textstyle\sum_{K\in\mathcal{T}_h} A_{h,K}^{\Delta}(\mathbf{u}_h, \mathbf{v}_h);\\
&A_h^{\nabla} : \mathbb{H}_h \times \mathbb{H}_h \to \mathbb{R}; && A_h^{\nabla}(\mathbf{u}_h, \mathbf{v}_h) && := \textstyle\sum_{K\in\mathcal{T}_h} A_{h,K}^{\nabla}(\mathbf{u}_h, \mathbf{v}_h);\\
&F_h : \mathbb{H}_h \to \mathbb{R}; && F_h(\mathbf{v}_h) && := \textstyle\sum_{K\in\mathcal{T}_h} F_{h,K}(\mathbf{v}_h);\\
&B_h : \mathbb{H}_h \times \mathbb{H}_h \times \mathbb{H}_h \to \mathbb{R}; && B_h(\mathbf{w}_h; \mathbf{u}_h, \mathbf{v}_h) && := \textstyle\sum_{K\in\mathcal{T}_h} B_{h,K}(\mathbf{w}_h; \mathbf{u}_h, \mathbf{v}_h);
\end{aligned}$$

where

$$\begin{aligned}
&A_{h,K}^{\Delta}(\mathbf{u}_h, \mathbf{v}_h) := a_{h,K}^{\Delta}(u_h, v_h) + a_{h,K}^{\Delta}(\psi_h, \varphi_h);\\
&A_{h,K}^{\nabla}(\mathbf{u}_h, \mathbf{v}_h) := a_{h,K}^{\nabla}(u_h, v_h);\\
&F_{h,K}(\mathbf{v}_h) := \int_K \Pi_K^2 f v_h \equiv \int_K \Pi_K^2 f \Pi_K^{2,D} v_h \equiv \int_K f \Pi_K^{2,D} v_h;\\
&B_{h,K}(\mathbf{w}_h; \mathbf{u}_h, \mathbf{v}_h) := b_{h,K}(w_h; \psi_h, v_h) + b_{h,K}(\xi_h; u_h, v_h) - b_{h,K}(w_h; u_h, \varphi_h)\\
&= -\frac{1}{2}\int_K \Big\{[\Pi_K^{2,D} w_h, \Pi_K^{2,D}\psi_h]\Pi_K^2 v_h + [\Pi_K^{2,D}\xi_h, \Pi_K^{2,D} u_h]\Pi_K^2 v_h - [\Pi_K^{2,D} w_h, \Pi_K^{2,D} u_h]\Pi_K^2\varphi_h\Big\},
\end{aligned}$$

with $\mathbf{u}_h := (u_h, \psi_h), \mathbf{v}_h := (v_h, \varphi_h), \mathbf{w}_h := (w_h, \xi_h) \in \mathbb{H}_h$.

Now, we are ready to propose the virtual element scheme to approximate the isolated solutions of the von Kármán problem: given $(f, \lambda) \in L^2(\Omega) \times \mathbb{R}$, find $\mathbf{u}_h := (u_h, \psi_h) \in \mathbb{H}_h$ such that

$$A_h^{\Delta}(\mathbf{u}_h, \mathbf{v}_h) + \lambda A_h^{\nabla}(\mathbf{u}_h, \mathbf{v}_h) + B_h(\mathbf{u}_h; \mathbf{u}_h, \mathbf{v}_h) = F_h(\mathbf{v}_h) \qquad \forall\, \mathbf{v}_h := (v_h, \varphi_h) \in \mathbb{H}_h. \tag{3.3.15}$$

In the next section we are going to prove the well posedness of the discrete problem (3.3.15), provided that (f, λ) is small enough. To do that we will use a fix point argument. With this aim, we present that following discrete version of Lemma 3.2.1.

Lemma 3.3.3. *There exist positive constants α, C and C_B independent of h such that*

$$|A_h^{\Delta}(\mathbf{u}_h, \mathbf{v}_h)| \leq ||\,\mathbf{u}_h\,||\;||\,\mathbf{v}_h\,|| \qquad \forall\, \mathbf{u}_h, \mathbf{v}_h \in \mathbb{H}_h; \tag{3.3.16a}$$

$$|A_h^{\nabla}(\mathbf{u}_h, \mathbf{v}_h)| \leq |\lambda|\;||\,\mathbf{u}_h\,||\;||\,\mathbf{v}_h\,|| \qquad \forall\, \mathbf{u}_h, \mathbf{v}_h \in \mathbb{H}_h; \tag{3.3.16b}$$

$$A_h^{\Delta}(\mathbf{v}_h, \mathbf{v}_h) \geq \alpha||\,\mathbf{v}_h\,||^2 \qquad \forall\, \mathbf{v}_h \in \mathbb{H}_h; \tag{3.3.16c}$$

$$|F_h(\mathbf{v}_h)| \leq ||f||_{0,\Omega}||\,\mathbf{v}_h\,|| \qquad \forall\, \mathbf{u}_h, \mathbf{v}_h \in \mathbb{H}_h; \tag{3.3.16d}$$

$$|B_h(\mathbf{w}_h; \mathbf{u}_h, \mathbf{v}_h)| \leq C||\,\mathbf{w}_h\,||\;||\,\mathbf{u}_h\,||\;||\,\mathbf{v}_h\,|| \qquad \forall\, \mathbf{w}_h, \mathbf{u}_h, \mathbf{v}_h \in \mathbb{H}_h; \tag{3.3.16e}$$

$$B_h(\mathbf{w}_h; \mathbf{u}_h, \mathbf{v}_h) = B_h(\mathbf{u}_h; \mathbf{w}_h, \mathbf{v}_h) \qquad \forall\, \mathbf{w}_h, \mathbf{u}_h, \mathbf{v}_h \in \mathbb{H}_h. \tag{3.3.16f}$$

Proof. The proof follows from (3.3.8)-(3.3.9) and Proposition 3.3.1. □

We end this section with some definitions and results which will be used in Section 3.4 to prove the solvability of the discrete problem (3.3.15).

First, we introduce the following broken seminorm and projectors:

$$|v|_{\ell,h}^2 := \sum_{K\in\mathcal{T}_h} |v|_{\ell,K}^2 \quad \forall v \in L^2(\Omega) : v|_K \in H^\ell(K) \qquad \ell = 1, 2.$$

Now, for all $v \in L^2(\Omega)$ such that $v|_K \in H^2(K)$ for all $K \in \mathcal{T}_h$, we define $\Pi_h^{2,D}$ in $L^2(\Omega)$ as follows

$$(\Pi_h^{2,D} v)|_K := \Pi_K^{2,D}(v|_K) \quad \forall K \in \mathcal{T}_h. \tag{3.3.17}$$

Next, we present the following standard approximation results. Proposition 3.3.2 is derived by interpolation between Sobolev spaces from the analogous result for integer values of s. In fact, this result for integer values is stated in [12, Proposition 4.2] and follows from the classical Scott-Dupont theory (see [38] and [7, Proposition 3.1]). Proposition 3.3.3 has been proved in [27, Proposition 4.2]. Proposition 3.3.4 and Lemma 3.3.4 can be seen for instance in [108, Section 3] and [105, Lemma 3.5], respectively.

Proposition 3.3.2. *If the assumption* **A1** *is satisfied, then there exists a constant $C > 0$, such that for every $v \in H^\delta(K)$ there exists $v_\pi \in \mathbb{P}_k(K)$, $k \geq 0$ such that*

$$|v - v_\pi|_{\ell,K} \leq C h_K^{\delta-\ell} |v|_{\delta,K} \quad 0 \leq \delta \leq k+1, \ell = 0, \ldots, [\delta],$$

with $[\delta]$ denoting the largest integer equal or smaller than $\delta \in \mathbb{R}$.

Proposition 3.3.3. *Assume* ***A1***–***A2*** *are satisfied, let $v \in H^{2+s}(\Omega)$ with $s \in (1/2, 1]$. Then, there exist $v_I \in H_h$ and $C > 0$ independent of h such that*

$$|v - v_I|_{2,\Omega} \leq C h_K^s |v|_{2+s,\Omega}.$$

Proposition 3.3.4. *There exists $C > 0$ independent of h such that for all $\mathbf{v} \in H^\delta(K)^2$*

$$\|\mathbf{v} - \boldsymbol{\Pi}_K^1 \mathbf{v}\|_{0,K} \leq C h_K^\delta |\mathbf{v}|_{\delta,K} \quad 0 \leq \delta \leq 2,$$

where $\boldsymbol{\Pi}_K^1 : L^2(K)^2 \to \mathbb{P}_1(K)^2$ is the standard L^2-orthogonal projector (cf. Remark 3.3.1).

Lemma 3.3.4. *Let $v_h \in H_h$. Then, there exists $C > 0$ such that*

$$\|v_h - \Pi_h^{2,D} v_h\|_{0,\Omega} \leq C h^2 \|v_h\|_{2,\Omega}.$$

3.4 Analysis of the discrete problem

The purpose of this section is to prove that problem (3.3.15) admits a unique solution. With this end, from now on, we assume that $\mathbf{u}$ is an isolated solution of the von Kármán system (3.2.12).

Now, from Theorem 3.2.1, we know that $\mathbf{u} = (u, \psi) \in [H^{2+s}(\Omega)]^2$ with $s \in (1/2, 1]$. Then, from Proposition 3.3.3 we have that there exists $\mathbf{u}_I := (u_I, \psi_I) \in \mathbb{H}_h$ (from now on $\mathbf{u}_I$ denotes the interpolated of $\mathbf{u}$) such that

$$|| \mathbf{u} - \mathbf{u}_I || \leq C h^s || \mathbf{u} ||_{2+s,\Omega}, \tag{3.4.18}$$

where, u_I and ψ_I are the interpolants of u and ψ, respectively.

In order to establish the well posedness of the discrete problem (3.3.15), we need to introduce some definitions. Let $A_{h,\mathbf{u}_I} : \mathbb{H}_h \times \mathbb{H}_h \to \mathbb{R}$ be the discrete form defined by

$$A_{h,\mathbf{u}_I}(\mathbf{w}_h, \mathbf{v}_h) := A_h^{\Delta}(\mathbf{w}_h, \mathbf{v}_h) + \lambda A_h^{\nabla}(\mathbf{w}_h, \mathbf{v}_h) + 2B_h(\mathbf{u}_I; \mathbf{w}_h, \mathbf{v}_h) \quad \forall\, \mathbf{w}_h, \mathbf{v}_h \in \mathbb{H}_h. \tag{3.4.19}$$

We also define the operator

$$\begin{aligned} T : \ \mathbb{H}_h &\longrightarrow \mathbb{H}_h \\ \mathbf{w}_h &\longmapsto T\,\mathbf{w}_h, \end{aligned}$$

where, $T\,\mathbf{w}_h \in \mathbb{H}_h$ is the unique solution (to be proved below) of the following problem. Find $T\,\mathbf{w}_h \in \mathbb{H}_h$ such that

$$A_{h,\mathbf{u}_I}(T\,\mathbf{w}_h, \mathbf{v}_h) = 2B_h(\mathbf{u}_I; \mathbf{w}_h, \mathbf{v}_h) - B_h(\mathbf{w}_h; \mathbf{w}_h, \mathbf{v}_h) + F_h(\mathbf{v}_h) \quad \forall\, \mathbf{v}_h \in \mathbb{H}_h. \tag{3.4.20}$$

It is easy to check that any solution $\mathbf{u}_h$ of the discrete problem (3.3.15) is a fixed point of T and reciprocally.

Now, we focus on proving that T is well defined and then we will use contraction and fixed point arguments to establish that T has a unique fixed point. To do that, we first need to prove an auxiliary lemma, which follows the argument presented in the proof of [40, Lemma 2].

Lemma 3.4.1. *Let $\widetilde{\mathbf{v}} \in \mathbb{H}$ such that $||\widetilde{\mathbf{v}}|| = 1$. Then, the following problem: find $\widetilde{\mathbf{v}}_h \in \mathbb{H}_h$ such that*

$$A_h^{\Delta}(\widetilde{\mathbf{v}}_h, \mathbf{z}_h) = A^{\Delta}(\widetilde{\mathbf{v}}, \mathbf{z}_h) \quad \forall\, \mathbf{z}_h \in \mathbb{H}_h, \tag{3.4.21}$$

has a unique solution and satisfies the following a priori estimates

$$||\widetilde{\mathbf{v}} - \widetilde{\mathbf{v}}_h||_{0,\Omega} \leq C h^t \qquad \text{and} \qquad ||\widetilde{\mathbf{v}} - \widetilde{\mathbf{v}}_h||_{\infty,\Omega} \leq C h^{t/4},$$

where, the constant $t \in (1/2, 1]$ is the Sobolev regularity for the biharmonic equation with the right-hand side in $H^{-1}(\Omega)$ and homogeneous Dirichlet boundary conditions (see e.g. [85]), and C is a positive constant independent of h.

Proof. We know from Lemma 3.2.1 that $A^{\Delta}(\widetilde{\mathbf{v}}, \mathbf{z}_h) \leq C|| \mathbf{z}_h ||$ for all $\mathbf{z}_h \in \mathbb{H}_h$. Then, from (3.3.16a), (3.3.16c), and Lax-Milgram Lemma, we obtain that the problem (3.4.21) has a unique solution and satisfies the following estimate (see [38])

$$||\widetilde{\mathbf{v}} - \widetilde{\mathbf{v}}_h|| \leq C||\widetilde{\mathbf{v}}|| = C \tag{3.4.22}$$

for some positive constant C independent of h.

On the other hand, we will use duality arguments to obtain an error bound for $||\widetilde{\mathbf{v}} - \widetilde{\mathbf{v}}_h||_{0,\Omega}$. In fact, we consider the following problem: find $\mathbf{r} \in \mathbb{H}$ such that

$$\begin{aligned} \Delta^2 \mathbf{r} &= \widetilde{\mathbf{v}} - \widetilde{\mathbf{v}}_h \qquad \text{in } \Omega, \\ \mathbf{r} = \partial_\nu \mathbf{r} &= 0 \qquad \text{on } \partial\Omega. \end{aligned} \tag{3.4.23}$$

It is well known that problem (3.4.23) has a unique solution (see for instance [85]) and that there exists a positive constant $t \in (1/2, 1]$ such that

$$|| \mathbf{r} ||_{2+t,\Omega} \leq C||\widetilde{\mathbf{v}} - \widetilde{\mathbf{v}}_h||_{0,\Omega}. \tag{3.4.24}$$

Now, from (3.4.24) and Proposition 3.3.3 we have that there exist $\mathbf{r}_I \in \mathbb{H}_h$ and $C > 0$ independent of h such that

$$|| \mathbf{r} - \mathbf{r}_I ||_{2,\Omega} \leq Ch^t || \mathbf{r} ||_{2+t,\Omega}. \tag{3.4.25}$$

Next, by multiplying the system (3.4.23) by $\widetilde{\mathbf{v}} - \widetilde{\mathbf{v}}_h \in \mathbb{H}$, integrating by parts twice, adding and subtracting $\mathbf{r}_I$, using the symmetry of $A_h^\Delta(\cdot,\cdot)$ and (3.4.21) we obtain

$$\begin{aligned} ||\widetilde{\mathbf{v}} - \widetilde{\mathbf{v}}_h||_{0,\Omega}^2 &= A^\Delta(\mathbf{r}, \widetilde{\mathbf{v}} - \widetilde{\mathbf{v}}_h) = A^\Delta(\mathbf{r} - \mathbf{r}_I, \widetilde{\mathbf{v}} - \widetilde{\mathbf{v}}_h) + A^\Delta(\mathbf{r}_I, \widetilde{\mathbf{v}} - \widetilde{\mathbf{v}}_h) \\ &= A^\Delta(\mathbf{r} - \mathbf{r}_I, \widetilde{\mathbf{v}} - \widetilde{\mathbf{v}}_h) + A^\Delta(\widetilde{\mathbf{v}}, \mathbf{r}_I) - A^\Delta(\widetilde{\mathbf{v}}_h, \mathbf{r}_I) \\ &= A^\Delta(\mathbf{r} - \mathbf{r}_I, \widetilde{\mathbf{v}} - \widetilde{\mathbf{v}}_h) + A_h^\Delta(\widetilde{\mathbf{v}}_h, \mathbf{r}_I) - A^\Delta(\widetilde{\mathbf{v}}_h, \mathbf{r}_I). \end{aligned} \tag{3.4.26}$$

Now, from (3.4.24) and Proposition 3.3.2 there exists $\mathbf{r}_\pi \in [\mathbb{P}_2(K)]^2$ such that

$$| \mathbf{r} - \mathbf{r}_\pi |_{2,K} \leq Ch^t | \mathbf{r} |_{2+t,K} \quad \forall K \in \mathcal{T}_h. \tag{3.4.27}$$

Thus, adding and subtracting $\mathbf{r}_\pi$, and using the consistency property (3.3.10) on the right hand side of (3.4.26), we obtain that

$$||\widetilde{\mathbf{v}} - \widetilde{\mathbf{v}}_h||_{0,\Omega}^2 = A^\Delta(\mathbf{r} - \mathbf{r}_I, \widetilde{\mathbf{v}} - \widetilde{\mathbf{v}}_h) + \sum_{K \in \mathcal{T}_h} \{A_{h,K}^\Delta(\widetilde{\mathbf{v}}_h, \mathbf{r}_I - \mathbf{r}_\pi) + A_K^\Delta(\widetilde{\mathbf{v}}_h, \mathbf{r}_\pi - \mathbf{r}_I)\}.$$

Next, using Lemma 3.2.1, Cauchy-Schwarz inequality, Poincaré inequality, (3.3.12) and finally adding and subtracting $\mathbf{r}$ on the right hand side of the above term, we obtain

$$\begin{aligned} &||\widetilde{\mathbf{v}} - \widetilde{\mathbf{v}}_h||_{0,\Omega}^2 \\ &\leq C|| \mathbf{r} - \mathbf{r}_I || \, ||\widetilde{\mathbf{v}} - \widetilde{\mathbf{v}}_h|| + \sum_{K \in \mathcal{T}_h} \{A_{h,K}^\Delta(\widetilde{\mathbf{v}}_h, \widetilde{\mathbf{v}}_h)^{1/2} A_{h,K}^\Delta(\mathbf{r}_I - \mathbf{r}_\pi, \mathbf{r}_I - \mathbf{r}_\pi)^{1/2} \\ &+ A_K^\Delta(\widetilde{\mathbf{v}}_h, \widetilde{\mathbf{v}}_h)^{1/2} A_K^\Delta(\mathbf{r}_I - \mathbf{r}_\pi, \mathbf{r}_I - \mathbf{r}_\pi)^{1/2}\} \\ &\leq C|| \mathbf{r} - \mathbf{r}_I || \, ||\widetilde{\mathbf{v}} - \widetilde{\mathbf{v}}_h|| + (\alpha_2 + 1) \sum_{K \in \mathcal{T}_h} |\widetilde{\mathbf{v}}_h|_{2,K} | \mathbf{r}_I - \mathbf{r}_\pi |_{2,K} \\ &\leq C|| \mathbf{r} - \mathbf{r}_I || \, ||\widetilde{\mathbf{v}} - \widetilde{\mathbf{v}}_h|| + (\alpha_2 + 1) \sum_{K \in \mathcal{T}_h} |\widetilde{\mathbf{v}}_h|_{2,K} \Big(| \mathbf{r} - \mathbf{r}_\pi |_{2,K} + | \mathbf{r} - \mathbf{r}_I |_{2,K} \Big). \end{aligned}$$

Then, using (3.4.25), (3.4.22), (3.4.27), and (3.4.24) in the above term, we infer

$$||\widetilde{\mathbf{v}} - \widetilde{\mathbf{v}}_h||^2_{0,\Omega} \leq Ch^t|| \,\mathbf{r}\, ||_{2+t,\Omega}||\widetilde{\mathbf{v}}|| = Ch^t|| \,\mathbf{r}\, ||_{2+t,\Omega} \leq Ch^t||\widetilde{\mathbf{v}} - \widetilde{\mathbf{v}}_h||_{0,\Omega},$$

and therefore, we conclude that

$$||\widetilde{\mathbf{v}} - \widetilde{\mathbf{v}}_h||_{0,\Omega} \leq Ch^t. \tag{3.4.28}$$

Now, using interpolation theory [38, Chapter 14] on the estimates (3.4.22) and (3.4.28), we obtain that for all $\delta \in [0, 2]$ the following estimate holds true

$$||\widetilde{\mathbf{v}} - \widetilde{\mathbf{v}}_h||_{\delta,\Omega} \leq Ch^{t(2-\delta)/2}.$$

Then, using the Sobolev injection of $H^{1+\sigma}(\Omega)$ (for all $\sigma > 0$) in $L^\infty(\Omega)$ (see e.g [1, Theorem 4.12]) we have in particular that

$$||\widetilde{\mathbf{v}} - \widetilde{\mathbf{v}}_h||_{\infty,\Omega} \leq ||\widetilde{\mathbf{v}} - \widetilde{\mathbf{v}}_h||_{\tilde{\delta},\Omega} \leq Ch^{t(2-\tilde{\delta})/2}$$

for some $\tilde{\delta} \in (1, 2)$. In particular, taking $\tilde{\delta} = 3/2$, we conclude the proof. □

Now, we will use Lemma 3.4.1 to prove that operator T is well defined. More precisely, we will show in the following result that $A_{h,\mathbf{u}_I}(\cdot,\cdot)$ is non singular (cf. (3.2.18)) on $\mathbb{H}_h \times \mathbb{H}_h$.

Lemma 3.4.2. *Let $\mathbf{u} = (u, \psi) \in \mathbb{H}$ be an isolated solution of problem (3.2.12). Then, for h small enough we have that the bilinear form $A_{h,\mathbf{u}_I}(\cdot,\cdot)$ (cf. (3.4.19)) is non singular on $\mathbb{H}_h \times \mathbb{H}_h$.*

Proof. Since the discrete space $\mathbb{H}_h \subseteq \mathbb{H}$ we will proceed as in [40, Lemma 2]. However, we have to deal with the approximation of the bilinear and trilinear forms in our case. We recall that at the discrete level it is enough to verify one of the two inequality in (3.2.18) for bilinear form $A_{h,\mathbf{u}_I}(\cdot,\cdot)$. We will prove that there exists a constant $C > 0$ independent of h such that

$$\sup_{\substack{\mathbf{v}_h \in \mathbb{H}_h \\ ||\,\mathbf{v}_h\,|| = 1}} A_{h,\mathbf{u}_I}(\mathbf{w}_h, \mathbf{v}_h) \geq C|| \,\mathbf{w}_h\, || \quad \forall\, \mathbf{w}_h \in \mathbb{H}_h. \tag{3.4.29}$$

Indeed, because of $\mathbf{u}$ is isolated, we have from Definition 3.2.1 that $A_{\mathbf{u}}(\cdot,\cdot)$ (cf. (3.2.17)) is non singular on $\mathbb{H} \times \mathbb{H}$. Then, the following result is a consequence of the fact that $A_{\mathbf{u}}(\cdot,\cdot)$ is non singular, $\mathbf{u}_I, \mathbf{w}_h \in \mathbb{H}_h \subset \mathbb{H}$, (3.4.18) and Theorem 3.2.3.

$$\sup_{\substack{\mathbf{v} \in \mathbb{H} \\ ||\mathbf{v}|| = 1}} A_{\mathbf{u}_I}(\mathbf{w}_h, \mathbf{v}) \geq \overline{c}_1|| \,\mathbf{w}_h\, || \qquad \forall\, \mathbf{w}_h := (w_h, \xi_h) \in \mathbb{H}_h.$$

Next, we can choose $\widetilde{\mathbf{v}} := (\widetilde{v}, \widetilde{\varphi}) \in \mathbb{H}$ with $||\widetilde{\mathbf{v}}|| = 1$ such that

$$A_{\mathbf{u}_I}(\mathbf{w}_h, \widetilde{\mathbf{v}}) \geq \overline{c}_1|| \,\mathbf{w}_h\, ||. \tag{3.4.30}$$

Moreover, from Lemma 3.4.1 we have that: given $\widetilde{\mathbf{v}} = (\widetilde{v}, \widetilde{\varphi})$, there exists $\widetilde{\mathbf{v}}_h := (\widetilde{v}_h, \widetilde{\varphi}_h)$ and $t \in (1/2, 1]$ such that

$$||\widetilde{v} - \widetilde{v}_h||_{0,\Omega} \leq ||\widetilde{\mathbf{v}} - \widetilde{\mathbf{v}}_h||_{0,\Omega} \leq Ch^t, \tag{3.4.31}$$

and

$$||\widetilde{\mathbf{v}} - \widetilde{\mathbf{v}}_h||_{\infty,\Omega} \leq Ch^{t/4}. \tag{3.4.32}$$

Now, from the left hand side of (3.4.29), normalizing $\widetilde{\mathbf{v}}_h$, using the definition of $A_{h,\mathbf{u}_I}(\cdot,\cdot)$ in (3.4.20) and $A_{\mathbf{u}_I}(\cdot,\cdot)$ in (3.2.17), we obtain

$$\begin{aligned}
&\sup_{\substack{\mathbf{v}_h \in \mathbb{H}_h \\ ||\,\mathbf{v}_h\,||=1}} A_{h,\mathbf{u}_I}(\mathbf{w}_h,\mathbf{v}_h) \geq A_{h,\mathbf{u}_I}(\mathbf{w}_h,\widetilde{\mathbf{v}}_h) = A_{\mathbf{u}_I}(\mathbf{w}_h,\widetilde{\mathbf{v}}) + \big\{A_{h,\mathbf{u}_I}(\mathbf{w}_h,\widetilde{\mathbf{v}}_h) - A_{\mathbf{u}_I}(\mathbf{w}_h,\widetilde{\mathbf{v}})\big\} \\
&= A_{\mathbf{u}_I}(\mathbf{w}_h,\widetilde{\mathbf{v}}) + \lambda\Big\{A_h^{\nabla}(\mathbf{w}_h,\widetilde{\mathbf{v}}_h) - A^{\nabla}(\mathbf{w}_h,\widetilde{\mathbf{v}})\Big\} + 2\Big\{B_h(\mathbf{u}_I;\mathbf{w}_h,\widetilde{\mathbf{v}}_h) - B(\mathbf{u}_I;\mathbf{w}_h,\widetilde{\mathbf{v}})\Big\} \\
&\geq \bar{c}_1||\,\mathbf{w}_h\,|| + \lambda\Big\{\underbrace{A_h^{\nabla}(\mathbf{w}_h,\widetilde{\mathbf{v}}_h) - A^{\nabla}(\mathbf{w}_h,\widetilde{\mathbf{v}})}_{E_1}\Big\} + 2\Big\{\underbrace{B_h(\mathbf{u}_I;\mathbf{w}_h,\widetilde{\mathbf{v}}_h) - B(\mathbf{u}_I;\mathbf{w}_h,\widetilde{\mathbf{v}})}_{E_2}\Big\},
\end{aligned} \tag{3.4.33}$$

where, in the last step we have used (3.4.30). We note that the terms E_1 and E_2 have appeared because of the approximation of the bilinear and trilinear forms.

In what follows, we will prove that the terms E_1, E_2 are bounded. Indeed, for E_1 we use the definition of $\mathbf{\Pi}_K^1$, add and subtract the term $\nabla w_h \cdot \nabla\widetilde{v}_h$ and integrate by parts to obtain

$$\begin{aligned}
E_1 &= \sum_{K\in\mathcal{T}_h}\Big\{\int_K \{\nabla w_h\cdot\nabla\widetilde{v} - \mathbf{\Pi}_K^1\nabla w_h\cdot\mathbf{\Pi}_K^1\nabla\widetilde{v}_h\} + s_K^{\nabla}(w_h - \Pi_K^{2,\nabla}w_h, \widetilde{v}_h - \Pi_K^{2,\nabla}\widetilde{v}_h)\Big\} \\
&= \sum_{K\in\mathcal{T}_h}\Big\{\int_K \nabla w_h\cdot\{\nabla\widetilde{v} - \mathbf{\Pi}_K^1\nabla\widetilde{v}_h\} + s_K^{\nabla}(w_h - \Pi_K^{2,\nabla}w_h, \widetilde{v}_h - \Pi_K^{2,\nabla}\widetilde{v}_h)\Big\} \\
&= \sum_{K\in\mathcal{T}_h}\int_K\Big\{\nabla w_h\cdot\{\nabla\widetilde{v}_h - \mathbf{\Pi}_K^1\nabla\widetilde{v}_h\} + \nabla w_h\cdot\nabla(\widetilde{v} - \widetilde{v}_h) + s_K^{\nabla}(w_h - \Pi_K^{2,\nabla}w_h, \widetilde{v}_h - \Pi_K^{2,\nabla}\widetilde{v}_h)\Big\} \\
&= \sum_{K\in\mathcal{T}_h}\int_K\Big\{\nabla w_h\cdot\{\nabla\widetilde{v}_h - \mathbf{\Pi}_K^1\nabla\widetilde{v}_h\} + s_K^{\nabla}(w_h - \Pi_K^{2,\nabla}w_h, \widetilde{v}_h - \Pi_K^{2,\nabla}\widetilde{v}_h)\Big\} + \int_\Omega \Delta w_h(\widetilde{v}_h - \widetilde{v}).
\end{aligned}$$

Next, applying Cauchy-Schwarz inequality three times, using (3.3.9) and the definition of $\Pi_K^{2,\nabla}$ on the right hand side above, we get

$$\begin{aligned}
E_1 &\leq \sum_{K\in\mathcal{T}_h}\Big\{|w_h|_{1,K}||\mathbf{\Pi}_K^1\nabla\widetilde{v}_h - \nabla\widetilde{v}_h||_{0,K} + s_K^{\nabla}(w_h - \Pi_K^{2,\nabla}w_h, w_h - \Pi_K^{2,\nabla}w_h)^{1/2} \\
&\quad\times s_K^{\nabla}(\widetilde{v}_h - \Pi_K^{2,\nabla}\widetilde{v}_h, \widetilde{v}_h - \Pi_K^{2,\nabla}\widetilde{v}_h)^{1/2}\Big\} + ||\Delta w_h||_{0,\Omega}||\widetilde{v} - \widetilde{v}_h||_{0,\Omega} \\
&\leq \sum_{K\in\mathcal{T}_h}\Big\{|w_h|_{1,K}||\mathbf{\Pi}_K^1\nabla\widetilde{v}_h - \nabla\widetilde{v}_h||_{0,K} + c_3|w_h - \Pi_K^{2,\nabla}w_h|_{1,K}|\widetilde{v}_h - \Pi_K^{2,\nabla}\widetilde{v}_h|_{1,K}\Big\} \\
&\quad + ||\Delta w_h||_{0,\Omega}||\widetilde{v} - \widetilde{v}_h||_{0,\Omega} \\
&\leq \sum_{K\in\mathcal{T}_h}\Big\{|w_h|_{1,K}||\mathbf{\Pi}_K^1\nabla\widetilde{v}_h - \nabla\widetilde{v}_h||_{0,K} + c_3|w_h - w_h^{\pi}|_{1,K}|\widetilde{v}_h - \widetilde{v}_h^{\pi}|_{1,K}\Big\} \\
&\quad + ||\Delta w_h||_{0,\Omega}||\widetilde{v} - \widetilde{v}_h||_{0,\Omega},
\end{aligned}$$

for $w_h^{\pi}, \widetilde{v}_h^{\pi} \in \mathbb{P}_2(K)$ such that Proposition 3.3.2 holds true with respect to w_h and $\widetilde{v}_h$. Therefore, from Propositions 3.3.4 and 3.3.2, and (3.4.31), we conclude that

$$E_1 \leq C\sum_{K\in\mathcal{T}_h}\Big\{h_K|w_h|_{1,K}|\nabla\widetilde{v}_h|_{1,K} + c_3Ch_K^2|w_h|_{2,K}|\widetilde{v}_h|_{2,K}\Big\} + Ch^t||\Delta w_h||_{0,\Omega} \leq Ch^t||w_h||, \tag{3.4.34}$$

with $t \in (1/2, 1]$ and where we have used in the last inequality the fact that $||\widetilde{v}_h||_{2,\Omega} \leq ||\widetilde{\mathbf{v}}_h|| = 1$.

Now, let us find a bound for the term E_2 in (3.4.33). Indeed, in E_2, we add and subtract $B(\mathbf{u}_I; \mathbf{w}_h, \widetilde{\mathbf{v}}_h)$ to obtain

$$\begin{aligned} E_2 &= \big\{B_h(\mathbf{u}_I; \mathbf{w}_h, \widetilde{\mathbf{v}}_h) - B(\mathbf{u}_I; \mathbf{w}_h, \widetilde{\mathbf{v}}_h)\big\} + B(\mathbf{u}_I; \mathbf{w}_h, \widetilde{\mathbf{v}}_h - \widetilde{\mathbf{v}}) \\ &= B(\mathbf{u}_I; \mathbf{w}_h, \widetilde{\mathbf{v}}_h - \widetilde{\mathbf{v}}) + \Big\{B_h(\mathbf{u}_I; \mathbf{w}_h, \widetilde{\mathbf{v}}_h) - B(\mathbf{u}_I; \mathbf{w}_h, \widetilde{\mathbf{v}}_h)\Big\}. \end{aligned} \tag{3.4.35}$$

Now, for first term on the right hand side above we have the following estimate,

$$B(\mathbf{u}_I; \mathbf{w}_h, \widetilde{\mathbf{v}}_h - \widetilde{\mathbf{v}}) = \int_\Omega [\mathbf{u}_I, \mathbf{w}_h](\widetilde{\mathbf{v}}_h - \widetilde{\mathbf{v}}) \leq C|| \mathbf{u}_I || \, || \mathbf{w}_h || \, ||\widetilde{\mathbf{v}}_h - \widetilde{\mathbf{v}}||_{\infty,\Omega} \leq Ch^{t/4}|| \mathbf{u}_I || \, || \mathbf{w}_h ||, \tag{3.4.36}$$

with, $t \in (1/2, 1]$ and where we have used the fact that $(\widetilde{\mathbf{v}} - \widetilde{\mathbf{v}}_h) \in L^\infty(\Omega)$ and estimate (3.4.32).

On the other hand, for the second term on right hand side of (3.4.35), we use the definitions of $B_h(\cdot;\cdot,\cdot)$ and $B(\cdot;\cdot,\cdot)$ to get

$$\begin{aligned} &B_h(\mathbf{u}_I; \mathbf{w}_h, \widetilde{\mathbf{v}}_h) - B(\mathbf{u}_I; \mathbf{w}_h, \widetilde{\mathbf{v}}_h) \\ &= -\frac{1}{2} \sum_{K \in \mathcal{T}_h} \int_K \Big\{ \Big([\Pi_K^{2,D} u_I, \Pi_K^{2,D} \xi_h] \Pi_K^2 \widetilde{v}_h - [u_I, \xi_h] \widetilde{v}_h\Big) + \Big([\Pi_K^{2,D} \psi_I, \Pi_K^{2,D} w_h] \Pi_K^2 \widetilde{v}_h - [\psi_I, w_h] \widetilde{v}_h\Big) \\ &- \Big([\Pi_K^{2,D} u_I, \Pi_K^{2,D} w_h] \Pi_K^2 \widetilde{\varphi}_h - [u_I, w_h] \widetilde{\varphi}_h\Big) \Big\} =: -\frac{1}{2} \sum_{K \in \mathcal{T}_h} \int_K \Big\{ \mathbf{B}^{1,K} + \mathbf{B}^{2,K} - \mathbf{B}^{3,K} \Big\}. \end{aligned} \tag{3.4.37}$$

Now, we will prove that the terms $\sum_{K \in \mathcal{T}_h} \int_K \mathbf{B}^{1,K}$, $\sum_{K \in \mathcal{T}_h} \int_K \mathbf{B}^{2,K}$ and $\sum_{K \in \mathcal{T}_h} \int_K (-\mathbf{B}^{3,K})$ are bounded. Indeed, for $\sum_{K \in \mathcal{T}_h} \int_K \mathbf{B}^{1,K}$, we use the definitions of Π_K^2 and $[\cdot,\cdot]$ (cf. (3.3.3) and (3.2.2), respectively) to obtain

$$\begin{aligned} &\sum_{K \in \mathcal{T}_h} \int_K \mathbf{B}^{1,K} = \sum_{K \in \mathcal{T}_h} \int_K \Big([\Pi_K^{2,D} u_I, \Pi_K^{2,D} \xi_h] - [u_I, \xi_h]\Big) \widetilde{v}_h \\ &= \sum_{K \in \mathcal{T}_h} \int_K \Big\{ \Big\{ \Big(\partial_{xx} \Pi_K^{2,D} u_I\Big) \Big(\partial_{yy} \Pi_K^{2,D} \xi_h\Big) \widetilde{v}_h - (\partial_{xx} u_I)(\partial_{yy} \xi_h) \widetilde{v}_h \Big\} \\ &+ \Big\{ \Big(\partial_{yy} \Pi_K^{2,D} u_I\Big) \Big(\partial_{xx} \Pi_K^{2,D} \xi_h\Big) \widetilde{v}_h - (\partial_{yy} u_I)(\partial_{xx} \xi_h) \widetilde{v}_h \Big\} \\ &- 2\Big\{ \Big(\partial_{xy} \Pi_K^{2,D} u_I\Big) \Big(\partial_{xy} \Pi_K^{2,D} \xi_h\Big) \widetilde{v}_h - (\partial_{xy} u_I)(\partial_{xy} \xi_h) \widetilde{v}_h \Big\} \Big\} =: \sum_{K \in \mathcal{T}_h} \int_K \Big\{ \boldsymbol{\alpha} + \boldsymbol{\beta} - 2\boldsymbol{\gamma} \Big\}. \end{aligned} \tag{3.4.38}$$

Next, we will estimate the term $\sum_{K \in \mathcal{T}_h} \int_K \boldsymbol{\alpha}$. The terms $\sum_{K \in \mathcal{T}_h} \int_K \boldsymbol{\beta}$ and $\sum_{K \in \mathcal{T}_h} \int_K (-2)\boldsymbol{\gamma}$ can be treated with the same arguments. Thus, applying the identity $\partial_{ij} \Pi_K^{2,D} v_h = \Pi_K^0(\partial_{ij} v_h)$ for all $v_h \in H_h^K$ and for all $i, j = x, y$, (which is a consequence of the definitions of the projectors $\Pi_K^{2,D}$ and Π_K^0 (cf. (3.3.1a) and (3.3.3), respectively)) in the expression $\int_K \boldsymbol{\alpha}$, we obtain

$$\sum_{K \in \mathcal{T}_h} \int_K \boldsymbol{\alpha} = \sum_{K \in \mathcal{T}_h} \int_K \Big\{ \Pi_K^0(\partial_{xx} u_I) \Pi_K^0(\partial_{yy} \xi_h) \widetilde{v}_h - (\partial_{xx} u_I)(\partial_{yy} \xi_h) \widetilde{v}_h \Big\}. \tag{3.4.39}$$

Now, adding and subtracting the terms $\Pi_K^0(\partial_{xx}u)\Pi_K^0(\partial_{yy}\xi_h)\widetilde{v}_h$, $\Pi_K^0(\partial_{xx}u)(\partial_{yy}\xi_h)\widetilde{v}_h$ and $(\partial_{yy}\xi_h)(\partial_{xx}u)\widetilde{v}_h$, and using the definitions of Π_K^0 on the right hand side of (3.4.39), we get

$$\begin{aligned}
\sum_{K\in\mathcal{T}_h}\int_K \boldsymbol{\alpha} &= \sum_{K\in\mathcal{T}_h}\int_K \Big\{\Big\{\Pi_K^0(\partial_{xx}(u_I-u))\Big\}\Pi_K^0(\partial_{yy}\xi_h)\widetilde{v}_h + \Pi_K^0(\partial_{xx}u)\Big\{(\Pi_K^0-I)(\partial_{yy}\xi_h)\Big\}\widetilde{v}_h \\
&\quad + (\partial_{yy}\xi_h)\Big\{(\Pi_K^0-I)(\partial_{xx}u)\Big\}\widetilde{v}_h + (\partial_{yy}\xi_h)(\partial_{xx}(u-u_I))\widetilde{v}_h\Big\} \\
&= \sum_{K\in\mathcal{T}_h}\int_K \Big\{\Big\{\Pi_K^0(\partial_{xx}(u_I-u))\Big\}\Pi_K^0(\partial_{yy}\xi_h)\widetilde{v}_h \\
&\quad + \Pi_K^0(\partial_{xx}u)\Big\{(\Pi_K^0-I)(\partial_{yy}\xi_h)\Big\}\Big\{(I-\Pi_K^0)\widetilde{v}_h\Big\} \\
&\quad + (\partial_{yy}\xi_h)\Big\{(\Pi_K^0-I)(\partial_{xx}u)\Big\}\widetilde{v}_h + (\partial_{yy}\xi_h)(\partial_{xx}(u-u_I))\widetilde{v}_h\Big\}
\end{aligned}$$

Then, applying Cauchy-Schwarz and Hölder inequalities, using the fact that $\widetilde{v}_h \in L^\infty(K)$, and Π_K^0 is bounded in the L^2-norm, on the right hand side of the last equality, we obtain

$$\begin{aligned}
\sum_{K\in\mathcal{T}_h}\int_K \boldsymbol{\alpha} &\le \sum_{K\in\mathcal{T}_h}\Big\{||\Pi_K^0(\partial_{xx}(u_I-u))||_{0,K}||\Pi_K^0(\partial_{yy}\xi_h)||_{0,K}||\widetilde{v}_h||_{\infty,K} \\
&\quad + ||\Pi_K^0(\partial_{xx}u)||_{L^4(K)}||(\Pi_K^0-I)(\partial_{yy}\xi_h)||_{0,K}||(I-\Pi_K^0)\widetilde{v}_h||_{L^4(K)} \\
&\quad + ||\partial_{yy}\xi_h||_{0,K}||(\Pi_K^0-I)(\partial_{xx}u)||_{0,K}||\widetilde{v}_h||_{\infty,K} + ||\partial_{yy}\xi_h||_{0,K}||\partial_{xx}(u-u_I)||_{0,K}||\widetilde{v}_h||_{\infty,K}\Big\} \\
&\le \sum_{K\in\mathcal{T}_h}\Big\{||\partial_{xx}(u_I-u)||_{0,K}||\partial_{yy}\xi_h||_{0,K}||\widetilde{v}_h||_{\infty,K} \\
&\quad + ||\Pi_K^0(\partial_{xx}u)||_{L^4(K)}||\partial_{yy}\xi_h||_{0,K}||(I-\Pi_K^0)\widetilde{v}_h||_{L^4(K)} \\
&\quad + ||\partial_{yy}\xi_h||_{0,K}||(\Pi_K^0-I)(\partial_{xx}u)||_{0,K}||\widetilde{v}_h||_{\infty,K} + ||\partial_{yy}\xi_h||_{0,K}||\partial_{xx}(u-u_I)||_{0,K}||\widetilde{v}_h||_{\infty,K}\Big\} \\
&\le \sum_{K\in\mathcal{T}_h}\Big\{Ch_K^s|u|_{2+s,K}|\xi_h|_{2,K}\Big\} + \sum_{K\in\mathcal{T}_h}\Big\{||\Pi_K^0(\partial_{xx}u)||_{L^4(K)}||\partial_{yy}\xi_h||_{0,K}||(I-\Pi_K^0)\widetilde{v}_h||_{L^4(K)}\Big\},
\end{aligned} \tag{3.4.40}$$

where in the last step, we have used Theorem 3.2.1, Propositions 3.3.3 and 3.3.2, and the fact that $||\widetilde{v}_h||_{\infty,K} \le ||\widetilde{v}_h||_{\infty,\Omega} \le C||\widetilde{v}_h||_{2,\Omega} \le C||\widetilde{\mathbf{v}}_h|| = C$ (which is a consequence of $H^{1+\sigma}(\Omega) \subseteq L^\infty(\Omega)$ for all $\sigma > 0$, see e.g., [1, Theorem 4.12]).

Now, to bound the second term on the right hand side of (3.4.40), it is easy to check that $||\Pi_K^0(\partial_{xx}u)||_{L^4(K)} \le C||\partial_{xx}u||_{L^4(K)}$ (see Proposition 3.3 in [24]). Thus, applying Hölder inequality (for sequences), [80, Lemma 3.7], and using the Sobolev imbeddings $H^s(\Omega) \hookrightarrow L^4(\Omega)$ for $s \in (1/2, 1]$

and $H^2(\Omega) \hookrightarrow W^{1,4}(\Omega)$ (see [10, Theorem 7.3.7(a-b)]), we get

$$\begin{aligned}
\sum_{K\in\mathcal{T}_h}\int_K \boldsymbol{\alpha} &\leq Ch^s||u||_{2+s,\Omega}|\xi_h|_{2,\Omega} + \sum_{K\in\mathcal{T}_h}\Big\{||\partial_{xx}u||_{L^4(K)}|\xi_h|_{2,K}||(I-\Pi_K^0)\widetilde{v}_h||_{L^4(K)}\Big\}\\
&\leq Ch^s||u||_{2+s,\Omega}|\xi_h|_{2,\Omega}\\
&+\Big(\sum_{K\in\mathcal{T}_h}||\partial_{xx}u||^4_{L^4(K)}\Big)^{1/4}\Big(\sum_{K\in\mathcal{T}_h}||\partial_{yy}\xi_h||^2_{0,K}\Big)^{1/2}\Big(\sum_{K\in\mathcal{T}_h}||(I-\Pi_K^0)\widetilde{v}_h||^4_{L^4(K)}\Big)^{1/4}\\
&\leq Ch^s||u||_{2+s,\Omega}|\xi_h|_{2,\Omega} + ||\partial_{xx}u||_{L^4(\Omega)}||\partial_{yy}\xi_h||_{0,\Omega}\Big(\sum_{K\in\mathcal{T}_h}||(I-\Pi_K^0)\widetilde{v}_h||^4_{L^4(K)}\Big)^{1/4}\\
&\leq Ch^s||u||_{2+s,\Omega}|\xi_h|_{2,\Omega} + ||\partial_{xx}u||_{L^4(\Omega)}||\partial_{yy}\xi_h||_{0,\Omega}\Big(C\sum_{K\in\mathcal{T}_h}h_K^4|\widetilde{v}_h|^4_{W^{1,4}(K)}\Big)^{1/4}\\
&\leq Ch^s||u||_{2+s,\Omega}|\xi_h|_{2,\Omega} + Ch||\partial_{xx}u||_{L^4(\Omega)}||\partial_{yy}\xi_h||_{0,\Omega}|\widetilde{v}_h|_{W^{1,4}(\Omega)}\\
&\leq Ch^s||u||_{2+s,\Omega}|\xi_h|_{2,\Omega} + Ch|\partial_{xx}u|_{s,\Omega}||\partial_{yy}\xi_h||_{0,\Omega}|\widetilde{v}_h|_{2,\Omega}\\
&\leq Ch^s||u||_{2+s,\Omega}||\xi_h||_{2,\Omega} + Ch||u||_{2+s,\Omega}||\xi_h||_{2,\Omega}||\widetilde{v}_h||_{2,\Omega}\\
&\leq Ch^s||u||_{2+s,\Omega}||\xi_h||_{2,\Omega}, \qquad (3.4.41)
\end{aligned}$$

where, in the two last steps we have used the definition of norm $||\cdot||_{2,\Omega}$ and the fact that $||\widetilde{v}_h||_{2,\Omega} \leq ||\widetilde{\mathbf{v}}_h|| \leq C||\widetilde{\mathbf{v}}|| = C$. Note that C is independent of the parameter h.

Moreover, repeating the same steps used in (3.4.39)-(3.4.41), we can prove the following estimates

$$\sum_{K\in\mathcal{T}_h}\int_K \boldsymbol{\beta} \leq Ch^s||\xi_h||_{2,\Omega}||u||_{2+s,\Omega} \quad \text{and} \quad \sum_{K\in\mathcal{T}_h}\int_K(-2)\boldsymbol{\gamma} \leq Ch^s||\xi_h||_{2,\Omega}||u||_{2+s,\Omega}. \qquad (3.4.42)$$

Hence, from (3.4.38) and (3.4.40),(3.4.42), we obtain

$$\sum_{K\in\mathcal{T}_h}\int_K \mathbf{B}^{1,K} \leq Ch^s||u||_{2+s,\Omega}||\xi_h||_{2,\Omega}. \qquad (3.4.43)$$

Now, we observe that the terms in (3.4.37) can be bounded repeating the same arguments used to bound $\sum_{K\in\mathcal{T}_h}\mathbf{B}^{1,K}$. Thus,

$$\sum_{K\in\mathcal{T}_h}\int_K \mathbf{B}^{2,K} \leq Ch^s||\psi||_{2+s,\Omega}||w_h||_{2,\Omega} \quad \text{and} \quad \sum_{K\in\mathcal{T}_h}\int_K(-1)\mathbf{B}^{3,K} \leq Ch^s||u||_{2+s,\Omega}||w_h||_{2,\Omega}.$$

As a consequence, we have that

$$\sum_{K\in\mathcal{T}_h}\left\{\int_K \mathbf{B}^{2,K} - \int_K \mathbf{B}^{3,K}\right\} \leq Ch^s\{||\psi||_{2+s,\Omega}||w_h||_{2,\Omega} + ||u||_{2+s,\Omega}||w_h||_{2,\Omega}\}. \qquad (3.4.44)$$

Therefore, we have the following bound for the term E_2 in (3.4.35)

$$E_2 \leq Ch^{\tilde{s}}||\,\mathbf{u}\,||_{2+s,\Omega}||\,\mathbf{w}_h\,||, \qquad (3.4.45)$$

with $\tilde{s} := \min\{s, t/4\}$, and where $s, t \in (1/2, 1]$.

Hence, from (3.4.34), (3.4.45) and Theorem 3.2.1 we get the following estimate

$$\lambda E_1 + 2E_2 \leq Ch^{\tilde{s}} || \mathbf{u} ||_{2+\tilde{s},\Omega} || \mathbf{w}_h || \leq Ch^{\tilde{s}} ||f||_{0,\Omega} || \mathbf{w}_h ||. \tag{3.4.46}$$

Finally, from (3.4.46), there exists $h_0 := \left(\frac{\overline{c}_1}{2C||f||_{0,\Omega}}\right)^{1/\tilde{s}} > 0$ such that for all $h \leq h_0$, the following result is deduced from (3.4.33)

$$\sup_{\substack{\mathbf{v}_h \in \mathbb{H}_h \\ || \mathbf{v}_h || = 1}} A_{h,\mathbf{u}_I}(\mathbf{w}_h, \mathbf{v}_h) \geq \overline{c}_1 || \mathbf{w}_h || - Ch^{\tilde{s}} ||f||_{0,\Omega} || \mathbf{w}_h || \geq \frac{\overline{c}_1}{2} || \mathbf{w}_h ||.$$

The proof is complete. □

Now, in what follows, we will focus on proving that the operator T satisfies the hypotheses of Banach fixed-point theorem [39, Theorem 5.7]. With this aim, first from Lemma 3.4.2 we will prove that the operator T maps the ball

$$\mathcal{B}(\mathbf{u}_I, R) := \{\mathbf{w}_h \in \mathbb{H}_h : || \mathbf{w}_h - \mathbf{u}_I || \leq R\}$$

to itself, where $R := R(h) > 0$ is a positive real number depending on h which will be specified later in Lemma 3.4.4 and we recall that $\mathbf{u}_I$ is the interpolant of the isolated solution $\mathbf{u}$. We first need to prove a technical lemma.

Lemma 3.4.3. *Let $\mathbf{w}_h \in \mathbb{H}_h$. For h small enough, there exists a positive constant C, independent of h, such that*

$$||T \mathbf{w}_h - \mathbf{u}_I || \leq C(h^s + || \mathbf{u}_I - \mathbf{w}_h ||^2),$$

where $s \in (1/2, 1]$ is the Sobolev exponent for the solution of the von Kármán problem (see Theorem 3.2.1).

Proof. Let $\mathbf{w}_h \in \mathbb{H}_h$. Since $T \mathbf{w}_h - \mathbf{u}_I \in \mathbb{H}_h$, we have from Lemma 3.4.2 (cf. (3.4.29)) that there exists $\widetilde{c}_1 > 0$ such that

$$\widetilde{c}_1 ||T \mathbf{w}_h - \mathbf{u}_I || \leq \sup_{\substack{\mathbf{v}_h \in \mathbb{H}_h \\ || \mathbf{v}_h || = 1}} A_{h,\mathbf{u}_I}(T \mathbf{w}_h - \mathbf{u}_I, \mathbf{v}_h).$$

Now, we can choose $\overline{\mathbf{v}}_h \in \mathbb{H}_h \subseteq \mathbb{H}$ with $||\overline{\mathbf{v}}_h|| = 1$ such that

$$\widetilde{c}_1 ||T \mathbf{w}_h - \mathbf{u}_I || \leq A_{h,\mathbf{u}_I}(T \mathbf{w}_h - \mathbf{u}_I, \overline{\mathbf{v}}_h). \tag{3.4.47}$$

Next, using the definitions of T and $A_{h,\mathbf{u}_I}(\cdot,\cdot)$ (cf. (3.4.20) and (3.4.19)), and adding the continuous

variational formulation (3.2.12) tested with $\overline{\mathbf{v}}_h$ on the right hand side of (3.4.47), we obtain

$$
\begin{aligned}
&\widetilde{c}_1||T\,\mathbf{w}_h-\mathbf{u}_I\,||\leq A_{h,\mathbf{u}_I}(T\,\mathbf{w}_h-\mathbf{u}_I,\overline{\mathbf{v}}_h)=A_{h,\mathbf{u}_I}(T\,\mathbf{w}_h,\overline{\mathbf{v}}_h)-A_{h,\mathbf{u}_I}(\mathbf{u}_I,\overline{\mathbf{v}}_h)\\
&=2B_h(\mathbf{u}_I;\mathbf{w}_h,\overline{\mathbf{v}}_h)-B_h(\mathbf{w}_h;\mathbf{w}_h,\overline{\mathbf{v}}_h)+F_h(\overline{\mathbf{v}}_h)-A_h^{\Delta}(\mathbf{u}_I,\overline{\mathbf{v}}_h)-\lambda A_h^{\nabla}(\mathbf{u}_I,\overline{\mathbf{v}}_h)-2B_h(\mathbf{u}_I;\mathbf{u}_I,\overline{\mathbf{v}}_h)\\
&=2B_h(\mathbf{u}_I;\mathbf{w}_h,\overline{\mathbf{v}}_h)-B_h(\mathbf{w}_h;\mathbf{w}_h,\overline{\mathbf{v}}_h)+F_h(\overline{\mathbf{v}}_h)-A_h^{\Delta}(\mathbf{u}_I,\overline{\mathbf{v}}_h)-\lambda A_h^{\nabla}(\mathbf{u}_I,\overline{\mathbf{v}}_h)-2B_h(\mathbf{u}_I;\mathbf{u}_I,\overline{\mathbf{v}}_h)\\
&+A^{\Delta}(\mathbf{u},\overline{\mathbf{v}}_h)+\lambda A^{\nabla}(\mathbf{u},\overline{\mathbf{v}}_h)+B(\mathbf{u};\mathbf{u},\overline{\mathbf{v}}_h)-F(\overline{\mathbf{v}}_h)\\
&=\underbrace{\Big\{2B_h(\mathbf{u}_I;\mathbf{w}_h,\overline{\mathbf{v}}_h)-B_h(\mathbf{w}_h;\mathbf{w}_h,\overline{\mathbf{v}}_h)-B_h(\mathbf{u}_I;\mathbf{u}_I,\overline{\mathbf{v}}_h)\Big\}}_{G_1}+\underbrace{\Big\{F_h(\overline{\mathbf{v}}_h)-F(\overline{\mathbf{v}}_h)\Big\}}_{G_2}\\
&+\underbrace{\Big\{A^{\Delta}(\mathbf{u},\overline{\mathbf{v}}_h)-A_h^{\Delta}(\mathbf{u}_I,\overline{\mathbf{v}}_h)\Big\}}_{G_3}+\underbrace{\lambda\Big\{A^{\nabla}(\mathbf{u},\overline{\mathbf{v}}_h)-A_h^{\nabla}(\mathbf{u}_I,\overline{\mathbf{v}}_h)\Big\}}_{G_4}+\underbrace{\Big\{B(\mathbf{u};\mathbf{u},\overline{\mathbf{v}}_h)-B_h(\mathbf{u}_I;\mathbf{u}_I,\overline{\mathbf{v}}_h)\Big\}}_{G_5}.
\end{aligned}
\tag{3.4.48}
$$

In what follows, we want to bound all the terms $G_i, i=1,\ldots,5$ defined in (3.4.48). Indeed, using the properties of the trilinear form, we rewrite G_1, then applying the identity (3.3.16f) and (3.3.16e) and the fact that $||\overline{\mathbf{v}}_h||=1$, we get

$$
\begin{aligned}
G_1&=B_h(\mathbf{u}_I;\mathbf{w}_h,\overline{\mathbf{v}}_h)-B_h(\mathbf{w}_h;\mathbf{w}_h,\overline{\mathbf{v}}_h)-B_h(\mathbf{u}_I;\mathbf{u}_I,\overline{\mathbf{v}}_h)+B_h(\mathbf{u}_I;\mathbf{w}_h,\overline{\mathbf{v}}_h)\\
&=B_h(\mathbf{u}_I-\mathbf{w}_h;\mathbf{w}_h,\overline{\mathbf{v}}_h)+B_h(\mathbf{u}_I;\mathbf{w}_h-\mathbf{u}_I,\overline{\mathbf{v}}_h)\\
&=B_h(\mathbf{u}_I-\mathbf{w}_h;\mathbf{w}_h,\overline{\mathbf{v}}_h)+B_h(\mathbf{u}_I-\mathbf{w}_h;-\mathbf{u}_I,\overline{\mathbf{v}}_h)\\
&=B_h(\mathbf{u}_I-\mathbf{w}_h;\mathbf{w}_h-\mathbf{u}_I,\overline{\mathbf{v}}_h)\\
&\leq C||\,\mathbf{u}_I-\mathbf{w}_h\,||\;||\,\mathbf{w}_h-\mathbf{u}_I\,||\;||\overline{\mathbf{v}}_h||=C||\,\mathbf{u}_I-\mathbf{w}_h\,||^2.
\end{aligned}
\tag{3.4.49}
$$

For G_2, we use Cauchy-Schwarz inequality and Lemma 3.3.4 to obtain

$$
G_2=\sum_{K\in\mathcal{T}_h}\int_K f(\Pi_K^{2,D}\widetilde{v}_h-\widetilde{v}_h)\leq||f||_{0,\Omega}||\Pi_K^{2,D}\widetilde{v}_h-\widetilde{v}_h||_{0,\Omega}\leq Ch^2||f||_{0,\Omega}||\overline{\mathbf{v}}_h||=Ch^2||f||_{0,\Omega}.
\tag{3.4.50}
$$

Next, to bound G_3, we use Theorem 3.2.1 and Proposition 3.3.2 to find $\mathbf{u}_\pi\in[\mathbb{P}_k(K)]^2$ such that

$$
|\,\mathbf{u}-\mathbf{u}_\pi\,|_{2,K}\leq Ch^s|\,\mathbf{u}\,|_{2+s,K}\leq Ch^s||f||_{0,K}\quad\forall K\in\mathcal{T}_h,
\tag{3.4.51}
$$

with $s\in(1/2,1]$.

Now, in the definition of G_3, we add and subtract the term $\mathbf{u}_\pi$, use the definition of $A_{h,K}^{\Delta}(\cdot,\cdot)$, property (3.3.10), Cauchy-Schwarz inequality, and apply the estimate (3.3.12) in the definition of $A_{h,K}(\cdot,\cdot)$ to obtain

$$
\begin{aligned}
G_3&=\sum_{K\in\mathcal{T}_h}\Big\{A_K^{\Delta}(\mathbf{u}-\mathbf{u}_\pi,\overline{\mathbf{v}}_h)+A_{h,K}^{\Delta}(\mathbf{u}_\pi-\mathbf{u}_I,\overline{\mathbf{v}}_h)\Big\}\\
&\leq\sum_{K\in\mathcal{T}_h}\Big\{|\,\mathbf{u}-\mathbf{u}_\pi\,|_{2,K}|\overline{\mathbf{v}}_h|_{2,K}+A_{h,K}^{\Delta}(\mathbf{u}_\pi-\mathbf{u}_I,\mathbf{u}_\pi-\mathbf{u}_I)^{1/2}A_{h,K}^{\Delta}(\overline{\mathbf{v}}_h,\overline{\mathbf{v}}_h)^{1/2}\Big\}\\
&\leq\sum_{K\in\mathcal{T}_h}\Big\{|\,\mathbf{u}-\mathbf{u}_\pi\,|_{2,K}|\overline{\mathbf{v}}_h|_{2,K}+\alpha_2|\,\mathbf{u}_\pi-\mathbf{u}_I\,|_{2,K}|\overline{\mathbf{v}}_h|_{2,K}\Big\}.
\end{aligned}
$$

Next, adding and subtracting the term $\mathbf{u}$, using the estimates (3.4.51) and (3.4.18) on the right hand side of the above term, we get

$$\begin{aligned} G_3 &\leq \sum_{K\in\mathcal{T}_h} \Big\{(1+\alpha_2)|\,\mathbf{u}-\mathbf{u}_\pi\,|_{2,K}|\overline{\mathbf{v}}_h|_{2,K} + \alpha_2|\,\mathbf{u}-\mathbf{u}_I\,|_{2,K}|\overline{\mathbf{v}}_h|_{2,K}\Big\} \\ &\leq Ch^s||\,\mathbf{u}\,||_{2+s,\Omega}||\overline{\mathbf{v}}_h|| = Ch^s||\,\mathbf{u}\,||_{2+s,\Omega} \leq Ch^s||f||_{0,\Omega}. \end{aligned} \tag{3.4.52}$$

For the term G_4, we use the definition of $\mathbf{\Pi}^1_K$, Cauchy Schwarz inequality, and (3.3.9) to obtain

$$\begin{aligned} G_4 &= \sum_{K\in\mathcal{T}_h} \Big\{ \int_K \{\mathbf{\Pi}^1_K\nabla u_I - \nabla u\}\cdot\nabla\widetilde{v}_h + s^\nabla_K(\Pi^{2,\nabla}_K u_I - u_I, \widetilde{v}_h - \Pi^{2,\nabla}_K\widetilde{v}_h)\Big\} \\ &\leq \sum_{K\in\mathcal{T}_h} \Big\{||\mathbf{\Pi}^1_K\nabla u_I - \nabla u||_{0,K}|\widetilde{v}_h|_{1,K} + s^\nabla_K(\Pi^{2,\nabla}_K u_I - u_I, \Pi^{2,\nabla}_K u_I - u_I)^{1/2} \\ &+ s^\nabla_K(\widetilde{v}_h - \Pi^{2,\nabla}_K\widetilde{v}_h), \widetilde{v}_h - \Pi^{2,\nabla}_K\widetilde{v}_h)^{1/2}\Big\}. \\ &\leq \sum_{K\in\mathcal{T}_h} \Big\{||\mathbf{\Pi}^1_K\nabla u_I - \nabla u||_{0,K}|\widetilde{v}_h|_{1,K} + c_3|u_I - \Pi^{2,\nabla}_K u_I|_{1,K}|\widetilde{v}_h - \Pi^{2,\nabla}_K\widetilde{v}_h|_{1,K}\Big\} \\ &\leq \sum_{K\in\mathcal{T}_h} \Big\{||\mathbf{\Pi}^1_K\nabla u_I - \nabla u_I||_{0,K}|\widetilde{v}_h|_{1,K} + ||\nabla(u-u_I)||_{0,K}|\widetilde{v}_h|_{1,K} \\ &+ c_3|u_I - \Pi^{2,\nabla}_K u_I|_{1,K}|\widetilde{v}_h - \Pi^{2,\nabla}_K\widetilde{v}_h|_{1,K}\Big\}, \end{aligned}$$

where in the last step we have added and subtracted ∇u_I.

Now, on the right hand side above, we apply Propositions 3.3.4 and 3.3.3, the definition of $\Pi^{2,\nabla}_K$, Proposition 3.3.2 and finally Theorem 3.2.1, to deduce that

$$\begin{aligned} G_4 &\leq C\sum_{K\in\mathcal{T}_h} \Big\{\{h_K|u_I|_{2,K} + h^{1+s}_K|u|_{2,K}\}|\widetilde{v}_h|_{1,K} + h^2_K|u_I|_{2,K}|\widetilde{v}_h|_{2,K}\Big\} \\ &\leq Ch||\,\mathbf{u}\,||_{2+s,\Omega}\,||\overline{\mathbf{v}}_h|| = Ch||\,\mathbf{u}\,||_{2+s,\Omega} \leq Ch||f||_{0,\Omega}. \end{aligned} \tag{3.4.53}$$

It is easy to check that G_5 can be bounded using the same arguments as those applied to estimate (3.4.37). Hence, we obtain the following result

$$G_5 \leq Ch^s||\,\mathbf{u}\,||_{2+s,\Omega}||\overline{\mathbf{v}}_h|| = Ch^s||\,\mathbf{u}\,||_{2+s,\Omega} \leq Ch^s||f||_{0,\Omega}. \tag{3.4.54}$$

Therefore, by combining (3.4.48) and the estimates (3.4.49)-(3.4.50), (3.4.52)-(3.4.54), we obtain that

$$||T\,\mathbf{w}_h - \mathbf{u}_I\,|| \leq C(h^s + ||\,\mathbf{u}_I - \mathbf{w}_h\,||^2),$$

where C is a positive constant depending on $||f||_{0,\Omega}$, and $s\in(1/2,1]$ is the Sobolev exponent for the solution of the von Kármán problem (see Theorem 3.2.1). □

Now, we are in position to prove that T maps the ball $\mathcal{B}(\mathbf{u}_I,R)$ to itself.

Lemma 3.4.4. *For h small enough, there exists a positive constant $R(h)$, depending on h, such that*

$$T(\mathcal{B}(\mathbf{u}_I,R(h))) \subseteq \mathcal{B}(\mathbf{u}_I,R(h)).$$

Proof. Let $\mathbf{z}_h \in T(\mathcal{B}(\mathbf{u}_I, R))$, then there exists $\widetilde{\mathbf{w}}_h \in \mathbb{H}_h$ such that $\mathbf{z}_h = T\widetilde{\mathbf{w}}_h$ and $||\widetilde{\mathbf{w}}_h - \mathbf{u}_I|| \leq R$. Then, applying Lemma 3.4.3, we have

$$||\mathbf{z}_h - \mathbf{u}_I|| = ||T\widetilde{\mathbf{w}}_h - \mathbf{u}_I|| \leq \widetilde{C}(h^s + ||\mathbf{u}_I - \widetilde{\mathbf{w}}_h||^2).$$

Now, for all $h \leq h_1 := (2\widetilde{C})^{-2/s}$, we choose $2\widetilde{C}h^s =: R(h) = R$ and obtain

$$||\mathbf{z}_h - \mathbf{u}_I|| \leq \widetilde{C}h^s + \widetilde{C}||\widetilde{\mathbf{w}}_h - \mathbf{u}_I||^2 \leq \widetilde{C}h^s + \widetilde{C}R(h)^2 = \frac{R(h)}{2} + \frac{R(h)}{2}4\widetilde{C}^2h^s \leq R(h).$$

Therefore $\mathbf{z}_h \in \mathcal{B}(\mathbf{u}_I, R(h))$. □

In the following result, we will prove that the operator T is a contraction in $\mathcal{B}(\mathbf{u}_I, R(h))$.

Lemma 3.4.5. *For h small enough, the operator T is a contraction in $\mathcal{B}(\mathbf{u}_I, R(h))$.*

Proof. Let $\mathbf{w}_h, \widetilde{\mathbf{w}}_h \in \mathcal{B}(\mathbf{u}_I, R(h))$, hence

$$||\mathbf{w}_h - \mathbf{u}_I||, ||\widetilde{\mathbf{w}}_h - \mathbf{u}_I|| \leq R(h) = 2\widetilde{C}h^s. \tag{3.4.55}$$

Now, from the definition of operator T (cf. (3.4.20)), we have

$$\begin{aligned} A_{h,\mathbf{u}_I}(T\mathbf{w}_h, \mathbf{v}_h) &= 2B_h(\mathbf{u}_I; \mathbf{w}_h, \mathbf{v}_h) - B_h(\mathbf{w}_h; \mathbf{w}_h, \mathbf{v}_h) + F_h(\mathbf{v}_h) \qquad \forall\, \mathbf{v}_h \in \mathbb{H}_h; \\ A_{h,\mathbf{u}_I}(T\widetilde{\mathbf{w}}_h, \mathbf{v}_h) &= 2B_h(\mathbf{u}_I; \widetilde{\mathbf{w}}_h, \mathbf{v}_h) - B_h(\widetilde{\mathbf{w}}_h; \widetilde{\mathbf{w}}_h, \mathbf{v}_h) + F_h(\mathbf{v}_h) \qquad \forall\, \mathbf{v}_h \in \mathbb{H}_h, \end{aligned}$$

which implies

$$A_{h,\mathbf{u}_I}(T(\mathbf{w}_h - \widetilde{\mathbf{w}}_h), \mathbf{v}_h) = 2B_h(\mathbf{u}_I; \mathbf{w}_h - \widetilde{\mathbf{w}}_h, \mathbf{v}_h) - B_h(\mathbf{w}_h; \mathbf{w}_h, \mathbf{v}_h) + B_h(\widetilde{\mathbf{w}}_h; \widetilde{\mathbf{w}}_h, \mathbf{v}_h) \quad \forall\, \mathbf{v}_h \in \mathbb{H}_h. \tag{3.4.56}$$

Using Lemma 3.4.2, we can choose $\overline{\mathbf{v}}_h \in \mathbb{H}_h$ with $||\overline{\mathbf{v}}_h|| = 1$ such that

$$C||T\mathbf{w}_h - T\widetilde{\mathbf{w}}_h|| = C||T(\mathbf{w}_h - \widetilde{\mathbf{w}}_h)|| \leq A_{h,\mathbf{u}_I}(T(\mathbf{w}_h - \widetilde{\mathbf{w}}_h), \overline{\mathbf{v}}_h). \tag{3.4.57}$$

Therefore, by combining (3.4.56) and (3.4.57), using (3.3.16e) and (3.3.16f), we get

$$\begin{aligned} ||T\mathbf{w}_h - T\widetilde{\mathbf{w}}_h|| &\leq \frac{1}{C}\Big\{2B_h(\mathbf{u}_I; \mathbf{w}_h - \widetilde{\mathbf{w}}_h, \overline{\mathbf{v}}_h) - B_h(\mathbf{w}_h; \mathbf{w}_h, \overline{\mathbf{v}}_h) + B_h(\widetilde{\mathbf{w}}_h; \widetilde{\mathbf{w}}_h, \overline{\mathbf{v}}_h)\Big\} \\ &= \frac{1}{C}\Big\{B_h(\widetilde{\mathbf{w}}_h - \mathbf{w}_h; \mathbf{w}_h - \mathbf{u}_I, \overline{\mathbf{v}}_h) + B_h(\widetilde{\mathbf{w}}_h - \mathbf{u}_I; \widetilde{\mathbf{w}}_h - \mathbf{w}_h, \overline{\mathbf{v}}_h)\Big\} \\ &\leq \frac{1}{C}\Big\{||\widetilde{\mathbf{w}}_h - \mathbf{w}_h||\,||\mathbf{w}_h - \mathbf{u}_I||\,||\overline{\mathbf{v}}_h|| + ||\widetilde{\mathbf{w}}_h - \mathbf{w}_h||\,||\widetilde{\mathbf{w}}_h - \mathbf{u}_I||\,||\overline{\mathbf{v}}_h||\Big\} \\ &= \frac{1}{C}||\widetilde{\mathbf{w}}_h - \mathbf{w}_h||\Big\{||\mathbf{w}_h - \mathbf{u}_I|| + ||\widetilde{\mathbf{w}}_h - \mathbf{u}_I||\Big\}. \end{aligned} \tag{3.4.58}$$

Finally, for all $h \leq h_2 := \left(\frac{1}{8}\right)^{1/s}$, we apply (3.4.55) on the right hand side of (3.4.58) to obtain

$$||T\mathbf{w}_h - T\widetilde{\mathbf{w}}_h||| \leq \frac{2R(h)}{C}||\mathbf{w}_h - \widetilde{\mathbf{w}}_h|| = 4h^s||\mathbf{w}_h - \widetilde{\mathbf{w}}_h|| \leq \frac{1}{2}||\mathbf{w}_h - \widetilde{\mathbf{w}}_h||.$$

Therefore, we have finished the proof. □

Finally, we are ready to prove that the discrete problem (3.3.15) admits a unique solution.

Theorem 3.4.1. *Let* $\mathbf{u}$ *be an isolated solution of* (3.2.12)*. Then, for* h *small enough, the discrete problem* (3.3.15) *has a unique solution* $\mathbf{u}_h \in \mathbb{H}_h$*. Moreover, we have that*

$$|| \mathbf{u}_h - \mathbf{u}_I || = ||T \mathbf{u}_h - \mathbf{u}_I || \leq Ch^s.$$

Proof. We know that the solution of (3.3.15) is a fixed point of operator T. Thus, the proof follows from Lemmas 3.4.4 and 3.4.5, and Banach fixed-point theorem.

□

We finish this section presenting the following result, which provides the rate of convergence of our virtual element scheme.

Theorem 3.4.2. *Let* $\mathbf{u}$ *and* $\mathbf{u}_h$ *the isolated solution of* (3.2.12) *and the unique solution of the discrete problem* (3.3.15)*, respectively. Then, there exists a positive constant* C*, independent of* h*, such that for all* $h \leq \min\{h_1, h_2\}$ *we have that*

$$|| \mathbf{u} - \mathbf{u}_h || \leq Ch^s,$$

where $s \in (1/2, 1]$ *is the Sobolev exponent for the solution of von Kármán problem (see Theorem 3.2.1).*

Proof. For all $h \leq \min\{h_1, h_2\}$, we have from Theorem 3.4.1 the following estimate

$$|| \mathbf{u}_h - \mathbf{u}_I || \leq Ch^s. \tag{3.4.59}$$

Hence, applying triangle inequality in the term $|| \mathbf{u} - \mathbf{u}_h ||$, and using the estimates (3.4.18) and (3.4.59), we deduce

$$|| \mathbf{u} - \mathbf{u}_h || \leq || \mathbf{u} - \mathbf{u}_I || + || \mathbf{u}_I - \mathbf{u}_h || \leq Ch^s.$$

The proof is complete. □

3.5 Numerical results

We report in this section a series of numerical experiments to approximate the isolated solutions of the von Kàrmàn problem (3.2.12), using the Virtual Element Method proposed and analyzed in this paper. We have implemented in a MATLAB code the proposed VEM on arbitrary polygonal meshes (see [16]).

We will test the method by using different families of meshes (see Figure 3.2):

- $\mathcal{T}_h^1$: trapezoidal meshes which consist of partitions of the domain into $N \times N$ congruent trapezoids, all similar to the trapezoid with vertices $(0,0)$, $(1/2,0)$, $(1/2,2/3)$ and $(0,1/3)$;
- $\mathcal{T}_h^2$: hexagonal meshes;
- $\mathcal{T}_h^3$: triangular meshes;

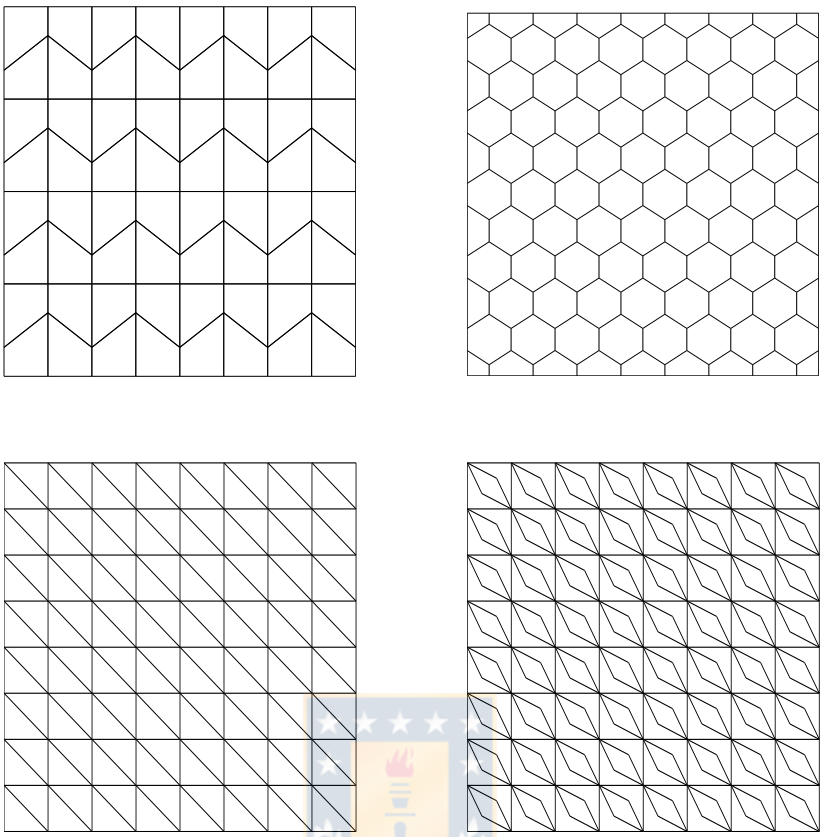

Figure 3.2: Sample meshes: $\mathcal{T}_h^1$ (top left), $\mathcal{T}_h^2$ (top right), $\mathcal{T}_h^3$ (bottom left) and $\mathcal{T}_h^4$ (bottom right) (figure produced by the author).

- $\mathcal{T}_h^4$: distorted concave rhombic quadrilaterals.

Now, in order to complete the choice of the VEM, we have to fix the bilinear forms $S_K^D(\cdot,\cdot)$ and $S_K^\nabla(\cdot,\cdot)$ satisfying (3.3.8) and (3.3.9), respectively. First, we consider the following symmetric bilinear forms (see for instance [12, 105]):

$$s_K^D(u_h,v_h) := \sigma_K \sum_{i=1}^{N_K} [u_h(\mathrm{v}_i)v_h(\mathrm{v}_i) + h_{\mathrm{v}_i}^2 \nabla u_h(\mathrm{v}_i)\cdot\nabla v_h(\mathrm{v}_i)] \qquad \forall u_h, v_h \in H_h^K,$$

$$s_K^\nabla(u_h,v_h) := \overline{\sigma}_K \sum_{i=1}^{N_K} [u_h(\mathrm{v}_i)v_h(\mathrm{v}_i) + \nabla u_h(\mathrm{v}_i)\cdot\nabla v_h(\mathrm{v}_i)] \qquad \forall u_h, v_h \in H_h^K,$$

where, $\mathrm{v}_1,\ldots,\mathrm{v}_{N_K}$ denote the vertices of K, h_{v_i} is chosen as the maximum diameter of the elements K with v_i as a vertex. Moreover, σ_K and $\overline{\sigma}_K$ are multiplicative factors to consider the h-scaling and the physical constant of the problem. For instance, in the numerical tests we have considered $\sigma_K, \overline{\sigma}_K > 0$ as the mean value of the eigenvalues of the local matrices $a_K^\Delta\big(\Pi_K^{2,D}\phi_i, \Pi_K^{2,D}\phi_j\big)$ and $a_K^\nabla\big(\Pi_K^{2,\nabla}\phi_i, \Pi_K^{2,\nabla}\phi_j\big)$, respectively, where $\{\phi_i\}_{i=1}^{\dim H_h^K}$ corresponds to a basis of H_h^K.

Then, we set $S_K^D(\cdot,\cdot)$ and $S_K^\nabla(\cdot,\cdot)$ as follows

$$S_K^D(\mathbf{u}_h,\mathbf{v}_h) := s_K^D(u_h,v_h) + s_K^D(\psi_h,\varphi_h) \qquad \forall\, \mathbf{u}_h,\mathbf{v}_h \in \mathbb{H}_h^K,$$
$$S_K^\nabla(\mathbf{u}_h,\mathbf{v}_h) := s_K^\nabla(u_h,v_h) \qquad \forall\, \mathbf{u}_h,\mathbf{v}_h \in \mathbb{H}_h^K.$$

In order to present the numerical tests, we have taken as computational domain $\Omega := (0,1)^2$. The discrete solution associated to problem (3.3.15) was obtained by a classical Newton method. In particular, we have considered the usual incremental loading procedure (see for instance [21, Section 3.2]) to approximate the discrete solution of the nonlinear von Kármán problem: given a positive integer $\hat{N}$, let $F_h^\ell(\mathbf{v}_h) = (\ell/\hat{N})F_h(\mathbf{v}_h)$ $\forall \ell = 1,2,\ldots,\hat{N}$ be the partial loadings. Therefore, given the initial guest $\mathbf{u}_h^0$ (for instance the zero function), one applies for $\ell = 1,2,\ldots,\hat{N}$ the following iterative procedure

Given $\mathbf{u}_h^0$ **do**

for $\ell = 1 : \hat{N}$ **do**

$F_h^\ell(\mathbf{v}_h) = (\ell/\hat{N})F_h(\mathbf{v}_h)$

Solve Newton iterates

$A_h^\Delta(\mathbf{u}_h^\ell,\mathbf{v}_h) + \lambda A_h^\nabla(\mathbf{u}_h^\ell,\mathbf{v}_h) + 2B_h(\mathbf{u}_h^{\ell-1};\mathbf{v}_h^\ell,\mathbf{v}_h) = B_h(\mathbf{u}_h^{\ell-1};\mathbf{u}_h^{\ell-1},\mathbf{v}_h) + F_h^\ell(\mathbf{v}_h)$

end

Thus, the final solution is $\mathbf{u}_h = \mathbf{u}_h^{\hat{N}}$.

Moreover, we define the individual errors by:

$$\mathrm{e}_0(w_h) := ||w - \Pi_h^{2,D} w_h||_{0,\Omega}, \quad \mathrm{e}_1(w_h) := |w - \Pi_h^{2,D} w_h|_{1,h}, \quad \mathrm{e}_2(w_h) := |w - \Pi_h^{2,D} w_h|_{2,h},$$

where, $\Pi_h^{2,D}$ has been defined in (3.3.17).

We have computed the experimental rates of convergence for each individual errors as follows:

$$\mathrm{rc}(\cdot) := \frac{\log(\mathrm{e}_\star(\cdot)/\mathrm{e}'_\star(\cdot))}{\log(N_{dof}/N'_{dof})} \qquad \text{for all subscripts } \star \in \{0,1,2\},$$

with N_{dof} and N'_{dof} denote the degrees of freedom of two consecutive polygonal decomposition with respectively errors $\mathrm{e}_\star$ and $\mathrm{e}'_\star$. For each mesh $\mathcal{T}_h$, the degrees of freedom are $N_{dof} = 6N_v$, where N_v denotes the number of interior vertices of the polygonal mesh.

In what follows, we present three numerical tests illustrating the performance of our virtual element scheme. For reasons of brevity, we do not report the results obtained with all meshes for all test problems. However, all non reported results are in accordance with the ones shown.

3.5.1 Test 1

In this test, we have taken $\lambda = 5$. In addition, we modify the right hand side of the second equation in (3.2.4) to compare the discrete solution with the continuous one, i.e.

$$\begin{cases} \Delta^2 u + \lambda\Delta u - [\psi,u] &= f \quad \text{in} \quad \Omega, \\ \Delta^2\psi + \frac{1}{2}[u,u] &= g \quad \text{in} \quad \Omega, \\ u = \partial_\nu u &= 0 \quad \text{on} \quad \Gamma, \\ \psi = \partial_\nu \psi &= 0 \quad \text{on} \quad \Gamma. \end{cases} \tag{3.5.60}$$

Thus, we consider f and g so that the exact solution of (3.5.60) are

$$u(x,y) = x^2y^2(x-1)^2(y-1)^2 \quad \text{in } \Omega, \quad \text{and} \quad \psi(x,y) = \sin^2(\pi x)\sin^2(\pi y) \quad \text{in } \Omega.$$

We report in Table 3.1 the convergence history of our virtual element scheme (3.3.15). For each ℓ the Newton's method used up to 5 iterations with a tolerance Tol $= 10^{-9}$. In particular, Table 3.1 summarizes the convergence history for the transverse displacements u_h and for the Airy stress function ψ_h. As predicted by Theorem 3.4.2, an $\mathcal{O}(h)$ of convergence is clearly seen for $e_2(u_h)$ and $e_2(\psi_h)$. We also report $e_0(u_h)$, $e_1(u_h)$, $e_0(\psi_h)$ and $e_1(\psi_h)$, where an $\mathcal{O}(h^2)$ is observed. The discrete solutions obtained with the virtual element method proposed in this work, are depicted in Figure 3.3.

Table 3.1: Test 1: Errors and experimental convergence rates $\mathrm{e}_0(u_h)$, $\mathrm{e}_1(u_h)$, $\mathrm{e}_2(u_h)$, $\mathrm{e}_0(\psi_h)$, $\mathrm{e}_1(\psi_h)$ and $\mathrm{e}_2(\psi_h)$ of the discrete solution to the von Kármán problem (table produced by the author).

$\mathcal{T}_h$	N_{dof}	$\mathrm{e}_0(u_h)$	$\mathrm{rc}(u_h)$	$\mathrm{e}_1(u_h)$	$\mathrm{rc}(u_h)$	$\mathrm{e}_2(u_h)$	$\mathrm{rc}(u_h)$
	54	0.000431704768438	-	0.003262724422857	-	0.031728922182966	-
	294	0.000118318604331	1.87	0.000935470949060	1.80	0.016255461918515	0.96
$\mathcal{T}_h^3$	1350	0.000029867487367	1.99	0.000239063199567	1.97	0.008150175184542	1.00
	5766	0.000007461004475	2.00	0.000059929912000	2.00	0.004079547948378	1.00
	23814	0.000001863069256	2.00	0.000014979870677	2.00	0.002040881649304	1.00
	246	0.000480588388535	-	0.003317993901837	-	0.031341253980477	-
	1062	0.000136460315064	1.72	0.000988414232088	1.66	0.015733875049155	0.94
$\mathcal{T}_h^4$	4422	0.000034563080364	1.93	0.000256091744078	1.89	0.007800044026566	0.98
	18054	0.000008594114090	1.98	0.000064363787275	1.96	0.003890338441267	0.99
	72966	0.000002136931492	1.99	0.000016086825337	1.99	0.001944197375647	0.99
$\mathcal{T}_h$	N_{dof}	$\mathrm{e}_0(\psi_h)$	$\mathrm{rc}(\psi_h)$	$\mathrm{e}_1(\psi_h)$	$\mathrm{rc}(\psi_h)$	$\mathrm{e}_2(\psi_h)$	$\mathrm{rc}(\psi_h)$
	54	0.073050506944122	-	0.846040099702635	-	8.159441640704209	-
	294	0.012011400077328	2.60	0.292568564494940	1.53	4.341739275488559	0.91
$\mathcal{T}_h^1$	1350	0.002294277174721	2.39	0.083090515350743	1.81	2.174289254445207	1.00
	5766	0.000499349745906	2.20	0.021622526054148	1.94	1.083299492719920	1.01
	23814	0.000119140487292	2.08	0.005465045349110	1.98	0.540966031106735	1.00
	192	0.061884511675239	-	0.679874909970360	-	7.512913582695741	-
	768	0.026172828966453	1.46	0.249463389030945	1.71	4.077763689322426	1.04
$\mathcal{T}_h^2$	3072	0.008664638440498	1.74	0.071485859700407	1.97	2.055397431297525	1.08
	12288	0.002491920671679	1.88	0.018172983843658	2.06	1.024040359048393	1.05
	49152	0.000669515058352	1.94	0.004531873249613	2.05	0.510867678265516	1.03

3.5.2 Test 2

In this test we consider the canonical von Kármán equations (cf. (3.2.1)) with non-homogeneous boundary conditions. In addition, we modify the right side of the second equation in (3.2.1) to

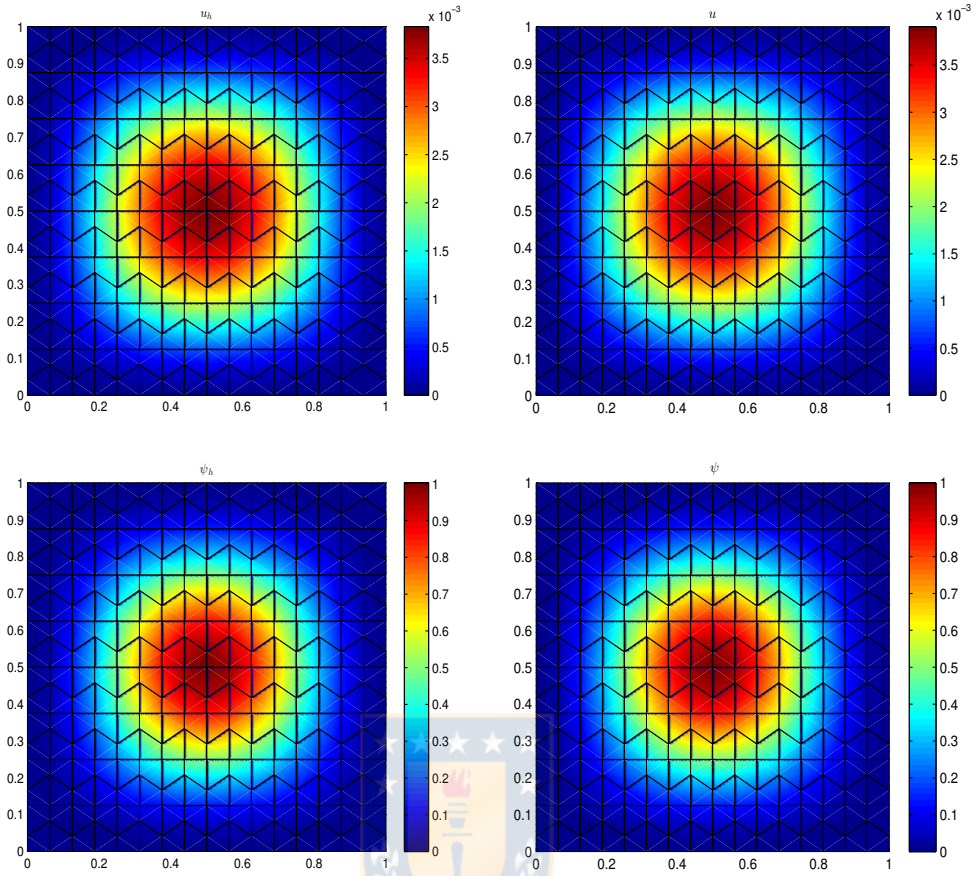

Figure 3.3: Test 1. u_h (top left), u (top right), ψ_h (bottom left) and ψ (bottom right) (figure produced by the author).

compare the discrete solution with the continuous one, i.e.

$$\begin{cases} \Delta^2 u - [\psi, u] &= f \quad \text{in} \quad \Omega, \\ \Delta^2 \psi + \frac{1}{2}[u, u] &= g \quad \text{in} \quad \Omega, \\ u = \partial_\nu u &= 0 \quad \text{on} \quad \Gamma, \\ \psi &= \varphi_0 \quad \text{on} \quad \Gamma, \\ \partial_\nu \psi &= \varphi_1 \quad \text{on} \quad \Gamma. \end{cases} \tag{3.5.61}$$

Next, we consider the following lateral forces φ_0 and φ_1

$$\begin{aligned} \varphi_0(x, y) &= \sin^2(\pi x) && \text{on } \Gamma, \\ \varphi_1(x, y) &= 2\pi\nu_1(x, y)\cos(\pi x)\sin(\pi x) && \text{on } \Gamma, \end{aligned}$$

and transverse loads f and g so that the exact solution of (3.5.61) is

$$u(x, y) = x^2 \sin(\pi y)^2 \log(2 - x)^2 \quad \text{in } \Omega, \quad \text{and} \quad \psi(x, y) = \sin^2(\pi x) \quad \text{in } \Omega.$$

Table 3.2 reports the convergence history of our virtual element scheme (3.3.15) applied to solve (3.5.61). Once again, for each ℓ, the Newton's method used up to 5 iterations with a tolerance Tol

$= 10^{-9}$. In particular, Table 3.1 summarizes the convergence history for the transverse displacements u_h (resp. to Airy stress function ψ_h). Once again an $\mathcal{O}(h)$ of convergence is clearly seen for $e_2(u_h)$ (resp. $e_2(\psi_h)$). We again report the errors $e_0(u_h)$ and $e_1(u_h)$ (resp. $e_0(\psi_h)$ and $e_1(\psi_h)$), where an $\mathcal{O}(h^2)$ is observed. The discrete solutions associated to the Test 2, and obtained with the virtual element method proposed in this work, are depicted in Figure 3.4.

Table 3.2: Test 2: Errors and experimental convergence rates $\mathrm{e}_0(u_h)$, $\mathrm{e}_1(u_h)$, $\mathrm{e}_2(u_h)$, $\mathrm{e}_0(\psi_h)$, $\mathrm{e}_1(\psi_h)$ and $\mathrm{e}_2(\psi_h)$ of the discrete solution to the von Kármán problem (table produced by the author).

$\mathcal{T}_h$	N_{dof}	$\mathrm{e}_0(u_h)$	$\mathrm{rc}(u_h)$	$\mathrm{e}_1(u_h)$	$\mathrm{rc}(u_h)$	$\mathrm{e}_2(u_h)$	$\mathrm{rc}(u_h)$
	54	0.003331813500703	-	0.040541588728628	-	0.392326399686893	-
	294	0.000666755182746	1.90	0.013573656090400	1.29	0.211617144042376	0.73
$\mathcal{T}_h^1$	1350	0.000139272569159	2.05	0.003744148938304	1.69	0.107073487968784	0.89
	5766	0.000032059141547	2.02	0.000964443541553	1.87	0.053613559930229	0.95
	23814	0.000007817172339	1.99	0.000243151609540	1.94	0.026821738028166	0.98
	192	0.003338044048468	-	0.029905766623389	-	0.331352206962454	-
	768	0.001214026245280	1.46	0.011071959441869	1.43	0.188066935651525	0.82
$\mathcal{T}_h^2$	3072	0.000374019547265	1.70	0.003255655646633	1.77	0.098467208145884	0.93
	12288	0.000107769516445	1.80	0.000862676994761	1.92	0.050139745754829	0.97
	49152	0.000029635952218	1.86	0.000221290022671	1.96	0.025284764141485	0.99
$\mathcal{T}_h$	N_{dof}	$\mathrm{e}_0(\psi_h)$	$\mathrm{rc}(\psi_h)$	$\mathrm{e}_1(\psi_h)$	$\mathrm{rc}(\psi_h)$	$\mathrm{e}_2(\psi_h)$	$\mathrm{rc}(\psi_h)$
	54	0.029494648554614	-	0.412210903728138	-	6.003264759584535	-
	294	0.004591865781598	2.20	0.101028788029534	1.66	3.069362969416609	0.79
$\mathcal{T}_h^3$	1350	0.000940086309599	2.08	0.025008571679680	1.83	1.540413925828407	0.90
	5766	0.000222681115380	1.98	0.006215447146812	1.92	0.770497464565608	0.95
	23814	0.000055123897439	1.97	0.001548657099701	1.96	0.385190062299381	0.98
	246	0.027814402349946	-	0.372966458416872	-	5.590747627283569	-
	1062	0.004522053574370	2.62	0.094464604014345	1.98	2.885848302050357	0.95
$\mathcal{T}_h^4$	4422	0.000957131357883	2.24	0.023604212432399	2.00	1.453857116146261	0.99
	18054	0.000229063918352	2.06	0.005877183318359	2.01	0.728469592800096	1.00
	72966	0.000056858787426	2.01	0.001464852130236	2.00	0.364490348651261	1.00

3.5.3 Test 3

In this test we present a numerical example, illustrating the performance of our virtual element scheme applied to the von Kármán system (3.2.4), with $f = 0$ and different values of the parameter λ (cf. Remark 3.2.1). Let $\lambda^\star = 52.34469...$ (see for instance [32, 106, 108]) be the smallest eigenvalue λ of the following buckling spectral problem (cf. (3.2.5)):

$$a^{\Delta}(u, v) = -\lambda a^{\nabla}(u, v) \qquad \forall v \in H_0^2(\Omega),$$

where, the bilinear forms $a^{\Delta}(\cdot, \cdot)$ and $a^{\nabla}(\cdot, \cdot)$ were defined in (3.2.8) and (3.2.9), respectively. In this particular case as predicted by the theory in [65, Theorem 5.9-2], there exist at least 3 solutions of the problem (3.2.4) for $\lambda > \lambda^\star$ (see Remark 3.2.1).

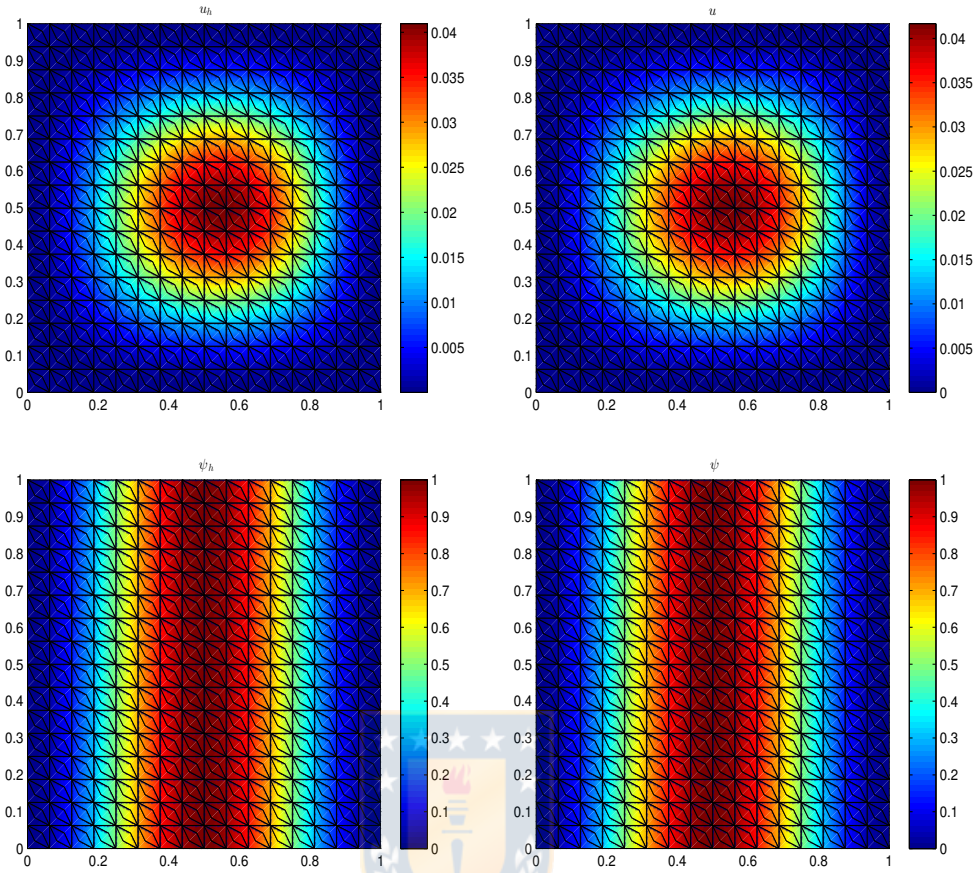

Figure 3.4: Test 2. u_h (top left), u (top right), ψ_h (bottom left) and ψ (bottom right) (figure produced by the author).

Once again, we have solved our discrete problem (3.3.15), using three values for λ, namely: $\lambda = 53$, $\lambda = 55$ and $\lambda = 60$. In addition, for each value of the parameter λ, we used two different initial guess and trapezoidal meshes $\mathcal{T}_h^1$. On the left hand side of Figures 3.5–3.7, we illustrate the approximation of $u_h =: u_1$ obtained with the initial guess $\mathbf{u}_h^0(x,y) = (\frac{1}{4}(yx^2+1), \frac{1}{4}(yx^2+1))$, and $\lambda = 53, 55$ and 60, respectively. While, on the right hand side of Figures 3.5–3.7, we illustrate the approximation of $u_h =: u_2$ obtained with the initial guess $\mathbf{u}_h^0(x,y) = -(\frac{1}{4}(yx^2+1), \frac{1}{4}(yx^2+1))$ and $\lambda = 53, 55$ and 60, respectively. We can appreciate that $u_1 \neq 0$ and $u_2 = -u_1$, which confirm the existence of non zero solutions with opposite displacements, as established in [65, Theorem 5.9-2]. On the other hand, for $\mathbf{u}_h^0 \equiv 0$, we obtained $\mathbf{u}_h = 0$ for any value of λ, as established in [65, Theorem 5.9-2].

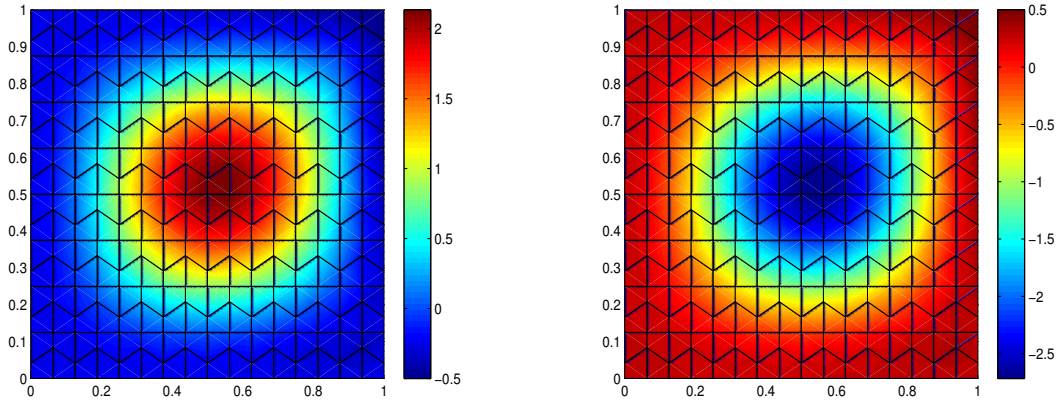

Figure 3.5: Test 3. $u_1 := u_h$ obtained from Newton iterates, with $\lambda = 53$, $f = 0$ and $\mathbf{u}^0(x,y) = (\frac{1}{4}(yx^2+1), \frac{1}{4}(yx^2+1))$ (left). $u_2 := u_h$ obtained from Newton iterates, with $\lambda = 53$, $f = 0$ and $\mathbf{u}^0(x,y) = -(\frac{1}{4}(yx^2+1), \frac{1}{4}(yx^2+1))$ (right) (figure produced by the author).

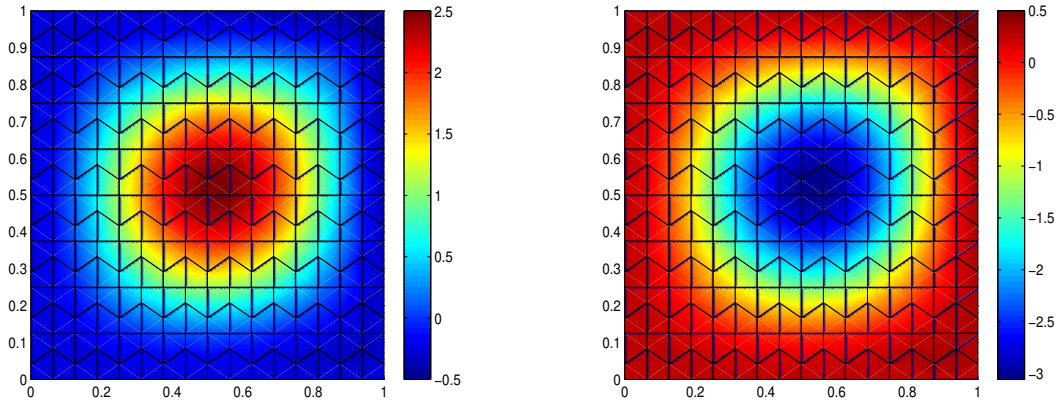

Figure 3.6: Test 3. $u_1 := u_h$ obtained from Newton iterates, with $\lambda = 55$, $f = 0$ and $\mathbf{u}^0(x,y) = (\frac{1}{4}(yx^2+1), \frac{1}{4}(yx^2+1))$ (left). $u_2 := u_h$ obtained from Newton iterates, with $\lambda = 55$, $f = 0$ and $\mathbf{u}^0(x,y) = -(\frac{1}{4}(yx^2+1), \frac{1}{4}(yx^2+1))$ (right) (figure produced by the author).

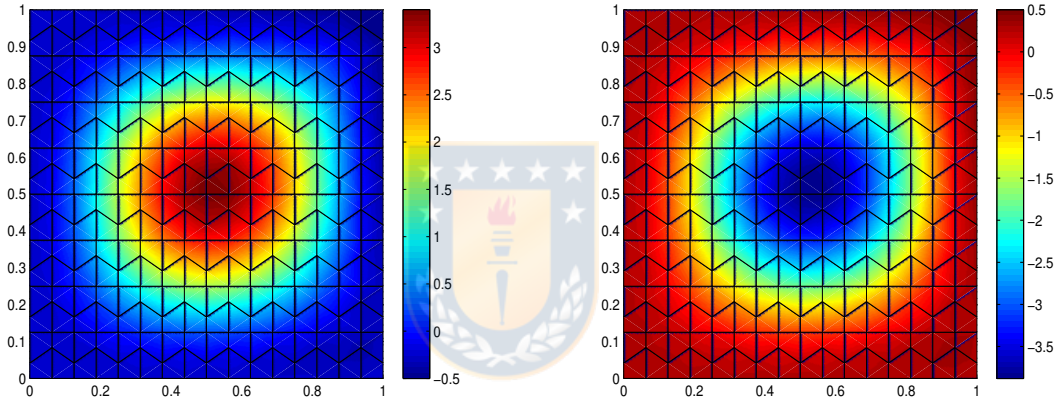

Figure 3.7: Test 3. $u_1 := u_h$ obtained from Newton iterates, with $\lambda = 60$, $f = 0$ and $\mathbf{u}^0(x, y) = (\frac{1}{4}(yx^2 + 1), \frac{1}{4}(yx^2 + 1))$ (left). $u_2 := u_h$ obtained from Newton iterates, with $\lambda = 60$, $f = 0$ and $\mathbf{u}^0(x, y) = -(\frac{1}{4}(yx^2 + 1), \frac{1}{4}(yx^2 + 1))$ (right) (figure produced by the author).

CHAPTER 4

A virtual element method for the transmission eigenvalue problem

4.1 Introduction

In this work, we study a Virtual Element Method for an eigenvalue problem arising in scattering theory. The *Virtual Element Method* (VEM), introduced in [12, 16], is a generalization of the Finite Element Method which is characterized by the capability of dealing with very general polygonal/polyhedral meshes, and it also permits to easily implement highly regular discrete spaces. Indeed, by avoiding the explicit construction of the local basis functions, the VEM can easily handle general polygons/polyhedrons without complex integrations on the element (see [16] for details on the coding aspects of the method). The VEM has been developed and analyzed for many problems, see for instance [6, 7, 15, 21, 23, 27, 30, 35, 41, 42, 43, 55, 64, 76, 112, 121]. Regarding VEM for spectral problems, we mention [28, 78, 79, 102, 103, 105]. We note that there are other methods that can make use of arbitrarily shaped polygonal/polyhedral meshes, we cite as a minimal sample of them [20, 52, 75, 118].

Due to their important role in many application areas, there has been a growing interest in recent years towards developing numerical schemes for spectral problems (see [33]). In particular, we are going to analyze a virtual element approximation of the transmission eigenvalue problem. The motivation for considering this problem is that it plays an important role in inverse scattering theory [47, 71]. This is due to the fact that transmission eigenvalues can be determined from the far-field data of the scattered wave and used to obtain estimates for the material properties of the scattering object [45, 48].

In recent years various numerical methods have been proposed to solve this eigenvalue problem see for example the following references [49, 50, 60, 72, 83, 126, 88, 115]. In particular, the transmission eigenvalue problem is often solved by reformulating it as a fourth-order eigenvalue problem. In [49], a C^1 finite element method using Argyris elements has been proposed, a complete analysis of the method including error estimates are proved using the theory for compact non-self-adjoint operators. However, the construction of H^2-conforming finite elements is difficult in general, since they usually involve a large number of degrees of freedom (see [67]). More recently, in [83] a discontinuous Galerkin method has been proposed and analyzed to solve the fourth-order transmission eigenvalue problem; moreover, in [60] a C^0 linear finite element method has been introduced to solve the spectral problem.

The purpose of the present chapter is to introduce and analyze a C^1-VEM for solving a fourth-order spectral problem derived from the transmission eigenvalue problem. We consider a variational formulation of the problem written in $H^2(\Omega) \times H^1(\Omega)$ as in [49, 83], where an auxiliary variable is introduced to transform the problem into a linear eigenvalue problem. Here, we exploit the capability of VEM to build highly regular discrete spaces (see [25, 41]) and propose a conforming $H^2(\Omega) \times H^1(\Omega)$ discrete formulation, which makes use of a very simple set of degrees of freedom, namely 4 degrees of freedom per vertex of the mesh. Then, we use the classical spectral theory for non-selfadjoint compact operators (see [11, 110]) to deal with the continuous and discrete solution operators, which appear as the solution of the continuous and discrete source problems, and whose spectra are related with the solutions of the transmission eigenvalue problem. Under rather mild assumptions on the polygonal meshes (made by possibly non-convex elements), we establish that the resulting VEM scheme provides a correct approximation of the spectrum and prove optimal-order error estimates for the eigenfunctions and a double order for the eigenvalues. Finally, we note that, differently from the FEM where building globally conforming $H^2(\Omega)$ approximation is complicated, here the virtual space can be built with a rather simple construction due to the flexibility of the VEM. In a summary, the advantages of the present virtual element discretization are the possibility to use general polygonal meshes and to build conforming $H^2(\Omega)$ approximations.

The chapter is structured as follows: In Section 4.2, we introduce the variational formulation of the transmission eigenvalue problem, define a solution operator and establish its spectral characterization. In Section 4.3, we introduce the virtual element discrete formulation, describe the spectrum of a discrete solution operator and establish some auxiliary results. In Section 4.4, we prove that the numerical scheme provides a correct spectral approximation and establish optimal order error estimates for the eigenvalues and eigenfunctions using the standard theory for compact and non-selfadjoint operators. Finally, we report some numerical tests that confirm the theoretical analysis developed in Section 4.5.

In this article, we will employ standard notations for Sobolev spaces, norms and seminorms. In addition, we will denote by C a generic constant independent of the mesh parameter h, which may take different values in different occurrences. When the constant depends on the index of refraction, we will write C_n.

4.2 The transmission eigenvalue problem

Let $\Omega \subset \mathbb{R}^2$ be the polygonal domain. We denote by ν the outward unit normal vector to $\partial\Omega$ and by ∂_ν the normal derivative. Let n be a real value function in $L^\infty(\Omega)$ such that $n-1$ is strictly positive (or strictly negative) almost everywhere in Ω. The transmission eigenvalue problem reads as follows:

Find the so-called transmission eigenvalue $k \in \mathbb{C}$ and a non-trivial pair of functions $(w_1, w_2) \in$

$L^2(\Omega) \times L^2(\Omega)$, such that $(w_1 - w_2) \in H^2(\Omega)$ and

$$\Delta w_1 + k^2 n(x) w_1 = 0 \quad \text{in } \Omega, \tag{4.2.1}$$

$$\Delta w_2 + k^2 w_2 = 0 \quad \text{in } \Omega, \tag{4.2.2}$$

$$w_1 = w_2 \quad \text{on } \partial\Omega, \tag{4.2.3}$$

$$\partial_\nu w_1 = \partial_\nu w_2 \quad \text{on } \partial\Omega. \tag{4.2.4}$$

Now, we rewrite the problem above in the following equivalent form in the new variable $u := (w_1 - w_2) \in H_0^2(\Omega)$ (see [49]):

Find $(k, u) \in \mathbb{C} \times H_0^2(\Omega)$ such that

$$(\Delta + k^2 n)\frac{1}{n-1}(\Delta + k^2)u = 0 \quad \text{in } \Omega. \tag{4.2.5}$$

The variational formulation of problem (4.2.5) can be stated as: Find $(k, u) \in \mathbb{C} \times H_0^2(\Omega)$, $u \neq 0$ such that

$$\int_\Omega \frac{1}{n-1}(\Delta u + k^2 u)(\Delta \overline{v} + k^2 n \overline{v}) = 0 \quad \forall v \in H_0^2(\Omega), \tag{4.2.6}$$

where $\overline{v}$ denotes the complex conjugate of v. Now, expanding the previous expression we obtain the following quadratic eigenvalue problem:

$$\int_\Omega \frac{1}{n-1}\Delta u \Delta \overline{v} + \tau \int_\Omega \frac{1}{n-1} u \Delta \overline{v} + \tau \int_\Omega \frac{1}{n-1}\Delta u \overline{nv} + \tau^2 \int_\Omega \frac{1}{n-1} u \overline{nv} = 0 \tag{4.2.7}$$

for all $v \in H_0^2(\Omega)$, where $\tau := k^2$. It is easy to show that $k = 0$ is not an eigenvalue of the problem (see [49]). Moreover, for the sake of simplicity, we will assume that the index of refraction function $n(x)$ is a real constant. Nevertheless, this assumption do not affect the generality of the forthcoming analysis.

For the theoretical analysis it is convenient to transform problem (4.2.7) into a linear eigenvalue problem. With this aim, let ϕ be the solution of the problem: Find $\phi \in H_0^1(\Omega)$ such that

$$\Delta \phi = \tau \frac{n}{n-1} u \quad \text{in } \Omega, \tag{4.2.8}$$

$$\phi = 0 \quad \text{on } \partial\Omega. \tag{4.2.9}$$

Therefore, by testing problem (4.2.8)-(4.2.9) with functions in $H_0^1(\Omega)$, we arrive at the following weak formulation of the problem:

Problem 3. *Find $(\lambda, u, \phi) \in \mathbb{C} \times H_0^2(\Omega) \times H_0^1(\Omega)$ with $(u, \phi) \neq 0$ such that*

$$a((u,\phi),(v,\psi)) = \lambda b((u,\phi),(v,\psi)) \quad \forall (v,\psi) \in H_0^2(\Omega) \times H_0^1(\Omega),$$

where $\lambda = -\tau$ and the sesquilinear forms $a(\cdot,\cdot)$ and $b(\cdot,\cdot)$ are defined by

$$a((u,\phi),(v,\psi)) := \frac{1}{n-1}\int_\Omega D^2 u : D^2 \overline{v} + \int_\Omega \nabla\phi \cdot \nabla\overline{\psi},$$

$$b((u,\phi),(v,\psi)) := \frac{n}{n-1}\int_\Omega \Delta u \overline{v} + \frac{1}{n-1}\int_\Omega u \Delta \overline{v} - \int_\Omega \nabla\phi \cdot \nabla \overline{v} + \frac{n}{n-1}\int_\Omega u\overline{\psi},$$

for all $(u,\phi),(v,\psi) \in H_0^2(\Omega)\times H_0^1(\Omega)$. Moreover, " : " denotes the usual scalar product of 2×2-matrices, $D^2u := (\partial_{ij}u)_{1\le i,j\le 2}$ denotes the Hessian matrix of u.

Remark 4.2.1. *In the definition of $a(\cdot,\cdot)$ (cf. Problem 3), we have considered $a^{\Delta}(u,v) := \int_\Omega D^2u : D^2\overline{v}$ instead of $a^*(u,v) := \int_\Omega \Delta u\Delta\overline{v}$; since, we are considering functions in $H_0^2(\Omega)$, both are equivalent (see [67]). This fact will facilitate the presentation and the analysis of the VEM method. In particular, we will use $a_K^{\Delta}(u,v)$ to construct the projector Π_2^{Δ} (cf. (4.3.1a)-(4.3.1b)) which will be used to write the discrete scheme. However, once the projector Π_2^{Δ} is built, it can be used to discretize the $a_K^*(u,v)$ as well (see Appendix of [29]).*

We endow $H_0^2(\Omega)\times H_0^1(\Omega)$ with the corresponding product norm, which we will simply denote with $\|(\cdot,\cdot)\|$.

Now, we note that the sesquilinear forms $a(\cdot,\cdot)$ and $b(\cdot,\cdot)$ are bounded forms (with constants which depend on the index of refraction). Moreover, we have that $a(\cdot,\cdot)$ is elliptic.

Lemma 4.2.1. *There exists a constant $C_n > 0$, such that*

$$a((v,\psi),(v,\psi)) \ge C_n \|(v,\psi)\|^2 \qquad \forall (v,\psi)\in H_0^2(\Omega)\times H_0^1(\Omega).$$

Proof. The result follows immediately from the fact that $\{\|D^2v\|_{0,\Omega}^2 + \|\nabla\psi\|_{0,\Omega}^2\}^{1/2}$ is a norm on $H_0^2(\Omega)\times H_0^1(\Omega)$, equivalent with the norm $||(\cdot,\cdot)||$ (see Chapter 6 of [116]). □

We define the solution operator associated with Problem 3:

$$\begin{array}{rcl} T : H_0^2(\Omega)\times H_0^1(\Omega) & \longrightarrow & H_0^2(\Omega)\times H_0^1(\Omega) \\ (f,g) & \longmapsto & T(f,g) = (\tilde{u},\tilde{\phi}) \end{array}$$

as the unique solution (as a consequence of Lemma 4.2.1) of the corresponding source problem:

$$a((\tilde{u},\tilde{\phi}),(v,\psi)) = b((f,g),(v,\psi)) \quad \forall (v,\psi)\in H_0^2(\Omega)\times H_0^1(\Omega). \tag{4.2.10}$$

The linear operator T is then well defined and bounded. Notice that $(\lambda,u,\phi)\in\mathbb{C}\times H_0^2(\Omega)\times H_0^1(\Omega)$ solves Problem 3 if and only if (μ,u,ϕ), with $\mu := \frac{1}{\lambda}$, is an eigenpair of T, i.e., $T(u,\phi) = \mu(u,\phi)$.

We observe that no spurious eigenvalues are introduced into the problem since if $\mu\neq 0$, $(0,\phi)$ is not an eigenfunction of the problem.

The following is an additional regularity result for the solution of the source problem (4.2.10) and consequently, for the generalized eigenfunctions of T.

Lemma 4.2.2. *There exist $s,t\in(1/2,1]$ and $C_n>0$ such that, for all $(f,g)\in H_0^2(\Omega)\times H_0^1(\Omega)$, the solution $(\tilde{u},\tilde{\phi})$ of problem (4.2.10) satisfies $\tilde{u}\in H^{2+s}(\Omega)$, $\tilde{\phi}\in H^{1+t}(\Omega)$, and*

$$\|\tilde{u}\|_{2+s,\Omega} + \|\tilde{\phi}\|_{1+t,\Omega} \le C_n\|(f,g)\|.$$

Proof. The estimate for $\tilde{\phi}$ follows from the classical regularity result for the Laplace problem with its right-hand side in $L^2(\Omega)$. The estimate for $\tilde{u}$ follows from the classical regularity result for the biharmonic problem with its right-hand side in $H^{-1}(\Omega)$ (cf. [85]). □

Remark 4.2.2. *The constant s in the lemma above is the Sobolev regularity for the biharmonic equation with the right-hand side in $H^{-1}(\Omega)$ and homogeneous Dirichlet boundary conditions. The constant t is the Sobolev exponent for the Laplace problem with homogeneous Dirichlet boundary conditions. These constants only depend on the domain Ω. If Ω is convex, then $s = t = 1$. Otherwise, the lemma holds for all $s < s_0$ and $t < t_0$, where $s_0, t_0 \in (1/2, 1]$ depend on the largest reentrant angle of Ω.*

Hence, because of the compact inclusions $H^{2+s}(\Omega) \hookrightarrow H^2_0(\Omega)$ and $H^{1+t}(\Omega) \hookrightarrow H^1_0(\Omega)$, we can conclude that T is a compact operator. So, we obtain the following spectral characterization result.

Lemma 4.2.3. *The spectrum of T satisfies $\mathrm{sp}(T) = \{0\} \cup \{\mu_k\}_{k\in\mathbb{N}}$, where $\{\mu_k\}_{k\in\mathbb{N}}$ is a sequence of complex eigenvalues which converges to 0 and their corresponding eigenspaces lie in $H^{2+s}(\Omega) \times H^{1+t}(\Omega)$. In addition $\mu = 0$ is an infinite multiplicity eigenvalue of T.*

Proof. The proof is obtained from the compactness of T and Lemma 4.2.2. □

4.3 The virtual element discretization

In this section, we will write the C^1-VEM discretization of Problem 3. With this aim, we start with the mesh construction and the assumptions considered to introduce the discrete virtual element spaces.

Let $\{\mathcal{T}_h\}_h$ be a sequence of decompositions of Ω into polygons K we will denote by h_K the diameter of the element K and by h the maximum of the diameters of all the elements of the mesh, i.e., $h := \max_{K\in\mathcal{T}_h} h_K$. In what follows, we denote by N_K the number of vertices of K, by e a generic edge of $\{\mathcal{T}_h\}_h$ and for all $e \in \partial K$, we denote with ν^e_K the unit normal vector that points outside of K.

In addition, we will make the following assumptions as in [12, 28]: there exists a positive real number $C_{\mathcal{T}}$ such that, for every h and every $K \in \mathcal{T}_h$,

A1: the ratio between the shortest edge and the diameter h_K of K is larger than $C_{\mathcal{T}}$;

A2: $K \in \mathcal{T}_h$ is star-shaped with respect to every point of a ball of radius $C_{\mathcal{T}} h_K$.

In order to introduce the method, we first define two preliminary discrete spaces as follows: For each polygon $K \in \mathcal{T}_h$ (meaning open simply connected set whose boundary is a non-intersecting line made of a finite number of straight line segments) we define the following finite dimensional spaces

$$\widetilde{W}^K_h := \big\{ v_h \in H^2(K) : \Delta^2 v_h \in \mathbb{P}_2(K), v_h|_{\partial K} \in C^0(\partial K), v_h|_e \in \mathbb{P}_3(e)\ \forall e \in \partial K, \\ \nabla v_h|_{\partial K} \in C^0(\partial K)^2, \partial_\nu v_h|_e \in \mathbb{P}_1(e)\ \forall e \in \partial K \big\},$$

and

$$\widetilde{V}^K_h := \{ \psi_h \in H^1(K) : \Delta\psi_h \in \mathbb{P}_1(K), \psi_h|_{\partial K} \in C^0(\partial K), \psi_h|_e \in \mathbb{P}_1(e)\ \forall e \in \partial K \},$$

where Δ^2 represents the biharmonic operator and we have denoted by $\mathbb{P}_k(S)$ the space of polynomials of degree up to k defined on the subset $S \subseteq \mathbb{R}^2$.

The following conditions hold:

- for any $v_h \in \widetilde{W}_h^K$ the trace on the boundary of K is continuous and on each edge is a polynomial of degree 3;
- for any $v_h \in \widetilde{W}_h^K$ the gradient on the boundary is continuous and on each edge its normal (respectively tangential) component is a polynomial of degree 1 (respectively 2);
- for any $\psi_h \in \widetilde{V}_h^K$ the trace on the boundary of K is continuous and on each edge is a polynomial of degree 1;
- $\mathbb{P}_2(K) \times \mathbb{P}_1(K) \subseteq \widetilde{W}_h^K \times \widetilde{V}_h^K$.

Next, with the aim to choose the degrees of freedom for both spaces, we will introduce three sets of linear operators $\mathbf{D_1}$, $\mathbf{D_2}$ and $\mathbf{D_3}$. The first two sets $(\mathbf{D_1}, \mathbf{D_2})$ are provided by linear operators from $\widetilde{W}_h^K$ into $\mathbb{R}$ and the set $\mathbf{D_3}$ by linear operators from $\widetilde{V}_h^K$ into $\mathbb{R}$. For all $(v_h, \psi_h) \in \widetilde{W}_h^K \times \widetilde{V}_h^K$ they are defined as follows:

- $\mathbf{D_1}$ contains linear operators evaluating v_h at the N_K vertices of K,
- $\mathbf{D_2}$ contains linear operators evaluating ∇v_h at the N_K vertices of K,
- $\mathbf{D_3}$ contains linear operators evaluating ψ_h at the N_K vertices of K.

Note that, as a consequence of definition of the discrete spaces, the output values of the three sets of operators $\mathbf{D_1}$, $\mathbf{D_2}$ and $\mathbf{D_3}$ are sufficient to uniquely determine v_h and ∇v_h on the boundary of K, and ψ_h on the boundary of K, respectively.

In order to construct the discrete scheme, we need some preliminary definitions. First, we split the forms $a(\cdot,\cdot)$ and $b(\cdot,\cdot)$, introduced in the previous section, as follows:

$$a((u,\phi),(v,\psi)) = \sum_{K\in\mathcal{T}_h} \frac{1}{n-1} a_K^{\Delta}(u,v) + a_K^{\nabla}(\phi,\psi), \qquad \forall (u,\phi),(v,\psi) \in H_0^2(\Omega)\times H_0^1(\Omega),$$

$$b((u,\phi),(v,\psi)) = \sum_{K\in\mathcal{T}_h} b_K((u,\phi),(v,\psi)), \qquad \forall (u,\phi),(v,\psi) \in H_0^2(\Omega)\times H_0^1(\Omega),$$

with

$$a_K^{\Delta}(u,v) := \int_K D^2u : D^2\overline{v}, \qquad \forall u,v \in H^2(K),$$

$$a_K^{\nabla}(\phi,\psi) := \int_K \nabla\phi\cdot\nabla\overline{\psi}, \qquad \forall \phi,\psi \in H^1(K),$$

and for all $(u,\phi),(v,\phi) \in H^2(K)\times H^1(K)$,

$$b_K((u,\phi),(v,\psi)) := \frac{n}{n-1}\int_K \Delta u\overline{v} + \frac{1}{n-1}\int_K u\Delta\overline{v} - \int_K \nabla\phi\cdot\nabla\overline{v} + \frac{n}{n-1}\int_K u\overline{\psi}.$$

Now, we define the projector $\Pi_2^{\Delta}: H^2(K) \longrightarrow \mathbb{P}_2(K) \subseteq \widetilde{W}_h^K$ for each $v \in H^2(K)$ as the solution of

$$a_K^{\Delta}\big(\Pi_2^{\Delta}v, q\big) = a_K^{\Delta}(v,q) \qquad \forall q \in \mathbb{P}_2(K), \tag{4.3.1a}$$

$$((\Pi_2^{\Delta}v, q))_K = ((v,q))_K \qquad \forall q \in \mathbb{P}_1(K), \tag{4.3.1b}$$

where $((\cdot,\cdot))_K$ is defined as follows:

$$((u,v))_K = \sum_{i=1}^{N_K} u(P_i)v(P_i) \qquad \forall u,v \in C^0(\partial K),$$

where $P_i, 1 \leq i \leq N_K$, are the vertices of K. We note that the bilinear form $a_K^{\Delta}(\cdot,\cdot)$ has a non-trivial kernel, given by $\mathbb{P}_1(K)$. Hence, the role of condition (4.3.1b) is to select an element of the kernel of the operator. We observe that operator Π_2^{Δ} is well defined on $\widetilde{W}_h^K$ and, most important, for all $v \in \widetilde{W}_h^K$ the polynomial $\Pi_2^{\Delta} v$ can be computed using only the values of the operators $\mathbf{D_1}$ and $\mathbf{D_2}$ calculated on v. This follows easily with an integration by parts (see [7]).

In a similar way, we define the projector $\Pi_1^{\nabla} : H^1(K) \longrightarrow \mathbb{P}_1(K) \subseteq \widetilde{V}_h^K$ for each $\psi \in H^1(K)$ as the solution of

$$a_K^{\nabla}(\Pi_1^{\nabla}\psi, q) = a_K^{\nabla}(\psi, q) \qquad \forall q \in \mathbb{P}_1(K), \tag{4.3.2a}$$

$$(\Pi_1^{\nabla}\psi, 1)_{\partial K} = (\psi, 1)_{\partial K}. \tag{4.3.2b}$$

We observe that operator Π_1^{∇} is well defined on $\widetilde{V}_h^K$ and, as before, for all $\psi \in \widetilde{V}_h^K$ the polynomial $\Pi_1^{\nabla}\psi$ can be computed using only the values of the operators $\mathbf{D_3}$ calculated on ψ, which follows by an integration by parts (see [2]).

Now, we introduce our local virtual spaces (see [7, 2]):

$$W_h^K := \left\{ v_h \in \widetilde{W}_h^K : \int_K (\Pi_2^{\Delta} v_h) q = \int_K v_h q \qquad \forall q \in \mathbb{P}_2(K) \right\},$$

and

$$V_h^K := \left\{ \psi_h \in \widetilde{V}_h^K : \int_K (\Pi_1^{\nabla} \psi_h) q = \int_K \psi_h q \qquad \forall q \in \mathbb{P}_1(K) \right\}.$$

It is clear that $W_h^K \times V_h^K \subseteq \widetilde{W}_h^K \times \widetilde{V}_h^K$. Thus, the linear operators Π_2^{Δ} and Π_1^{∇} are well defined on W_h^K and V_h^K, respectively.

In Lemma 2.1 of [7]. has been established that the sets of operators $\mathbf{D_1}$ and $\mathbf{D_2}$ constitutes a set of degrees of freedom for the space W_h^K. Moreover, the set of operators $\mathbf{D_3}$ constitutes a set of degrees of freedom for the space V_h^K (see [2]).

We also have that $\mathbb{P}_2(K) \times \mathbb{P}_1(K) \subseteq W_h^K \times V_h^K$. This will guarantee the good approximation properties for the spaces.

To continue the construction of the discrete scheme, we will need to consider new projectors. First, we define the projector $\Pi_2^{\nabla} : H^2(K) \longrightarrow \mathbb{P}_2(K)$ for each $w \in H^2(K)$ as the solution of

$$a_K^{\nabla}(\Pi_2^{\nabla} w, q) = a_K^{\nabla}(w, q) \qquad \forall q \in \mathbb{P}_2(K), \tag{4.3.3a}$$

$$(\Pi_2^{\nabla} w, 1)_{0,K} = (w, 1)_{0,K}. \tag{4.3.3b}$$

Moreover, we consider the $L^2(\Omega)$ orthogonal projectors onto $\mathbb{P}_l(K)$, $l = 1, 2$ as follows: we define $\Pi_l^0 : L^2(\Omega) \to \mathbb{P}_l(K)$ for each $p \in L^2(\Omega)$ by

$$\int_K (\Pi_l^0 p) q = \int_K pq \qquad \forall q \in \mathbb{P}_l(K). \tag{4.3.4}$$

Now, due to the particular property appearing in definition of the space W_h^K, it can be seen that the right hand side in (4.3.4) is computable using $\Pi_2^\Delta v_h$, and thus $\Pi_2^0 v_h$ depends only on the values of the degrees of freedom for v_h and ∇v_h. Actually, it is easy to check that on the space W_h^K the projectors Π_2^0 and Π_2^Δ are the same operator. In fact:

$$\int_K (\Pi_2^0 v_h) q = \int_K v_h q = \int_K (\Pi_2^\Delta v_h) q \qquad \forall q \in \mathbb{P}_2(K). \tag{4.3.5}$$

By definition of V_h^K, we have that Π_1^0 and Π_1^∇ are the same operator in V_h^K.

Now, for every decomposition $\mathcal{T}_h$ of Ω into simple polygons K, we introduce the global virtual space denoted by Z_h as follow:

$$Z_h := W_h \times V_h,$$

where

$$W_h := \{v_h \in H_0^2(\Omega) : v_h|_K \in W_h^K\} \quad \text{and} \quad V_h := \{\psi_h \in H_0^1(\Omega) : \psi_h|_K \in V_h^K\}.$$

A set of degrees of freedom for Z_h is given by all pointwise values of v_h and ψ_h on all vertices of $\mathcal{T}_h$ together with all pointwise values of ∇v_h on all vertices of $\mathcal{T}_h$, excluding the vertices on $\partial\Omega$ (where the values vanishes). Thus, the dimension of Z_h is four times the number of interior vertices of $\mathcal{T}_h$.

In what follows, we discuss the construction of the discrete version of the local forms. With this aim, we consider $s_K^\Delta(\cdot,\cdot)$ and $s_K^\nabla(\cdot,\cdot)$ any hermitian positive definite forms satisfying:

$$c_0 a_K^\Delta(v_h, v_h) \leq s_K^\Delta(v_h, v_h) \leq c_1 a_K^\Delta(v_h, v_h) \quad \forall v_h \in W_h^K \quad \text{with} \quad \Pi_2^\Delta v_h = 0, \tag{4.3.6}$$

$$c_2 a_K^\nabla(\psi_h, \psi_h) \leq s_K^\nabla(\psi_h, \psi_h) \leq c_3 a_K^\nabla(\psi_h, \psi_h) \quad \forall \psi_h \in V_h^K \quad \text{with} \quad \Pi_1^\nabla \psi_h = 0. \tag{4.3.7}$$

We define the discrete sesquilinear forms $a_h(\cdot,\cdot) : Z_h \times Z_h \to \mathbb{C}$ and $b_h(\cdot,\cdot) : Z_h \times Z_h \to \mathbb{C}$ by

$$a_h((u_h,\phi_h),(v_h,\psi_h)) := \sum_{K\in\mathcal{T}_h} \frac{1}{n-1} a_{h,K}^\Delta(u_h, v_h) + a_{h,K}^\nabla(\phi_h, \psi_h) \qquad \forall (u_h,\phi_h),(v_h,\psi_h) \in Z_h,$$

$$b_h((u_h,\phi_h),(v_h,\psi_h)) := \sum_{K\in\mathcal{T}_h} b_{h,K}((u_h,\phi_h),(v_h,\psi_h)) \qquad \forall (u_h,\phi_h),(v_h,\psi_h) \in Z_h,$$

where $a_{h,K}^\Delta(\cdot,\cdot)$, $a_{h,K}^\nabla(\cdot,\cdot)$ and $b_{h,K}(\cdot,\cdot)$ are local forms on $W_h^K \times W_h^K$, $V_h^K \times V_h^K$ and $Z_h^K := W_h^K \times V_h^K$, respectively, defined by

$$a_{h,K}^\Delta(u_h, v_h) := a_K^\Delta\big(\Pi_2^\Delta u_h, \Pi_2^\Delta v_h\big) + s_K^\Delta\big(u_h - \Pi_2^\Delta u_h, v_h - \Pi_2^\Delta v_h\big), \quad \forall u_h, v_h \in W_h^K,$$
$$a_{h,K}^\nabla(\phi_h, \psi_h) := a_K^\nabla\big(\Pi_1^\nabla \phi_h, \Pi_1^\nabla \psi_h\big) + s_K^\nabla\big(\phi_h - \Pi_1^\nabla \phi_h, \psi_h - \Pi_1^\nabla \psi_h\big), \quad \forall \phi_h, \psi_h \in V_h^K,$$

$$\begin{aligned} b_{h,K}((u_h,\phi_h),(v_h,\psi_h)) :=& \frac{n}{n-1}\int_K \Pi_2^0(\Delta u_h)\Pi_2^0 \overline{v}_h + \frac{1}{n-1}\int_K \Pi_2^0 u_h \Pi_2^0(\Delta \overline{v}_h) \\ &- \int_K \nabla\Pi_1^\nabla \phi_h \cdot \nabla \Pi_2^\nabla \overline{v}_h + \frac{n}{n-1}\int_K \Pi_2^0 u_h \Pi_1^0 \overline{\psi}_h \quad \forall (u_h,\phi_h),(v_h,\psi_h) \in Z_h^K. \end{aligned}$$

The construction of the local sesquilinear forms guarantees the usual consistency and stability properties, as is stated in the proposition below. Since the proof follows standard arguments in the VEM literature, it is omitted.

Proposition 4.3.1. *The local forms $a^{\Delta}_{h,K}(\cdot,\cdot)$ and $a^{\nabla}_{h,K}(\cdot,\cdot)$ on each element K satisfy*

- *Consistency: for all $h>0$ and for all $K\in\mathcal{T}_h$ we have that*

$$a^{\Delta}_{h,K}(v_h,q)=a^{\Delta}_{K}(v_h,q)\qquad \forall q\in\mathbb{P}_2(K),\quad \forall v_h\in W_h^K, \tag{4.3.8}$$

$$a^{\nabla}_{h,K}(\psi_h,q)=a^{\nabla}_{K}(\psi_h,q)\qquad \forall q\in\mathbb{P}_1(K),\quad \forall \psi_h\in V_h^K. \tag{4.3.9}$$

- *Stability and boundedness: There exist positive constants $\alpha_i, i=1,2,3,4$, independent of K, such that:*

$$\alpha_1 a^{\Delta}_{K}(v_h,v_h)\leq a^{\Delta}_{h,K}(v_h,v_h)\leq \alpha_2 a^{\Delta}_{K}(v_h,v_h)\qquad \forall v_h\in W_h^K, \tag{4.3.10}$$

$$\alpha_3 a^{\nabla}_{K}(\psi_h,\psi_h)\leq a^{\nabla}_{h,K}(\psi_h,\psi_h)\leq \alpha_4 a^{\nabla}_{K}(\psi_h,\psi_h)\qquad \forall \psi_h\in V_h^K. \tag{4.3.11}$$

Now, we are in a position to write the virtual element discretization of Problem 3.

Problem 4. *Find $(\lambda_h,u_h,\phi_h)\in\mathbb{C}\times Z_h$, $(u_h,\psi_h)\neq 0$ such that*

$$a_h((u_h,\phi_h),(v_h,\psi_h))=\lambda_h b_h((u_h,\phi_h),(v_h,\psi_h)). \tag{4.3.12}$$

It is clear that by virtue of (4.3.10) and (4.3.11) the hermitian form $a_h(\cdot,\cdot)$ is bounded. Moreover, we will show in the following lemma that $a_h(\cdot,\cdot)$ is also uniformly elliptic.

Lemma 4.3.1. *There exists constant $C_n>0$, independent of h, such that*

$$a_h((v_h,\psi_h),(v_h,\psi_h))\geq C_n\|(v_h,\psi_h)\|^2\qquad \forall (v_h,\psi_h)\in Z_h.$$

Proof. The result is deduced from Lemma 4.2.1, (4.3.10) and (4.3.11). □

Now, we introduce the discrete solution operator T_h which is given by

$$\begin{array}{rccc} T_h: & H_0^2(\Omega)\times H_0^1(\Omega) & \longrightarrow & H_0^2(\Omega)\times H_0^1(\Omega)\\ & (f,g) & \longmapsto & T_h(f,g)=(\tilde{u}_h,\tilde{\phi}_h)\end{array}$$

where $(\tilde{u}_h,\tilde{\phi}_h)\in Z_h$ is the unique solution of the corresponding discrete source problem

$$a_h((\tilde{u}_h,\tilde{\phi}_h),(v_h,\psi_h))=b_h((f,g),(v_h,\psi_h))\qquad \forall (v_h,\psi_h)\in Z_h. \tag{4.3.13}$$

Because of Lemma 4.3.1, the linear operator T_h is well defined and bounded uniformly with respect to h. Once more, as in the continuous case, $(\lambda_h,u_h,\phi_h)\in\mathbb{C}\times Z_h$ solves Problem 4 if and only if (μ_h,u_h,ϕ_h), with $\mu_h:=\frac{1}{\lambda_h}$, is an eigenpair of T_h, i.e., $T_h(u_h,\phi_h)=\mu_h(u_h,\phi_h)$.

We end this section with the following remark.

Remark 4.3.1. *In the first and second terms in the definition of $b_{h,K}(\cdot,\cdot)$, we have employed the projector $\Pi^0_2(\Delta\cdot)$ which is a projector of high order. This definition will be useful in the forthcoming analysis of the VEM method. However, this is not the only posibility to discretize $b_K(\cdot,\cdot)$, we can also consider the following alternative definition:*

$$\begin{aligned}\tilde{b}_{h,K}((u_h,\phi_h),(v_h,\psi_h)):=&\frac{n}{n-1}\int_K\Pi^0_1(\Delta u_h)\Pi^0_2\overline{v}_h+\frac{1}{n-1}\int_K\Pi^0_2u_h\Pi^0_1(\Delta\overline{v}_h)\\ &-\int_K\nabla\Pi^{\nabla}_1\phi_h\cdot\nabla\Pi^{\nabla}_2\overline{v}_h+\frac{n}{n-1}\int_K\Pi^0_2u_h\Pi^0_1\overline{\psi}_h\quad\forall(u_h,\phi_h),(v_h,\psi_h)\in Z_h^K,\end{aligned}$$

where the projector $\Pi^0_1(\Delta\cdot)$ has been used. The VEM discretization in this case is:

Problem 5. *Find* $(\lambda_h, u_h, \psi_h) \in \mathbb{C} \times Z_h$, $(u_h, \phi_h) \neq 0$ *such that*

$$a_h((u_h, \phi_h), (v_h, \psi_h)) = \lambda_h \tilde{b}_h((u_h, \phi_h), (v_h, \psi_h)). \tag{4.3.14}$$

We are going to analize in detail the VEM method (4.3.12) *and summarize the results for the VEM discretization* (4.3.14) *(see Remark 4.4.3).*

4.4 Spectral approximation and error estimates

To prove that T_h provides a correct spectral approximation of T, we will resort to the classical theory for compact operators (see [11]). First, we recall the following approximation result which is derived by interpolation between Sobolev spaces (see for instance Theorem I.1.4 of [84] from the analogous result for integer values of s). In its turn, the result for integer values is stated in Proposition 4.2 of [12] and follows from the classical Scott-Dupont theory (see [38] and Proposition 3.1 of [7]):

Proposition 4.4.1. *There exists a constant* $C > 0$, *such that for every* $v \in H^\delta(K)$ *there exists* $v_\pi \in \mathbb{P}_k(K)$, $k \geq 0$ *such that*

$$|v - v_\pi|_{\ell,K} \leq C h_K^{\delta-\ell} |v|_{\delta,K} \quad 0 \leq \delta \leq k+1, \ell = 0, \ldots, [\delta],$$

with $[\delta]$ *denoting the largest integer equal or smaller than* $\delta \in \mathbb{R}$.

For the analysis we will introduce the broken seminorms:

$$|\psi|_{1,h}^2 := \sum_{K \in \mathcal{T}_h} |\psi|_{1,K}^2 \quad \text{and} \quad |v|_{2,h}^2 := \sum_{K \in \mathcal{T}_h} |v|_{2,K}^2,$$

which are well defined for every $(\psi, v) \in [L^2(\Omega)]^2$ such that $(\psi, v)|_K \in H^1(K) \times H^2(K)$ for all polygon $K \in \mathcal{T}_h$.

In what follows, we derive several auxiliary results which will be used in the following to prove convergence and error estimates for the spectral approximation.

Proposition 4.4.2. *Assume* ***A1–A2*** *are satisfied, let* $\psi \in H^{1+t}(\Omega)$ *with* $t \in (0, 1]$. *Then, there exist* $\psi_I \in V_h$ *and* $C > 0$ *such that*

$$\|\psi - \psi_I\|_{1,\Omega} \leq C h^t |\psi|_{1+t,\Omega}.$$

Proof. This result has been proved in Theorem 11 of [53] (see also Proposition 4.2 of [103]). □

Proposition 4.4.3. *Assume* ***A1–A2*** *are satisfied, let* $v \in H^{2+s}(\Omega)$ *with* $s \in (0, 1]$. *Then, there exist* $v_I \in W_h$ *and* $C > 0$ *such that*

$$\|v - v_I\|_{2,\Omega} \leq C h^s |v|_{2+s,\Omega}.$$

Proof. This result has been establish in Proposition 3.1 of [7]. □

Now, we establish a result which will be useful to prove the convergence of the operator T_h to T as h goes to zero.

Lemma 4.4.1. *There exists C_n independent of h such that for all $(f,g) \in H_0^2(\Omega)\times H_0^1(\Omega)$, if $(\tilde{u},\tilde{\phi}) := T(f,g)$ and $(\tilde{u}_h,\tilde{\phi}_h) := T_h(f,g)$, then*

$$\|(T-T_h)(f,g)\| \leq C_n h\|(f,g)\| + |\tilde{u}-\tilde{u}_I|_{2,\Omega} + |\tilde{u}-\tilde{u}_\pi|_{2,h} + |\tilde{\phi}-\tilde{\phi}_I|_{1,\Omega} + |\tilde{\phi}-\tilde{\phi}_\pi|_{1,h},$$

for all $(\tilde{u}_I,\tilde{\phi}_I) \in Z_h$ and for all $(\tilde{u}_\pi,\tilde{\phi}_\pi) \in [L^2(\Omega)]^2$ such that $(\tilde{u}_\pi,\tilde{\phi}_\pi)|_K \in \mathbb{P}_2(K)\times\mathbb{P}_1(K)$.

Proof. Let $(f,g) \in H_0^2(\Omega)\times H_0^1(\Omega)$, for any $(\tilde{u}_I,\tilde{\phi}_I) \in W_h \times V_h$, we have,

$$\|(T-T_h)(f,g)\| \leq \|(\tilde{u},\tilde{\phi})-(\tilde{u}_I,\tilde{\phi}_I)\| + \|(\tilde{u}_I,\tilde{\phi}_I)-(\tilde{u}_h,\tilde{\phi}_h)\|. \tag{4.4.1}$$

Now, we define $(v_h,\psi_h) = (\tilde{u}_h-\tilde{u}_I,\tilde{\phi}_h-\tilde{\phi}_I) \in Z_h$, then from the ellipticity of $a_h(\cdot,\cdot)$ and the definition of T and T_h, we have

$$\begin{aligned}
&\beta\|(v_h,\psi_h)\|^2 \leq a_h((v_h,\psi_h),(v_h,\psi_h)) = a_h((\tilde{u}_h,\tilde{\phi}_h),(v_h,\psi_h)) - a_h((\tilde{u}_I,\tilde{\phi}_I),(v_h,\psi_h))\\
&= b_h((f,g),(v_h,\psi_h)) - \sum_{K\in\mathcal{T}_h}\Big\{\frac{1}{n-1}a_{h,K}^{\Delta}(\tilde{u}_I,v_h) + a_{h,K}^{\nabla}(\tilde{\phi}_I,\psi_h)\Big\}\\
&= b_h((f,g),(v_h,\psi_h))\\
&- \sum_{K\in\mathcal{T}_h}\Big\{\frac{1}{n-1}\{a_{h,K}^{\Delta}(\tilde{u}_I-\tilde{u}_\pi,v_h) + a_{h,K}^{\Delta}(\tilde{u}_\pi,v_h)\} + a_{h,K}^{\nabla}(\tilde{\phi}_I-\tilde{\phi}_\pi,\psi_h) + a_{h,K}^{\nabla}(\tilde{\phi}_\pi,\psi_h)\Big\}\\
&= b_h((f,g),(v_h,\psi_h)) - \sum_{K\in\mathcal{T}_h}\Big\{\frac{1}{n-1}\{a_{h,K}^{\Delta}(\tilde{u}_I-\tilde{u}_\pi,v_h) + a_K^{\Delta}(\tilde{u}_\pi-\tilde{u},v_h) + a_K^{\Delta}(\tilde{u},v_h)\}\\
&\qquad + a_{h,K}^{\nabla}(\tilde{\phi}_I-\tilde{\phi}_\pi,\psi_h) + a_K^{\nabla}(\tilde{\phi}_\pi-\tilde{\phi},\psi_h) + a_K^{\nabla}(\tilde{\phi},\psi_h)\Big\}\\
&= \underbrace{\sum_{K\in\mathcal{T}_h}\Big\{b_{h,K}((f,g),(v_h,\psi_h)) - b_K((f,g),(v_h,\psi_h))\Big\}}_{E_1}\\
&- \frac{1}{n-1}\underbrace{\sum_{K\in\mathcal{T}_h}\Big\{a_{h,K}^{\Delta}(\tilde{u}_I-\tilde{u}_\pi,v_h) + a_K^{\Delta}(\tilde{u}_\pi-\tilde{u},v_h)\Big\}}_{E_2}\\
&- \underbrace{\sum_{K\in\mathcal{T}_h}\Big\{a_{h,K}^{\nabla}(\tilde{\phi}_I-\tilde{\phi}_\pi,\psi_h) + a_K^{\nabla}(\tilde{\phi}_\pi-\tilde{\phi},\psi_h)\Big\}}_{E_3},
\end{aligned}\tag{4.4.2}$$

where we have used the consistency properties (4.3.8)-(4.3.9). We now bound each term $E_i|_K$, $i = 1,2,3$.

First, the term $E_1|_K$ can be written as follows:

$$
\begin{aligned}
&b_{h,K}((f,g),(v_h,\psi_h)) - b_K((f,g),(v_h,\psi_h)) \\
&= \frac{n}{n-1}\Big\{ \underbrace{\int_K \Pi_2^0(\Delta f)\Pi_2^0\overline{v}_h - \int_K \Delta f\overline{v_h}}_{E_{11}} \Big\} + \frac{1}{n-1}\Big\{ \underbrace{\int_K \Pi_2^0 f\Pi_2^0(\Delta\overline{v}_h) - \int_K f\Delta\overline{v_h}}_{E_{12}} \Big\} \\
&- \Big\{ \underbrace{\int_K \nabla\Pi_1^\nabla g\cdot\nabla\Pi_2^\nabla\overline{v}_h - \int_K \nabla g\cdot\nabla\overline{v_h}}_{E_{13}} \Big\} + \frac{n}{n-1}\Big\{ \underbrace{\int_K (\Pi_2^0 f)(\Pi_1^0\overline{\psi}_h) - \int_K f\overline{\psi_h}}_{E_{14}} \Big\}. \qquad (4.4.3)
\end{aligned}
$$

Now, we will bound each term $E_{1i}|_K$ $i=1,2,3,4$. The term E_{11} can be bounded as follows. Using the definition of Π_2^0 and Proposition 4.4.1, we have

$$
\begin{aligned}
E_{11} &= \int_K \Delta f(\overline{v}_h - \Pi_2^0\overline{v}_h) \le |f|_{2,K}||v_h - \Pi_2^0 v_h||_{0,K} \\
&= |f|_{2,K}\inf_{q\in\mathbb{P}_2(K)}||v_h - q||_{0,K} \le Ch_K^2|f|_{2,K}|v_h|_{2,K}.
\end{aligned}
$$

For the term E_{12}, we repeat the same arguments to obtain:

$$
E_{12} \le Ch_K^2|f|_{2,K}|v_h|_{2,K}.
$$

Now, we bound E_{13}. From the definition of Π_2^∇, we have

$$
\begin{aligned}
E_{13} &= \int_K \nabla\Pi_1^\nabla g\cdot\nabla\overline{v_h} - \int_K \nabla g\cdot\nabla\overline{v_h} = \int_K \nabla(\Pi_1^\nabla g - g)\cdot\nabla\overline{v_h} \\
&= \int_K \nabla(\Pi_1^\nabla g - g)\cdot\nabla(\overline{v_h} - \tilde{v}_\pi) \le |\Pi_1^\nabla g - g|_{1,K}|v_h - \tilde{v}_\pi|_{1,K} \\
&\le Ch_K|g|_{1,K}|v_h|_{2,K},
\end{aligned}
$$

where we have used the definition and the stability of Π_1^∇ with $\tilde{v}_\pi \in \mathbb{P}_1(K)$ such that Proposition 4.4.1 holds true.

For the term E_{14}, we first use the definition of Π_2^0, the definition and the stability of Π_1^0 with respect to $\hat{f}_\pi \in \mathbb{P}_1(K)$ such that Proposition 4.4.1 holds true, thus, we have

$$
\begin{aligned}
E_{14} &= \int_K f\Pi_1^0\overline{\psi}_h - \int_K f\overline{\psi_h} = \int_K (f - \hat{f}_\pi)(\Pi_1^0\overline{\psi}_h - \overline{\psi_h}) \le Ch_K^2|f|_{2,K}||\Pi_1^0\psi_h - \psi_h||_{0,K} \\
&\le Ch_K^2|f|_{2,K}\inf_{q\in\mathbb{P}_1(K)}||\psi_h - q||_{0,K} \le Ch_K^3|f|_{2,K}|\psi_h|_{1,K}.
\end{aligned}
$$

Therefore, using the Cauchy-Schwarz inequality, we can deduce from (4.4.3) that

$$
E_1 \le C_n h||(f,g)||||(v_h,\psi_h)||.
$$

Now, for the terms E_2 and E_3, we use the Cauchy-Schwarz inequality and the stability of $a_{h,K}^\Delta(\cdot,\cdot)$ and $a_{h,K}^\nabla(\cdot,\cdot)$, to obtain

$$
E_2 + E_3 \le C_n\big\{|\tilde{u} - \tilde{u}_I|_{2,\Omega} + |\tilde{u} - \tilde{u}_\pi|_{2,h}\big\} + |\tilde{\phi} - \tilde{\phi}_I|_{1,\Omega} + |\tilde{\phi} - \tilde{\phi}_\pi|_{1,h}.
$$

Finally, from (4.4.2) we have

$$\beta||(v_h,\psi_h)|| \leq C_n\Big\{h||(f,g)|| + |\tilde{u}-\tilde{u}_I|_{2,\Omega} + |\tilde{u}-\tilde{u}_\pi|_{2,h} + |\tilde{\phi}-\tilde{\phi}_I|_{1,\Omega} + |\tilde{\phi}-\tilde{\phi}_\pi|_{1,h}\Big\}.$$

Therefore, the proof follows from (4.4.1) and the previous inequality. □

For the convergence and error analysis of the proposed virtual element scheme for the transmission eigenvalue problem, we first establish that $T_h \to T$ in norm as $h \to 0$. Then, we prove a similar convergence result for the adjoint operators T^* and T_h^* of T and T_h, respectively.

Lemma 4.4.2. *There exist C_n and $\tilde{s} \in (0,1]$, independent of h, such that*

$$\|T - T_h\| \leq C_n h^{\tilde{s}}.$$

Proof. Let $(f,g) \in H_0^2(\Omega) \times H_0^1(\Omega)$ such that $||(f,g)|| = 1$, let $(\tilde{u},\tilde{\phi})$ and $(\tilde{u}_h,\tilde{\phi}_h)$ be the solution of problems (4.2.10) and (4.3.13), respectively, so that $(\tilde{u},\tilde{\phi}) := T(f,g)$ and $(\tilde{u}_h,\tilde{\phi}_h) := T_h(f,g)$. From Lemma 4.4.1 and Poincaré inequality, we have

$$\begin{aligned}\|(T-T_h)(f,g)\| &\leq C_n h||(f,g)|| + \|\tilde{u}-\tilde{u}_I\|_{2,\Omega} + |\tilde{u}-\tilde{u}_\pi|_{2,h} + \|\tilde{\phi}-\tilde{\phi}_I\|_{1,\Omega} + |\tilde{\phi}-\tilde{\phi}_\pi|_{1,h}\\ &\leq C_n\left(h||(f,g)|| + h^s||f||_{2,\Omega} + h^t||g||_{1,\Omega}\right)\\ &\leq C_n h^{\tilde{s}}||(f,g)||\end{aligned}$$

where we have used the Propositions 4.4.1, 4.4.2 and 4.4.3, and Lemma 4.2.2, with $\tilde{s} := \min\{s,t\}$. Thus, we conclude the proof. □

Let T^* and $T_h^* : H_0^2(\Omega) \times H_0^1(\Omega) \to H_0^2(\Omega) \times H_0^1(\Omega)$ the adjoint operators of T and T_h, respectively, defined by $T^*(f,g) := (\tilde{u}^*,\tilde{\phi}^*)$ and $T_h^*(f,g) := (\tilde{u}_h^*,\tilde{\phi}_h^*)$, where $(\tilde{u}^*,\tilde{\phi}^*)$ and $(\tilde{u}_h^*,\tilde{\phi}_h^*)$ are the unique solutions of the following problems:

$$a((v,\psi),(\tilde{u}^*,\tilde{\phi}^*)) = b((v,\psi),(f,g)) \qquad \forall (v,\psi) \in H_0^2(\Omega) \times H_0^1(\Omega), \tag{4.4.4}$$

$$a_h((v_h,\psi_h),(\tilde{u}_h^*,\tilde{\phi}_h^*)) = b_h((v_h,\psi_h),(f,g)) \qquad \forall (v_h,\psi_h) \in Z_h. \tag{4.4.5}$$

It is simple to prove that if μ is an eigenvalue of T with multiplicity m, $\overline{\mu}$ is an eigenvalue of T^* with the same multiplicity m.

Now, we will study the convergence in norm of T_h^* to T^* as h goes to zero. With this aim, first we establish an additional regularity result for the solution $(\tilde{u}^*,\tilde{\phi}^*)$ of problem (4.4.4).

Lemma 4.4.3. *There exist $s,t \in (1/2,1]$ and C_n such that, for all $(f,g) \in H_0^2(\Omega) \times H_0^1(\Omega)$, the solution $(\tilde{u}^*,\tilde{\phi}^*)$ of problem (4.4.4) satisfies $\tilde{u}^* \in H^{2+s}(\Omega)$, $\tilde{\phi}^* \in H^{1+t}(\Omega)$, and*

$$\|\tilde{u}^*\|_{2+s,\Omega} + \|\tilde{\phi}^*\|_{1+t,\Omega} \leq C_n||(f,g)||.$$

Proof. The result follows repeating the same arguments used in the proof of Lemma 4.2.2. □

Remark 4.4.1. *We note that the constants s and t in Lemma 4.4.3 are the same as in Lemma 4.2.2.*

Now, we are in a position to establish the following result.

Lemma 4.4.4. *There exist C_n and $\tilde{s} \in (0,1]$, independent of h, such that*

$$\|T^* - T_h^*\| \leq C_n h^{\tilde{s}}.$$

Proof. It is essentially identical to that of Lemma 4.4.1 and Lemma 4.4.2. □

Our final goal is to show convergence and obtain error estimates. With this aim, we will apply to our problem the theory from [11, 110] for non-selfadjoint compact operators.

We first recall the definition of spectral projectors. Let μ be a nonzero eigenvalue of T with algebraic multiplicity m and let Γ be an open disk in the complex plane centered at μ, such that μ is the only eigenvalue of T lying in Γ and $\partial\Gamma \cap \mathrm{sp}(T) = \emptyset$. The spectral projectors E and E^* are defined as follows:

- The spectral projector of T relative to μ: $E := (2\pi i)^{-1} \int_{\partial\Gamma} (z - T)^{-1} dz$;
- The spectral projector of T^* relative to $\overline{\mu}$: $E^* := (2\pi i)^{-1} \int_{\partial\Gamma} (z - T^*)^{-1} dz$.

E and E^* are projections onto the space of generalized eigenvectors $R(E)$ and $R(E^*)$, respectively. It is simple to prove that $R(E), R(E^*) \in H^{2+s}(\Omega) \times H^{1+t}(\Omega)$ (see [49]).

Now, since $T_h \to T$ in norm, there exist m eigenvalues (which lie in Γ) $\mu_h^{(1)}, \ldots, \mu_h^{(m)}$ of T_h (repeated according to their respective multiplicities) will converge to μ as h goes to zero.

In a similar way, we introduce the following spectral projector $E_h := (2\pi i)^{-1} \int_{\partial\Gamma} (z - T_h)^{-1} dz$, which is a projector onto the invariant subspace $R(E_h)$ of T_h spanned by the generalized eigenvectors of T_h corresponding to $\mu_h^{(1)}, \ldots, \mu_h^{(m)}$.

We recall the definition of the *gap* $\widehat{\delta}$ between two closed subspaces $\mathcal{X}$ and $\mathcal{Y}$ of a Hilbert space $\mathcal{V}$:

$$\widehat{\delta}(\mathcal{X}, \mathcal{Y}) := \max\left\{\delta(\mathcal{X}, \mathcal{Y}), \delta(\mathcal{Y}, \mathcal{X})\right\},$$

where

$$\delta(\mathcal{X}, \mathcal{Y}) := \sup_{\mathbf{x} \in \mathcal{X}:\ \|x\|_{\mathcal{V}} = 1} \delta(x, \mathcal{Y}), \quad \text{with } \delta(x, \mathcal{Y}) := \inf_{y \in \mathcal{Y}} \|x - y\|_{\mathcal{V}}.$$

Let $\mathcal{P}_h := \mathcal{P}_h^2 \times \mathcal{P}_h^1 : H_0^2(\Omega) \times H_0^1(\Omega) \to Z_h \subseteq H_0^2(\Omega) \times H_0^1(\Omega)$ be the projector defined by

$$a(\mathcal{P}_h(u,\phi) - (u,\phi), (v_h, \psi_h)) = a^{\Delta}(\mathcal{P}_h^2 u - u, v_h) + a^{\nabla}(\mathcal{P}_h^1 \phi - \phi, \psi_h) = 0 \quad \forall (v_h, \psi_h) \in Z_h.$$

We note that the form $a(\cdot,\cdot)$ is the inner product of $H_0^2(\Omega) \times H_0^1(\Omega)$. Therefore, we have

$$|(u,\phi) - \mathcal{P}(u,\phi)|_{H_0^2(\Omega)\times H_0^1(\Omega)} = \inf_{(v_h,\psi_h)\in Z_h} |(u,\phi) - (v_h,\psi_h)|_{H_0^2(\Omega)\times H_0^1(\Omega)}, \tag{4.4.6}$$

and

$$|\mathcal{P}(u,\phi)|_{H_0^2(\Omega)\times H_0^1(\Omega)} \leq |(u,\phi)|_{H_0^2(\Omega)\times H_0^1(\Omega)} \qquad \forall (u,\phi) \in H_0^2(\Omega) \times H_0^1(\Omega). \tag{4.4.7}$$

The following error estimates for the approximation of eigenvalues and eigenfunctions hold true.

Theorem 4.4.1. *There exists a strictly positive constant C_n such that*

$$\widehat{\delta}(R(E), R(E_h)) \leq C_n h^{\min\{s,t\}}, \tag{4.4.8}$$

$$|\mu - \hat{\mu}_h| \leq C_n h^{2\min\{s,t\}}, \tag{4.4.9}$$

where $\hat{\mu}_h := \frac{1}{m}\sum_{k=1}^{m} \mu_h^{(k)}$ and with the constants s and t as in Lemmas 4.2.2 and 4.4.3 (see also Remark 4.2.2).

Proof. As a consequence of Lemma 4.4.2, T_h converges in norm to T as h goes to zero. Then, the proof of (4.4.8) follows as a direct consequence of Theorem 7.1 from [11] and the fact that, for $(f,g) \in R(E)$, $\|(f,g)\|_{H^{2+s}(\Omega)\times H^{1+t}(\Omega)} \leq \|(f,g)\|$, because of Lemma 4.2.2.

In what follows we will prove (4.4.9): assume that $T(u_k,\phi_k) = \mu(u_k,\phi_k)$, $k = 1,\ldots,m$. Since $a(\cdot,\cdot)$ is an inner product in $H_0^2(\Omega)\times H_0^1(\Omega)$, we can choose a dual basis for $R(E^*)$ denoted by $(u_k^*,\phi_k^*) \in H_0^2(\Omega)\times H_0^1(\Omega)$ satisfying

$$a((u_k,\phi_k),(u_l^*,\phi_l^*)) = \delta_{k,l}.$$

Now, from Theorem 7.2 of [11], we have that

$$|\mu - \hat{\mu}_h| \leq \frac{1}{m}\sum_{k=1}^{m} |\langle (T-T_h)(u_k,\phi_k),(u_k^*,\phi_k^*)\rangle| + C_n ||(T-T_h)|_{R(E)}|| ||(T^*-T_h^*)|_{R(E^*)}||,$$

where $\langle\cdot,\cdot\rangle$ denotes the corresponding duality pairing.

Thus, in order to obtain (4.4.9), we need to bound the two terms on the right hand side above.

The second term can be easily bounded from Lemmas 4.4.2 and 4.4.4. In fact, we have

$$||(T-T_h)|_{R(E)}|| ||(T^*-T_h^*)|_{R(E^*)}|| \leq C_n h^{2\min\{s,t\}}. \tag{4.4.10}$$

Next, we manipulate the first term as follows: adding and subtracting $(v_h,\psi_h) \in Z_h$ and using the definition of T and T_h, we obtain,

$$\begin{aligned}
&\langle (T-T_h)(u_k,\phi_k),(u_k^*,\phi_k^*)\rangle = a((T-T_h)(u_k,\phi_k),(u_k^*,\phi_k^*)) \\
&= a((T-T_h)(u_k,\phi_k),(u_k^*,\phi_k^*)-(v_h,\psi_h)) + a(T(u_k,\phi_k),(v_h,\psi_h)) \\
&\quad - a(T_h(u_k,\phi_k),(v_h,\psi_h)) \\
&= a((T-T_h)(u_k,\phi_k),(u_k^*,\phi_k^*)-(v_h,\psi_h)) + b((u_k,\phi_k),(v_h,\psi_h)) \\
&- a(T_h(u_k,\phi_k),(v_h,\psi_h)) + a_h(T_h(u_k,\phi_k),(v_h,\psi_h)) - b_h((u_k,\phi_k),(v_h,\psi_h)) \\
&= \Big\{a((T-T_h)(u_k,\phi_k),(u_k^*,\phi_k^*)-(v_h,\psi_h))\Big\} \\
&+ \Big\{b((u_k,\phi_k),(v_h,\psi_h)) - b_h((u_k,\phi_k),(v_h,\psi_h))\Big\} \\
&+ \Big\{a_h(T_h(u_k,\phi_k),(v_h,\psi_h)) - a(T_h(u_k,\phi_k),(v_h,\psi_h))\Big\} \qquad \forall (v_h,\psi_h)\in Z_h.
\end{aligned} \tag{4.4.11}$$

Now, we estimate each bracket in (4.4.11) separately. First, to bound the second bracket, we use the additional regularity of $(u_k,\phi_k) \in R(E) \subset H^{2+s}(\Omega)\times H^{1+t}(\Omega)$ and repeating the same steps used to derive (4.4.3) (in this case with (u_k,ϕ_k) instead of (f,g)), we have

$$b_{h,K}((u_k,\phi_k),(v_h,\psi_h)) - b_K((u_k,\phi_k),(v_h,\psi_h)) = E_{11}+E_{12}+E_{13}+E_{14}.$$

Now, we will bound each term E_{1i} $i = 1, 2, 3, 4$, as in the proof of Lemma 4.4.1, but in this case exploiting the additional regularity and the estimates in Lemmas 4.2.2 and 4.4.3 for $(u_k, \phi_k) \in R(E)$ and $(u_k^*, \phi_k^*) \in R(E^*)$, respectively.

In particular, the terms E_{11}, E_{12} and E_{14} can be bound exactly as in the proof of Lemma 4.4.1. However, for the term E_{13}, we proceed as follows:

$$\begin{aligned}
E_{13} &= \int_K \nabla \Pi_1^\nabla \phi_k \cdot \nabla \overline{v_h} - \int_K \nabla \phi_k \cdot \nabla \overline{v_h} = \int_K \nabla(\Pi_1^\nabla \phi_k - \phi_k) \cdot \nabla \overline{v_h} \\
&= \int_K \nabla(\Pi_1^\nabla \phi_k - \phi_k) \cdot \nabla(\overline{v_h} - \tilde{v}_h^\pi) \leq |\Pi_1^\nabla \phi_k - \phi_k|_{1,K} |v_h - \tilde{v}_h^\pi|_{1,K} \\
&= \inf_{q_h \in \mathbb{P}_1(K)} |\phi_k - q_h|_{1,K} |v_h - \tilde{v}_h^\pi|_{1,K} \leq C h_K^{1+t} |\phi_k|_{1+t,K} |v_h|_{2,K} \\
&\leq C h_K^{2\min\{s,t\}} |\phi_k|_{1+t,K} |v_h|_{2,K},
\end{aligned}$$

where we have used the definition of Π_1^∇ with $\tilde{v}_h^\pi \in \mathbb{P}_1(K)$ such that Proposition 4.4.1 holds true and the fact that $\phi_k \in H^{1+t}(\Omega)$ together with Proposition 4.4.1 again.

Therefore taking sum and using the additional regularity for ϕ_k, together with Lemma 4.2.2, we obtain for all $(v_h, \psi_h) \in Z_h$ that

$$\Big\{ b((u_k, \phi_k), (v_h, \psi_h)) - b_h((u_k, \phi_k), (v_h, \psi_h)) \Big\} \leq C_n h^{2\min\{s,t\}} ||(u_k, \phi_k)|| ||(v_h, \psi_h)||. \tag{4.4.12}$$

Now, we estimate the third bracket in (4.4.11). Let $(w_h, \xi_h) := T_h(u_k, \phi_k)$ and Π_h^K be defined by $(\Pi_h^K(v, \psi))|_K := (\Pi_2^\Delta v, \Pi_1^\nabla \psi)$ for all $K \in \mathcal{T}_h$ and for all $(v, \psi) \in H_0^2(\Omega) \times H_0^1(\Omega)$, where Π_2^Δ and Π_1^∇ have been defined in (4.3.1a)-(4.3.1b) and (4.3.2a)-(4.3.2b), respectively. Hence, we have

$$\begin{aligned}
&a_h((w_h, \xi_h),(v_h, \psi_h)) - a((w_h, \xi_h), (v_h, \psi_h)) \\
&\qquad = \sum_{K \in \mathcal{T}_h} \Big\{ a_{h,K}((w_h, \xi_h), (v_h, \psi_h)) - a_K((w_h, \xi_h), (v_h, \psi_h)) \Big\} \\
&\qquad = \sum_{K \in \mathcal{T}_h} \Big\{ a_{h,K}((w_h, \xi_h) - (\Pi_2^\Delta w_h, \Pi_1^\nabla \xi_h), (v_h, \psi_h) - (\Pi_2^\Delta v_h, \Pi_1^\nabla \psi_h)) \\
&\qquad + a_K((\Pi_2^\Delta w_h, \Pi_1^\nabla \xi_h) - (w_h, \xi_h), (v_h, \psi_h) - (\Pi_2^\Delta v_h, \Pi_1^\nabla \psi_h)) \Big\} \\
&\qquad \leq C_n \sum_{K \in \mathcal{T}_h} \Big\{ |(w_h, \xi_h) - (\Pi_2^\Delta w_h, \Pi_1^\nabla \xi_h)|_{H^2(K) \times H^1(K)} \\
&\qquad\qquad \times |(v_h, \psi_h) - (\Pi_2^\Delta v_h, \Pi_1^\nabla \psi_h)|_{H^2(K) \times H^1(K)} \Big\} \\
&\qquad = C_n \sum_{K \in \mathcal{T}_h} \Big\{ |T_h(u_k, \phi_k) - \Pi_h^K T_h(u_k, \phi_k)|_{H^2(K) \times H^1(K)} \\
&\qquad\qquad \times |(v_h, \psi_h) - \Pi_h^K (v_h, \psi_h)|_{H^2(K) \times H^1(K)} \Big\},
\end{aligned} \tag{4.4.13}$$

for all $(v_h, \psi_h) \in Z_h$, where we have used (4.3.8)-(4.3.9), Cauchy-Schwarz inequality and (4.3.10)-

(4.3.11). Now, using the triangular inequality, we have that

$$\begin{aligned}|T_h(u_k,\phi_k)-\Pi_h^K T_h(u_k,\phi_k)|_{H^2(K)\times H^1(K)} &\leq |T_h(u_k,\phi_k)-T(u_k,\phi_k)|_{H^2(K)\times H^1(K)}\\ &+|\Pi_h^K T_h(u_k,\phi_k)-\Pi_h^K T(u_k,\phi_k)|_{H^2(K)\times H^1(K)}\\ &+|\Pi_h^K T(u_k,\phi_k)-T(u_k,\phi_k)|_{H^2(K)\times H^1(K)}.\end{aligned}$$

Thus, from (4.4.13), the above estimate, the stability of Π_h^K and the additional regularity for (u_k,ϕ_k) together with Lemma 4.2.2, we have

$$\begin{aligned}&a_h(T_h(u_k,\phi_k),(v_h,\psi_h))-a(T_h(u_k,\phi_k),(v_h,\psi_h))\\ &\leq C_n h^{\min\{s,t\}}||(u_k,\phi_k)||\sum_{K\in\mathcal{T}_h}|(v_h,\psi_h)-\Pi_h^K(v_h,\psi_h)|_{H^2(K)\times H^1(K)}\quad \forall (v_h,\psi_h)\in Z_h.\end{aligned}\tag{4.4.14}$$

Finally, we take $(v_h,\psi_h):=\mathcal{P}(u_k^*,\phi_k^*)\in Z_h$ in (4.4.11). Thus, on the one hand, we bound the first bracket in (4.4.11) as follows,

$$\begin{aligned}&a((T-T_h)(u_k,\phi_k),(u_k^*,\phi_k^*)-(v_h,\psi_h))=a((T-T_h)(u_k,\phi_k),(u_k^*,\phi_k^*)-\mathcal{P}(u_k^*,\phi_k^*))\\ &\leq |(T-T_h)(u_k,\phi_k)|_{H_0^2(\Omega)\times H_0^1(\Omega)}|(u_k^*,\phi_k^*)-\mathcal{P}(u_k^*,\phi_k^*)|_{H_0^2(\Omega)\times H_0^1(\Omega)}\\ &=|(T-T_h)(u_k,\phi_k)|_{H_0^2(\Omega)\times H_0^1(\Omega)}\inf_{(r_h,s_h)\in Z_h}|(u_k^*,\phi_k^*)-(r_h,s_h)|_{H_0^2(\Omega)\times H_0^1(\Omega)}\\ &\leq |(T-T_h)(u_k,\phi_k)|_{H_0^2(\Omega)\times H_0^1(\Omega)}|(u_k^*,\phi_k^*)-((u_k^*)_I,(\phi_k^*)_I)|_{H_0^2(\Omega)\times H_0^1(\Omega)}\\ &\leq Ch^{2\min\{s,t\}}||(u_k^*,\phi_k^*)||,\end{aligned}$$

where we have used (4.4.6), Propositions 4.4.2 and 4.4.3, the additional regularity for (u_k^*,ϕ_k^*), Lemma 4.4.3 and Lemma 4.4.2.

On the other hand, from (4.4.14) we have that

$$\begin{aligned}|(v_h,\psi_h)-\Pi_h^K(v_h,\psi_h)|_{H^2(K)\times H^1(K)} &= |\mathcal{P}(u_k^*,\phi_k^*)-\Pi_h^K\mathcal{P}(u_k^*,\phi_k^*)|_{H^2(K)\times H^1(K)}\\ &\leq |\mathcal{P}(u_k^*,\phi_k^*)-(u_k^*,\phi_k^*)|_{H^2(K)\times H^1(K)}\\ &+|(u_k^*,\phi_k^*)-\Pi_h^K(u_k^*,\phi_k^*)|_{H^2(K)\times H^1(K)}\\ &+|\Pi_h^K((u_k^*,\phi_k^*)-\mathcal{P}(u_k^*,\phi_k^*))|_{H^2(K)\times H^1(K)}.\end{aligned}$$

Then, using again (4.4.6), Propositions 4.4.2 and 4.4.3, the additional regularity for (u_k^*,ϕ_k^*), Lemma 4.4.3 and Lemma 4.4.2, we obtain from (4.4.14) that

$$a_h(T_h(u_k,\phi_k),(v_h,\psi_h))-a(T_h(u_k,\phi_k),(v_h,\psi_h))\leq C_n h^{2\min\{s,t\}}||(u_k,\phi_k)||||(u_k^*,\phi_k^*)||.\tag{4.4.15}$$

Thus, from (4.4.11), (4.4.12) and (4.4.15), we obtain

$$|\langle (T-T_h)(u_k,\phi_k),(u_k^*,\phi_k^*)\rangle|\leq C_n h^{2\min\{s,t\}}.\tag{4.4.16}$$

Therefore, the proof follows from estimates (4.4.10) and (4.4.16). □

Remark 4.4.2. *The error estimate for the eigenvalue μ of T yields analogous estimate for the approximation of the eigenvalue $\lambda=1/\mu$ of Problem 3 by means of $\hat{\lambda}_h:=\frac{1}{m}\sum_{k=1}^{m}\lambda_h^{(k)}$, where $\lambda_h^{(k)}=1/\mu_h^{(k)}$.*

Now, we state in the following remark the approximation properties of Problem 5.

Remark 4.4.3. *A result analogous to Theorem 4.4.1 can be proven for the alternative discretization of Problem 3 proposed in Remark 4.3.1. We do not include proofs to avoid repeating step by step those of Section 4.4. However, we will present a numerical test to confirm the error estimates in this case.*

4.5 Numerical results

In this section we present a series of numerical experiments to solve the transmission eigenvalue problem with the Virtual Element schemes (4.3.12) and (4.3.14). However, to complete the choice of the VEM, we had to fix the forms $s_K^{\Delta}(\cdot,\cdot)$ and $s_K^{\nabla}(\cdot,\cdot)$ satisfying (4.3.6) and (4.3.7), respectively. For $s_K^{\Delta}(\cdot,\cdot)$, we consider the same definition as in [105]:

$$s_K^{\Delta}(u_h, v_h) := \sigma_K \sum_{i=1}^{N_K} [u_h(P_i)v_h(P_i) + h_{P_i}^2 \nabla u_h(P_i) \cdot \nabla v_h(P_i)] \quad \forall u_h, v_h \in W_h^K,$$

where $P_1, \ldots, P_{N_K}$ are the vertices of K, h_{P_i} corresponds to the maximum diameter of the elements with P_i as a vertex and $\sigma_K > 0$ is a multiplicative factor to take into account the magnitude of the parameter and the h-scaling, for instance, in the numerical tests we have picked $\sigma_K > 0$ as the mean value of the eigenvalues of the local matrix $a_K^{\Delta}(\Pi_2^{\Delta}\varphi_i, \Pi_2^{\Delta}\varphi_j)$, $i, j = 1, \ldots, \dim W_h^K$ and $\{\varphi_i\}_{i=1}^{\dim W_h^K}$ is a basis of W_h^K. This ensures that the stabilizing term scales as $a_K^{\Delta}(v_h, v_h)$. Now, a choice for $s_K^{\nabla}(\cdot,\cdot)$ is given by

$$s_K^{\nabla}(\phi_h, \psi_h) := \sum_{i=1}^{N_K} \phi_h(P_i)\psi_h(P_i) \quad \forall \phi_h, \psi_h \in V_h^K,$$

which corresponds to the identity matrix of dimension N_K. A proof of (4.3.6) and (4.3.7) for the above choices could be derived following the arguments in [22]. Finally, we mention that the previous definitions are in accordance with the analysis presented in [103, 105] in order to avoid spectral pollution.

We have implemented in a MATLAB code the proposed VEM on arbitrary polygonal meshes, by following the ideas presented in [16]. Moreover, we compare our results with those existing in the literature, for example [49, 60, 72, 88]. We have considered three different domains, namely: square domain, a circular domain centered at the origin and an L-shaped domain.

4.5.1 Test 1: Square domain

The goal of this test is to assess and compare the performance of the VEM discretizations (4.3.12) and (4.3.14). With this aim, we have taken $\Omega := (0,1)^2$ and index of refraction $n = 4$ and $n = 16$. We have tested the methods by using different families of meshes (see Figure 4.1):

- $\mathcal{T}_h^1$: triangular meshes;
- $\mathcal{T}_h^2$: rectangular meshes;

- $\mathcal{T}_h^3$: hexagonal meshes;
- $\mathcal{T}_h^4$: non-structured hexagonal meshes made of convex hexagons.

The refinement parameter N used to label each mesh is the number of elements on each edge of the domain.

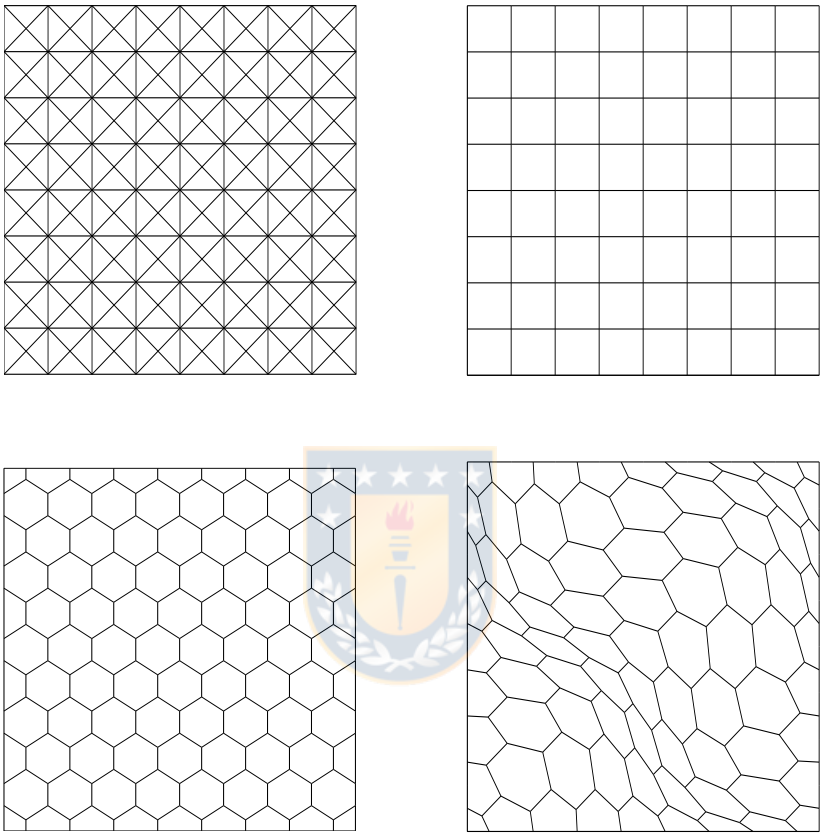

Figure 4.1: Sample meshes: $\mathcal{T}_h^1$ (top left), $\mathcal{T}_h^2$ (top right), $\mathcal{T}_h^3$ (bottom left) and $\mathcal{T}_h^4$ (bottom right), for $N = 8$ (figure produced by the author).

We report in Tables 4.1 and 4.2 the lowest transmission eigenvalues k_{ih}, $i = 1, 2, 3, 4$ computed by the scheme (4.3.12) with two different families of meshes and $N = 32, 64, 128$, and with the index of refraction $n = 4$ and $n = 16$, respectively. The tables include computed orders of convergence, as well as more accurate values extrapolated by means of a least-squares fitting. Moreover, we compare the performance of the proposed method with those presented in [72, 88]. With this aim, we include in the last row of Tables 4.1 and 4.2 the results reported in that references, for the same problem.

It can be seen from Tables 4.1 and 4.2 and that the eigenvalue approximation order of method (4.3.12) is quadratic (as predicted by the theory for convex domains).

On the other hand, in Table 4.3 we report the five lowest transmission eigenvalues computed with

Table 4.1: Test 1: Lowest transmission eigenvalues k_{ih}, $i = 1, 2, 3, 4$ computed on different meshes and with index of refraction $n = 4$ (table produced by the author).

Meshes	k_{ih}	k_{1h}	k_{2h}	k_{3h}	k_{4h}
$\mathcal{T}_h^3$	$N = 32$	4.2835-1.1367i	4.2835+1.1367i	5.3373	5.4172
	$N = 64$	4.2745-1.1446i	4.2745+1.1446i	5.4375	5.4599
	$N = 128$	4.2724-1.1467i	4.2724+1.1467i	5.4661	5.4719
	Order	2.10& 1.89	2.10& 1.89	1.81	1.84
	Extrapolated	4.2717-1.1475i	4.2717+1.1475i	5.4775	5.4765
$\mathcal{T}_h^4$	$N = 32$	4.2870-1.1341i	4.2870+1.1341i	5.3245	5.4178
	$N = 64$	4.2753-1.1438i	4.2753+1.1438i	5.4329	5.4602
	$N = 128$	4.2726-1.1465i	4.2726+1.1465i	5.4647	5.4719
	Order	2.12 &1.86	2.12&1.86	1.77	1.85
	Extrapolated	4.2718-1.1475i	4.2718+1.1475i	5.4779	5.4765
	[88]	4.2717-1.1474i	4.2717+1.1474i	5.4761	5.4761

the virtual element method (4.3.14). The table includes orders of convergence, as well as accurate values extrapolated by means of a least-squares fitting.

It can be seen from Table 4.3 that the computed lowest transmission eigenvalues converge with an optimal quadratic order as predicted by the theory (see Remark 4.4.3). It can be observed that the two methods agree perfectly well (see Tables 4.2 and 4.3).

4.5.2 Test 2: Circular domain

In this test, we have taken as domain the circle $\Omega := \{(x, y) \in \mathbb{R}^2 : x^2 + y^2 < 1/4\}$. We have used polygonal meshes created with PolyMesher [119] (see Figure 4.2). The refinement parameter N is the number of elements intersecting the boundary.

We report in Table 4.4 the five lowest transmission eigenvalues computed with the virtual element method (4.3.12). The table includes orders of convergence, as well as accurate values extrapolated by means of a least-squares fitting. Once again, the last rows show the values obtained by extrapolating those computed with different methods presented in [49, 60, 72].

Once more, a quadratic order of convergence can be clearly appreciated from Table 4.4.

We show in Figure 4.2 the eigenfunctions corresponding to the four lowest transmission eigenvalues.

Table 4.2: Test 1: Lowest transmission eigenvalues k_{ih}, $i = 1, 2, 3, 4$ computed on different meshes and with index of refraction $n = 16$ (table produced by the author).

Meshes	k_{ih}	k_{1h}	k_{2h}	k_{3h}	k_{4h}
$\mathcal{T}_h^1$	$N = 32$	1.8805	2.4467	2.4467	2.8691
	$N = 64$	1.8798	2.4449	2.4449	2.8671
	$N = 128$	1.8796	2.4444	2.4444	2.8666
	Order	2.01	2.00	2.00	2.01
	Extrapolated	1.8796	2.4442	2.4442	2.8664
$\mathcal{T}_h^2$	$N = 32$	1.8764	2.4318	2.4318	2.8645
	$N = 64$	1.8788	2.4410	2.4410	2.8658
	$N = 128$	1.8794	2.4434	2.4434	2.8663
	Order	1.95	1.95	1.95	1.61
	Extrapolated	1.8796	2.4443	2.4443	2.8665
	[72][Argyris method]	1.8651	2.4255	2.4271	2.8178
	[72][Continuous method]	1.9094	2.5032	2.5032	2.9679
	[72][Mixed method]	1.8954	2.4644	2.4658	2.8918
	[88]	1.8796	2.4442	2.4442	2.8664

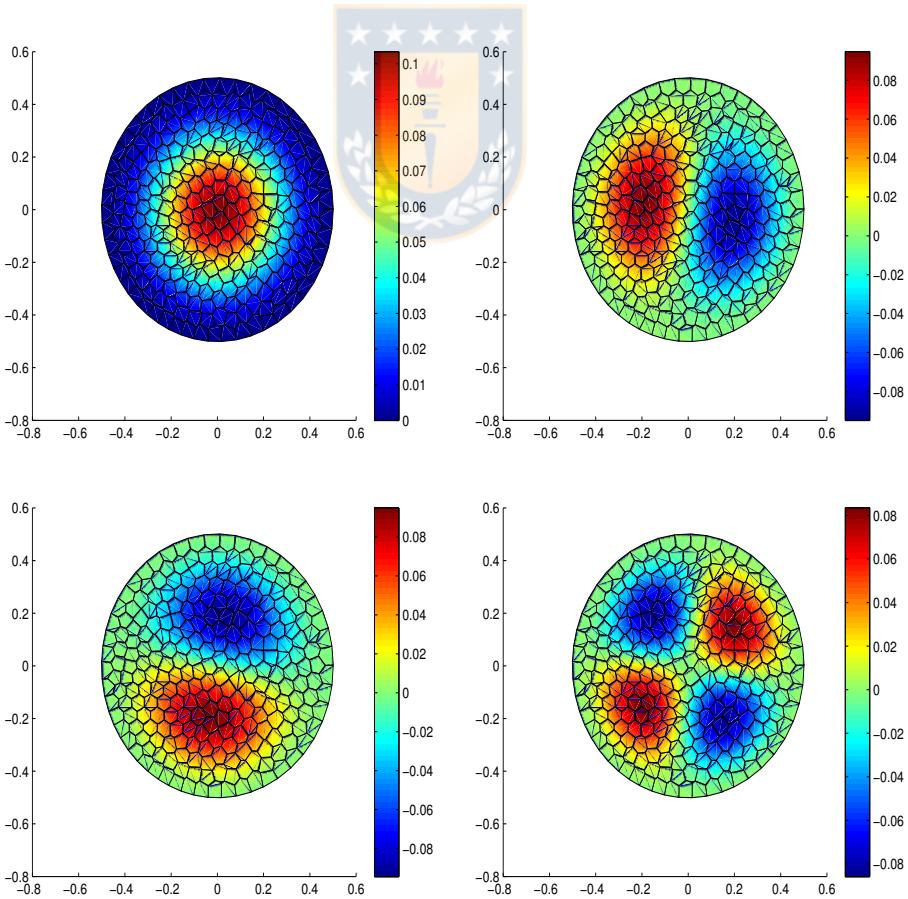

Figure 4.2: Test 2. Eigenfunctions u_{1h} (top left), u_{2h} (top right), u_{3h} (bottom left) and u_{4h} (bottom right) (figure produced by the author).

Table 4.3: Test 1: Lowest transmission eigenvalues k_{ih}, $i = 1, 2, 3, 4$ computed on different meshes and with index of refraction $n = 16$ (table produced by the author).

Meshes	k_{ih}	k_{1h}	k_{2h}	k_{3h}	k_{4h}
$\mathcal{T}_h^1$	$N = 32$	1.8823	2.4504	2.4504	2.8749
	$N = 64$	1.8803	2.4458	2.4458	2.8686
	$N = 128$	1.8798	2.4446	2.4446	2.8670
	Order	1.99	1.99	1.99	1.99
	Extrapolated	1.8796	2.4442	2.4442	2.8664
$\mathcal{T}_h^2$	$N = 32$	1.8815	2.4421	2.4421	2.8811
	$N = 64$	1.8801	2.4438	2.4438	2.8702
	$N = 128$	1.8797	2.4441	2.4441	2.8674
	Order	1.91	2.15	2.15	1.96
	Extrapolated	1.8796	2.4442	2.4442	2.8664

Table 4.4: Test 2: Computed lowest transmission eigenvalues k_{ih}, $i = 1, 2, 3, 4, 5$ with index of refraction $n = 16$ (table produced by the author).

	k_{1h}	k_{2h}	k_{3h}	k_{4h}	k_{5h}
$N = 32$	1.9835	2.6032	2.6037	3.2115	3.2117
$N = 64$	1.9869	2.6105	2.6106	3.2225	3.2227
$N = 128$	1.9877	2.6123	2.6123	3.2255	3.2256
Order	1.98	1.97	2.01	1.86	1.90
Extrapolated	1.9880	2.6129	2.6129	3.2267	3.2267
[49]	1.9881	-	-	-	-
[60]	1.9879	2.6124	2.6124	3.2255	3.2255
[72][Argyris method]	2.0076	2.6382	2.6396	3.2580	3.2598
[72][Continuous method]	2.0301	2.6937	2.6974	3.3744	3.3777
[72][Mixed method]	1.9912	2.6218	2.6234	3.2308	3.2397

4.5.3 Test 3: L-shaped domain

Finally, we have considered an L-shaped domain: $\Omega := (-1/2, 1/2)^2 \backslash ([0, 1/2] \times [-1/2, 0])$. We have used uniform triangular meshes as those shown in Figure 4.3. The meaning of the refinement parameter N is the number of elements on each edge.

We report in Table 4.5 the four lowest transmission eigenvalues computed with the virtual scheme (4.3.12). The table includes orders of convergence, as well as accurate values extrapolated by means of a least-squares fitting. Once again, we compare the performance of the proposed virtual scheme with the one presented in [49] for the same problem, using triangular meshes.

In this numerical test, according to [85, 86], we have that for the Laplace problem the Lemma 4.2.2 holds for all $t < t_0$, where $t_0 := \pi/\omega$ with ω being the largest interior angle of Ω (in this test, $\omega = 3\pi/2$). On the other hand, for the biharmonic equation the Lemma 4.2.2 holds for all $s < s_0 := \alpha - 1$, where

Table 4.5: Test 3: Computed lowest transmission eigenvalues k_{ih}, $i = 1, 2, 3, 4$ with index of refraction $n = 16$ (table produced by the author).

k_{ih}	k_{1h}	k_{2h}	k_{3h}	k_{4h}
$N = 32$	2.9690	3.1480	3.4216	3.5744
$N = 64$	2.9590	3.1417	3.4136	3.5683
$N = 128$	2.9551	3.1400	3.4113	3.5667
Order	1.37	1.94	1.76	2.00
Extrapolated	2.9527	3.1395	3.4103	3.5662
[49]	2.9553	-	-	-

$\alpha > 1$ is the smallest positive root of the following characteristic equation:

$$\sin^2(\alpha - 1)\omega = (\alpha - 1)^2 \sin^2 \omega.$$

As a consequence, for the first transmission eigenvalue, since the singularity of the solution in the L-shaped domain, the method converges with order close to $\min\{1.089, 1.333\}$, which corresponds to the Sobolev regularity for the biharmonic equation and Laplace equation, respectively. Moreover, the method converges with larger orders for the rest of the transmission eigenvalues.

Finally, Figure 4.3 shows the eigenfunctions corresponding to the four lowest transmission eigenvalues with index of refraction $n = 16$.

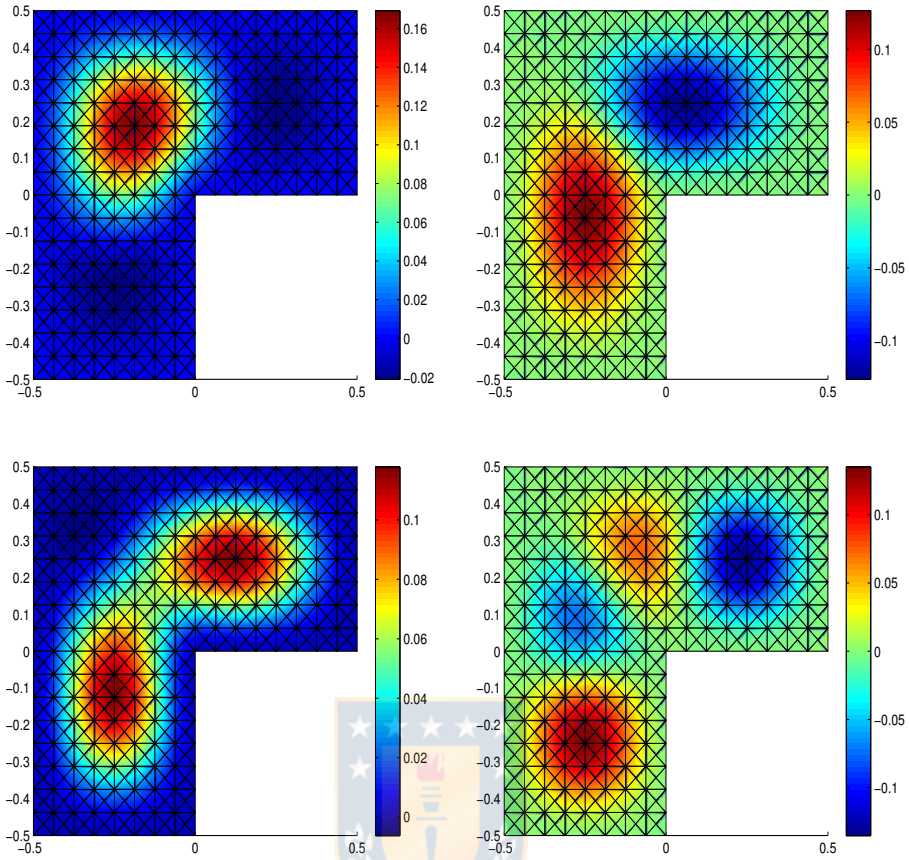

Figure 4.3: Test 3. Eigenfunctions u_{1h} (top left), u_{2h} (top right), u_{3h} (bottom left) and u_{4h} (bottom right) (figure produced by the author).

Conclusions

We analyzed and applied, several H^2 conforming virtual element methods constructed with few degrees of freedom and easy to implement on general polygonal meshes for solving linear and nonlinear problems that arise in solid mechanics and are modelled by fourth order partial differential equations. Theoretical and numerical results of the virtual element methods applied to the vibration and buckling problems of Kirchhoff plates, von Kármán plate problem and transmission eigenvalue problem have been provided.

The main conclusions of this thesis are:

1. In **Chapter 1**, we studied the vibration problem of a clamped polygonal non-convex plate and modelled by Kirchhoff equations. A variational formulation based only in terms of the transverse displacement of the plate was introduced. Next, a conforming scheme of $H^2(\Omega)$ by means of the virtual element method was developed to obtain analitically and numerically results of the eigenvalue problem. It was established that the resulting scheme provides a correct spectral approximation. Moreover, optimal error estimates results for the eigenfunctions and eigenvalues are provided. We reported a set of numerical tests which confirmed the good performance of the C^1-VEM applied to vibration problem. Moreover, we included a numerical test to check the influence of the stabilizing bilinear forms. In this test, non spurious eigenvalues were found for any chosen stability parameter. We conclude that the computed eigenvalues for the vibration problem are sensitive with respect to stabilization parameter in case of coarse meshes i.e., the lowest eigenvalues converge to wrong results for very small values of α when coarse meshes are considered. Hence, finer meshes are needed for the computed eigenvalues to lie close to the reference value. However, the numerical results deduce that the methods is robust for $\alpha \in [1/4, 4]$ in any coarse meshes. Moreover, we found that the small eigenvalues were well approximated for a wide range of the stability parameters in case of fine meshes (verified for $\alpha \in [1/4, 64]$).

2. In **Chapter 2**, we analyzed a C^1 virtual element method of arbitrary order $k \geq 2$ to study the buckling problem of a clamped polygonal non-convex plate and governed by Kirchhoff equations. The plate has been subjected to a general symmetric stress tensor field. It is established that the resulting scheme provides a correct spectral approximation and that the error estimations are of the optimal order for the eigenvalues and buckling modes. The C^1-VEM analyzed provides an attractive and competitive alternative to solve the fourth order plate buckling eigenvalue problem without use of a lot of degrees of freedom. For instance, in the lowest order case ($k = 2$), the total

degrees of freedom used were $3N_v$, where N_v denoted the number of vertices in the polygonal mesh. For $k = 3$, the quantity of degrees of freedom employed were $3N_v + N_e$, where N_e denoted the number of edges in the polygonal mesh. Several numerical examples which confirm the good performance of our method were developed (including examples for a non positive definite strain tensor). In addition, even though our theoretical analysis has been developed only for clamped plates, once again, additional tests were considered and we evidenced that the results developed in the chapter hold true for a simply supported-free plate.

3. We proposed and analyzed a lowest-order C^1 Virtual Element Method ($k = 2$) on general polygonal meshes in **Chapter 3** to approximate the isolated solutions of a von Kármán plate. Under sufficiently small data assumptions the uniqueness of the isolated solution is guaranteed. In addition, we approximated the isolated solution by means of VEM. This was made by considering fixed-point arguments together with sufficiently small discretization parameter assumptions. As a consequence, we established optimal order error estimates in energy H^2-norm. Finally, a set of numerical tests were reported in order to validate the good performance of the method and confirm the corresponding order of convergence. In addition, we reported a numerical test which shows that the discrete solutions near a simple bifurcation point of the continuous problem behave as it was expected. Which makes us to think that it is possible to extend the analysis in such situations.

4. The mathematical and numerical analysis of the approximation by virtual elements for the transmission eigenvalue problem was addressed in **Chapter 4**. We obtained a spectral characterization of the solution operator applying the spectral theory for non-self-adjoint compact operators. The numerical method has been based in a $C^1 \times C^0$-virtual elements discretization. The standard spectral theory for compact non-self-adjoint operators was applied in order to obtain convergence and optimal order error estimates, for the discrete scheme as well as for adjoint discrete problem. Several numerical tests for circular, L-shaped and squared domains were considered.

Future work

1. To derive a posteriori error estimators, reliable and efficient for the topics studied in **Chapters 1,2,3** and **4**.
2. To extend the results in **Chapters 1** and **2** considering more general boundary conditions.
3. To use other mathematical models of thin structures to study the vibration or buckling problems.
4. To study virtual element methods applied to the bifurcation theory for the von Kármán equations.
5. To study virtual element methods for the von Kármán evolution equations.
6. To study virtual element methods in two and three dimensions for the transmission eigenvalue problem.

Conclusiones y trabajos futuros

Conclusiones

Analizamos y aplicamos varios métodos de elementos virtuales conformes de H^2, construidos con pocos grados de libertad y fáciles de implementar en mallas poligonales generales, para resolver problemas lineales y no lineales de cuarto orden que surgen en la mecánica de sólidos. Se han proporcionado resultados teóricos y numéricos de los métodos de elementos virtuales aplicados a los problemas de vibración y de pandeo de las placas de Kirchhoff, para el problema de placa de von Kármán y a el problema de valores propios de transmisión.

Las principales conclusiones de esta tesis son:

1. En el **Capítulo 1**, estudiamos el problema de vibración de una placa poligonal no convexa empotrada y modelado por las ecuaciones de Kirchhoff. Se introdujo una formulación variacional basada únicamente en términos del desplazamiento transversal de la placa. A continuación, se desarrolló un esquema conforme de $H^2(\Omega)$ mediante el método del elemento virtual para obtener resultados analíticos y numéricos del problema de valores propios. Se estableció que el esquema resultante proporciona una aproximación espectral correcta. Además, se establecieron estimaciones de error óptimas para las funciones propias y los valores propios. Presentamos resultados numéricos que confirmaron el buen desempeño del C^1-VEM aplicado al problema de vibración de placas. Además, incluimos una prueba numérica para verificar la influencia de las formas bilineales estabilizadoras. En esta prueba, se encontraron valores propios no espurios para cualquier parámetro de estabilidad elegido. Concluimos que los valores propios calculados para el problema de vibración son sensibles con respecto al parámetro de estabilización en caso de mallas gruesas, es decir, los valores propios más bajos convergen en resultados incorrectos para valores muy pequeños de α cuando se consideran mallas gruesas. Por lo tanto, se necesitan mallas finas para que los valores propios calculados se encuentren cerca del valor de referencia. Sin embargo, los resultados numéricos deducen que el método es robusto para $\alpha \in [1/4, 4]$ en cualquier malla gruesa. Además, encontramos que los pequeños valores propios son bien aproximados para una amplia gama del parámetro de estabilidad en caso de mallas finas (verificado por $\alpha \in [1/4, 64]$).

2. En el **Capítulo 2**, analizamos un método de elemento virtual C^1 de orden arbitrario $k \geq 2$, para estudiar el problema de pandeo de una placa empotrada poligonal no convexa y gobernada por las ecuaciones de Kirchhoff. La placa se ha sometido a un campo tensorial de esfuerzo simétrico no necesariamente definido positivo. Se estableció que el esquema resultante proporciona una aproximación espectral correcta y que las estimaciones de error son del orden óptimo para los

valores propios y los modos de pandeo. El C^1 -VEM analizado ofrece una alternativa atractiva y competitiva para resolver el problema de valor propio de la placa de cuarto orden, sin usar muchos grados de libertad. Por ejemplo, en el caso del orden más bajo ($k = 2$), el total de grados de libertad empleados fue de $3N_v$, donde N_v denotó el número de vértices en la malla poligonal. Para $k = 3$, la cantidad de grados de libertad empleados fue de $3N_v + N_e$, donde N_e denotó el número de lados en la malla poligonal. Se desarrollaron varios ejemplos numéricos que confirman el buen desempeño de nuestro método. Además, aún cuando nuestro análisis teórico se ha desarrollado sólo para placas empotradas, una vez más, se consideraron pruebas adicionales y se evidenció que los resultados desarrollados en el capítulo son válidos para una placa con condiciones de frontera mixta, mas precisamente, con frontera libre y simplemente apoyada.

3. En el **Capítulo 3** propusimos y analizamos un método de elemento virtual C^1 de orden $k = 2$ en mallas poligonales generales, para aproximar las soluciones aisladas de una placa modelada por las ecuaciones de von Kármán. Bajo supuestos de datos suficientemente pequeños, se garantizó la unicidad de la solución aislada. Además, aproximamos la solución aislada mediante VEM. Esto se hizo considerando argumentos de punto fijo, junto con suposiciones de parámetros de discretización suficientemente pequeños. Como consecuencia, establecimos estimaciones de error de orden óptimas en norma H^2. Finalmente, se presentó un conjunto de pruebas numéricas para validar el buen desempeño del método y confirmar el orden de convergencia correspondiente.

4. El análisis matemático y numérico de la aproximación por elementos virtuales para el problema de autovalores de transmisión se abordó en el **Capítulo 4**. Se obtuvo una caracterización espectral del operador de solución, aplicando la teoría espectral para operadores compactos no autoadjuntos. El método numérico se basó en una discretización de elementos virtuales $C^1 \times C^0$. La teoría espectral estándar para operadores compactos no autoadjuntos se aplicó para obtener convergencia y estimaciones de error de orden óptimas, tanto para el esquema discreto como para el problema discreto adjunto. Se consideraron varias pruebas numéricas para dominios circulares, en forma de L y cuadrados.

Trabajo futuro

1. Derivar estimadores de error a posteriori, confiables y eficientes para los problemas estudiados en los **Capítulos 1,2,3** and **4**.

2. Extender los resultados presentados en los **Capítulos 1** and **2** considerando condiciones de contornos más generales.

3. Usar otros modelos matemáticos de estructuras delgadas para los problemas de vibración y pandeo.

4. Estudiar los métodos de elementos virtuales aplicados a la teoría de la bifurcación para las ecuaciones de von Kármán.

5. Estudiar los métodos de elementos virtuales para las ecuaciones de evolución de von Kármán.

6. Estudiar métodos de elementos virtuales en dos y tres dimensiones para el problema del valores propios de transmisión.

References

[1] R. A. Adams and J. J. Fournier, *Sobolev Spaces*, Elsevier, 2003.

[2] B. Ahmad, A. Alsaedi, F. Brezzi, L. D. Marini, and A. Russo, *Equivalent projectors for virtual element methods*, Comput. Math. Appl., 66 (2013), pp. 376–391.

[3] M. Amara, D. Capatina-Papaghiuc, and A. Chatti, *Bending moment mixed method for the Kirchhoff-Love plate model*, SIAM J. Numer. Anal., 40 (2002), pp. 1632–1649.

[4] V. Anaya, M. Bendahmane, D. Mora and M. Sepúlveda, *A virtual element method for a nonlocal FitzHugh–Nagumo model of cardiac electrophysiology*, IMA J. Numer. Anal., DOI: https://doi.org/10.1093/imanum/drz001 (2019).

[5] A. B. Andreev, R. D. Lazarov, and M. R. Racheva, *Postprocessing and higher order convergence of the mixed finite element approximations of biharmonic eigenvalue problems*, J. Comput. Appl. Math., 182 (2005), pp. 333–349.

[6] P. F. Antonietti, L. Beirão da Veiga, D. Mora, and M. Verani, *A stream virtual element formulation of the Stokes problem on polygonal meshes*, SIAM J. Numer. Anal., 52 (2014), pp. 386–404.

[7] P. F. Antonietti, L. Beirão da Veiga, S. Scacchi, and M. Verani, *A C^1 virtual element method for the Cahn-Hilliard equation with polygonal meshes*, SIAM J. Numer. Anal., 54 (2016), pp. 34–56.

[8] E. Artioli, S. de Miranda, C. Lovadina, and L. Patruno, *A stress/displacement virtual element method for plane elasticity problems*, Comput. Methods Appl. Mech. Engrg., 325 (2017), pp. 155–174.

[9] E. Artioli, S. de Miranda, C. Lovadina, and L. Patruno, *A family of virtual element methods for plane elasticity problems based on the Hellinger-Reissner principle*, Comput. Methods Appl. Mech. Engrg., 340 (2018), pp. 978–999.

[10] K. Atkinson and W. Han, *Theoretical Numerical Analysis*, Texts in Applied Mathematics, Springer, Dordrecht, 2009.

[11] I. Babuška and J. Osborn, *Eigenvalue Problems*, Elsevier,North-Holland, 1991.

[12] L. Beirão da Veiga, F. Brezzi, A. Cangiani, G. Manzini, L. D. Marini, and A. Russo, *Basic principles of virtual element methods*, Math. Models Methods Appl. Sci., 23 (2013), pp. 199–214.

[13] L. Beirão da Veiga, F. Brezzi, F. Dassi, L. D. Marini, and A. Russo, *Virtual element approximation of 2D magnetostatic problems*, Comput. Methods Appl. Mech. Engrg., 327 (2017), pp. 173–195.

[14] L. Beirão da Veiga, F. Brezzi, F. Dassi, L. D. Marini, and A. Russo, *Lowest order virtual element approximation of magnetostatic problems*, Comput. Methods Appl. Mech. Engrg., 332 (2018), pp. 343–362.

[15] L. Beirão da Veiga, F. Brezzi, and L. D. Marini, *Virtual elements for linear elasticity problems*, SIAM J. Numer. Anal., 51 (2013), pp. 794–812.

[16] L. Beirão da Veiga, F. Brezzi, L. D. Marini, and A. Russo, *The hitchhiker's guide to the virtual element method*, Math. Models Methods Appl. Sci., 24 (2014), pp. 1541–1573.

[17] L. Beirão da Veiga, F. Brezzi, L. D. Marini, and A. Russo, *Mixed virtual element methods for general second order elliptic problems on polygonal meshes*, ESAIM Math. Model. Numer. Anal., 50 (2016), pp. 727–747.

[18] L. Beirão da Veiga, F. Brezzi, L. D. Marini, and A. Russo, *Virtual element implementation for general elliptic equations*, in Building Bridges: Connections and Challenges in Modern Approaches to Numerical Partial Differential Equations, Springer, Cham, 2016, pp. 39–71.

[19] L. Beirão da Veiga, F. Dassi, and A. Russo, *C^1 virtual element method on polyhedral meshes*, arXiv preprint arXiv:1808.01105, (2018).

[20] L. Beirão da Veiga, K. Lipnikov, and G. o. Manzini, *The Mimetic Finite Difference Method for Elliptic Problems*, Springer, 2014.

[21] L. Beirão da Veiga, C. Lovadina, and D. Mora, *A virtual element method for elastic and inelastic problems on polytope meshes*, Comput. Methods Appl. Mech. Engrg., 295 (2015), pp. 327–346.

[22] L. Beirão da Veiga, C. Lovadina, and A. Russo, *Stability analysis for the virtual element method*, Math. Models Methods Appl. Sci., 27 (2017), pp. 2557–2594.

[23] L. Beirão da Veiga, C. Lovadina, and G. Vacca, *Divergence free virtual elements for the Stokes problem on polygonal meshes*, ESAIM Math. Model. Numer. Anal., 51 (2017), pp. 509–535.

[24] L. Beirão da Veiga, C. Lovadina, and G. Vacca, *Virtual elements for the Navier-Stokes problem on polygonal meshes*, SIAM J. Numer. Anal., 56 (2018), pp. 1210–1242.

[25] L. Beirão da Veiga and G. Manzini, *A virtual element method with arbitrary regularity*, IMA J. Numer. Anal., 34 (2014), pp. 759–781.

[26] L. Beirão da Veiga and G. Manzini, *Residual a posteriori error estimation for the virtual element method for elliptic problems*, ESAIM Math. Model. Numer. Anal., 49 (2015), pp. 577–599.

[27] L. Beirão da Veiga, D. Mora, and G. Rivera, *Virtual elements for a shear-deflection formulation of Reissner-Mindlin plates*, Math. Comp., 88 (2019), pp. 149–178.

[28] L. Beirão da Veiga, D. Mora, G. Rivera, and R. Rodríguez, *A virtual element method for the acoustic vibration problem*, Numer. Math., 136 (2017), pp. 725–763.

[29] L. Beirão da Veiga, D. Mora, and G. Vacca, *The stokes complex for virtual elements with application to navier–stokes flows*, arXiv preprint arXiv:1807.10650, (2018).

[30] M. F. Benedetto, S. Berrone, A. Borio, S. Pieraccini, and S. Scialò, *Order preserving SUPG stabilization for the virtual element formulation of advection-diffusion problems*, Comput. Methods Appl. Mech. Engrg., 311 (2016), pp. 18–40.

[31] S. Berrone and A. Borio, *A residual a posteriori error estimate for the Virtual Element Method*, Math. Models Methods Appl. Sci., 27 (2017), pp. 1423–1458.

[32] P. E. Bjørstad and B. P. Tjøstheim, *High precision solutions of two fourth order eigenvalue problems*, Computing, 63 (1999), pp. 97–107.

[33] D. Boffi, *Finite Element Approximation of Eigenvalue Problems*, Acta Numerica, 1979.

[34] D. Boffi, F. Gardini, and L. Gastaldi, *Some remarks on eigenvalue approximation by finite elements*, in Frontiers in numerical analysis–Durham 2010, Springer, Heidelberg, 2012, pp. 1–77.

[35] S. C. Brenner, Q. Guan, and L.-Y. Sung, *Some estimates for virtual element methods*, Comput. Methods Appl. Math., 17 (2017), pp. 553–574.

[36] S. C. Brenner, P. Monk, and J. Sun, *C^0 interior penalty galerkin method for biharmonic eigenvalue problems*, in Spectral and High Order Methods for Partial Differential Equations–ICOSAHOM 2014, Springer, Cham, 2015, pp. 3–15.

[37] S. C. Brenner, M. Neilan, A. Reiser, and L.-Y. Sung, *A C^0 interior penalty method for a von Kármán plate*, Numer. Math., 135 (2017), pp. 803–832.

[38] S. C. Brenner and L. R. Scott, *The Mathematical Theory of Finite Element Methods*, Springer, New York, 2008.

[39] H. Brezis, *Functional Analysis, Sobolev Spaces and Partial Differential Equations*, Springer, New York, 2011.

[40] F. Brezzi, *Finite element approximations of the von Kármán equations*, RAIRO Anal. Numér., 12 (1978), pp. 303–312.

[41] F. Brezzi and L. D. Marini, *Virtual element methods for plate bending problems*, Comput. Methods Appl. Mech. Engrg., 253 (2013), pp. 455–462.

[42] E. Cáceres and G. N. Gatica, *A mixed virtual element method for the pseudostress-velocity formulation of the Stokes problem*, IMA J. Numer. Anal., 37 (2017), pp. 296–331.

[43] E. Cáceres, G. N. Gatica, and F. A. Sequeira, *A mixed virtual element method for the Brinkman problem*, Math. Models Methods Appl. Sci., 27 (2017), pp. 707–743.

[44] E. Cáceres, G. N. Gatica, and F. A. Sequeira, *A mixed virtual element method for a pseudostress-based formulation of linear elasticity*, Appl. Numer. Math., 135 (2019), pp. 423–442.

[45] F. Cakoni, M. Çayören, and D. Colton, *Transmission eigenvalues and the nondestructive testing of dielectrics*, Inverse Problems, 24 (2008), pp. 065016, 15.

[46] F. Cakoni, D. Colton, and H. Haddar, *Inverse Scattering Theory and Transmission Eigenvalues*, vol. 88, SIAM, 2016.

[47] F. Cakoni, D. Colton, P. Monk, and J. Sun, *The inverse electromagnetic scattering problem for anisotropic media*, Inverse Problems, 26 (2010), pp. 074004, 14.

[48] F. Cakoni, D. Gintides, and H. Haddar, *The existence of an infinite discrete set of transmission eigenvalues*, SIAM J. Math. Anal., 42 (2010), pp. 237–255.

[49] F. Cakoni, P. Monk, and J. Sun, *Error analysis for the finite element approximation of transmission eigenvalues*, Comput. Methods Appl. Math., 14 (2014), pp. 419–427.

[50] J. Camaño, R. Rodríguez, and P. Venegas, *Convergence of a lowest-order finite element method for the transmission eigenvalue problem*, Calcolo, 55 (2018), pp. Art. 33, 14.

[51] A. Cangiani, P. Chatzipantelidis, G. Diwan, and E. H. Georgoulis, *Virtual element method for quasilinear elliptic problems*, arXiv preprint arXiv:1707.01592, (2017).

[52] A. Cangiani, E. H. Georgoulis, and P. Houston, *hp-version discontinuous Galerkin methods on polygonal and polyhedral meshes*, Math. Models Methods Appl. Sci., 24 (2014), pp. 2009–2041.

[53] A. Cangiani, E. H. Georgoulis, T. Pryer, and O. J. Sutton, *A posteriori error estimates for the virtual element method*, Numer. Math., 137 (2017), pp. 857–893.

[54] A. Cangiani, V. Gyrya, and G. Manzini, *The nonconforming virtual element method for the Stokes equations*, SIAM J. Numer. Anal., 54 (2016), pp. 3411–3435.

[55] A. Cangiani, G. Manzini, and O. J. Sutton, *Conforming and nonconforming virtual element methods for elliptic problems*, IMA J. Numer. Anal., 37 (2017), pp. 1317–1354.

[56] C. Canuto, *Eigenvalue approximations by mixed methods*, RAIRO Anal. Numér., 12 (1978), pp. 27–50.

[57] C. Canuto, *A hybrid finite element method to compute the free vibration frequencies of a clamped plate*, RAIRO Anal. Numér., 15 (1981), pp. 101–118.

[58] J. Cao, Z. Wang, W. Cao, and L. Chen, *A mixed Legendre-Galerkin spectral method for the buckling problem of simply supported Kirchhoff plates*, Bound. Value Probl., 34 (2017), pp. 1–12.

[59] C. Carstensen, G. Mallik, and N. Nataraj, *A priori and a posteriori error control of discontinuous galerkin finite element methods for the von kármán equations*, IMA J. Numer. Anal., 39 (2018), pp. 167–200.

[60] H. Chen, H. Guo, Z. Zhang, and Q. Zou, *A C^0 linear finite element method for two fourth-order eigenvalue problems*, IMA J. Numer. Anal., 37 (2017), pp. 2120–2138.

[61] L. Chen and F. Wang, *A divergence free weak virtual element method for the Stokes problem on polytopal meshes*, J. Sci. Comput., 78 (2019), pp. 864–886.

[62] H. Chi, L. Beirão da Veiga, and G. H. Paulino, *A simple and effective gradient recovery scheme and a posteriori error estimator for the virtual element method (VEM)*, Comput. Methods Appl. Mech. Engrg., 347 (2019), pp. 21–58.

[63] C. Chinosi, *Virtual elements for the Reissner-Mindlin plate problem*, Numer. Methods Partial Differential Equations, 34 (2018), pp. 1117–1144.

[64] C. Chinosi and L. D. Marini, *Virtual element method for fourth order problems: L^2-estimates*, Comput. Math. Appl., 72 (2016), pp. 1959–1967.

[65] P. G. Ciarlet, *Mathematical Elasticity: Volume II: Theory of Plates*, Elsevier, 1997.

[66] P. G. Ciarlet, *Basic error estimates for elliptic problems*, in Handbook of numerical analysis, Vol. II, Handb. Numer. Anal., II, North-Holland, Amsterdam, 1991, pp. 17–351.

[67] P. G. Ciarlet, *The Finite Element Method for Elliptic Problems*, SIAM, 2002.

[68] P. G. Ciarlet and P. Rabier, *Les équations de von Kármán*, Springer, Berlin, 1980.

[69] P. G. Ciarlet and P.-A. Raviart, *A mixed finite element method for the biharmonic equation*, in Mathematical aspects of finite elements in partial differential equations, Elsevier, 1974, pp. 125–145.

[70] Ö. Civalek, A. Korkmaz, and Ç. Demir, *Discrete singular convolution approach for buckling analysis of rectangular Kirchhoff plates subjected to compressive loads on two-opposite edges*, Advances in Engineering Software, 41 (2010), pp. 557–560.

[71] D. Colton and R. Kress, *Inverse Acoustic and Electromagnetic Scattering Theory*, Springer, New York, 2013.

[72] D. Colton, P. Monk, and J. Sun, *Analytical and computational methods for transmission eigenvalues*, Inverse Problems, 26 (2010), pp. 045011, 16.

[73] J. Descloux, N. Nassif, and J. Rappaz, *On spectral approximation. part 1. the problem of convergence*, RAIRO Anal. Numér, 12 (1978), pp. 97–112.

[74] J. Descloux, N. Nassif, and J. Rappaz, *On spectral approximation. part 2. error estimates for the galerkin method*, RAIRO Anal. Numér, 12 (1978), pp. 113–119.

[75] D. A. Di Pietro and A. Ern, *A hybrid high-order locking-free method for linear elasticity on general meshes*, Comput. Methods Appl. Mech. Engrg., 283 (2015), pp. 1–21.

[76] M. Frittelli and I. Sgura, *Virtual element method for the Laplace-Beltrami equation on surfaces*, ESAIM Math. Model. Numer. Anal., 52 (2018), pp. 965–993.

[77] A. L. Gain, C. Talischi, and G. H. Paulino, *On the virtual element method for three-dimensional linear elasticity problems on arbitrary polyhedral meshes*, Comput. Methods Appl. Mech. Engrg., 282 (2014), pp. 132–160.

[78] F. Gardini, G. Manzini, and G. Vacca, *The nonconforming Virtual Element Method for eigenvalue problems*, ESAIM Math. Model. Numer. Anal., 53 (2019), pp. 749–774.

[79] F. Gardini and G. Vacca, *Virtual element method for second-order elliptic eigenvalue problems*, IMA J. Numer. Anal., 38 (2018), pp. 2026–2054.

[80] G. N. Gatica, M. Munar, and F. A. Sequeira, *A mixed virtual element method for the navier-stokes equations*, Math. Models Methods Appl. Sci, 28 (2018), pp. 2719–2762.

[81] G. N. Gatica, M. Munar and F.A. Sequeira, *A mixed virtual element method for the Boussinesq problem on polygonal mesh*, CI^{2}MA preprint 2019-32, available from http://www.ci2ma.udec.cl.

[82] F. Gazzola and Y. Wang, *Modeling suspension bridges through the von Kármán quasilinear plate equations*, in Contributions to nonlinear elliptic equations and systems, Birkhäuser/Springer, Cham, 2015, pp. 269–297.

[83] H. Geng, X. Ji, J. Sun, and L. Xu, *C^0IP methods for the transmission eigenvalue problem*, J. Sci. Comput., 68 (2016), pp. 326–338.

[84] V. Girault and P.-A. Raviart, *Finite Element Methods for Navier-Stokes Equations*, Springer-Verlag, Berlin, 1986.

[85] P. Grisvard, *Elliptic Problems in Non-Smooth Domains*, Pitman, Boston, 1985.

[86] P. Grisvard, *Problèmes aux limites dans les polygones. Mode d'emploi*, EDF Bull. Direction Études Rech. Sér. C Math. Inform., (1986), pp. 21–59.

[87] T. Gustafsson, R. Stenberg, and J. Videman, *A posteriori estimates for conforming Kirchhoff plate elements*, SIAM J. Sci. Comput., 40 (2018), pp. A1386–A1407.

[88] J. Han, Y. Yang, and H. Bi, *A new multigrid finite element method for the transmission eigenvalue problems*, Appl. Math. Comput., 292 (2017), pp. 96–106.

[89] P. Hansbo and M. G. Larson, *A posteriori error estimates for continuous/discontinuous Galerkin approximations of the Kirchhoff-Love buckling problem*, Comput. Mech., 56 (2015), pp. 815–827.

[90] J. Huang, L. Guo, and Z. Shi, *Vibration analysis of Kirchhoff plates by the Morley element method*, J. Comput. Appl. Math., 213 (2008), pp. 14–34.

[91] K. Ishihara, *On the mixed finite element approximation for the buckling of plates*, Numer. Math., 33 (1979), pp. 195–210.

[92] G. H. Knightly, *An existence theorem for the von Kármán equations*, Arch. Rational Mech. Anal., 27 (1967), pp. 233–242.

[93] X. Liu and Z. Chen, *The nonconforming virtual element method for the Navier-Stokes equations*, Adv. Comput. Math., 45 (2019), pp. 51–74.

[94] X. Liu, J. Li, and Z. Chen, *A nonconforming virtual element method for the Stokes problem on general meshes*, Comput. Methods Appl. Mech. Engrg., 320 (2017), pp. 694–711.

[95] G. Mallik and N. Nataraj, *Conforming and nonconforming finite element methods for canonical von Kármán equations*, Int. J. Adv. Eng. Sci. Appl. Math., 7 (2015), pp. 86–95.

[96] G. Mallik and N. Nataraj, *Conforming finite element methods for the von Kármán equations*, Adv. Comput. Math., 42 (2016), pp. 1031–1054.

[97] G. Mallik and N. Nataraj, *A nonconforming finite element approximation for the von Karman equations*, ESAIM Math. Model. Numer. Anal., 50 (2016), pp. 433–454.

[98] L. Mascotto, I. Perugia, and A. Pichler, *Non-conforming harmonic virtual element method: h- and p-versions*, J. Sci. Comput., 77 (2018), pp. 1874–1908.

[99] B. Mercier, J. Osborn, J. Rappaz, and P.-A. Raviart, *Eigenvalue approximation by mixed and hybrid methods*, Math. Comp., 36 (1981), pp. 427–453.

[100] F. Millar and D. Mora, *A finite element method for the buckling problem of simply supported Kirchhoff plates*, J. Comput. Appl. Math., 286 (2015), pp. 68–78.

[101] T. Miyoshi, *A mixed finite element method for the solution of the von kármán equations*, Numer. Math., 26 (1976), pp. 255–269.

[102] D. Mora and G. Rivera, *A priori and a posteriori error estimates for a virtual element spectral analysis for the elasticity equations*, IMA J. Numer. Anal., DOI: https://doi.org/10.1093/imanum/dry063, (2019).

[103] D. Mora, G. Rivera, and R. Rodríguez, *A virtual element method for the Steklov eigenvalue problem*, Math. Models Methods Appl. Sci., 25 (2015), pp. 1421–1445.

[104] D. Mora, G. Rivera, and R. Rodríguez, *A posteriori error estimates for a virtual element method for the Steklov eigenvalue problem*, Comput. Math. Appl., 74 (2017), pp. 2172–2190.

[105] D. Mora, G. Rivera, and I. Velásquez, *A virtual element method for the vibration problem of Kirchhoff plates*, ESAIM Math. Model. Numer. Anal., 52 (2018), pp. 1437–1456.

[106] D. Mora and R. Rodríguez, *A piecewise linear finite element method for the buckling and the vibration problems of thin plates*, Math. Comp., 78 (2009), pp. 1891–1917.

[107] D. Mora and I. Velásquez, *A virtual element method for the transmission eigenvalue problem*, Math. Models Methods Appl. Sci., 28 (2018), pp. 2803–2831.

[108] D. Mora and I. Velásquez, *Virtual element for the buckling problem of Kirchhoff-Love plates*, arXiv preprint arXiv:1905.02030, (2019).

[109] M. R. Nelson, J. R. King, and O. E. Jensen, *Buckling of a growing tissue and the emergence of two-dimensional patterns*, Math. Biosci., 246 (2013), pp. 229–241.

[110] J. E. Osborn, *Spectral approximation for compact operators*, Math. Comput., 29 (1975), pp. 712–725.

[111] G. H. Paulino and A. L. Gain, *Bridging art and engineering using Escher-based virtual elements*, Struct. Multidiscip. Optim., 51 (2015), pp. 867–883.

[112] I. Perugia, P. Pietra, and A. Russo, *A plane wave virtual element method for the Helmholtz problem*, ESAIM Math. Model. Numer. Anal., 50 (2016), pp. 783–808.

[113] R. Rannacher, *Nonconforming finite element methods for eigenvalue problems in linear plate theory*, Numer. Math., 33 (1979), pp. 23–42.

[114] N. Sukumar and A. Tabarraei, *Conforming polygonal finite elements*, Internat. J. Numer. Methods Engrg., 61 (2004), pp. 2045–2066.

[115] J. Sun, *Iterative methods for transmission eigenvalues*, SIAM J. Numer. Anal., 49 (2011), pp. 1860–1874.

[116] J. Sun and A. Zhou, *Finite Element Methods for Eigenvalue Problems*, Chapman and Hall/CRC, 2016.

[117] O. J. Sutton, *The virtual element method in 50 lines of matlab*, Numer. Algorithms, 75 (2017), pp. 1141–1159.

[118] C. Talischi, G. H. Paulino, A. Pereira, and I. F. Menezes, *Polygonal finite elements for topology optimization: A unifying paradigm*, Int. J. Numer. Meth. Eng., 82 (2010), pp. 671–698.

[119] C. Talischi, G. H. Paulino, A. Pereira, and I. F. Menezes, *Polymesher: a general-purpose mesh generator for polygonal elements written in matlab*, Struct. Multidiscip. Optim., 45 (2012), pp. 309–328.

[120] S. P. Timoshenko, *Theory of Elastic Stability*, McGraw-Hill Book Co., Inc., New York-Toronto-London, 1961.

[121] G. Vacca, *An H^1-conforming virtual element for Darcy and Brinkman equations*, Math. Models Methods Appl. Sci., 28 (2018), pp. 159–194.

[122] O. Čertík, F. Gardini, G. Manzini, and G. Vacca, *The virtual element method for eigenvalue problems with potential terms on polytopic meshes*, Appl. Math., 63 (2018), pp. 333–365.

[123] T. Von Kármán, *Festigkeitsprobleme im maschinenbau*, Encycl. der Mathematischen Wissenschaften, Leipzig, 4 (1910), pp. 348–352.

[124] Y. Wang, *An evolution von Kármán equation modeling suspension bridges*, Nonlinear Anal., 169 (2018), pp. 59–78.

[125] P. Wriggers, W. T. Rust, and B. D. Reddy, *A virtual element method for contact*, Comput. Mech., 58 (2016), pp. 1039–1050.

[126] Y. Yang, J. Han, and H. Bi, *Non-conforming finite element methods for transmission eigenvalue problem*, Comput. Methods Appl. Mech. Engrg., 307 (2016), pp. 144–163.

[127] J. Zhao, S. Chen, and B. Zhang, *The nonconforming virtual element method for plate bending problems*, Math. Models Methods Appl. Sci., 26 (2016), pp. 1671–1687.

[128] J. Zhao, B. Zhang, S. Chen, and S. Mao, *The Morley-type virtual element for plate bending problems*, J. Sci. Comput., 76 (2018), pp. 610–629.